

Emission of biogenic halocarbons in temperate and tropical coastal zones

A thesis submitted to the School of Environmental Sciences of the University of East
Anglia in candidature for the degree of

Doctor of Philosophy

By

Emma C. Leedham

March 2013

© This copy of the thesis has been supplied on condition that anyone who consults it is understood to recognise that its copyright rests with the author and that use of any information derived there from must be in accordance with current UK Copyright Law. In addition, any quotation or extract must include full attribution.

Abstract

Biogenically-produced halocarbons play an important role in regional and global biogeochemical processes. These compounds are short-lived (lifetimes <6 months) and so have temporal and spatial variability in their atmospheric distributions. Marine regions, in particular coastlines, have been identified as important source regions for these compounds, and within these regions macroalgae (seaweeds) are an important source. Despite their short lifetime, it is believed that biogenic bromocarbons may contribute to stratospheric inorganic bromine (Br_y). Measurement and model studies have identified a 6 (1-8) ppt excess of stratospheric Br_y that cannot be accounted for via known sources of longer-lived halocarbons. Tropical regions are believed to play an important role in this process, as deep convection may act as a rapid transport mechanism allowing these compounds to reach the upper troposphere within their atmospheric lifetimes. Despite this potential importance, gaps still remain in our knowledge of halocarbon biogeochemistry in this region. This study provides the first dedicated measurements of tropical macroalgae via laboratory incubations of 15 species. Laboratory studies on temperate macroalgae were also performed, with a focus on the impact of exposure and desiccation on halocarbon emissions. Desiccation-related halocarbon emissions are of interest due to a growing seaweed aquaculture industry; seaweeds are often left to dry before processing. In situ atmospheric measurements of halocarbons around Malaysia as part of the SHIVA campaign are also reported here. A study of halocarbon concentrations in Malaysia allowed the identification of different regions characterised by different source and atmospheric transport processes. We identified that strong coastal sources do exist in this region, but that their distribution is patchy and model studies should not assume a constant, strong coastal source. Laboratory and field measurements were combined in a final discussion providing annual emission estimates for the Malaysian and south east Asian region. Of particular interest is the potential impact of aquaculture, which, if projected expansions in production are met, could account for a considerable proportion of future Malaysian annual bromoform emissions.

Publications

Work contributing to, or done alongside, this thesis has been published in:

Leedham, E. C., Hughes, C., Keng, F. S. L., Phang, S.-M., Malin, G. and Sturges, W. T.: Emission of atmospherically significant halocarbons by naturally occurring and farmed tropical macroalgae, *Biogeosciences Discussions*, 10(1), 483-528, 2013

Keng, F. S.-L., Phang, S.-M., Rahman, N. A., Leedham, E. C., Hughes, C., Robinson, A. D., Harris, N. R. P., Pyle, J. A. and Sturges, W. T.: Volatile halocarbon emissions by three tropical brown seaweeds under different irradiances, *Journal of Applied Phycology* (pre-print) 2013

Gómez Martín J. C., Mahajan, A. S., Hay, T. D., Prados-Román, C., Ordóñez, C., MacDonald, S. M., Plane, J. M., Sorribas, M., Paredes Mora, J. F., Agama Reyes, M. V., Oram, D. E., Leedham, E. C. and Saiz-Lopez, A.: Iodine chemistry in the Eastern Pacific marine boundary layer, *Journal of Geophysical Research – Atmospheres*, 118, 2013

Acknowledgements

This thesis is a culmination of three years learning, collaboration and research, and I am indebted to the many people that have made this possible. To my supervisory team - Bill, Gill, David and Claire – thank you for getting this project off the ground, and supporting me through the whole process. You've all been amazing role models with respect to scientific curiosity and rigorous attention to details. I've also been lucky to be part of two research groups, to members past and present of the MTGB/Liss Group and the TGL group thanks for support, friendship and scientific discussions. Technical support at UEA has been brilliant. The help of Gareth, Steve W., Andy M. and Stephen H. has been invaluable at many points over the past few years when shipping crates of field equipment or just working in UEA labs. Rob – thanks for putting up with my complete lack of microbiological knowledge, large tanks of seawater and occasional temper – I could not have conducted lab work without you. There are many, many other people in ENV to thank, but to name a few...Graham, I think you probably made things better in the lab slightly more times than you made things worse, but, joking aside, you've been invaluable. Adam (I'm still waiting for donuts), Amy, Chris, Clare, Imke, Katrin, Martin, Moritz, Nat, Ollie and Raf – thanks for tea, cake, hugs, laughter and the (not so occasional) glass of wine.

Fieldwork would have been impossible without the more-than-generous support of Prof. Phang Siew-Moi and her research group in the Institute of Ocean and Earth Sciences (IOES) at the University of Malaya. The hospitality of the entire IOES team during time I spent there was staggering, in particular that of Fiona Keng (an amazing collaborator/provider of food) and Hui-Yin Yeong. Data in Chapter 5 forms part of the international SHIVA consortium and thanks must be given to everyone involved in SHIVA for a successful field campaign, useful collaborations, and the occasional bit of karaoke. In particular SHIVA coordinators, Klaus Pfeilsticker and Marcel Dorf, for having me on board and Birgit Quack for help with local boat logistics and seawater measurements.

Work aside, my sanity in the first two years of my PhD was greatly supported by my Norwich family; Sarah, David and Chris. Perhaps we can get back to watching the X-Files now I've finished my thesis? Friends near and far (mainly far, I do live in Norwich) – thank you for at least feigning an interest in what I do and battling the Greater Anglia trains to visit.

Love and thanks to my family. Mum, Dad and Han, thanks for your love and support that extends far beyond this thesis. You guys are the best. Porps, you once asked me if you could 'use up the smell of a flower', setting me on a course of scientific thinking (and I still don't know the answer) – this thesis is for you. And, finally, Andy – without you this is nothing.

Table of contents

Preliminary information

List of tables and figure	vii
List of acronyms, abbreviations and chemical formulae	xi
Appendices from page 194 and references from page 200	

Chapter 1 – An introduction to coastal halocarbon production

1.1	Terrestrial sources of biogenic halocarbon	3
1.2	Marine sources of biogenic halocarbons	4
1.2.1	Macroalgae	4
1.2.2	Other marine sources (both biotic and abiotic)	5
1.3	Macroalgal production of halocarbons	7
1.3.1	Accumulation and concentration of halides from seawater	7
1.3.2	Production of halocarbons	8
1.3.3	Release of halocarbons into the environment due to environmental stress	9
1.3.4	The role of inorganic iodine emissions	10
1.3.5	Release of halocarbons into the environment as a chemical defence compound	11
1.4	Loss processes in seawater	12
1.5	The sea-air flux of halocarbons	14
1.6	Role and fate in the atmosphere	15
1.6.1	Global biogeochemical cycles and human health	15
1.6.2	New particle formation	16
1.6.3	Halocarbons and their impact on tropospheric chemistry	18
1.6.4	Halocarbons and stratospheric ozone	20
1.7	The importance of tropical coastal halocarbon emissions	22
1.7.1	The coastal zone: An important halocarbon source region	22
1.7.2	Tropical deep convection	23
1.7.3	Tropical macroalgae	24
1.7.4	Knowledge gaps and the need for regional measurements	25
1.8	Halocarbons in a changing world	26
1.9	Key research questions and thesis structure	26

Chapter 2 – A methodology overview and method development

2.1	Introduction	28
2.2	The effects of storage on seawater samples	30
2.3	Flux chambers	33

Chapter 3 – Halocarbon production by tropical macroalgae

3.1	Introduction	41
3.2	Methodology	43
3.2.1	Malaysian macroalgae sample collection	43
3.2.2	Temperate macroalgae sample collection	47
3.2.3	Incubation protocol	48
3.2.4	Purge and trap (P&T) system	49
3.2.5	GCMS analysis	51
3.2.6	Calibration and use of internal standards	53
3.3	Results and discussion	57
3.3.1	The effect of incubation time on production	57
3.3.2	Halocarbon production by tropical macroalgae	59
3.3.3	Correlations between biogenic halocarbons	66
3.3.4	Comparison with temperate and polar halocarbon production	69
3.4	Conclusions	73
3.4.1	Further work	73

Chapter 4 – Halocarbon production by macroalgae during desiccation

4.1	Introduction	74
4.1.1	Natural tidal desiccation	74
4.1.2	Halocarbons and desiccation stress	76
4.1.3	Prolonged desiccation	77
4.1.4	Aims of this work	78
4.2	Methodology	80
4.2.1	Collection of seaweed samples	80
4.2.2	Incubation flasks and housing	81
4.2.3	Sorbent tube sampling	83
4.2.4	Analysis of sorbent tubes	86
4.2.5	Experimental protocols	87
4.2.6	Water loss and photosynthesis changes	90
4.2.7	Flux chamber experiments	91
4.3	Results	92
4.3.1	Replicate variability and the use of standardised concentration values	92
4.3.2	Treatment of potential sources of errors	93
4.3.3	Mass loss experiments	94
4.3.4	F_v/F_m experiments	95
4.3.5	Halocarbons emission patterns: submerged vs. exposed macroalgae	98
4.3.6	Halocarbons emission patterns during desiccation of macroalgae	103
4.3.7	Halocarbon production/emission rates	110
4.3.8	Rewetting experiments	113
4.4	Discussion - the halocarbon response to desiccation	116
4.4.1	Variation in desiccation rate between species	118
4.4.2	Variation in F_v/F_m between species	119
4.4.3	Reasons for decreasing bromocarbon emissions over time	120
4.4.4	The effects of rewetting with freshwater after a period of desiccation	121
4.5	Conclusions	122
4.5.1	Further work	122

Chapter 5 – Atmospheric distribution of halocarbons around Malaysia

5.1	Introduction	123
5.2	Method	123
5.2.1	Sampling sites – SHIVA 11	126
5.2.2	Sampling sites – JAM10	127
5.2.3	Sample collection	128
5.2.4	Sample analysis	128
5.2.5	Air standard concentrations, calibrations and intercalibrations	130
5.2.6	A comparison of system precision and detection limits	131
5.3	Results and discussion	133
5.3.1	Data overview	133
5.3.2	Differences between SHIVA11 sites	136
5.3.3	Extending the range of halocarbon measurements with other datasets	136
5.3.4	A comparison with previous studies	139
5.3.5	Mapping emissions	141
5.3.6	Back trajectories and air mass differences between sites	149
5.3.7	Halocarbon correlations	154
5.3.8	Three-factor correlations to determine regional emission rates	160
5.3.9	Contribution of biogenic VSLS to stratospheric bromine	163
5.4	Conclusions – regional halocarbon distributions around Malaysia	166

Chapter 6 - Conclusions

6.1	Introduction	168
6.2	A semiquantitative analysis of the halocarbon flux from macroalgae	169
6.2.1	Determining macroalgal biomass	169
6.2.2	Determining regional fluxes and annual emissions	171
6.2.3	A comparison of estimated fluxes and emissions	175
6.2.4	The impact of tropical aquaculture	178
6.3	A discursive summary of work covered in chapters 3-5	184
6.3.1	Regional halocarbon distributions around Malaysia	184
6.3.2	Tropical macroalgae – incubations and emission estimates	184
6.3.3	Macroalgae incubations – comparisons between different studies and methodologies	186
6.3.4	Halocarbon ratios	187
6.3.5	Desiccation of macroalgae	188
6.4	Future work ideas	190
6.4.1	Halocarbon measurement techniques	190
6.4.2	Halocarbons and their ecosystem role	191
6.4.3	Halocarbon emissions in a changing climate	192

List of tables and figures by chapter

Chapter 1 – An introduction to coastal halocarbon production

Figures

1	Thesis outline	27
---	----------------	----

Tables

1	Target VSLS & their atmospheric lifetimes	2
2	Concentration of bromine & iodine in a range of macroalgae	7
3	Seawater loss processes & lifetime of CHBr_3	12

Chapter 2 – A methodology overview and method development

Figures

1	Overview of key stages in analysis of samples for [halocarbon] & a comparison of methods used in each chapter	29
2	Changes in [halocarbon] during seawater storage in amber bottles	32
3	Changes in [halocarbon] during seawater storage in glass syringes	33
4	Flux chamber photograph	35
5	UVB transmission through flux chamber materials	38
6	UVA transmission through flux chamber materials	39
7	Visible light transmission through flux chamber materials	40

Tables

1	Flux chamber materials tested for ability to transmit light	37
---	---	----

Chapter 3 – Halocarbon production by tropical macroalgae

Figures

1	Location of macroalgae sampling sites	44
2	Photographs of tropical macroalgae species	45
3	Diagram of purge & trap system	50
4	Variations in internal standard over time	55
5	Correlations between two internal standards	56
6	Correlations between calculated production at t4 & t24	58
7	Halocarbon production by tropical macroalgae	60
8	Macroalgae ranked with respect to halocarbon production	62
9	Correlations between halocarbon production rates	67
10	A comparison with reported halocarbon production rates from existing literature	70

Tables

1	Details of tropical macroalgae species	46
2	Details of temperate macroalgae species	47
3	Target halocarbons	52
4	Ratio between calculated production at t4 & t24	57
5	Total halides emitted during incubations	63
6	Changes in 'production rank' when calculated for fresh weight and dry weight	65

Chapter 4 – Halocarbon production by macroalgae during desiccation

Figures

1	Photograph of seaweed drying at a commercial farm	77
2	Photographs of <i>Fucus vesiculosus</i> & <i>Ulva intestinalis</i>	78
3	Photograph of seaweed collection site & shore position	79
4	Diagram of desiccation chamber	82
5	Results from sorbent tube methodological tests	85
6	Changes in F_v/F_m (<i>Fucus</i>) during desiccation, relative to time	96
7	Changes in F_v/F_m (<i>Fucus</i>) during desiccation, relative to water loss	97
8	Changes in $[CH_2Br_2]$ & $[CHBr_3]$ upon emersion (<i>Fucus</i>)	100
9	Changes in $[CH_2Br_2]$ & $[CHBr_3]$ upon emersion (<i>Ulva</i>)	101
10	Changes in $[CH_2Br_2]$ during <i>Fucus</i> desiccation	105
11	Changes in $[CHBr_3]$ during <i>Fucus</i> desiccation	106
12	Changes in $[CH_2Br_2]$ during <i>Ulva</i> desiccation	107
13	Changes in $[CHBr_3]$ during <i>Ulva</i> desiccation	108
14	Changes in $[CH_2Br_2]$ and $[CHBr_3]$ during <i>Porphyra</i> desiccation	109

15	Histogram: CH ₂ Br ₂ & CHBr ₃ production rates during <i>Fucus</i> desiccation	111
16	Histogram: CH ₂ Br ₂ & CHBr ₃ production rates during <i>Ulva</i> desiccation	112
17	Changes in [CH ₂ Br ₂] during desiccation & rewetting of <i>Ulva</i>	114
18	Changes in [CHBr ₃] during desiccation & rewetting of <i>Ulva</i>	115

Tables

1	Summary of desiccation experiments conducted	88
2	Mass (water) loss rates for <i>Fucus</i> & <i>Ulva</i>	94
3	A comparison between bromocarbon production rates for exposed & submerged specimens	102

Chapter 5 – Atmospheric distribution of halocarbons around Malaysia

Figures

1	Measurement sites and campaign locations, Malaysia	125
2	Small boats used for coastal transect sampling, photograph	126
3	Sampling sites visited during JAM10, photograph	127
4	Vertical distribution of halocarbons sampled from the Falcon aircraft	135
5	Atmospheric distribution of CH ₃ I around Malaysia	142
6	Atmospheric distribution of CH ₂ Br ₂ around Malaysia	143
7	Atmospheric distribution of CHBr ₃ around Malaysia	144
8	Atmospheric distribution of CHBrCl ₂ around Malaysia	145
9	Atmospheric distribution of CHBr ₂ Cl around Malaysia	146
10	Satellite chlorophyll-a map for Malaysia	148
11	HYSPLIT back trajectories for local boat stations	150
12	HYSPLIT back trajectories for R/V Sonne cruise and Falcon flights	151
13	An overview of regions R1-R4	153
14	Bromoalkane correlations measured during SHIVA11	156
15	Logarithmic bromoalkane correlations measured during SHIVA11	157
16	Log-log ratio plots for CHBr ₃ , CH ₂ Br ₂ and CHBr ₂ Cl determining emission source ratios	162
17	Satellite maps of convection over the western Pacific	164

Tables

1	Measurement platforms and techniques used to measure [halocarbon] around Malaysia	124
2	Precision, detection limits and error on standard concentrations for air standards	132
3	A summary of halocarbon concentrations observed during SHIVA11	134
4	A summary of halocarbon concentrations observed during JAM10	138
5	A summary of atmospheric mixing ratios from the literature	140
6	Summary of measurements made in regions R1-R4	153
7	Descriptive statistics for correlations in Fig. 14	156
8	Descriptive statistics for correlations in Fig. 15	157
9	Fisher's z statistic for correlations in Fig. 14	159

Chapter 6 - Conclusions

Figures

1	Visual representation of the seawater wedge used with assumptions A1-A6	173
---	---	-----

Tables

1	A summary of data sources used to derive regional emission estimates	180
2	A comparison of seawater concentrations, flux rates and annual emission estimates from this study and the existing literature	182

Abbreviations, acronyms and chemical formulae

Acronyms:

A

B

BD	Bohey Dulang
BrPO	bromoperoxidases
BV	breakthrough volume, see also SSV

C

CCN	cloud condensation nuclei
CFC(s)	chlorofluorocarbon(s)

D

DOM	dissolved organic matter
DMS	dimethyl sulphide
DW	dry weight

E

EI	electron ionisation mode (MS analysis)
----	--

F

FAO	Food and Agriculture Organisation (United Nations)
FW	fresh weight
F_v/F_m	Maximum potential quantum efficiency, used as part of a measure to determine photosynthetic efficiency.

G

GC	gas chromatograph (see also GCMS)
GCMS	gas chromatography mass spectrometry
GOME	Global Ozone Monitoring Experiment

H

HYSPLIT	HYbrid Single Particle Lagrangian Integrated Trajectory model
---------	---

I

IPO	iodoperoxidases
-----	-----------------

J

K

Ku	Kuching
KK	Kota Kinabalu

Abbreviations etc.

L

La Langkawi
LT (Malaysian) local time

M

MBL marine boundary layer
MS/MSD mass spectrometer/mass selective detector (see also GCMS)
m/z target masses defined during SIM MS analysis

N

n number of samples
NCI negative ion chemical ionisation (MS analysis)

O

ODR orthogonal distance regression
OFN oxygen-free nitrogen

P

PD Port Dickson
P&T purge and trap
PAM Pulse Amplitude Modulation (part of a system to measure F_v/F_m)
PARFORCE New Particle Formation and Fate in the Coastal Environment
PG product gas
PP polypropylene
PSII photosystem II

Q

R

R1-4 Used to denote regions 1-4 when discussing atmospheric halocarbons distributions around Borneo.
ROS Reactive oxygen species. This includes: singlet oxygen (1O_2), the superoxide radical ($^{\cdot}O_2^-$), hydrogen peroxide (H_2O_2) and the hydroxyl radical ($^{\cdot}OH$).

S

SAM S-adenosyl-L-methionine
SEA the south east Asian region (defined in Chapter 6)
sem Semporna
semcruise A local boat cruise in the Semporna region.
SCS South China Sea
SD/ σ standard deviation (usually given as 1SD or 1σ)
SG source gas
SIM single ion mode (MS analysis)
SSV safe sampling volume, see also BV.

T

TTL tropical tropopause layer

U

UEA University of East Anglia

UM University of Malaya

UNEP United Nations Environment Programme

U.S. E.P.A United States of America Environmental Protection Agency

UTC coordinated universal time

UV ultra violet light

V

VOCs volatile organic compounds

VSLS very short lived (halogenated) substances

W

WMO World Meteorological Organisation

X,Y,Z**Equation components:** τ lifetime (atmospheric) ΔC the concentration difference between C_a and C_w C_a concentration in bulk air C_w concentration in bulk seawater

F sea air flux, equations involve

H dimensionless henry's law constant

k rate constant (used for chemical decay in Chapter 5)

 K_a total transfer velocity expressed from gas phase K_m Michaelis-Menten constant K_w total transfer velocity expressed from liquid side K_H gas over liquid form of henry's law constant, H

m slope of regression line

 p_r significance of a regression statistic using Pearson's

Product-Moment Correlation coefficient

 p_p significance of a regression statistic using Spearman's

Rank Correlation Coefficient

u windspeed

Sc Schmidt number

Abbreviations etc.

Commonly used chemical formulae

The production and atmospheric distribution of the following **organic halocarbons** is investigated in this thesis. More details are provided in Chapter 1, in particular Table 1.

CH ₃ I	methyl iodide
CH ₂ I ₂	diiodomethane
CH ₂ Br ₂	dibromomethane
CHBr ₃	bromoform
CH ₂ BrCl	bromochloromethane
CHBrCl ₂	bromodichloromethane
CHBr ₂ Cl	dibromochloromethane
CH ₂ BrI	bromoiodomethane
CH ₂ ClI	chloroiodomethane

The following inorganic halogen-containing compounds and reactive oxygen species are mentioned frequently due to their role in halocarbon formation or atmospheric chemistry.

Br ₂	molecular bromine
BrO	bromine monoxide/bromine oxide radical
Br _y	collective term for reactive bromine species
Br _y ^{VSLs}	as above, the contribution from VSLs
H ₂ O ₂	hydrogen peroxide
HOX	hypohalous acids, including HOI and HOBr
HOI	hypoiodous acid
HOBr	hypobromous acid
I ₂	molecular iodine
I ⁻	iodide
IO	iodine monoxide/iodine oxide radical
IO ₂ /OIO	iodine dioxide
NO _x	a term combining NO and NO ₂
NO & NO ₂	nitric oxide and nitrogen dioxide
OH & HO ₂	hydroxyl and perhydroxyl radicals (also shown e.g. ·OH)
O ₃	ozone

CHAPTER 1

An introduction to coastal halocarbon production

The term 'halocarbon' refers to an organic molecule containing one or more halogen atoms; chlorine (Cl), bromine (Br), iodine (I) or fluorine (F). This broad group of compounds is usually divided into two groups:

- Longer-lived, generally anthropogenically produced, halocarbons.
- Shorter-lived halocarbons, which tend to have a biogenic source.

Anthropogenic halocarbons, notably chlorofluorocarbons (CFCs) and 'halons' (compounds containing bromine as well as chlorine and or fluorine e.g. CBr_2F_2) became widely used in the 1930s and 1960s respectively as their inert, non-flammable and non-toxic compounds were ideally suited for use in a range of commercial goods including refrigeration systems, air conditioners and fire extinguishers (Carlisle, 2004). It was this inert stability, the property that made them a commercial success, and which led to their environmentally damaging properties. These compounds were first detected in the atmosphere by James Lovelock in the early 1970s (Lovelock, 1971; Lovelock et al., 1973). Shortly after it was reported that they had the potential to destroy stratospheric ozone (O_3) (Molina & Rowland, 1974). However, it was not until 1985 and the discovery of the seasonal ozone hole over Antarctica (Farman et al., 1985) that the scientific community accepted that, due to their long atmospheric lifetimes (e.g. 100-120 years for CFC-11 (Montzka et al., 2010)), CFCs were persisting in the atmosphere long enough to reach the stratospheric ozone layer and provide halogens which were perturbing stratospheric ozone cycling (see Section 1.6.4). In 1987 the Montreal Protocol was signed, which, along with subsequent amendments, sought to restrict and eventually ban the production and consumption of ozone-depleting substances. The latest World Meteorological Organisation (WMO) and United Nations Environment Programme (UNEP) Scientific Assessment of Ozone Depletion report published in 2010, demonstrates declining or stabilising global surface mean mixing ratios of Montreal Protocol-controlled substances, including CFCs. Whilst the long lifetime and continuing emission from existing chemical and product stocks ensures these compounds will persist in the atmosphere for many more years, current and future emissions of these compounds are controlled and monitored.

Very short-lived (halogenated) substances (VSLS), so termed because their atmospheric lifetimes are less than six months (Montzka et al., 2010), are mainly of natural (biogenic) origin. There are some exceptions: methyl chloride (CH_3Cl) and methyl bromide (CH_3Br) have mainly natural sources (CH_3Br has a small contribution from anthropogenic sources such as agricultural quarantined shipment fumigants) yet have relatively long atmospheric lifetimes of 1 and 0.8 years respectively. They contribute about 17% of stratospheric chlorine and 30% of stratospheric bromine respectively (Fahey & Hegglin, 2010). There are also anthropogenic sources of VSLS. Water chlorination leads to a wide range of bromo- and bromochloro- compounds (Helz & Hsu, 1978; Richardson et al., 2010). Power plants (both fossil fuel and nuclear, coastal and inland), desalination plants; waste water treatment and the chlorination of water for public use also produce a small (~3% total) but locally significant contribution to VSLS (Quack & Wallace, 2003). This thesis will focus on biogenic VSLS, mainly those produced by macroalgae in coastal regions. These biogenic VSLS can play an important role in biogeochemical cycles (Section 1.6.1), particle formation (Section 1.6.2) and atmospheric chemistry including atmospheric oxidising capacity and ozone cycling (Sections 1.6.3, 1.6.4). Table 1 provides a list of biogenic halocarbons studied in this thesis, along with their chemical formulae, atmospheric lifetime and where they are discussed in this body of work.

Table 1. Target VSLS and their atmospheric lifetimes.

Compound	Chemical formula	Atmospheric lifetime / days*	Chapter		
			3	4	5
Iodocarbons					
	CH_3I	7	■		■
	CH_2I_2	0.003	■		
Bromocarbons					
	CH_2Br_2	123	■		
	CHBr_3	24	■		
Mixed bromochlorocarbons					
Bromochloromethane	CH_2BrCl	137	■		■
Bromodichloromethane	CHBrCl_2	78			■
Dibromochloromethane	CHBr_2Cl	59	■		■
Mixed iodocarbons					
Bromoiodomethane	CH_2BrI	0.04	■		
Chloroiodomethane	CH_2ClI	0.1	■		

* Atmospheric lifetimes from Montzka et al. (2010).

1.1 Terrestrial sources of biogenic halocarbons

Both terrestrial and marine systems produce biogenic halocarbons, although a wider range of compounds are produced from marine environments due to the generally higher concentrations of halogens in seawater (Moore & Tokarczyk, 1993). Volcanoes are also a source of a variety of halogenated compounds including methyl halides, chloroform (CHCl_3), carbon tetrachloride (CCl_4) and CFCs (Frische et al., 2006; Gribble, 2003). The main halocarbons produced by terrestrial environments, however, are methyl halides, CH_3Cl and CH_3Br . The main sources of CH_3Cl include biomass burning and coastal salt marshes whilst CH_3Br emissions have been observed from biomass burning, peatlands, rice paddies, salt marshes, mangroves, rapeseed, various fungal processes and woodlands (Montzka et al., 2010). Marine sources of both CH_3Cl and CH_3Br exist, with production reported for both compounds from phytoplankton cultures (Colomb et al., 2008), macroalgae (Baker et al., 2001) and an abiotic photochemical source via dissolved organic matter (Moore, 2008). Due the analytical systems used in this work CH_3Cl and CH_3Br could not be measured, but previous studies have suggested that production of these methyl halides from macroalgae is small and therefore unlikely to contribute greatly to global emission budgets (Baker et al., 2001).

1.2 Marine sources of biogenic halocarbons

Oceanic emissions account for 90-95% of brominated and iodinated VSLs (Law & Sturges, 2007). In coastal regions macroalgal emissions dominate (Section 1.2.1). However, other biotic and abiotic sources exist and will be discussed in Section 1.2.2.

1.2.1 Macroalgae

Since Bernard Courtois discovered iodine vapours from seaweed in 1811 (see Swain, 2005) many halogenated compounds from a range of marine organisms have been discovered. Burreson et al. (1976) reported over 42 halogenated products found in essential oil extracted from the red alga *Asparagopsis taxiformis*, including volatile halocarbons such as bromoform (CHBr_3) and dibromomethane (CH_2Br_2). This number has since been extended to over 100 halogenated products, many of which were previously unknown (Gribble, 2003).

That these halogenated compounds could have an environmental role was first noted by Lovelock in 1975. He reported concentrations of methyl iodide (CH_3I) in the water surrounding kelp beds that were up to one thousand times greater than those observed in the open ocean. A variety of studies soon followed, demonstrating production and emission of a range of halocarbons from marine algae; ranging from CH_3I to 1-bromopentane (e.g. Gschwend et al., 1985; Manley & Dastoor, 1987, 1988). A range of incubations demonstrated production from temperate (Carpenter & Liss, 2000; Nightingale et al., 1995), polar (Laternus, 1995, 1996; Schall et al., 1994) and subtropical (Giese et al., 1999) macroalgae. Few, if any, investigations into halocarbon production by tropical macroalgae were made, this will be discussed in further detail in Section 1.7.4.

1.2.2 Other marine sources (both biotic and abiotic)

i. Biotic sources

This thesis will focus on halocarbon production from macroalgae. However, a range of other biotic and abiotic sources exist. Ice algae were reported to produce a range of bromocarbons by Sturges et al. (1992), and other studies have demonstrated a phytoplankton source of volatile halocarbons (e.g. Hughes et al., 2006, 2011; Scarratt & Moore, 1998, 1999). Halogenated secondary metabolites and haloperoxidase enzymes (Section 1.3.2) have also been reported in some corals, sea squirts, nudibranches, bryozoans and worms (Gribble, 2003; Quack & Wallace, 2003 and references herein). However, these groups have not been proposed as sources of atmospherically important volatile halocarbons. Another little-studied group are the marine fungi. Terrestrial fungi are known to produce methyl halides (Watling & Harper, 1998) but the production of methyl halides from marine fungi has not been reported.

Bacteria have also been shown to produce CH_3I (Amachi, 2008; Amachi et al., 2001; Manley & Dastoor, 1988), but production of bromocarbons has not been reported. Axenic macroalgae cultures are rarely used for incubation experiments, some macroalgae have been shown to rely on natural bacterial assemblages for morphologically 'normal' growth and development (Spoerner et al., 2012). The possibility that halocarbon production is attributable to epiphytic bacteria or other organisms has been proposed. However, axenic macroalgae cultures, and microalgae cultures treated with prokaryotic inhibitors, still demonstrate halocarbon production (Manley & Dastoor, 1988; Sturges et al., 1992). A range of studies by Gschwend et al. (1985) on production from macroalgal epiphytes (both eukaryotic and prokaryotic) also suggests that the macroalgae themselves are responsible for a majority of the observed halocarbon emissions in non-axenic cultures. As measurements from macroalgae either in situ (e.g. Manley & Dastoor, 1987) or from culture are nearly always non-axenic, emission estimates will take into account epiphytic bacterial contribution. Bacteria are also believed to be involved in halocarbon breakdown in the marine environment (Section 1.4).

ii. Abiotic sources

A photochemical source of CH_3I has been proposed on the basis of laboratory and field experiments. Studies by Moore and Zafiriou (1994) demonstrated CH_3I production in $0.22 \mu\text{m}$ filtered seawater irradiated with natural light levels which they attributed to a non biological source. Filtration at the $0.22 \mu\text{m}$ should significantly reduce the microorganism community (Wurl, 2009), including many nanoplankton species, although some nanoplankton and many bacteria will pass through this level of filter. Using field measurements, Happell and Wallace (1996) demonstrated CH_3I production in regions of low biological productivity, and showed that only light levels were a significant predictor of CH_3I concentrations. Incubations of seawater samples collected in the tropical Atlantic by Richter and Wallace (2004) also demonstrated a photochemical, non-biologically dependent CH_3I source, which they calculated could contribute up to 50% of the average sea-air flux. Abiotic CH_3I production is not constant in all oceanic regions. Dissolved organic matter (DOM) is involved in the production of CH_3I , and so in coastal areas, with higher concentrations of DOM, the abiotic production rate of CH_3I may be up to six times greater than in pelagic regions (Moore & Zafiriou, 1994; Richter & Wallace, 2004). An abiotic source linked to dust inputs to the ocean has also been proposed (Williams et al., 2007), although the full impact of this process remains to be quantified. Further information on abiotic production of CH_3I is given in Section 1.6.2.

Abiotic production in surface seawater of several other iodocarbons, diiodomethane (CH_2I_2), chloriodomethane (CH_2ClI) and iodoform (CHI_3), was demonstrated by Martino et al. (2009). This processes occurs when seawater is exposed to ozone. Dissolved iodide reacts with ozone to form hypiodous acid (HOI) and molecular iodine (I_2), both of which then go on to react with DOM to form volatile iodocarbons. This process was observed in field-collected seawater with a range of biological productivity, and is therefore likely to be a ubiquitous source of volatile iodocarbons in the marine environment. Nucleophilic substitutions, for example production of CH_2ClI from CH_2I_2 and dibromochloromethane (CHBr_2Cl) and bromodichloromethane (CHBrCl_2) from CHBr_3 , have also been proposed (e.g. Moore & Tokarczyk, 1993). This is discussed further in Section 1.4.

1.3 Macroalgal production of halocarbons

1.3.1 Accumulation and concentration of halides from seawater

Macroalgae actively take up trace elements through contact with the algal surface or through pores in their cell walls (Rodríguez-Castañeda et al., 2006). With regards to iodine Küpper et al. (1998) demonstrated that uptake is linked to apoplastic oxidation, possibly by haloperoxidase-catalysed reactions with hydrogen peroxide (H₂O₂). Typical concentrations of bromine and iodine in seawater are about 6.6 x 10⁻³% and 5.1 x 10⁻⁶% (by weight) respectively (Saenko et al., 1978). Table 2 presents reported concentrations of bromine and iodine measured in macroalgae species from Japan, California and France. Note, rhodophyte, phaeophyte and chlorophyte are macroalgae classes also referred to as red, brown and green algae respectively. A wide range of values can be seen, but it is clear that seaweeds can concentrate halides from seawater, with reported iodine concentrations in *Laminaria digitata* of up to 30,000 the natural concentration of iodine in seawater (Küpper et al., 1998).

Table 2. Concentration, % dry weight (DW), of bromine and iodine in a range of macroalgae species. nr = not recorded.

	Description	Bromine	Iodine
Rhodophyta	Various species, Japan ^a	0.65 (0.02-3.74)	0.095 (0.002-0.75)
	Various species, California ^b	0.70 (0.16-1.24)	nr
Phaeophyta	Various species, Japan ^a	0.09 (0.02-0.55)	0.12 (0.005-0.56)
	Various species, California ^b	0.34 (0.14-0.71)	nr
	<i>L. digitata</i> , France ^c	nr	0.4-4.7
Chlorophyta	Various species, Japan ^a	0.04 (0.02-0.12)	0.006 (0.002-0.008)
	Various species, California ^b	0.36 (0.11-1.06)	nr

^aMean values taken from measurements of 17 rhodophytes, 21 phaeophytes and 5 chlorophytes by Saenko et al. (1978). ^bMean values taken from measurements of 10 rhodophytes, 8 phaeophytes and 19 chlorophytes by Rodríguez-Castañeda et al. (2006). ^c (Küpper et al., 1998).

1.3.2 Production of halocarbons

Once accumulated inside the alga some halides are incorporated into organic compounds. Two production mechanisms exist; methyl halides are produced via methyl transferases (i) and polyhalogenated compounds via haloperoxidases (ii).

i. Production of methyl halides

The production of methyl halides involves the methylation of halides with the methyl donor S-adenosyl-L-methionine (SAM), a process catalysed by methyl halide transferases (Wuosmaa & Hager, 1990). It has been suggested that methyl halide production is a means of regulating cellular halide levels by removing excess halides (Ni & Hager, 1999). However, a study of Michaelis-Menten constants, K_m , (a method of describing the rate of enzymatic reactions) in Manley (2002) shows relatively high K_m values which suggests a low affinity of methyl transferases to halides. A low affinity could reflect an abundance of halides but it could also suggest that halides are not the target substrate of these enzymes and that methyl halides could be a by-product of other metabolic processes such as the methylated secondary metabolites such as steroids and isoprenoids (Manley, 2002).

ii. Production of polyhalogenated compounds

Vanadium-dependent haloperoxidases are thought to be responsible for the production of polyhalomethanes from macroalgae (Theiler et al., 1978). Chloroperoxidases are mainly found in fungi and are not considered further here. Bromoperoxidases (BrPO), oxidising Br and I, are the most common in marine algae, but iodoperoxidases (IPO) which oxidise only I have also been reported (Manley, 2002). Haloperoxidases oxidise halogens to hypohalous acids, e.g. hypobromous acid (HOBr) in the presence of H_2O_2 (Wuosmaa & Hager, 1990). This has been demonstrated by Collen et al. (1994), who reported increasing bromocarbon production with the addition of H_2O_2 to algal incubations, and Pedersen et al. (1996) who reported that the addition of sodium azides (at a level to inhibits peroxidase activity and not kill all cells) leads to a decrease in halocarbon production. Further haloperoxidase-catalysed reactions with nucleophilic acceptors, such as ketones, then lead to the formation of halocarbons (Wever et al., 1991; Winter & Moore, 2009). Further nucleophilic substitution forms polyhalogenated compounds; for example the production of $CHBr_3$ can occur via multiple bromination of a ketone followed by non-enzymatic hydrolysis and liberation of $CHBr_3$ (Beissner et al., 1981).

Indirect production has also been proposed. In this case hypohalous acids are formed as described above. Then they diffuse into the surrounding seawater where they react with DOM to form halocarbons (Wever et al., 1991). A reduction in CHBr_3 production when DOM was removed from incubation seawater, reported by Manley and Barbero (2001) supports this theory. Nucleophilic halogen substitution reactions may lead to conversions, e.g. CHBr_3 to CHBr_2Cl , which may produce a wider suite of halocarbon emissions from macroalgae beds (Tokarczyk & Moore, 1994) (Section 1.4).

1.3.3 Release of halocarbons into the environment due to environmental stress

Reactive oxygen species (ROS) is a term that includes; singlet oxygen ($^1\text{O}_2$), the superoxide radical (O_2^-), H_2O_2 and the hydroxyl radical (OH) (Collen & Davison, 1999; Kumar et al., 2011). The term activated oxygen species (AOS) is also used, sometimes interchangeably, with ROS, although there are technical differences such as the inclusion of H_2O_2 under the term ROS. As the term ROS is used in most studies, this term will be used here (see Lesser, 2006) for further details). The production of ROS is a constant process in all living cells. However, if production and accumulation of ROS goes beyond the capacity of an organism to quench these species and limit their damage (Lesser, 2006) then 'oxidative stress' occurs and excess ROS may damage lipids, proteins and DNA (Collen & Davison, 1999). Reactive nitrogen species, such as NO , are also involved in oxidative stress (Lesser, 2006), although their involvement in halocarbon chemistry has not been reported. Oxidative stress may be caused by many factors, including, but not limited to; nutrient limitation, high light exposure and changes in salinity, temperature and pH (Mata et al., 2011; Mtolera et al., 1996; Palmer et al., 2005).

That polyhalogenated compounds scavenge H_2O_2 during their production was identified by H_2O_2 addition experiments (Section 1.3.2) aimed at understanding the roles of haloperoxidase enzymes. Several early studies demonstrated that production of polyhalogenated compounds was greater in incubations conducted in the light compared to those conducted in the dark (Collen et al., 1994; Klick, 1993; Nightingale et al., 1995; Pedersen et al., 1996). In one study, Goodwin et al. (1997a), who saw a reduction in CH_2Br_2 and CHBr_3 production by *Macrocystis pyrifera* with the addition of photosynthesis inhibitors, increases in polyhalocarbon compounds is likely linked to the production of H_2O_2 during photosynthesis. Methyl halides, which are produced by methyl halide transferase reactions which do not scavenge H_2O_2 , were not affected by light in studies by Collen et al. (1994) and Manley and Dastoor (1987). Respiration also leads to the production of ROS, and addition of respiratory inhibitors to macroalgae incubations also reduce CHBr_3 production (Manley & Barbero, 2001).

Intertidal macroalgae are exposed to oxidative stresses during tidal exposure on a daily basis (Collen & Davison, 1999) and field studies have reported increasing atmospheric concentrations of halocarbons over macroalgae beds at low tide (e.g. Carpenter et al., 1999, see also Section 1.6.2). As the algae are exposed they are subject to various factors which may cause oxidative stress and lead to halocarbon emissions. Increased halocarbon production during desiccation has been reported in several studies (Bravo-Linares et al., 2010; Nightingale et al., 1995) and is discussed further in Chapter 4.

The increased halocarbon flux at low tide could also be linked to physical processes. As the water retreats a thin film is left covering the macroalgae. Halocarbons and hypohalous acids then diffuse into a smaller volume of seawater and higher concentrations may lead to a higher flux into the atmosphere. This is of particular relevance for I_2 , which has a limited solubility and so is likely to volatilise and flux into the atmosphere (McFiggans et al., 2004).

1.3.4 The role of inorganic iodine emissions

In recent years it has been established that macroalgae produce I_2 alongside organic iodocarbons and that I_2 may actually be the dominant iodine-containing species involved in local atmospheric chemistry processes (Saiz-Lopez & Plane, 2004). Küpper et al. (2008) demonstrated that accumulated iodide in *L. digitata* acts as an antioxidant; reacting with ROS and ozone to form inorganic iodine species. At low tides iodide on the kelp surface is in direct contact with ozone and reactions between iodide and ozone can lead to a flux of I_2 directly into the coastal atmosphere (Palmer et al., 2005). The role of I_2 in new particle formation is discussed further in Section 1.6.2.

1.3.5 Release of halocarbons into the environment as a chemical defence compound

It is also believed that halogenated compounds may act as a method of chemical defence against herbivory or other biological interactions such as epiphytism or disease. Oxidative bursts have been elicited via the addition of oligoguluronates, which are cell wall components and mimic grazing, bacterial or epiphytic damage to algal cell walls (Küpper et al., 2001). As described in Section 1.3.3, halocarbon and inorganic iodine may act as antioxidant responses to these oxidative bursts. Herbivory or simulated herbivory (wounding) has been demonstrated to increase brominating activity by up to 120% (Palmer et al., 2005) and increases in halocarbon emission have also been observed (Nightingale et al., 1995). As well as the antioxidant response, herbivory may also lead to tissue and cell wounding and a flux of internal halocarbon stores into the surrounding seawater (Bravo-Linares & Mudge, 2009).

Aside from herbivory, other biological interactions may lead to increased production and emission of halocarbons. They may be produced in response to, or as protection from, microbial activity such as bacterial infection. The red seaweed *Bonnemaisonia hamifera*, for example, produces high concentrations of halogenated metabolites, and field studies have shown it to host fewer epiphytic bacteria than other species in the same area (Nylund et al., 2008). Little is known about the role viruses have to play in halocarbon biogeochemistry. As viruses release between 10^8 and 10^9 tonnes of carbon from the global marine pool per day (Brussaard et al., 2008) their role in triggering halocarbon production or release cellular halocarbon stores may potentially be significant.

1.4 Loss processes in seawater

The major loss process for halocarbons in seawater is the air-sea flux (Section 1.5). Other loss processes in seawater include hydrolysis, dehalogenation, halogen substitution and photolysis (Quack & Wallace, 2003). After losses to the atmosphere, photolysis is thought to be the largest seawater loss process and hydrolysis the slowest. Table 3 provides an example of differences in estimates lifetimes with respect to different loss processes using CHBr_3 as a case study. These loss processes are discussed in more detail after the table.

Table 3. Lifetime of CHBr_3 with respect to several seawater loss processes

Loss process	CHBr_3 lifetime / years	Source
Flux to atmosphere	0.01 – 0.03	Helz and Hsu (1978)
Photolysis	0.4 – 1.2	Carpenter and Liss (2000)
Bacterial breakdown	nr	Goodwin et al. (1997b)
Nucleophilic substitution	5 years at 25 °C 74 years at 2 °C	Geen et al. (1992) in Quack and Wallace (2003)
Abiotic reductive dehalogenation	Observed, no data on lifetime	Bouwer et al. (1981)
Hydrolysis	30 – 50 at 25 °C 680 – 1000 at 2 – 4 °C	Quack and Wallace (2003) and Goodwin et al. (1997b)

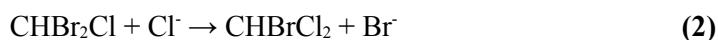
nr = not reported: Although Goodwin et al. (1997b) reported a lifetime of CH_2Br_2 relative to bacterial degradation of 0.05 years they did not observe CHBr_3 breakdown via this method. However, bacterial breakdown of CHBr_3 has been reported by Bouwer and McCarty (1983) and Bouwer et al. (1981), see section *iv* for further details.

i. Photolysis

Jones and Carpenter (2005) and Martino et al. (2005) reported photodissociation of CH_2I_2 , CH_2ClI and bromiodomethane (CH_2BrI) in seawater under natural light in the top few metres of the water column. Breakdown products included I^- and, for CH_2I_2 , CH_2XCl (where X = Cl, Br or I). Martino et al. (2005) suggest this source of iodine could contribute significantly to a marine source of atmospheric iodine for iodine oxide (IO) formation. Photolysis of CHBr_3 was considered by Carpenter and Liss (2000). They determined it to be a potentially important loss process in the top 1 m (on average – the depth penetration of light will be spatially dependent) of the water column. It is likely that photolysis is the largest internal seawater loss process of CHBr_3 , but it is still much smaller than loss via air-sea flux, equating to about 2% of the air-sea flux (Quack & Wallace, 2003).

ii. Nucleophilic substitution (chemical loss)

Bromocarbons undergo nucleophilic attack by chloride ions, for example the destruction of CHBr_3 in seawater following the steps outlined by Class & Ballschmiter (1988) in Eqs. 1-3 below. Broadly speaking it is thought that in coastal regions direct biological production of mixed bromochloro compounds is the dominant source whilst nucleophilic substitution may play a more important role in deeper oceanic waters (Carpenter & Liss, 2000; Moore & Tokarczyk, 1993).



Nucleophilic substitution of iodocarbons has also been reported, for example by Jones and Carpenter (2007) who reported the breakdown of iodocarbons, including CH_3I , via chlorination and hydrolysis. Loss rates via these processes were a function of seawater temperature as nucleophilic substitution of Cl^- increases within increasing temperatures. They predicted seawater lifetimes based on chemical destruction of 7 weeks at 15 °C and 7 days at 30 °C, faster than the respective loss rates for bromocarbons via nucleophilic substitution (Table 3).

iii. Hydrolysis

Hydrolysis of halocarbons in seawater is a slow process, the lifetime of CHBr_3 with respect to hydrolysis is thought to be between 680-1000 years at 2-4 °C and 30-50 years at 25 °C (Quack & Wallace, 2003 and references herein).

iv. Bacterial breakdown / reductive dehalogenation

Goodwin et al. (1997b, 1998) demonstrated bacterial breakdown of CH_2Br_2 in coastal seawater. Production of $^{14}\text{CO}_2$ in bacterial cultures exposed to $^{14}\text{CH}_2\text{Br}_2$ suggests the use of CH_2Br_2 as a carbon energy source. Goodwin and coworkers did not observe bacterial degradation of CHBr_3 in these experiments. However, other studies have demonstrated the breakdown of a suite of halogenated compounds, including CHBr_3 and CHBr_2Cl , by anaerobic methanogenic bacteria (Bouwer & McCarty, 1983; Bouwer et al., 1981). They also observed abiotic breakdown under sterile aerobic conditions, although this is thought to be much slower than biologically mediated reductive dehalogenation.

1.5 The sea-air flux of halocarbons

The sea to air flux (F) rate is governed by processes on both sides of the air-sea interface, commonly described by the Liss and Slater (1974) model. This model (Eq. 4) assumes that the flux rate is related to the total transfer velocities for the system (expressed from either the liquid (K_w) or gas phase (K_a)), the concentration in bulk air (C_a) and seawater (C_w), and the gas-over-liquid form of the Henry's Law constant (K_H).

$$F = K_a (C_a - K_H C_w) = K_w \left(\frac{C_a}{K_H} - C_w \right) \quad (4)$$

Fluxes of CHBr_3 and CH_2Br_2 are discussed in Chapter 6 Section 6.2. The flux of these two gases can be expressed relative to the K_w , the total transfer velocity based on the liquid phase, and so Eqs. 5 and 6 can be used to express the sea-air flux of these gases.

$$F = -K_w \Delta C \quad (5)$$

$$\Delta C = \frac{C_a}{H} - C_w \quad (6)$$

In Eqs. 5 and 6 H is the dimensionless Henry's law constant, a measure of the solubility of a gas in terms of its equilibrium between liquid and gas phases. Henry's law constants for halocarbons have been defined in several studies, e.g. Moore et al. (1995), which show good agreement (Sander, 1999). The transfer velocity, K_w , is less well quantified and the parametrisation of this factor is the largest source of error in the estimation of air-sea halocarbon fluxes (Johnson, 2010). Wind speed (u) is often considered to be the most important factor in calculating the air-sea transfer velocity and the parametrisations of Liss and Merlivat (1986) and Wanninkhof (1992) are commonly used when calculating fluxes. Temperature also plays a role, for example it affects compound diffusivity and the viscosity of the solvent (often defined by its Schmidt number, Sc) (Quack & Wallace, 2003). Errors may arise from a number of factors; wind speed parametrisations become less reliable at high wind speeds and a number of other factors also affect the flux, including wave types, bubbles, humidity gradients and surface films or surfactants (Nightingale et al., 2000). Regional and global bromocarbon fluxes have been derived from marine and atmospheric halocarbon measurements, these are discussed further in Chapter 6 Section 6.2.

1.6 Role and fate in the atmosphere

Atmospheric lifetimes for VSLS compounds discussed in this body of work were shown in Table 1. The major loss process for many of these halocarbons is photolysis and reactions with the OH radical (Krysztofiak et al., 2012; Montzka et al., 2010). Both iodo- and bromocarbons degrade in the atmosphere to form reactive species such as iodine and bromine oxides (IO and BrO), HOBr and iodine dioxide (OIO) (Mahajan et al., 2010; Saiz-Lopez and Plane, 2004; Tuckermann et al., 1997). These reactive species are very short lived and during daylight halogen atoms cycle between these reactive forms (see Eqs. 14-16, for example). In particular, Br[•] and I[•] are very short-lived intermediaries, for example only around 1% bromine in the atmosphere at any one time will be Br[•] (Monks, 2005).

Iodine and its degradation products are very short lived (lifetimes on the order of hours to days) and so have a localised impact on tropospheric chemistry (Section 1.6.3) and new particle formation (Section 1.6.2). They do play a global role in biogeochemical cycling of iodine, as discussed in Section 1.6.1. CHBr₃ and its degradation products not only impact local tropospheric chemistry (Section 1.6.3) but are also thought to have stratospheric impacts (Section 1.6.4).

1.6.1 Global biogeochemical cycles and human health.

Iodine deficiency can lead to growth and developmental problems in both humans and animals, including; thyroid problems (hypothyroidism), mental retardation, goitre and problems during pregnancy (de Benoist et al., 2004; Hetzel & Mano, 1989). On a local scale a study by Smyth et al. (2011) found that I₂ emissions from seaweeds may supply a significant fraction of the daily iodine intake of people living near the sea. Globally, marine sources of iodine are also important. The sea-to-air flux of iodine is a major component in global geochemical iodine cycling and marine sources of iodine are likely to be the largest contributor to atmospheric iodine that can be deposited in otherwise iodine-limited terrestrial environments (Fuge & Johnson, 1986; Whitehead, 1984).

1.6.2 New particle formation

Iodocarbons undergo rapid photolysis (e.g. Martino et al., 2005) and therefore have a short lifetime both in the upper water column and in the atmosphere (Bravo-Linares & Mudge, 2009; Donner et al., 2007). For this reason they contribute mainly to local atmospheric chemistry; providing a source for new particle formation in the coastal boundary layer. Iodocarbon and I_2 pulses from exposed macroalgae at low tide have been linked to measured increases in particle bursts, for example during the PARFORCE (New Particle Formation and Fate in the Coastal Environment) campaign at Mace Head, Ireland (Mäkelä et al., 2002; O'Dowd et al., 2002a, 2002b). It was originally thought that these particle bursts could have been due to fluxes of sulphur-containing compounds and the production of sulphuric acid, H_2SO_4 . However, field studies have shown that H_2SO_4 concentrations do not correlate as well as iodinated compounds with the observed tidal cycles and particle bursts (Greenberg et al., 2005). Examination of the chemical composition of these particles has also shown them to contain iodine (Mäkelä et al., 2002).

Particle bursts are believed to occur at low tide via the following sequence of events. Firstly, I_2 and iodocarbons are released from macroalgae at low tide (Sections 1.3.3 and 1.3.4). Iodocarbons and I_2 are then photolysed in the atmosphere and reactive iodine is produced. Whilst CH_3I is commonly the dominant iodocarbon in the marine boundary layer (MBL), more reactive but less abundant iodocarbons, such as CH_2I_2 and CH_2ClI , may contribute as much iodine as CH_3I (Saiz-Lopez et al., 2012 and references herein). A study by Jones et al. (2010) in the Atlantic Ocean found that the contribution of dihalomethanes (CH_2I_2 , CH_2ClI and CH_2BrI) to regional MBL iodine concentrations could be 3-4 times greater than the CH_3I contribution. However, this study also found that iodocarbon fluxes could not support observed IO levels, emphasising the potential importance of an abiotic source (Section 1.2.2).

Iodine quickly reacts with ozone to form IO. Further gas phase self-reactions, or reactions with the perhydroxyl radical (HO_2), OH and nitrogen dioxide (NO_2) form a range of condensable iodine vapours such as HOI, OIO and I_2O_2 (Grose et al., 2007; O'Dowd et al., 2002a). These products then go on to condense onto existing supercritical embryos, allowing rapid growth and an increase in their atmospheric lifetime which leads to a burst of ultra fine particles (McFiggans et al., 2004). 'Hot spots' of iodine oxides and particle bursts have been identified directly over macroalgae beds (Commane et al., 2011; Seitz et al., 2010), suggesting the impact of macroalgae-produced iodine on particle formation may be significant but localised. These particles may then provide condensation nuclei for other condensable vapours, potentially growing to the point of cloud condensation nuclei (CCN) (Saunders & Plane, 2005). Changes to CCN may then change the lifetime and albedo of clouds and impact the radiative balance of the earth system (Saiz-Lopez et al., 2012 and references herein).

Not all macroalgae species can impact local particle formation in this manner. *L. digitata*, accumulates and releases a large quantity of iodine, especially in the form of I_2 . Particle formation has been observed over exposed beds of *L. digitata*, for example during the aforementioned PARFORCE campaign. However, levels of CH_3I , IO and OIO over beds of another kelp, *Durvillaea potatorum*, are low and it is likely that it has little impact on coastal particle formation (Cainey et al., 2007). Flux chamber studies by Ball et al. (2010) also demonstrated substantial differences between phaeophyte species; again high I_2 emissions were observed from *L. digitata* whilst little, if any, I_2 was observed for several *Fucus* species.

Chamber studies have been used to investigate I_2 emissions during exposure (e.g. Ashu-Ayem et al., 2012; Ball et al., 2010; McFiggans et al., 2004). These are discussed in more detail in Chapter 4.

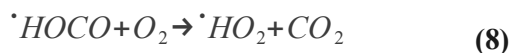
1.6.3 Halocarbons and their impact on tropospheric chemistry, in particular ozone chemistry

In all equations below X may be replaced with either Cl or Br.

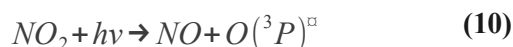
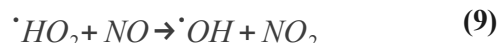
i. Tropospheric ozone chemistry

Tropospheric ozone is important with regards to human health, crop viability, general air quality (as an important constituent in photochemical smog) and is a greenhouse gas (Seinfeld & Pandis, 1997). To understand the role of halocarbons in ozone chemistry we first need to consider its production (Eqs. 7-11) and destruction (Eqs. 12-13) (Reeves et al., 2002).

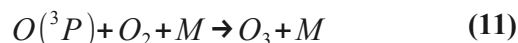
Formation of $\cdot\text{HO}_2$ via oxidation of carbon compounds with $\cdot\text{OH}$. Here carbon monoxide (CO) is given as an example, but many volatile organic compounds (VOCs) also play a role in ozone formation.



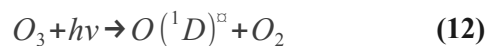
Formation of atomic oxygen via reactions between the $\cdot\text{HO}_2$ and NO_x ($\text{NO}_x = \text{NO}$ and NO_2).



Formation of ozone via reactions between molecular and atomic oxygen. M represents a third body which absorbs the excess energy from this reaction as heat. Commonly N_2 or O_2 , M may also represent particles or trace gases.



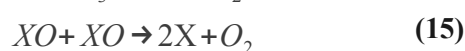
Loss via photolysis in the presence of water vapour. This is the major atmospheric chemical loss process, although ozone is also lost via deposition to the surface.



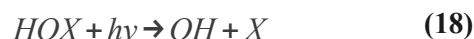
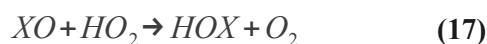
□ In these equations the bracketed oxygen suffix refers to the electron state of the oxygen atom. $\text{O}(^3\text{P})$ or “triplet P” is the ground state of atomic oxygen, here the oxygen atom has 2 unpaired electrons. $\text{O}(^1\text{D})$ or “singlet D” is the first excited state of atomic oxygen.

The balance between production and loss processes (Eqs. 7-13) determines whether a region is a source or a sink. The MBL may act as an important sink due to a lack of NO_x sources (transport and industry are major sources) and a high humidity (Read et al., 2008). The prevalence of halogen oxides is also thought to play an important role. Bromo- and iodocarbons released in the MBL are oxidised to form halogen oxides (XO , where $\text{XO} = \text{IO}$ or BrO). Halogen oxides can impact tropospheric ozone chemistry via a number of processes:

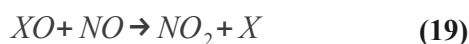
1. Catalytic ozone destruction via halogen oxidation and halogen oxide self reactions (Eqs. 14-16) (Read et al., 2008).



2. Perturbation of the HO_2/OH ratio (Eqs. 17 and 18) which suppresses ozone formation by impacting Eqs. 7-10. (Von Glasow et al., 2004).



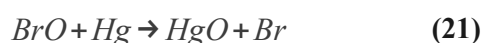
3. Suppression of NO_x due to reactions with halogen nitrates (Sander et al., 1999). It should be noted that halogen oxides also decrease the NO/NO_2 ratio via Eq. 19. However the production of X during this reaction means this process is unlikely to lead to increased ozone production (Platt and Hönninger, 2003; Read et al., 2008).



ii. Other tropospheric chemistry processes

As OH radicals are often involved in removal of greenhouse gases and other pollutants from the atmosphere (Tang et al., 1998) reactions between halogen oxides and HO₂, as described in the previous section, may also impact these processes.

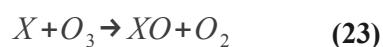
BrO is also thought to affect atmospheric processing of dimethyl sulphide (DMS) (von Glasow & Crutzen, 2004). DMS is a climatically important gas that plays a role in marine aerosol and CCN formation and potentially planetary albedo and climate regulation. In polar regions BrO is also thought to be involved in mercury chemistry. Observations of ozone loss and simultaneous depletion of mercury have been linked to bromine. Processes are thought to include Eqs. 20-22 which show the oxidation of bromine to form BrO (Eq. 20) which is then involved in the oxidation of mercury (Eqs. 21 and 22) (Goodsite et al., 2004). Mercury products from these reactions are more likely to undergo deposition, increasing the amount of mercury in the snow pack and also, potentially, the amount of bio-available mercury (Brooks et al., 2006).

**1.6.4 Halocarbons and stratospheric ozone**

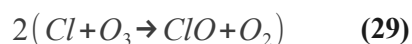
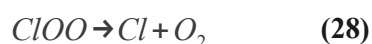
Biogenic bromocarbons have short atmospheric lifetimes (Table 1) as they are susceptible to chemical destruction or wash out in the troposphere. Despite this, studies suggest that they do provide reactive bromine species (Br_y) to the stratosphere via direct source gas (SG) injection or via their breakdown product gases (PG). Stratospheric balloon-borne measurements have reported an excess of Br_y above the known anthropogenic input (Dorf et al., 2006; Salawitch, 2006; Salawitch et al., 2005). These measurements have been supported by similar results from chemical transport model studies (e.g. Hossaini et al., 2012b). The latest estimations, based on both observations and model studies, suggest a total contribution of VSLS to stratospheric bromine of 6 (1-8) ppt (Montzka et al., 2010), a substantial amount compared to the total stratospheric Br_y abundance of around 20-25 ppt (Dorf et al., 2008; Yang et al., 2005).

Once in the stratosphere, halogens catalyse ozone loss via several destruction cycles. In low and mid latitudes Cycle 1 dominates (Eqs. 23-25). In polar regions less solar radiation is available for the production of atomic oxygen from ozone and O_2 , and there is also a greater abundance of ClO, therefore Cycles 2 and 3 dominate (Fahey & Hegglin, 2010; Newman & Pyle, 2002). All three cycles require sunlight. In polar regions this is demonstrated by an increase in ozone loss during the spring, when sunlight activates ClO which has formed on the surface of polar stratospheric clouds (PSCs) during the polar winter (Farman et al., 1985), hence the excess ClO driving cycles 2 and 3 in this region. These cycles are catalytic, and so one halogen atom may catalyse the destruction of many ozone molecules before it is lost from the stratosphere.

Cycle 1:

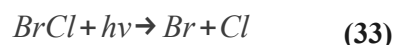
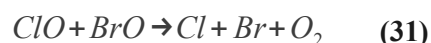


Cycle 2:



Cycle 3:

ClO may also react with BrO either via Eq. 31 or Eqs. 32 and 33. Br and Cl then react with ozone as Eqs. 23 and 24. (Bloss et al., 2001; Chipperfield & Pyle, 1998)



Stratospheric bromine inputs are less than those for chlorine, but Br_y species have a higher ozone depleting potential. One reason for this is that processes which remove halides from forms where they can destroy ozone, e.g. the production of HX and XONO₂, are less effective for bromine as BrX and BrONO₂ are less stable than their chlorine equivalents (Daniel et al., 1999).

The stratospheric ozone layer provides protection for plants and animals from harmful UV light (U.S. E.P.A, 2006). Natural ozone cycling was disrupted by the addition of anthropogenic chlorine-containing compounds, such as CFCs (as discussed in the opening paragraph of this chapter), leading to an enhanced loss of stratospheric ozone. The contribution of anthropogenic chlorine and bromine to stratospheric halogen loading is now controlled by the Montreal Protocol, and many of these anthropogenic source gases have stabilising or decreasing atmospheric concentrations (Montzka et al., 2010). Potential future effects of VSLs are discussed in Section 1.8.

1.7 The importance of tropical coastal halocarbon emissions

Due to their short atmospheric lifetime and biogenic sources VSLs have a patchy global distribution. Extensive field measurements have identified regions that are important in terms of global emissions. The tropics, in particular tropical coastlines, are thought to be important in terms of halocarbon sources, chemistry and stratospheric impact.

1.7.1 The coastal zone: An important halocarbon source region

Globally, coastlines have been shown to be an important halocarbon source region, this is largely thought to be due to macroalgae beds found in coastal regions (e.g. Carpenter et al., 1999; Ekdahl et al., 1998; Manley & Dastoor, 1987) although high bromocarbon concentrations have also been reported in coastal regions where there is little or no macroalgae, such as Cape Verde (O'Brien et al., 2009). High coastal and shelf seawater bromocarbon concentrations have been reported from several research cruises (e.g. Butler et al., 2007; Carpenter et al., 2009). A review by Quack and Wallace (2003) attributed 29% of global CHBr_3 emissions to open ocean waters, 48% to shelf waters and 23% to coastal waters. Another region where high halocarbon concentrations have been observed is upwelling regions, with elevated concentrations potentially linked to increased biological productivity. However the biological and physical processes that contribute to halocarbon sources and sinks in these regions are not fully understood, and from the data available it is thought that they are unlikely to contribute significantly to global halocarbon budgets (Carpenter et al., 2009; Quack & Wallace, 2003; Quack et al., 2007). Upwelling regions are not considered further within the remit of this work.

With respect to the tropics, Butler et al. (2007) assimilated data from several research cruises and estimated that the tropics contribute two thirds of open ocean CHBr_3 emissions. Other meridional transect surveys have shown similar peaks in halocarbon production in tropical waters (Quack & Wallace, 2003 and references herein). Tropical coastlines have also been highlighted as potentially strong source regions; for example Yokouchi et al. (2005) measured CHBr_3 mixing ratios up to 40 ppt near tropical island coastlines. Measurements of CH_3I also suggest the tropical ocean is a year-round source of this compound, compared to higher latitude waters which may sometimes act as a sink (Happell & Wallace, 1996). Chapter 5 Section 5.3.3 includes more detail, including a table comparing open ocean and coastal data for CH_2Br_2 , CHBr_3 and CH_3I , with particular focus on tropical regions. Chapter 6 (in particular, Table 2) also includes a comparison of calculated fluxes and annual emissions from several studies.

1.7.2 Tropical deep convection

In tropical regions areas of deep convection can transport halocarbons and their product gases from the MBL to the tropical tropopause layer (TTL) within a few hours, quicker than the atmospheric turnover of these compounds (Krysztofiak et al., 2012). Once in the TTL the likelihood of washout occurring is greatly reduced and these compounds may be transported into the stratosphere, making the tropics an important source region for VSLs contributions to stratospheric bromine (Montzka et al., 2010). In particular the tropical West Pacific is proposed as a strong source region, potentially accounting for 55% of the bromine from CHBr_3 transported to the stratosphere (Aschmann et al., 2009). This region is discussed in Chapters 5 and 6. Model studies focusing on the tropics suggest that deep convective regions may lead to up to 28% of surface CHBr_3 and up to 70% of surface CH_2Br_2 reaching the TTL (Gettelman et al., 2009). Another model study by Hossaini et al. (2010) suggests potential contributions from SGs and PGs; with 2.7 ppt of stratospheric bromine from direct SG injection of VSLs and 0.4-1.7 ppt of stratospheric bromine from PG injection. The PG contribution is harder to determine due to a lack of above-detection limit observations and a high solubility of many PGs leading to a variable atmospheric lifetime that is highly dependent on their location (Montzka et al., 2010).

1.7.3 Tropical macroalgae

Aquaculture is an important global industry with macroalgae produced for consumption and a wide range of products, including: phycocolloids, agar, carrageenans and alginates (Ask & Azanza, 2002). Aquaculture is commercially important, in 2006 the industry was worth about US\$7.2 billion (FAO, 2008). Currently, about 97% of Asian seaweed production is monoculture crops (where one species is farmed intensively) and this type of aquaculture is a fast growing global farming sector, with increases of around 8% per year (Bouwman et al., 2011; Buck & Buchholz, 2004; Chopin et al., 2001). Growth is driven by numerous factors, including the use of macroalgae as a biofuel and for carbon sequestration (Kheshgi et al., 2000; Singh et al., 2011). Compared to terrestrial biofuels, macroalgae do not compete with food crops for space or require intensive water inputs whilst providing high productivity and, in some cases, year round biomass with low cost harvesting procedures (Aresta et al., 2005). Macroalgae may also be utilised in integrated aquaculture. Here they remove waste nutrients and reduce the environmental impact of fish and shellfish fisheries (Neori, 2007). Further details on tropical aquaculture in Malaysia and south east Asia are provided in Chapter 6 Section 6.2.

Aquaculture may impact regional halocarbon emissions in several ways. Firstly an increase in the volume of halocarbon sources (macroalgae) is likely to increase halocarbon emissions. In the South East Asian region rhodophyte genera such as *Kappaphycus*, *Eucheuma*, *Gracilaria* and *Gelidium* are commonly farmed (Zemke-White & Ohno, 1999). These species have not been quantified in terms of their halocarbon production rates. In addition, farming practices could exacerbate halocarbon production from macroalgae. Aquaculture macroalgae are more likely to suffer from epiphytism, wounding, grazing and disease (Ask & Azanza, 2002). As discussed in Sections 1.3.3 and 1.3.5, halocarbon release may increase in response to these processes, either via an oxidative stress response or due to production as a grazing or epiphyte deterrent.

Harvested seaweeds are generally 'dewatered' (dried) before processing, especially in tropical regions where there is adequate heat and sunlight to enable drying before the algae rots. Even in commercial aquaculture processes this still involves spreading the seaweed out in the sun to dry for several days (Phang et al., 2006). As Section 1.6.2 showed, the flux of halogenated compounds during tidal exposure of temperate macroalgae has been the focus of numerous studies. However, the effects of longer exposure periods on halocarbon production is less well understood. Desiccation is discussed further in Chapter 4.

1.7.4 Knowledge gaps and the need for regional measurements

Despite the potential importance of the tropics with regards to global halocarbon budgets fewer measurements have been made in this region. In situ measurements are important as many processes involved in halocarbon production, transport and destruction cannot be extrapolated between regions. Seawater temperature, for example, is an important factor in loss process reaction rates. For example, hydrolysis and nucleophilic substitution rates are faster in warmer waters (Jones & Carpenter, 2007; Moore & Groszko, 1999).

Biological production of halocarbons can also vary between regions. As previous temperate and polar research has consistently shown large variations in emissions both between and within macroalgal species, species-specific measurements in different geographical regions are needed. Different macroalgal species are found in different climatic regions, which could lead to differences in halocarbon production and emission rates. The ratio of rhodophytes relative to phaeophytes and chlorophytes is also greater in the tropics (Santelices et al., 2009), and kelps are only found in deeper waters (Graham et al., 2007) where they are less likely to contribute to particle formation. Aquaculture is common in the tropics, and is set to increase (Section 1.7.3). Seaweed farms perturb the natural diversity and biomass of certain macroalgal species, potentially altering halocarbon emissions. Environmental conditions also vary, for example the occurrence and rate of herbivory is believed to be greater in the tropics (Cronin et al., 1997).

1.8 Halocarbons in a changing world

Current VSLS emissions make a “small but non-negligible” impact on stratospheric ozone chemistry (Montzka et al., 2010), but future climate change could alter this contribution. Changes to sea surface temperature, salinity, wind speed, mixed layer depth, pH and nutrients may all affect both biological halocarbon production (Section 1.3.3) and/or the sea-air flux of these halocarbons (Section 1.5) (Bravo-Linares & Mudge, 2009; Hense & Quack, 2009).

Atmospheric transport may also change with a changing climate, as demonstrated by chemistry-climate model studies. Dessens et al. (2009) demonstrated moderate increases in bromine in the TTL in a warmer world due to strong convection, leading to a 1-2 ppt increase in stratospheric bromine. A subsequent study by Hossaini et al. (2012a) reported increases in SG injection of VSLS of 0.3-1 ppt, depending on which climate change scenario was used. They attributed this increase to changes in tropical deep convection and OH chemistry. They did not take into account changes in biological productivity, which may change in a warmer climate, or the potential effect of changing sea surface temperatures and mixed layer depth on the sea-to-air halocarbon flux (Hense & Quack, 2009).

1.9 Key research questions and thesis structure

With the aim of building upon the current knowledge base, as described in this chapter, this thesis will focus on the following overarching aim:

**Improving our understanding of halocarbon production
in tropical and temperate coastal zones.**

Figure 1 outlines the research aims and objectives for each research chapter (3-5) as well as links between these chapters that help bring together the individual research strands. Chapter 6 brings together information from all chapters to discuss the current and projected future contribution of natural and farmed macroalgae to Malaysian and south east Asian halocarbon emissions.

Each chapter includes its own methodology section as each chapter involves different measurement and analytical techniques. An overview of methodological techniques used is provided in Chapter 2, alongside a description of two method development activities carried out during this research.

	Chapter 3 Halocarbon production by tropical macroalgae	Chapter 4 Halocarbon production during desiccation	Chapter 5 Halocarbon distributions around Malaysia
Aims:	Improve our knowledge of tropical macroalgae as halocarbon sources.	Improve our knowledge of the role exposure and desiccation plays in halocarbon emissions from macroalgae.	Study regional (Malaysian) tropical halocarbon distributions with a focus on the coastal region
Objectives:	Conduct incubations of 15 tropical macroalgae species (including red, brown and green algae) from a variety of habitats.	Desiccate temperate macroalgae under controlled laboratory conditions to investigate bromocarbon production during desiccation.	Combine observed atmospheric halocarbon concentrations from several field campaigns to study halocarbon distributions around Malaysia.
	Include incubations of farmed macroalgae.	Measure changes in photosynthetic capacity and water loss as the macroalgae dries to provide more information on the links between bromocarbon production and physiological stress.	Investigate differences in halocarbon concentrations in different regions using back trajectories.
	Compare calculated production rates with those reported for temperate and polar species.		
	Chapter 6 Draw conclusions from chapters 3-5. Use data from these chapters to estimate annual regional bromocarbon emissions from macroalgae, both farmed and natural, and discuss how this may change in the future.		

Figure 1. Thesis outline.

CHAPTER 2

A methodology overview and method development

2.1 Introduction

Throughout this thesis several analytical methods will be used to determine picomolar (10^{12}) concentrations of halocarbons in seawater and air samples. All these methods follow the same basic principles; a sample is collected, analytes of interest are removed from the bulk sample via pre-concentration, they are separated using gas chromatography (GC) and then identified and quantified via mass spectrometry (MS). Fig. 1 provides an overview of the methods used in each chapter to allow a comparison of the different techniques used for each strand of research. Individual experimental designs and nuances are discussed in their respective chapters, alongside relevant system characterisations such as detection limits and precision.

This chapter will also discuss two other method development activities that were conducted during the experimental activities discussed in this thesis. Section 2.2 covers the effect of storing seawater samples on observed halocarbon concentrations. Section 2.3 provides further information on the flux chamber used to provide some data for Chapter 4.

	Sample collection & storage	Analyte extraction & preconcentration	GCMS	Calibration
Chapter 3	Samples collected immediately prior to analysis. No sample storage. Chap. 2 Section 2.2	UEA built Purge & trap (P&T) system. Chap. 3 Section 3.2.4	Agilent 6890 GC with 60 m DB-VRX column. Agilent 5975 MS in electron impact (EI) single ion mode (SIM).	Calibration via multi-point calibration of aqueous standard. Chap. 3 Section 3.2.6
Chapter 4	Air samples collected onto sorbent tubes. Max. storage time 1 week at -18 °C. Chap. 4 Section 4.2.3	Commercial Markes ULTRA™ and UNITY™ system. Chap. 4 Section 4.2.4	Chap. 3 Section 3.2.5	SX074 air standard trapped onto sorbent tubes. Chap. 4 Section 4.2.4 Chap. 5 Section 5.2.6
	Air samples collected from flux chambers into canisters. Chap. 4 Section 4.2.7	A Markes Air Server™ allowed the connection of up to 6 canister samples to a Markes UNITY™.	Agilent 6890 GC with a 105 m Rtx 502.2 column. Agilent 5973 MS run in chemical ionization (CI) SIM.	Jana air standard. Chap. 5 Section 5.2.6
Chapter 5	Ambient canister air samples. Chap. 5 Section 5.2.3	Chap. 5 Section 5.2.4	Chap. 5 Section 5.2.4	SX074 air standard. Chap. 5 Section 5.2.6

Figure 1. An overview of the key stages in the analysis of seawater and air samples for halocarbon concentrations and a comparison of different techniques used for each chapter.

2.2 The effects of storage on seawater samples

Seawater is a complex sample matrix: various biologically (e.g. production by plankton), chemically (e.g. nucleophilic substitution) or physically (e.g. photolytic breakdown) mediated changes to halocarbon concentrations may occur in samples collected in the field, altering concentrations prior to analysis. Several methods are used to 'fix' seawater samples, that is, to halt biological activity so concentrations of biologically-affected compounds remain the same as they were upon collection. Common methods include treatment with mercuric chloride to poison the sample or filtration to remove microorganisms. The use of mercuric chloride as an effective method for preserving halocarbon samples has not been demonstrated. The use of filtration has three main issues; firstly the analysis of volatile halocarbons in seawater requires the need to keep a sample isolated from air between collection and analysis. Filtration must therefore be done with care to prevent ingress of air. Secondly, filtration may not be 100% effective at removing all biological activity (some bacteria, for example, may still be present). As described in Chapter 1 Sections 1.2.2 and 1.4 bacteria may mediate both halocarbon production and loss. Thirdly, filtration (as well as the use of poisons) may damage the cells causing a flux of halocarbons into the seawater. Little is known, or published, regarding these methods for storing seawater. For this reason, seawater measurements are usually measured as soon as possible, necessitating the transportation of analytical equipment (e.g. GCMS) into the field. This is a costly process, and, as demonstrated in Chapter 5 Section 5.4, may limit our ability to collect data in certain regions. An alternative is the use of sorbent tubes (see Hughes et al., 2012). With this technique halocarbons are purged from the seawater and trapped onto sorbent tubes (similar to those used for air samples in Chapter 4). However, this technique still requires compressed gases for purging and the facilities to keep tubes cooled during storage and transport. The use of tubes for the analysis of all halocarbons is also untested, for example problems with CH₃I storage on tubes has been identified in our laboratory.

With this in mind, a series of experiments were conducted at UEA on natural seawater taken from an aquarium containing temperate seaweeds. Four experiments were conducted:

- **E1 & E2:** Seawater samples were collected in amber bottles with ground glass stoppers by first rinsing the bottle in the seawater then filling via immersion until the bottle overflowed and adding the stopper to remove any remaining air from the sample. Samples were not filtered. Bottles were stored in the dark at 15 °C. E1 was conducted first followed the next day by E2.
- **E3:** Seawater samples were collected into 100 ml gas-tight glass syringes (ground glass barrel, Luer lock closure) via Tygon and ¼ inch diameter PFA tubing and then filtered into a second syringe via a GF/F filter (see Chapter 3 Section 3.2.4). Samples were stored in the dark at 4 °C.
- **E4:** Sampling as E3 but samples stored in the dark at 15 °C.

The results of these experiments (Figs. 2 and 3) were variable. In some instances little or no change was observed, (e.g. CH₃I and CH₂ClI in all 4 experiments). For other compounds changes in measured concentration were observed. For example, CHBr₂Cl, CHBr₃ and CH₂I₂ increased in E1 but not E2, despite the use of identical experimental protocols. Filtering into syringes which were then stored at 15 °C still resulted in increasing concentrations of CHBr₃ and CH₂I₂. However, this change was not seen in filtered samples stored at 4 °C. The results of these, preliminary, experiments suggest that whilst filtering and chilling helps to reduce changes in halocarbon concentrations further work would be needed to provide a method that provides a fully consistent response between experiments. Based on these results seawater samples taken from incubation experiments in Chapter 3 were analysed immediately to reduce the chance of changes occurring between sampling and analysis.

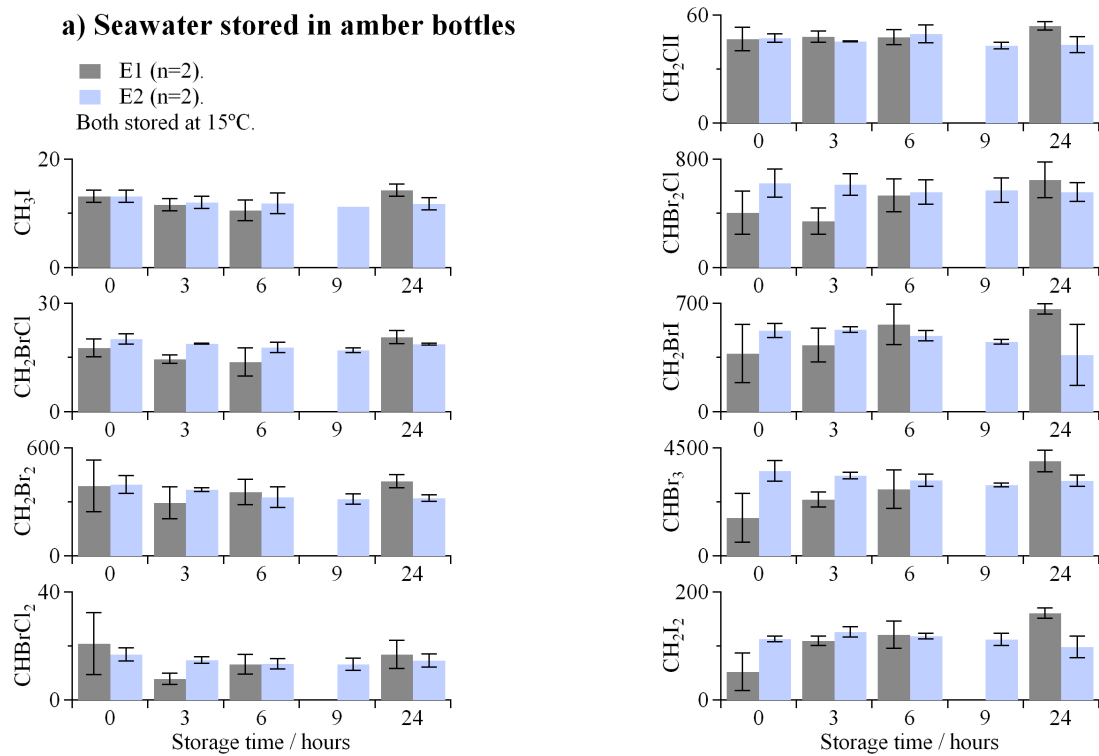


Figure 2. Changes in halocarbon concentration (pmol l⁻¹) during E1 and E2; storage of seawater in amber ground glass-stoppered bottles. Error bars are the range of duplicate sample measurements. Original in colour.

b) Seawater stored in glass syringes

- E3. Syringes stored at 4°C (n=2).
- E4. Syringes stored at 15°C (n=2).

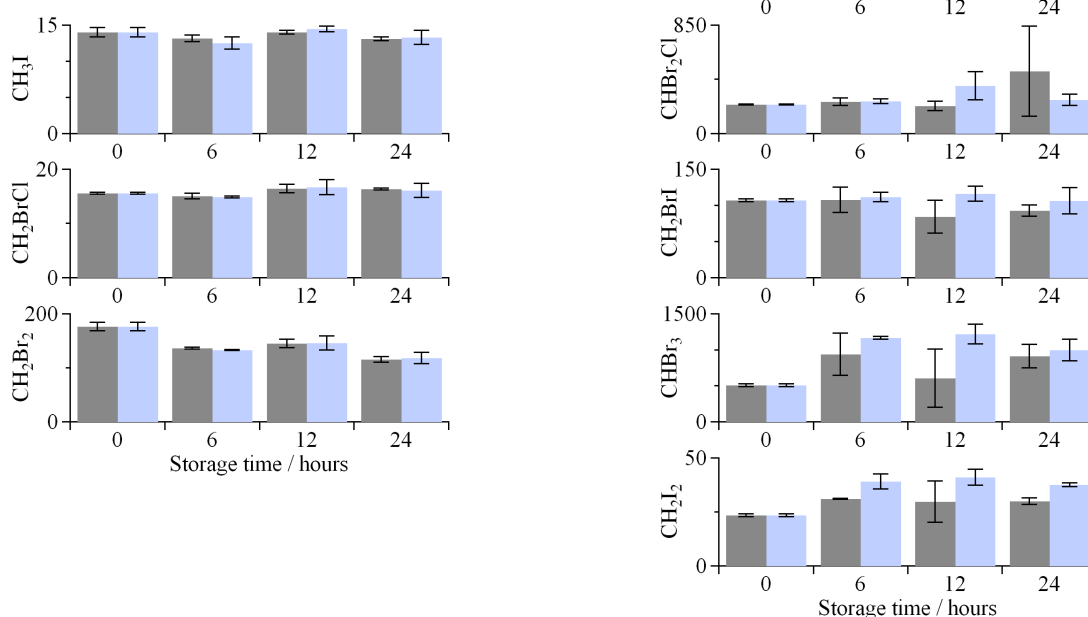


Figure 3. Changes in halocarbon concentration (pmol l⁻¹) during E3 and E4, storage of seawater in 100 ml glass syringes. Error bars are the range of duplicate sample measurements. Original in colour.

2.3 Flux chambers

To provide data on halocarbon emissions from exposed macroalgae canister samples were taken from a flux chamber (Chapter 4 Section 4.2.7). The flux chamber (Fig. 4) comprised a 35 l polypropylene (PP) storage box (Really Useful Boxes®, www.reallyusefulproducts.co.uk) measuring 370 x 310 x 280 mm (internal diameter) with two Swagelok ports fitted half way up the side of each box, one on each end. Ports were sealed during equilibration time (30 minutes) and connected to a canister and pump for sampling. In 2011 the chambers were modified by the addition of a small, battery powered hand-held fan to the inside top of the chamber to assist with the circulation of air inside the chamber and the achievement of equilibrium between sample/substrate and the atmosphere inside the chamber. Whilst we could not determine if equilibrium had been reached within our 30 minute flux chamber coverage time, maintaining a constant time allows for relative comparisons between chamber results, as described in Sartin et al. (2001)

Flux chambers were sealed over our target areas for 30 minutes before a sample was taken, a time also used by Sartin et al. (2001; 2002). It was hoped this would provide a balance between allowing a measurable concentration of halocarbons to flux into the chamber headspace without causing too large an increase in temperature within the chamber. Temperature increases within flux chambers of up to +15 °C have been reported (Dimmer et al., 2001) over a variety of (sometimes unspecified) time scales. We measured the increase in temperature within the flux chamber compared to ambient air on 8 occasions, covering different sites and meteorological conditions. The mean temperature increase was +4.1 °C and increases ranged from +0.9 °C to +7.9 °C.



Figure 4. Flux chambers. Swagelok sample port and battery-powered fans are visible. Whenever possible mud/sand was banked around the sides of the chamber to help seal the box.

Due to recent interest in the effect of UV on chamber results investigating methane (CH₄) fluxes from terrestrial plants (Beerling et al., 2008; Bloom et al., 2010) we tested the impact of our chamber material on both UV and visible light spectra. A Macam SR9910 UV spectroradiometer (Macam Photometrics Ltd.) was used to test the UV spectra beneath the flux chamber and several other materials. A Biospherical Instruments Inc. light meter model QSL-2102 was used to perform the same task for photosynthetically active radiation (PAR, 400-700 nm). Both light meters were set up in a UV light bench (constructed in-house) containing UVA (Q-Panel lab UVA-340, 40 W) and UVB (Q-Panel lab UVB-313, 40 W) lamps. The bench also delivered PAR (400-700 nm) via cool fluorescent bulbs (Philips Master TLD Reflex, 840 Cool White, 58 W). The spectroradiometer was set to scan through wavelengths between 280 and 400 nm.

The list of materials tested is displayed in Table 1. Three scans were conducted for each material, the mean value for these three scans (demonstrating the ability of these materials to transmit UV) are shown in Fig. 5 (UVB, 280-314 nm) and Fig. 6 (UVA, 315-400 nm). Standard deviation did not exceed ± 0.01 for any triplicate groups. Both figures show the same results. UV levels were highest inside Tedlar, glass and quartz containers, and lowest under acrylic. Polyethylene terephthalate (PET) and PP plastics displayed a range of transparency to UV, potentially linked to thickness. For example, PP transmitted more when a thin tuppaware box was used compared to the flux chamber whose walls were roughly double the thickness. The acrylic box, which showed the lowest transmission of UV, was also the thickest material.

The effect of these materials on blocking visible light was also investigated (Fig. 7) under both natural light (Panel a) and the same light bench as used for the UV experiments (Panel b). Again, acrylic showed the greatest reduction in light levels, with most other materials transmitting a significant percentage of ambient light. A small decrease in light levels was observed under the flux chamber when it was placed in natural (UEA roof) light conditions (Fig. 7, Panel a).

The choice of a PP box provided a low-cost chamber that was easily available and also light-weight and rugged for ease of use in the field. The results of these tests demonstrated that the selected PP flux chamber reduced the quantity of visible and UV light available inside the chamber by ~25% and ~33% respectively. However, the results provide reassurance that the chamber had little effect on the spectral distribution of light. Both visible and UV light was transmitted into the chamber allowing for semi-natural conditions to be experienced by samples within.

Table 1. Materials tested for ability to transmit UV and visible light.

Material	Source	Thickness
Thick PP	Flux chamber (used in Chapter 4)	4 mm
Thin PP	Plastic tuppaware (kitchen use)	2 mm
PET	Plastic water bottles, two brands	~1.5 mm
Acrylic	Box built for lab use	6 mm
Tedlar	Tedlar sampling bag (SKC Inc., USA)	<1 mm
Glass	Erlenmeyer flask	2 mm
Quartz	Erlenmeyer flask	2 mm

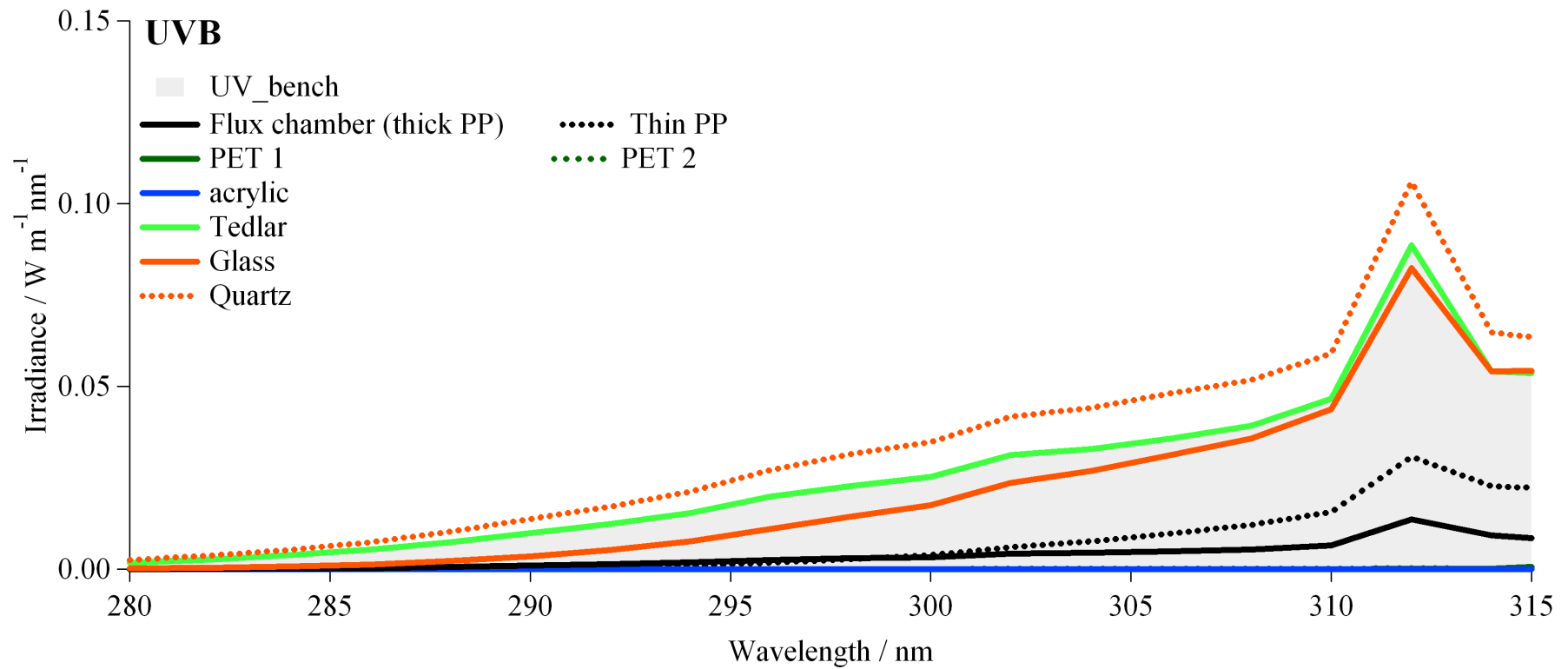


Figure 5. UVB transmission through possible flux chamber materials (Table 1). Measurements were taken under a light bench providing a constant UV and visible light source as described in the main body of the text. Original in colour.

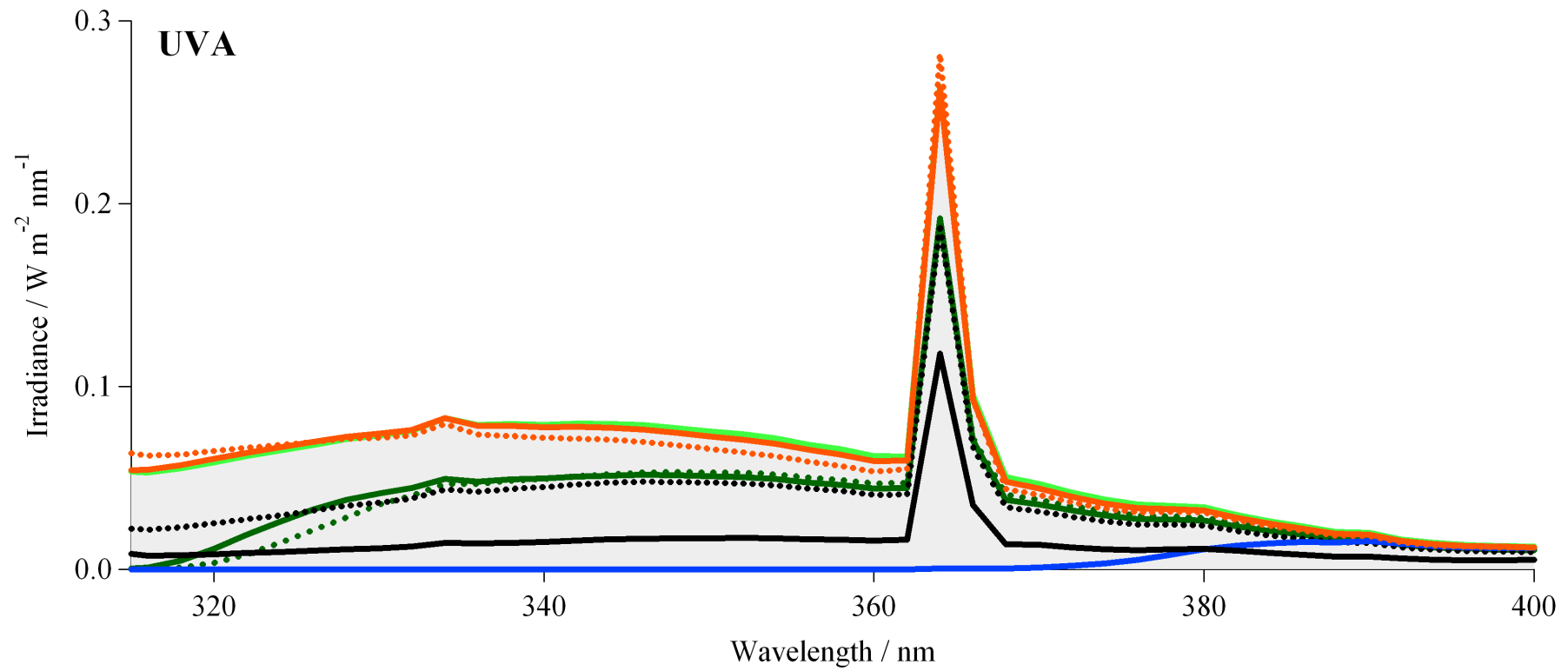


Figure 6. UVA transmission through possible flux chamber materials (Table 1). Measurements were taken under a light bench providing a constant UV and visible light source as described in the main body of the text. Original in colour.

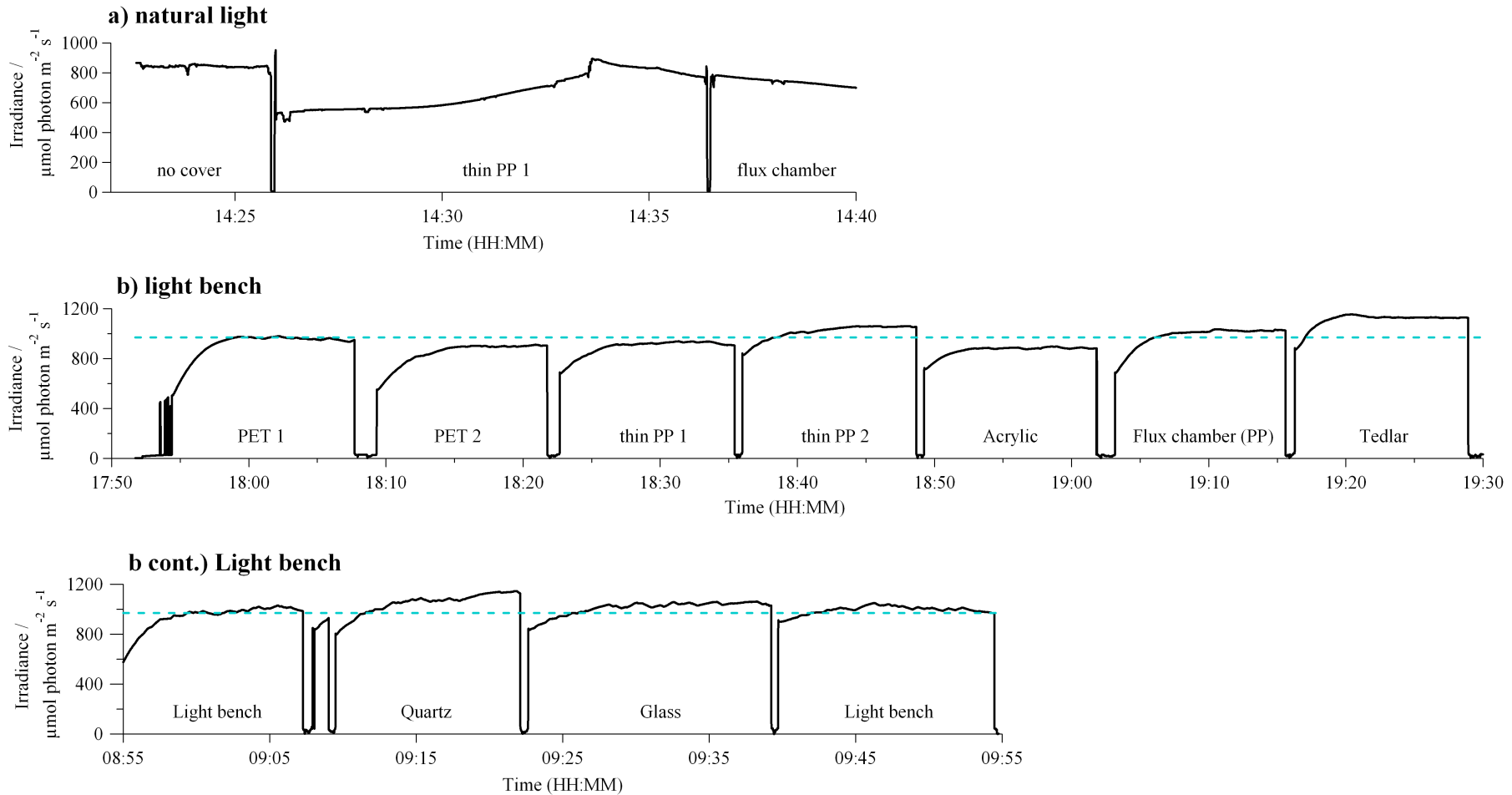


Figure 7. Transmission of visible light through potential flux chamber materials investigated (a) on the UEA roof and (b) under a light bench. Blue dashed lines in (b) represent the mean light level within the light bench.

CHAPTER 3

Halocarbon production by tropical macroalgae

3.1 Introduction

As described in Chapter 1 Sections 1.2 and 1.3, a number of incubation studies have investigated the production and emission of methyl halides and polyhalogenated compounds from polar and temperate macroalgae (Baker et al., 2001; Carpenter et al., 2000; Goodwin et al., 1997a; Gschwend et al., 1985; Laturmus, 1995; Manley & Dastoor, 1988; Marshall et al., 1999). Such studies have helped to quantify the production of halocarbons by macroalgae and develop our understanding of the complexity and variability involved in these biogenic processes. The broad suite of halogenated compounds found in, and released from, algae are thought to act as a defence mechanism (Chapter 1, Section 1.3.5). They help protect macroalgae from grazing; control bacterial, fungal and microalgal epiphytes; and limit fungal and bacterial infection (La Barre et al., 2010; Paul & Pohnert, 2010; Weinberger et al., 2007). It is also believed that halogenated compounds act as antioxidants, as discussed in Chapter 1 Section 1.3.3 and 1.3.4. This is consistent with previous work which suggests that environmental stresses such as desiccation, salinity and nutrient depletion influence halocarbon emission rates (Bondu et al., 2008; Mata et al., 2011; Nightingale et al., 1995).

These macroalgal emissions may impact local and regional atmospheric chemistry. The role organic and inorganic iodine species (e.g. I_2 , CH_3I and CH_2I_2) play on local atmospheric chemistry was discussed in Chapter 1 Section 1.6. Briefly they have three important impacts; they provide a route for iodine, an essential element for human health, to reach land; they contribute to the production of ultrafine aerosol particles and so potentially contribute to the number and distribution of cloud condensation nuclei and the atmospheric radiation balance; and they alter the balance of oxidising radicals in the troposphere, thereby changing the oxidising capacity of the atmosphere and its ability to process other gases, including pollutants and greenhouse gases (Saiz-Lopez et al., 2012 and references therein). Bromine-containing compounds are also involved in tropospheric (Chapter 1 Section 1.6.3) and stratospheric (Chapter 1 Section 1.6.4) chemistry.

Temperate regions have been the subject of various field studies demonstrating the importance of biogenic halocarbons (e.g. Carpenter et al., 1999; O'Dowd et al., 2002a, b). The short atmospheric lifetime of biogenic halocarbons, on the order of days to months, alongside geographical variation in biogenic sources leads to temporal and spatial heterogeneity in biogenic production and atmospheric mixing ratios. However, the tropical coastal region remains little-studied despite the potential importance of tropical regions in terms of halocarbon emissions and transport (Chapter 1 Section 1.7). Current hypotheses suggest tropical emissions may be particularly important due to deep stratospheric convective systems (Chapter 1 Section 1.7.2). These systems may provide a rapid transport mechanism delivering short-lived halocarbons and their product gases to the upper troposphere/lower stratosphere (Quack et al., 2004; Salawitch, 2006). Research cruises in tropical waters, however, have tended to consider emissions from oceanic, shelf sea and upwelling areas (Quack & Suess, 1999; Quack et al., 2004, 2007), and no study to date has focused on emissions from coastal tropical macroalgae. However, the tropical coastal zone has been identified as a potentially strong source region by Yokouchi et al. (2005) who measured up to 40 ppt of atmospheric CHBr_3 along the coast of tropical islands and a decreasing abundance relative to longer-lived halocarbons such as dibromomethane (CH_2Br_2) away from the coast; a pattern indicative of a localised coastal source such as macroalgae. Differences may also exist between tropical and other regions with regards to macroalgae abundance and species distribution, as discussed in Chapter 1 Sections 1.7.3 and 1.7.4.

This chapter presents the first dedicated study of halocarbon production by a range of tropical macroalgae. Alongside this work it also discusses the effects of incubation time on calculated production rates (Section 3.3.1) and compares tropical algal production rates with data from temperate and polar species (Section 3.3.4). Production rates for temperate and polar species were generally taken from the existing literature, but several temperate species were also incubated using the same method for a direct comparison. Work from this chapter can also be seen in Leedham et al. (2013).

3.2 Methodology

3.2.1 Malaysian macroalgae sample collection

In September and October 2011, 15 tropical macroalgae species were collected from several sites on the western coast of Peninsular Malaysia; including an intertidal reef, an aquaculture site and a mangrove stand (Fig. 1). *Kappaphycus alvarezii* was purchased from a small aquaculture site at Pangkor Island, *Ulva reticulata* was collected from a shrimp farm and *Gelidium elegans* was obtained from the University of Malaya (UM) hatchery where it is cultivated for use in aquaculture experiments. All other species were naturally occurring in the coastal environment and obtained from rock pools exposed at low tide or by snorkeling in water up to 1 m deep (see full details in Table 1). Care was taken to select intact, healthy looking specimens with a minimum of epiphytes. Species attached via a holdfast were removed by carefully cutting the holdfast from the substrate, ensuring minimal damage. One to four species were collected during each sampling trip and returned to the UM hatchery facility where they were stored in large tanks of aerated seawater which were changed about every 3 days. Samples were used within a week of collection. Prior to each incubation replicates of an individual species were chosen, again, only undamaged specimens were selected. In most cases triplicate samples were chosen, but for several incubations the quantity of collected material only allowed duplicate measurements (see Table 1).

As previous experiments have shown that different sections of some of the larger algae release different amount of halocarbons (Laternus, 1996) single whole plants, or multiple smaller plants for filamentous or mat forming algae, were used. In each case, samples of similar mass and appearance were selected. *Cladophora* sp., a mat forming alga, was removed in small sections maintaining the mud substrate to minimise disturbance, and a separate control containing mud and seawater was used for this incubation. Samples from Cape Rachado often had small sea anemones attached, these were gently removed. An individual incubation on anemones alone (species unknown) showed no appreciable halocarbon production (data not shown). Photographs of typical algal specimens can be seen in Fig. 2.



Figure 1. Location of sampling sites Peninsular Malaysia.

★ = Kuala Lumpur (laboratory)

● = sampling sites:

1. Seaweed farm, Pangkor Island, Perak.
2. Shrimp farm, Kuala Selangor, Selangor.
3. Mangroves, Morib, Selangor.
4. Port Dickson, Negeri Sembilan; including Cape Rachado, Pantai Dickson and Pantai Purnama.



Figure 2. Photographs of tropical seaweeds incubated in Malaysia in 2011. Details of each species are given in Table 1.

Table 1. Tropical macroalgae investigated, their collection sites and sample details. n = number of replicates used in incubation study.

Species	Collection site	Collection date	Incubation date	Sample composition	n
Rhodophyta					
<i>Gelidium elegans</i>	UM culture	17.10.11	18.10.11	Single specimen	3
<i>Gracilaria changii</i>	Morib mangrove	19.09.11	21.09.11	Single specimen	3
<i>Gracilaria salicornia</i> 1	Morib mangrove	19.09.11	21.09.11	Single specimen	3
<i>Gracilaria salicornia</i> 2	Pantai Dickson	17.10.11	18.10.11	Single specimen	3
<i>Kappaphycus alvarezii</i>	Seaweed farm, Pulau Pangkor	12.09.11	15.09.11	Single specimen	3
Phaeophyta					
<i>Padina australis</i>	Pantai Purnama	29.10.11	01.11.11	Selection of small plants	2
<i>Sargassum baccularia</i>	Pantai Purnama	29.10.11	01.11.11	Single specimen	2
<i>Sargassum binderi</i>	Cape Rachado	06.10.11	13.10.11	Single specimen	3
<i>Sargassum siliquosum</i>	Pantai Purnama	29.10.11	01.11.11	Single specimen	2
<i>Turbinaria conoides</i>	Cape Rachado	06.10.11	10.10.11	Single specimen	3
Chlorophyta					
<i>Bryopsis</i> sp.	Pantai Purnama	29.10.11	01.11.11	Selection of small plants	2
<i>Caulerpa racemosa</i>	Cape Rachado	06.10.11	09.10.11	Single specimen	3
<i>Caulerpa</i> sp.	Cape Rachado	06.10.11	09.10.11	Single specimen	3
<i>Cladophora</i> sp.	Pantai Dickson	05.10.11	09.10.11	Section of algal mat	3
<i>Ulva reticulata</i>	Shrimp farm, Kuala Selangor	21.09.11	23.09.11	Selection of small plants	3

3.2.2 Temperate macroalgae sample collection

Between January and August 2012 six temperate species were incubated to provide a comparison between temperate and tropical species using the same incubation and GCMS analytical method. Six species were collected from West Runton on the North Norfolk coast. As with tropical species, only whole, intact and healthy looking specimens were selected. Specimens were returned to UEA within two hours where they were sorted and gently cleaned to remove sand and epiphytic organisms before being placed in large tanks of artificial seawater made using Seachem Marine Salt™ (Seachem, USA) and distilled water which was aerated using two aquarium pumps connected to airstones. Salinity was checked regularly and maintained at 32-34. Tanks were stored in a constant temperature room held at 13 °C (± 0.5 °C) with a light level of 180 $\mu\text{mol photons m}^{-2} \text{ s}^{-1}$ and a 14:10 light:dark cycle. Samples were used within five days of collection. Table 2 provides details of the species, incubation dates and sample information. The results of these incubations are used in Section 3.3.4 and also in Chapter 4 Section 4.3.5.

Table 2. Temperate macroalgae investigated, their incubation dates and sample details.

n = number of replicates used in incubation studies.

Species	Incubation date	Sample composition	n
Rhodophyta			
<i>Corallina officinalis</i>	23.01.12	Single specimen	3
<i>Porphyra</i> sp.	16.02.12	Single specimen	3
<i>Polysiphonia fucoides</i>	29.06.12	Single specimen	2
Phaeophyta			
<i>Fucus vesiculosus</i>	01.08.12	Single specimen	3
Chlorophyta			
<i>Ulva intestinalis</i>	23.01.12	Selection of small plants	2
<i>Ulva lactuca</i>	29.06.12	Single specimen	2

3.2.3 Incubation protocol

Gas-tight incubation vessels comprised modified 500 ml Erlenmeyer flasks and Dreschel tops as described by Hughes et al. (2011). The Dreschel outlets were capped with 0.2 μm Minisart® filters (Sartorius, UK) and plastic Luer-type taps. During incubations all Luer taps were closed and during sample removal one was opened to allow the flask to re-equilibrate to atmospheric pressure, the filter preventing the ingress of bacteria, dust or other foreign matter. Filtered seawater (400 ml, 0.2 μm filtered) collected from a coastal site near to Kuala Lumpur was added to each flask leaving a 300 ml headspace. Seawater from this site was used for each incubation for standardisation. Algal samples were gently blotted dry and weighed before they were added to the flasks to obtain fresh weight values for use in production calculations. Two control flasks containing filtered seawater only were used for each incubation.

Flasks were transferred to an incubator at 35 °C which provided 120-130 $\mu\text{mol photons m}^{-2} \text{s}^{-1}$ constant light via fluorescent tubes (Philips). Jones and Carpenter (2005) reported UV photolysis of CH_2I_2 , CH_2BrI and CH_2ClI with lifetimes of 10 minutes (± 1 min), 4.5 hours (± 40 mins) and 9 hours (± 2 hours) respectively, lifetimes that could be significant within the 4 and 24 hour timescales of our incubations. However, no UVA or UVB light was measured in the incubator (Keng et al., 2013) and we therefore conclude that UV photolysis is negligible. Incubations lasted 24 hours, 40 ml samples were removed for analysis after 4 (t4) and 24 hours (t24). Samples were removed directly into 100 ml gas-tight syringes (ground glass barrel, Luer closure) using a Luer tap port near the base of each flask, taking care to prevent ingress of air. Samples were analysed immediately. After t4 the 40 ml removed for sampling was not replenished to avoid dilution or nutrient addition effects. After t24 macroalgae samples were re-weighed but no significant changes were noted for any of the incubations. Dry weight was calculated by drying samples for 3 days in an oven at 60 °C followed by 24 hours in a desiccator; a method used extensively by the UM algal lab. Losses to the headspace were estimated by calculating the solubility of each halocarbon with data from Sander (1999) and using this to compute partitioning between seawater and headspace. Percentage losses to the headspace at t24 varied between 3 and 13.5% for all gases with the exception of CH_3I , for which the calculated loss was 30%.

3.2.4 Purge and trap (P&T) system

Analysis was carried out via purge and trap pre-concentration followed by gas chromatography mass spectrometry (GCMS). After addition of an internal standard (Section 3.2.5) samples were passed through a 25 mm diameter WhatmanTM 0.7 μm filter directly into a purpose-built purge and trap (P&T) system (Fig. 3), described most recently for halocarbon analysis by Hughes et al. (2006, 2008). The system was constructed of glass and stainless steel and has a proven suitability for the analysis of halocarbons without loss or contamination problems. A flow of oxygen-free nitrogen, OFN, (BOC) scrubbed of organic contaminants using a hydrocarbon trap (Alltech®) passed through a frit into the glass purge tube containing the seawater sample. Samples were purged for 15 minutes in a 40 ml min⁻¹ flow of OFN. Purging efficiency is dependent on the Henry's Law coefficient (H), the concentration in air divided by the concentration in water at equilibrium (Moore et al., 1995). Low molecular weight compounds are purged more efficiently from the water sample than those with higher molecular weights. Purging efficiencies ranged from ~90% for CH₃I to ~70% for CHBr₃, in line with that reported by others using a similar technique (Chuck et al., 2005; Hopkins, 2010). Purging efficiencies were accounted for as calibrations were conducted via the P&T system (Section 3.2.5). Purge flow rates were checked daily to ensure consistency and the P&T system was frequently checked for leaks using the liquid leak detector SNOOP® (Swagelok, London). Periodic cleaning of the purge tube, replacement of the glass wool trap and conditioning of the hydrocarbon traps were conducted to maintain system performance.

The gas stream then passed through a glass wool trap to remove aerosols and was dried using two Nafion® counterflow driers (PermaPure, USA) with a 100 ml min⁻¹ counterflow flow rate arranged in series. Target analytes were pre-concentrated on a empty stainless steel sample loop held at -150 °C in the headspace of a thermostatically controlled liquid nitrogen-filled dewar. A VICI® Valco 6 port valve controlled flows of gases to the trap during trapping and injection.

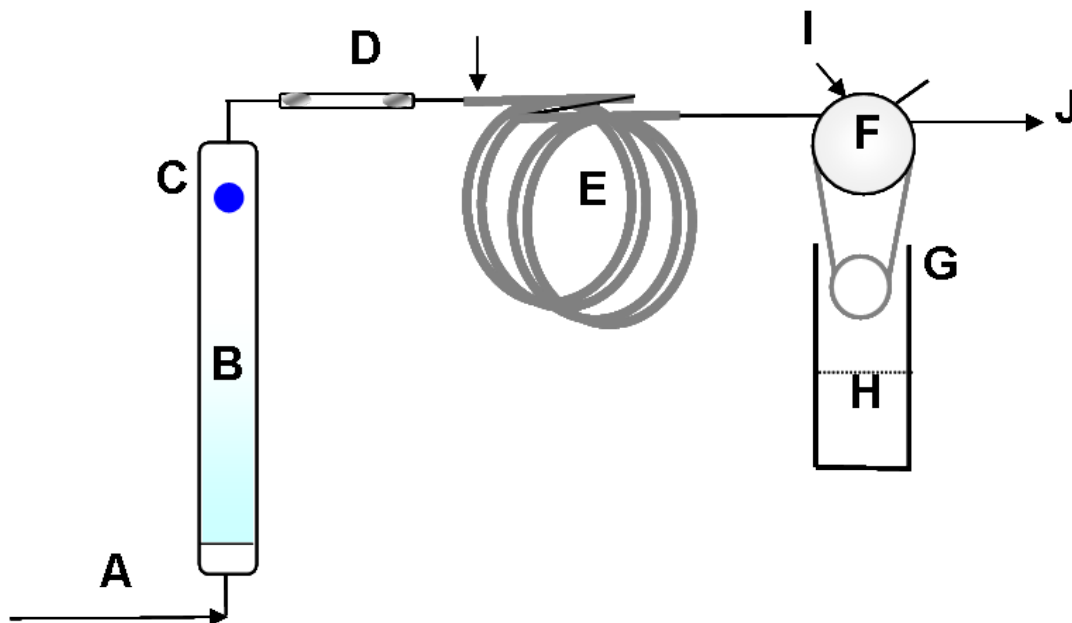


Figure 3. Purge and trap (P&T) system built at UEA. Letters denote:

A = Hydrocarbon-scrubbed OFN purge gas.

B = Purge vessel.

C = Luer port (sample enters here).

D = Glass wool trap.

E = Two Nafion® counterflow driers in series.

F = VICI® Valco 6 port valve.

G = Stainless steel trap.

H = Liquid nitrogen (trapping) or boiling water (injection) dewar. Liquid nitrogen headspace cooling was used, the dashed line represents the level of liquid nitrogen in the dewar. For injection the trap was fully submerged in boiling water.

I = Flow of high purity helium to sweep the trapped sample to the GC along a heated transfer line.

J = In-house built electronics controlled the liquid nitrogen thermostat and heated transfer line.

3.2.5 GCMS analysis

After the 15 minute P&T period the trap was immersed in boiling water and the halocarbons volatilised into a stream of CP grade helium (BOC) and transferred to an Agilent 6890 GC via a transfer line heated to 96 °C. A 60 m DB-VRX column (0.32 mm diameter, 1.8 µm film thickness, J&W Ltd.) provided separation of all target halocarbons with the following temperature programme: isothermal for 5 minutes at 40 °C, increasing to 200 °C at 20 °C min⁻¹, held at 200 °C for 2 minutes before increasing to 240 °C at 40 °C min⁻¹ and remaining isothermal at 240 °C for 4 minutes. Allowing for P&T time, data collection and oven cooling two samples could be analysed per hour.

An Agilent 5973 quadrupole Mass Selective Detector was connected to the GC and was run in electron ionisation (EI) selective ion monitoring (SIM) mode. SIM allows the creation of a custom sequence where the detector is set to filter out defined target masses (m/z values) for a set period of time. Reducing the masses to be identified at any one time increases the time the detector can dwell on each m/z value, therefore increasing the sensitivity of the system. Each compound was identified using two target ions and retention times identified from the analysis of commercial standards (Section 3.2.5). The 1 SD (standard deviation) precision of the system was around 13%. The detection limit of the complete system, at 1-6 pmol L⁻¹ (halocarbon dependant), was below the background halocarbon concentrations seen in the seawater control.

Table 3 provides a list of compounds (in order of elution from the column) which were quantified via this method. Their retention times and the m/z values used to identify them are also included in this table. Chapter 1 Table 1 provided further information on these compounds.

Table 3. Halocarbons quantified during tropical macroalgae incubations. Halocarbons are listed in order of elution.

Halocarbon	Chemical formula	Retention time	Target ions (m/z values)
Methyl iodide	CH ₃ I	6.8	142, 127
Bromochloromethane	CH ₂ BrCl	8.7	130, 93
Dibromomethane	CH ₂ Br ₂	10.3	174, 174
Bromodichloromethane	CHBrCl ₂	10.4	83, 85
Chloriodomethane	CH ₂ ClI	10.7	176, 127
Dibromochloromethane	CHBr ₂ Cl	11.8	129, 127
Bromiodomethane	CH ₂ BrI	12.03	222, 141
Bromoform	CHBr ₃	13.06	173, 175
Diiodomethane	CH ₂ I ₂	13.48	268, 141
Internal standards (Section 3.2.5)			
Deuterated methyl iodide	CD ₃ I	6.8	145, 127
¹³ C-dibromoethane	¹³ C ₂ H ₄ Br ₂	12.05	109, 107

3.2.6 Calibration and use of internal standards

Perfluorotributylamine (PFTBA), an internal MS standard provided by Agilent, was used to autotune the MS system after significant changes, e.g. system downtime. Commercial standards (generally Sigma-Aldrich®, UK) were used to calibrate the system for sample analysis. Neat (purity 97-99%) standards were diluted gravimetrically in a serial dilution in high purity methanol to produce primary, secondary and tertiary ('working') standards. Neat standards were sealed and refrigerated in the dark at ~4 °C. Diluted standards were stored in sealed 4 ml amber glass vials at -18 °C. Working standards were capped with Mininert™ tops (Valco Instruments Co. Inc.) which allowed syringe access, without the removal of the cap, through a septum valve which can be pressed shut to form a leak-tight closure when not in use. To calibrate the system microlitre (generally between 2-50 µl) volumes of the tertiary methanolic standards were added directly to 40 ml of 0.2 µm filtered seawater which had been pre-purged with hydrocarbon-scrubbed, compressed air (BOC) for at least 24 hours. Standards were added directly to the seawater in an 100 ml glass syringe, taking care to avoid ingress of air, to mimic sample injection into the P&T system. Multi-point calibrations containing at least 4 concentration values spanning the expected concentration range were regularly conducted. Calibrating in this way provided a calibration of the complete system, including purging efficiencies or any losses that may occur during drying or trapping. It therefore provided a more accurate result than calibrating only the detector. Values were blank corrected and a regression line plotted between these points was used to derive the relationship between concentration and peak area. Calibrations were accepted if the R² value of this line fell above 0.9, generally R² values were between 0.95-0.99.

Small fluctuations in sensitivity occur over time, to reflect these changes synthetic surrogate analytes were used to allow constant monitoring of sensitivity relative to recent calibrations. Two methanolic internal standards, deuterated methyl iodide (CD₃I) and ¹³C-dibromoethane (¹³C₂H₄Br₂) (Table 3) were prepared gravimetrically in the same way as the calibration standards. These compounds were used as they occur in extremely low natural concentrations and so would not be affected by natural fluctuations between samples. Small volumes (typically 2.5 µl) of a mixed internal standard were added to each sample immediately prior to analysis. Working solutions of these internal standards were checked daily or every two days for contamination by injection into a pre-purged water sample. Fresh working solutions were prepared regularly.

The mean daily internal standard peak area was used to correct each individual sample using Eq. 1 where the corrected target analyte peak area (TA_{corr}) is calculated from the raw target analyte peak area (TA_{raw}) using the daily mean internal standard peak area (IS_{av}) and the individual internal standard peak areas for each sample (IS_s). Internal standards that fell outside a distinct range, usually $\pm 1SD$, were not used to prevent distorting the data.

$$TA_{corr} = \left(\frac{IS_{av}}{IS_s} \right) \times TA_{raw} \quad (1)$$

Fig. 4 shows the response of $^{13}C_2H_4Br_2$ during the data collection period discussed in this chapter. Panel a shows the peak area response for $^{13}C_2H_4Br_2$ for consecutive sample numbers between 55-250. Samples 1-54 did not include the internal standard or were not part of this experiment (e.g. system installation tests). A decrease then plateau in system sensitivity following the initial set up and autotune is visible. The decrease is likely due to accumulation of decomposition products within the body of the MS and degradation or deformation of the filament (G. Mills, pers. comm.). Small increases in sensitivity following subsequent tunes (blue lines) can also be seen in Panel a. Panel b shows the same data grouped into days. Variation within each day, which can be corrected for using the surrogate analytes, is clearly visible. Generally a decrease in sensitivity was seen during each day. Where a decrease was seen it fell between 0.7-49% (mean 16%) for CD_3I and 4-39% (mean 19%) for $^{13}C_2H_4Br_2$. This daily sensitivity drift is somewhat reversible, with an increase between the last sample of one day and the first of the next commonly seen. This reversible drift has been potentially attributed to a build up of non-target analytes within the MS ionisation chamber (C. Hughes, pers. comm.).

Whilst the drift in the internal standards significantly correlated (Pearson's $r = 0.84$, $p = 3.09 \times 10^{-35}$, Fig. 5) the use of both an early (CD_3I at ~ 6.8 minutes) and later ($^{13}C_2H_4Br_2$ at ~ 12 minutes) eluting compound allowed IS correction for the range of target analytes. Different halocarbons may respond differently within the analytical system; for example, CH_3I has a higher purging efficiency than some of the later eluting and less volatile compounds, such as $CHBr_3$.

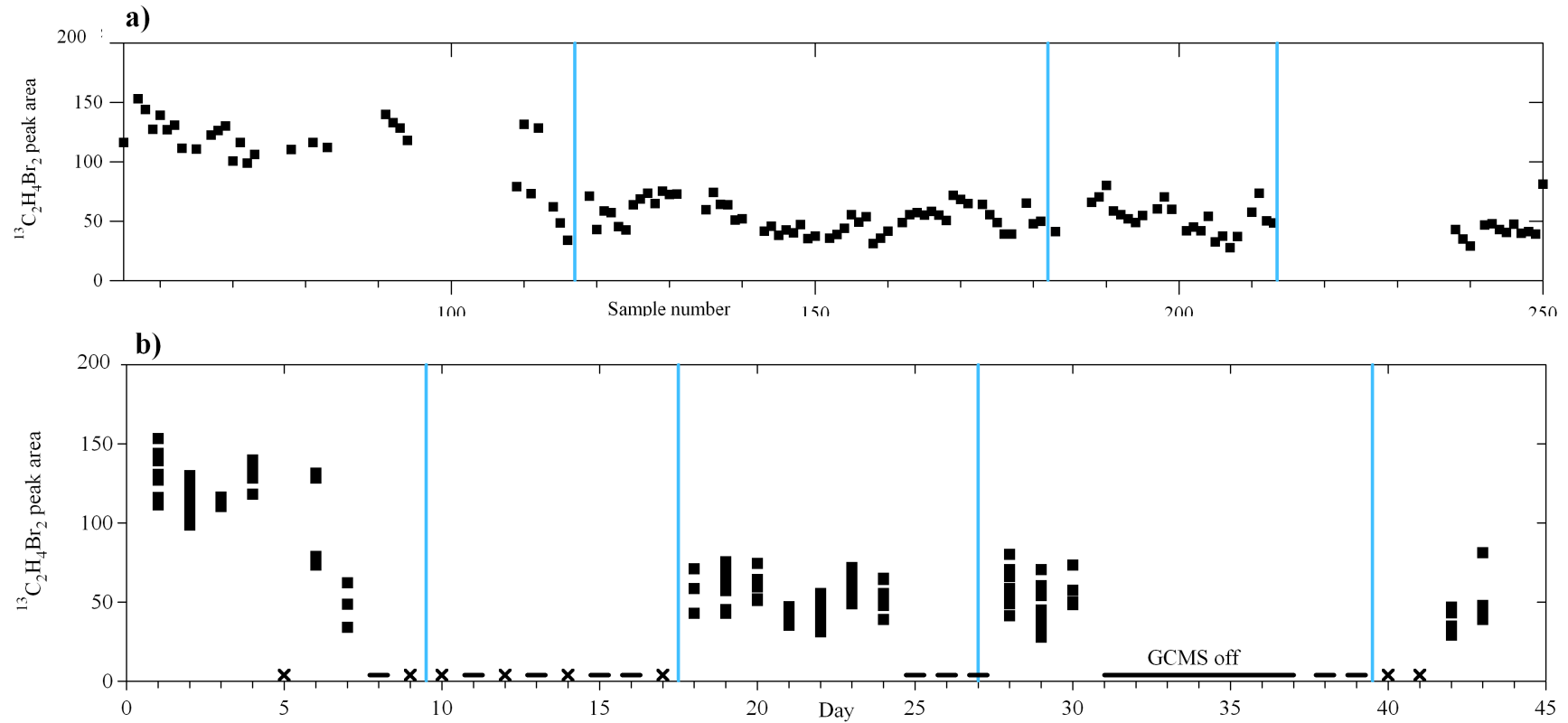


Figure 4. Variations in the peak area of the $^{13}\text{C}_2\text{H}_4\text{Br}_2$ surrogate analyte from September to November 2011. ■ represent individual samples displayed (a) in sample number order and (b) for each day. Blue lines represent autotunes of the GCMS due to instrument shut down or maintenance. Gaps represent times when the GCMS was run without addition of the internal standard (e.g. blanks or air samples). This is shown in more detail in (b) where x = days where no samples were run and - = days where samples were run without the internal standard (usually analysis of air samples). Only one GCMS shutdown period occurred during the experimental period, marked by the black horizontal line in (b). Original in colour.

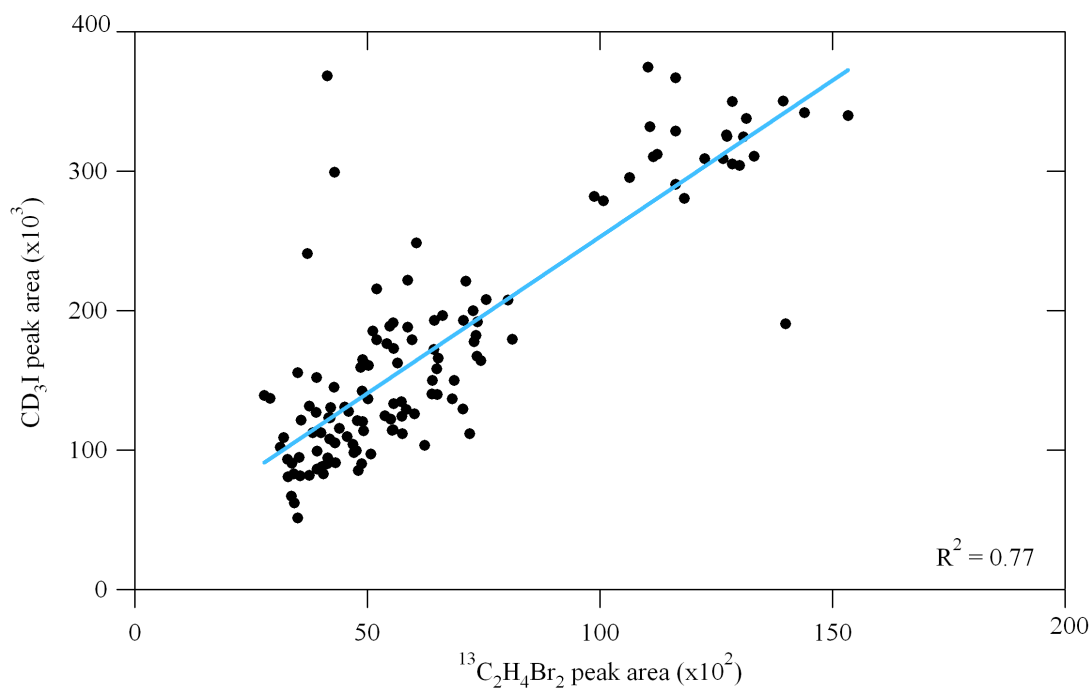


Figure 5. Correlation between peak area response of both surrogate analytes (CD_3I and $^{13}\text{C}_2\text{H}_4\text{Br}_2$) over the 2011 fieldwork season (September-November 2011). Original in colour.

3.3 Results and discussion

3.3.1 The effect of incubation time on production

Production rates for 10 of the 15 species were calculated at t4 and t24 (see Appendix 1). Table 4 shows the ratio between these values for each species. Over 50% of measurements were significantly higher at t4 compared to t24 (Student's t-test, $p=0.05$, on data which were first log-normalised to pass Kolmogorov-Smirnov tests of normality at $p=0.05$). Exceptions were the two *Caulerpa* species, both of which showed low overall production rates of less than 5 $\text{pmol g FW}^{-1} \text{ hr}^{-1}$ for all halocarbons. Both time periods show the same trends, with strong and significant correlations ($R^2 = 0.43-0.98$, $p=0.05$) between individual halocarbon and species datasets at t4 and t24 (Fig. 6). No individual halocarbon displayed a distinctive trend that may have indicated non-biogenic loss or production processes, this will be discussed in more detail later. As the t4 and t24 datasets both show the same patterns, from here on only the t24 dataset, which contains data for a greater number of species, will be discussed.

Table 4. Ratio t4:t24 halocarbon production ($\text{pmol g FW}^{-1} \text{ hr}^{-1}$) rates. nm = not measured, x = at one or both time points compound not detected. Production by *P. australis*, *S. baccularia*, *S. siliquosum* and *Bryopsis* sp. was not measured at t4.

Species	CH ₃ I	CH ₂ BrCl	CH ₂ Br ₂	CHBrCl ₂	CH ₂ ClI	CHBr ₂ Cl	CH ₂ BrI	CHBr ₃	CH ₂ I ₂
<i>G. elegans</i>	2.32	3.05	2.00	5.70	3.65	2.96	6.72	7.83	7.86
<i>G. changii</i>	2.72	16.47	11.80	3.56	7.20	3.25	13.26	3.95	3.16
<i>G. salicornia</i> 1	3.22	5.16	3.34	1.77	8.71	1.26	6.84	3.29	6.85
<i>G. salicornia</i> 2	2.36	12.45	10.87	4.36	13.08	3.71	26.36	5.39	14.72
<i>K. alvarezii</i>	nm	0.51	0.54	0.96	0.57	0.85	1.52	3.38	4.17
<i>S. binderi</i>	1.45	3.04	3.10	0.73	2.95	1.40	7.87	2.61	10.76
<i>T. conoides</i>	0.68	0.91	2.21	3.04	0	1.81	1.15	2.13	1.03
<i>C. racemosa</i>	4.98	x	0.59	x	1.75	1.39	1.51	2.07	1.91
<i>Caulerpa</i> sp.	0.93	x	0.08	x	1.75	1.39	1.51	2.07	1.91
<i>Cladophora</i> sp.	0.57	1.54	3.62	0.71	0.38	2.08	2.22	2.14	0.36
<i>U. reticulata</i>	x	x	2.39	4.99	8.81	6.14	4.39	6.68	6.75

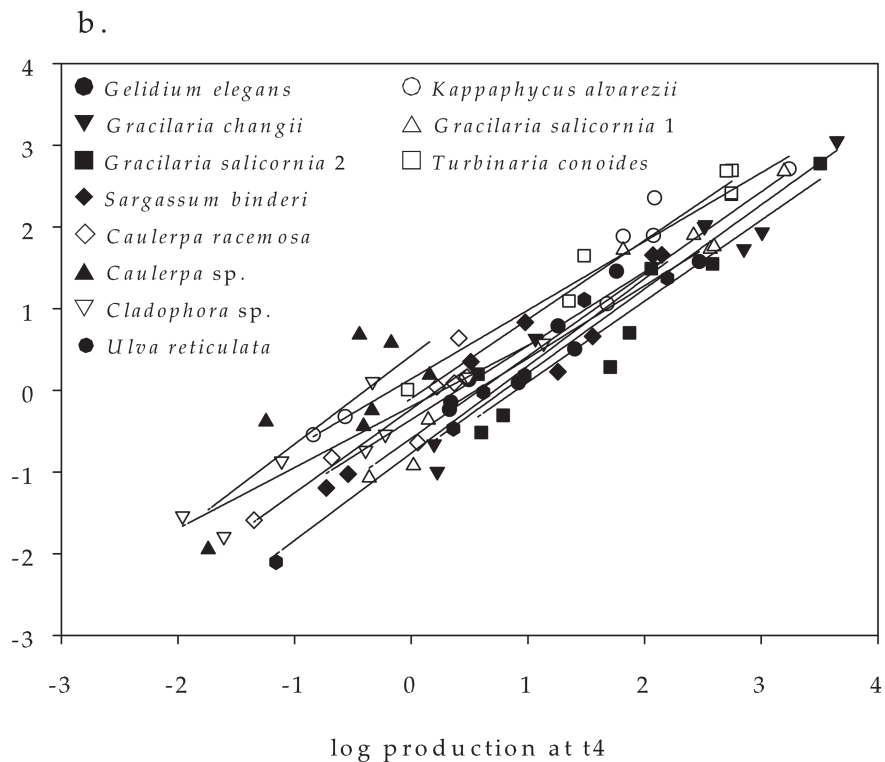
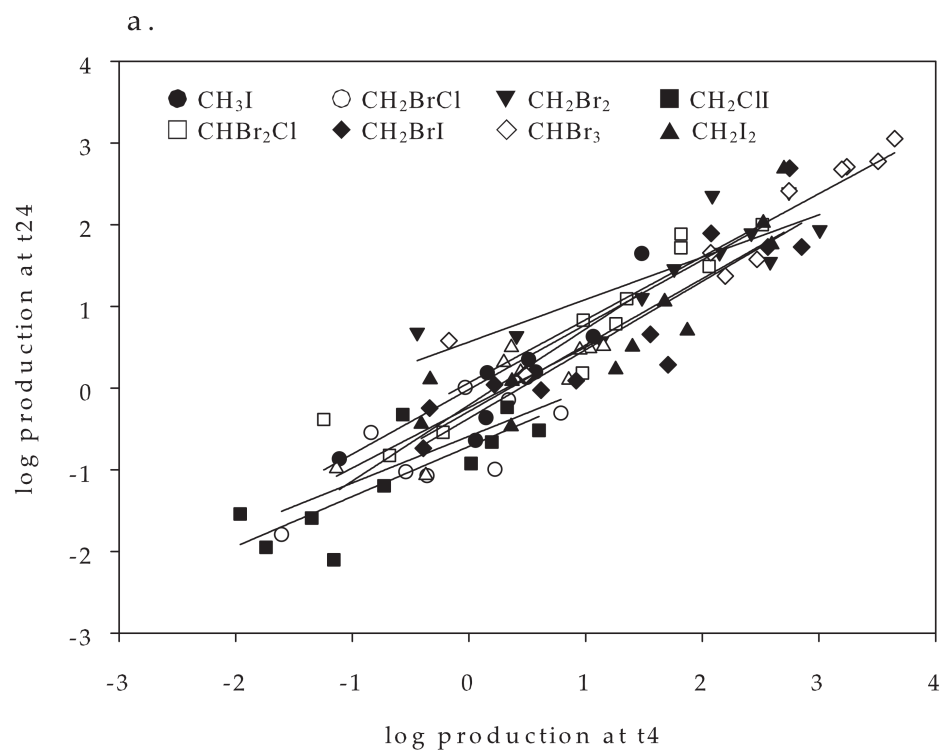


Figure 6. Correlation between log-normalised production (pmol g FW⁻¹ hr⁻¹) at t4 and t24 for (a) individual halocarbons and (b) seaweed species.

3.3.2 Halocarbon production by tropical macroalgae

T24 production values for each species are represented graphically in Fig. 7. Panels in Fig. 7 are ranked in order, with the highest individual halocarbon emission rate at the top. CH_2BrCl emission was low for all species and none was detected from *Bryopsis* sp., *Sargassum siliquosum*, *U. reticulata*, *Padina australis* and *Sargassum baccularia*. *U. reticulata* and *Caulerpa racemosa* showed no discernible production of CH_3I and CHBrCl_2 respectively. Otherwise, all other species produced all halocarbons. The bromocarbons, CH_2Br_2 and CHBr_3 , were produced ubiquitously. Generally CHBr_3 was produced in the highest quantities, followed by CH_2Br_2 . The exceptions to this were the chlorophytes, *Caulerpa* sp., *C. racemosa*, and *Cladophora* sp., which produced CH_2Br_2 at a similar or faster rate than CHBr_3 .

The rhodophyte *Gracilaria changii* was the strongest CHBr_3 producer with an average CHBr_3 production rate of $1129 \text{ pmol g FW}^{-1} \text{ hr}^{-1}$ (range $1037\text{-}1272 \text{ pmol g FW}^{-1} \text{ hr}^{-1}$). Another *Gracilaria* species, *Gracilaria salicornia* was also a strong halocarbon producer. *G. salicornia* was incubated twice, using specimens collected from two different sites within a month of each other (Table 1). Mean CHBr_3 production in September (*G. salicornia* 1) was $478 \text{ pmol g FW}^{-1} \text{ hr}^{-1}$ but variability was high, with individual incubations revealing rates ranging from $82 - 875 \text{ pmol g FW}^{-1} \text{ hr}^{-1}$. The second incubation (*G. salicornia* 2) also demonstrated high production with a mean CHBr_3 rate of $595 \text{ pmol g FW}^{-1} \text{ hr}^{-1}$ and a range of $298 - 791 \text{ pmol g FW}^{-1} \text{ hr}^{-1}$. Overall, the rhodophytes we tested tended to be the strongest producers, with *K. alvarezii* also producing CHBr_3 at a strong rate ($512.03 \text{ pmol g FW}^{-1} \text{ hr}^{-1}$, range $479\text{-}558 \text{ pmol g FW}^{-1} \text{ hr}^{-1}$).

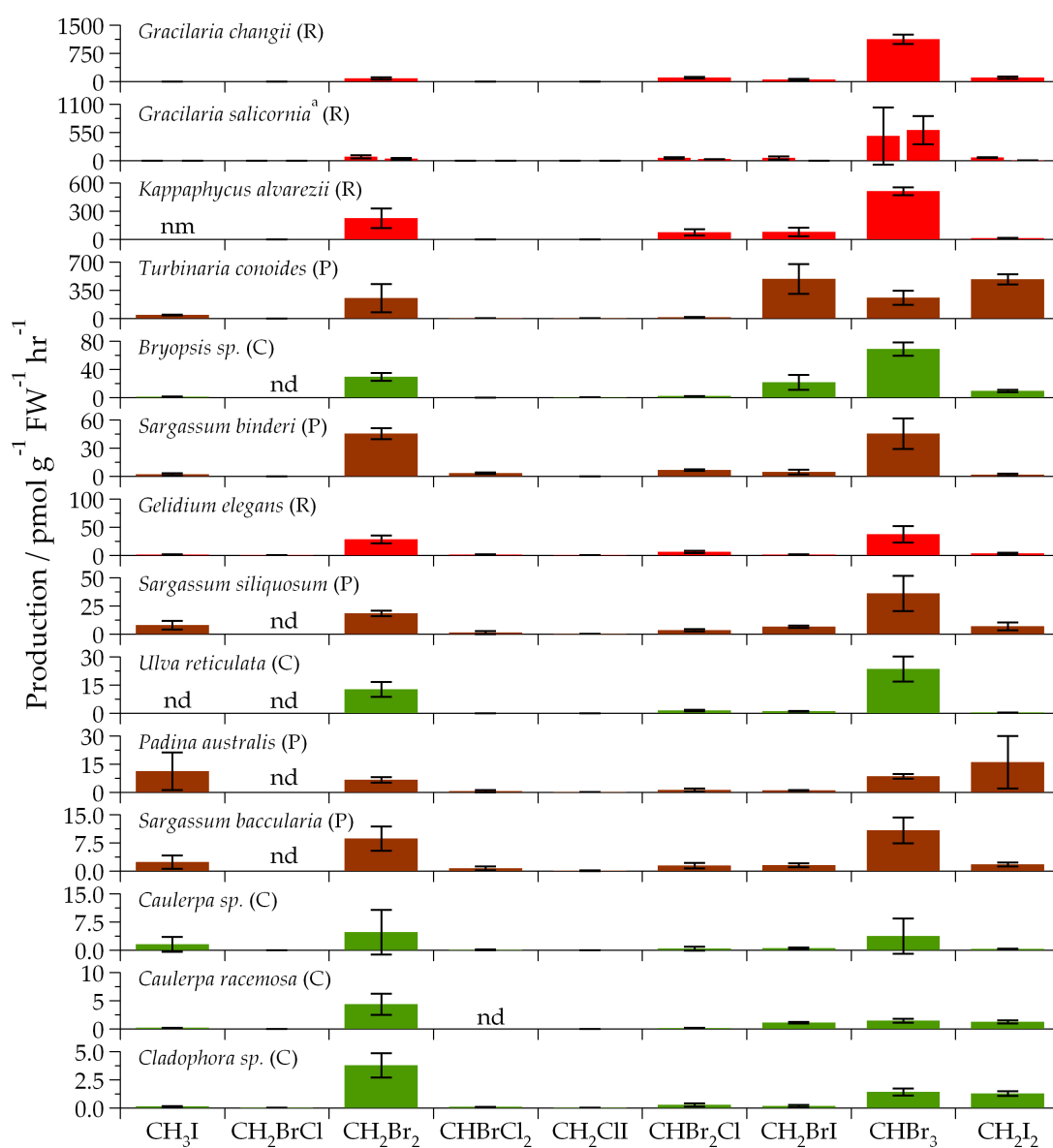


Figure 7. Halocarbon production by tropical macrophytes measured at t24. Bars are mean production of biological replicates (n=2 or 3, see Table 1) with error bars the 1σ standard deviation. Colour of bars and bracketed letter indicates: red (R) = rhodophyte, brown (P) = phaeophyte and green (C) = chlorophyte. 'nm' is 'not measured' and 'nd' is 'not detected'. (a) *G. salicornia* was incubated twice (see Table 1). Original in colour.

High intra-species variability was also seen amongst replicates in previous studies. Carpenter et al. (2000) saw replicate differences within a factor of 2, which they attributed, in part, to fluctuations in light and temperature as their incubations were conducted outdoors. However, fluctuations in environmental variables cannot explain all the variation as our study was conducted under laboratory-controlled light and temperature conditions and variations of the magnitude reported by Carpenter et al. were also observed in our study. Variability was also observed in other incubations conducted under controlled conditions, for example Collen et al. (1994) reported a percentage standard deviation on repeated incubations of up to 129%. This large variability is likely due to variations in both background seawater concentrations and biological variability between replicates. Giese et al. (1999) reported CHBr_3 variations in their seawater controls of ~10% and Laturus et al. (1996) reported varying production rates from different sections of algal tissue, with, on average, blades producing more CHBr_3 than stipes. Variability has been attributed to differences in environmental history (grazing pressure, stress, age) of different samples (e.g. Carpenter et al., 2000). An example of the effect of age can be seen in Mairh et al. (1989) where increasing internal iodine concentrations in older chlorophytes are reported. Variability between replicates is discussed further in Section 3.4.

Generally species that were strong bromocarbon producers also produced relatively high levels of other halocarbons. This was demonstrated by assigning each species a rank (1 lowest, 15 highest) for CHBr_3 production. They were then ranked again, independently, for CH_2Br_2 production, then for CH_3I and so on. The resulting spread of ranks are displayed as box and whisker plots in Fig. 8. Separate groups can be seen; prolific producers include the rhodophytes and *Turbinaria conoides*, phaeophytes are in the middle and chlorophytes are generally weaker producers. The strongest bromocarbon producer in this study, *G. changii*, also showed considerable production of other halocarbons, with CH_2I_2 production up to 300 times greater than most of the chlorophytes and CH_2Br_2 production 2-30 times greater than many of the other species studied. Some species, however, displayed a wide range of ranks. *Bryopsis*, for example, was one of the strongest producers of CH_2ClI with a rank of 13/15 but the weakest producer of CHBrCl_2 with a rank of 1/15.

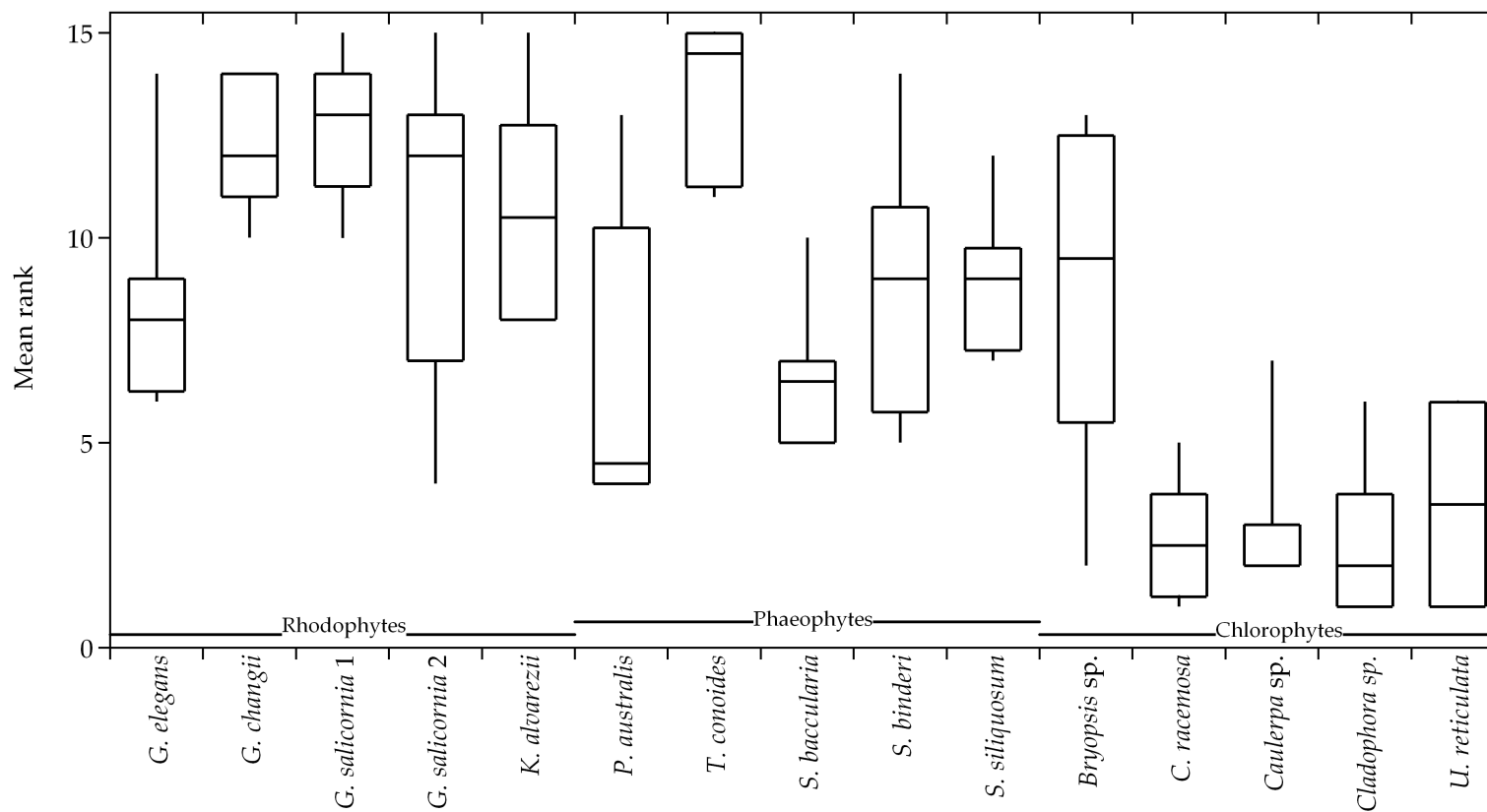


Figure 8. Production rank box and whisker plots for all halocarbons emitted by each seaweed species. Production data in pmol in g FW⁻¹ hr⁻¹ at t24 were used to rank the seaweeds for their production of each halocarbon. The lower and upper limits of the boxes represent the 25th and 75th percentiles, the horizontal lines are median values and whiskers represent the 10th and 90th percentiles. Species are ordered by class (rhodophyte, phaeophyte, chlorophyte) and alphabetically with these groups.

Whilst the rhodophytes produced large quantities of bromocarbons, some of the phaeophytes ranked highly for iodocarbon production. To investigate further, the proportions of bromine, chlorine and iodine emitted as halocarbons by each species was calculated and Table 5 shows the results with species ranked in order of decreasing total halogen emissions. *T. conoides* was the strongest producer of all iodine-containing compounds, with a CH_2I_2 production rate almost double that for CHBr_3 . Another phaeophyte, *P. australis*, showed a stronger production rate for CH_3I than for the bromocarbons. The phaeophytes in general showed a stronger propensity towards production of iodinated compounds, the mean percentage iodine emission for phaeophytes was 35% compared to 8% for rhodophytes. This corresponds to temperate studies which reported strong iodocarbon emissions from temperate macroalgae such as *Laminaria* (kelp) (Carpenter & Liss, 2000; Küpper et al., 2008). Chlorophytes also produced a higher percentage of iodine (18%) compared to the rhodophytes, but as overall production rates were lower for these species their contribution to local iodine chemistry is probably of less importance. In temperate regions kelps and other phaeophytes often dominate algal biomass in shallow coastal waters (Graham et al., 2007; de Vooy et al., 1979), but in tropical regions rhodophytes and chlorophytes are often more common (Santelices et al, 2009). This may potentially shift the balance of emissions towards brominated species.

Table 5. Total picomoles of halogens emitted as halocarbons during incubations and percentage contribution from bromine, chlorine and iodine. Species are arranged in order of decreasing total halogen emissions.

Species	Total halocarbons emitted / pmol	%Br	%Cl	%I
<i>G. changii</i>	1730945	89.2	4.5	6.3
<i>K. alvarezii</i>	1557254	84.4	11.7	3.9
<i>G. salicornia</i> (mean)	835449	87.6	6.4	6.0
<i>T. conoides</i>	435637	50.0	7.7	42.3
<i>Bryopsis</i> sp.	107250	79.9	8.8	11.4
<i>S. binderi</i>	62711	78.4	18.9	2.8
<i>G. elegans</i>	39696	83.9	12.8	3.3
<i>S. siliquosum</i>	36865	76.9	11.6	11.5
<i>U. reticulata</i>	33761	86.1	12.5	1.4
<i>S. baccularia</i>	20996	73.9	15.7	10.4
<i>P. australis</i>	11449	42.2	9.2	48.7
<i>C. racemosa</i>	12614	63.4	19.6	17.1
<i>Caulerpa</i> sp.	9312	73.4	17.8	8.8
<i>Cladophora</i> sp.	5312	64.8	21.9	13.3

With the exception of *Bryopsis*, the chlorophytes were the weakest producers, with production rates for all halocarbons below 30 pmol g FW⁻¹ hr⁻¹. Bromocarbons were still produced in the highest quantities, but production rates for iodinated and mixed bromochloro- compounds were generally less than 1 pmol g FW⁻¹ hr⁻¹ for *Ulva*, *Caulerpa*, and *Cladophora* spp.. In common with many chlorophytes, *Bryopsis* species are fast growing and opportunistic, with the potential to rapidly colonise an area. It has been suggested that halogenated metabolites within algal tissues help protect against epiphytes or grazers (Paul & Pohnert, 2010), perhaps the stronger halocarbon emissions from these species helps protect the algae, facilitating their rapid growth (see 'ideas for further research' in Chapter 6 Section 6.4).

Potential triggers for halocarbon emissions, such as grazing or oxidative stress, do not help to explain why different species found in the same environment and subjected to similar environmental conditions show such high variability in their halocarbon production rates. It is possible that some species may rely on other metabolites, for example some tropical *Caulerpa* species are reported to use high concentrations of sesquiterpenoid metabolites to deter herbivores (Paul et al., 1987). The *Caulerpa* species we studied all showed low halocarbon production, however no other metabolites were investigated. *T. conoides* also stood out from the general pattern of rhodophyte > phaeophyte > chlorophyte with respect to production rates. *T. conoides* is in the same phylogenetic family (Sargassaceae) as the weaker producing *Sargassum* species reported here. Variations between class, genus and species are not unexpected; despite the overarching terms 'seaweeds' or 'macroalgae', this group of organisms are an evolutionary diverse group, and the evolution and genetic control of halocarbon production is poorly understood.

In the literature to date halocarbon production has been expressed as production in picomoles or nanograms per unit of fresh weight (FW), dry weight (DW) or sometimes both, per unit of time. Fresh weight may provide an easier basis for scaling up to emission estimates as they better represent natural biomass, whereas dry weight potentially provides easier comparisons between algal species as some algae contain much higher water content than others. The ranking procedure used for Fig. 8 was repeated using production expressed per gram of DW instead of FW. FW and DW derived ranks are displayed alongside FW/DW ratios in Table 6. Despite the range of FW/DW ratios seen in this study the ranks assigned to each species and the overall pattern of weak or strong producers remains the same whether fresh or dry weight is used.

Table 6. Changes in mean 'production rank' when calculating production using fresh or dry weight. Species are ordered in increasing percentage DW.

Species	t24 mean rank		DW as % of FW
	FW	DW	
<i>C. racemosa</i>	2.5	5.6	4.3
<i>Caulerpa</i> sp.	2.7	6.8	4.8
<i>Bryopsis</i> sp.	8.3	8.6	5.9
<i>G. salicornia</i> 1	9.6	11.2	8.0
<i>G. elegans</i>	8.6	6.2	8.7
<i>Cladophora</i> sp.	2.3	1.3	8.9
<i>K. alvarezii</i>	12.4	13.5	9.8
<i>U. reticulata</i>	3.7	2.3	11.4
<i>G. changii</i>	12.3	11.0	11.4
<i>P. australis</i>	6.3	7.1	12.6
<i>S. binderi</i>	8.6	7.4	12.9
<i>S. siliquosum</i>	8.6	7.3	14.3
<i>T. conoides</i>	13.3	12.8	14.4
<i>S. baccularia</i>	6.1	6.0	15.4
<i>G. salicornia</i> 2	10.7	10.0	27.0

3.3.3 Correlations between biogenic halocarbons

Halocarbon correlations from incubation studies could improve our understanding of biological links between halocarbons and their production mechanisms. All log-normalised production values for each halocarbon (except CHBrCl_2 which failed normality tests even after log-normalisation) were correlated against one another (Fig. 9) and tested using Pearson's correlation coefficient (r). Significant correlations ($p < 0.05$) were common for the polyhalogenated halocarbons but the mono-halide CH_3I correlated only with two other iodinated compounds, CH_2ClI and CH_2I_2 . The strongest correlations were seen for the bromine-containing halocarbons, especially CHBr_3 , CH_2Br_2 and CHBr_2Cl with R^2 values between 0.79-0.94 ($p < 0.001$). The weakest correlations that passed the Pearson's correlation coefficient test included correlations between several of the bromine and iodine containing species, for example CHBr_3 and CH_2I_2 ($R^2 = 0.48$, $p = 0.004$) and CH_2ClI and CHBr_2Cl ($R^2 = 0.32$, $p = 0.027$). Our correlations support previous work to define the biochemical production of halocarbons. As described in Chapter 1 Section 1.3.2 methyl halides, in this case CH_3I , are produced via a methyltransferase-mediated reaction between halides and S-adenosyl-L-methionine (SAM), whereas the production of di- and tri-halogenated compounds involves vanadium-dependent haloperoxidases (Bravo-Linares et al., 2010; Goodwin et al., 1997a). Manley (2002) summarising his own and others' research, concluded that polyhalomethane production is functional, with polyhalogenated compounds acting as antioxidants, but that methyl halide production does not seem to serve a function and is possibly a by-product of normal metabolism. This difference in functionality supports the lack of correlation we observe between these two groups of halocarbons. However, despite the lack of statistical correlations between the production rates of CH_3I and the majority of other halocarbons, strong producers (e.g. *Gracilaria* spp.) produced large quantities of CH_3I and polyhalogenated compounds. This suggests that links may exist between these two production mechanisms. Further research into potential linkages between these two production pathways and the mechanisms that control or trigger them is needed.

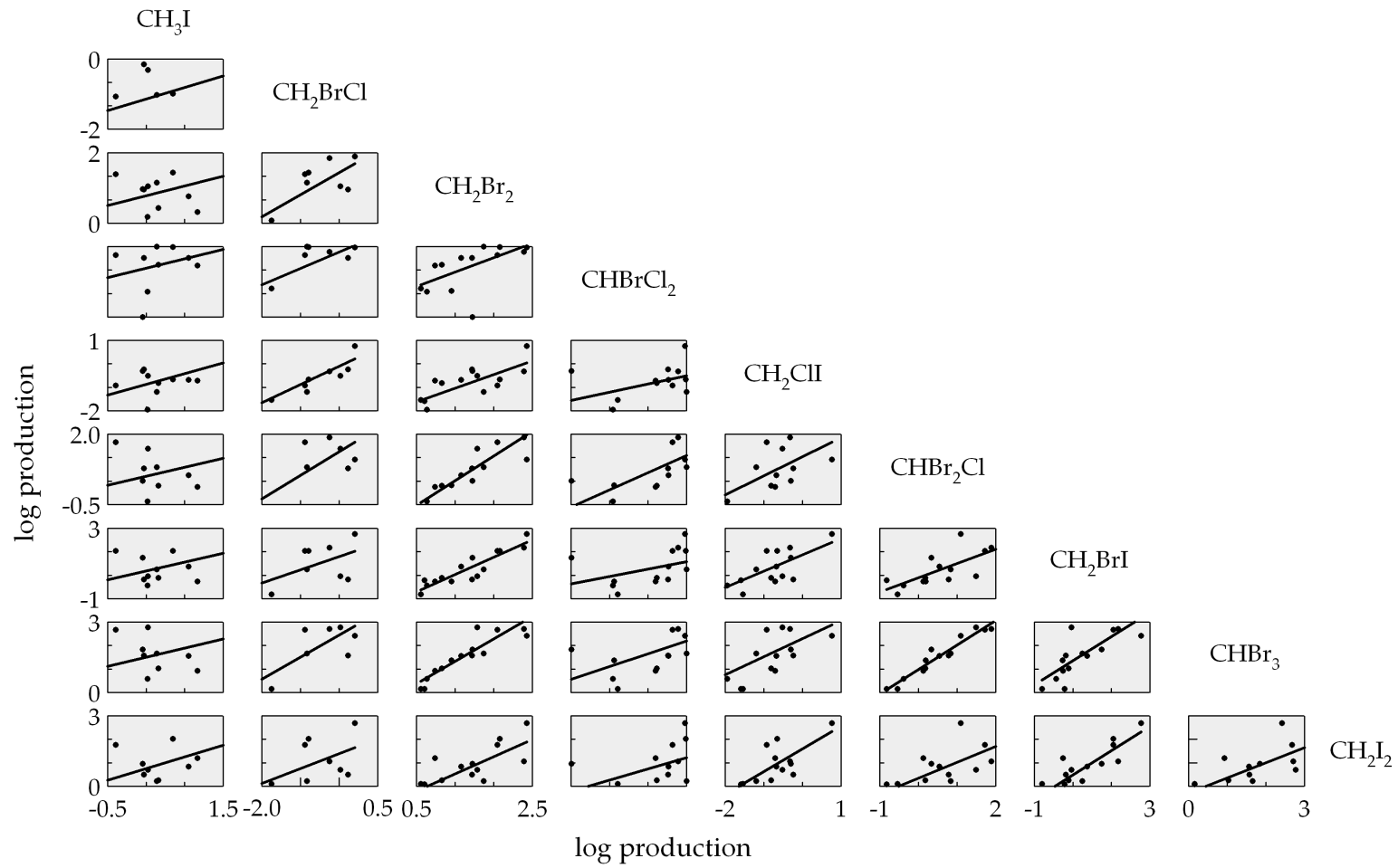


Figure 9. Halocarbon correlation plots of log-normalised production (pmol g FW⁻¹ hr⁻¹)

The highest correlation ($R^2 = 0.94$, $p < 0.001$) is between CHBr_3 and CHBr_2Cl . Tokarczyk and Moore (1994) suggested that CHBr_2Cl could be formed from CHBr_3 in laboratory cultures of diatoms, although their study did not see a time lag between CHBr_3 and CHBr_2Cl production. Although some evidence for the formation of CHBr_2Cl from CHBr_3 may be seen in this study, the ratio of $\text{CHBr}_3:\text{CHBr}_2\text{Cl}$ decreases from $\sim 18:1$ at t_4 to $\sim 11:1$ at t_{24} , the incubation time (max 24 hours) is less than the lifetime of CHBr_3 with respect to nucleophilic substitution (5 years at 25°C , see Chapter 1 Table 3) and so we would not expect this process to influence our results. Production of CH_2ClI from CH_2I_2 has also been proposed on the basis of data from incubations and the natural environment (Jones & Carpenter, 2005; Tokarczyk & Moore, 1994). Here CH_2I_2 and CH_2ClI have a relatively strong correlation ($R^2 = 0.64$, $p < 0.001$) but we did not see a change in ratio between t_4 and t_{24} . Overall, it seems that direct biogenic influence, either through direct biogenic halocarbon production or extracellular production via the emission of hypohalous acids which react with organic matter (Manley, 2002) is the important factor determining halocarbon concentrations in these incubations.

Atmospheric abundance ratios, typically from research cruises, are often used to determine regional and global oceanic halocarbon fluxes (O'Brien et al., 2009; Yokouchi et al., 2005). Ratios from this study are compared to observed atmospheric halocarbon ratios in Chapter 5.

3.3.4 Comparison with temperate and polar halocarbon production

Given that this is the first dedicated study of halocarbon production by tropical macroalgae it seemed pertinent to compare these results with existing data for temperate and polar macroalgae. CHBr_3 and CH_3I were selected for this comparison and production values were assimilated from 21 existing papers. Where production was expressed only per gram of DW production rates were converted (following Carpenter et al., 2000) using DW-FW conversion ratios in Baker et al. (2001) and Bravo-Linares et al. (2010). The resulting production value ranges are displayed alongside the results from our study in Fig. 6. Data collected from temperate incubations using an identical set up to the tropical incubations (Section 3.2.2) were also included. Appendix 2 contains figures showing all species included in these studies in order of increasing production of CH_3I and CHBr_3 . A simplification of these figures is shown in Fig. 10. Where errors were quoted alongside production rates these have been translated to error bars on Fig. 6. Determining error or variability from other studies was not always possible, but, as discussed in Section 3.3.2, previous studies have reported intra-species variability of a similar magnitude to those shown in this study

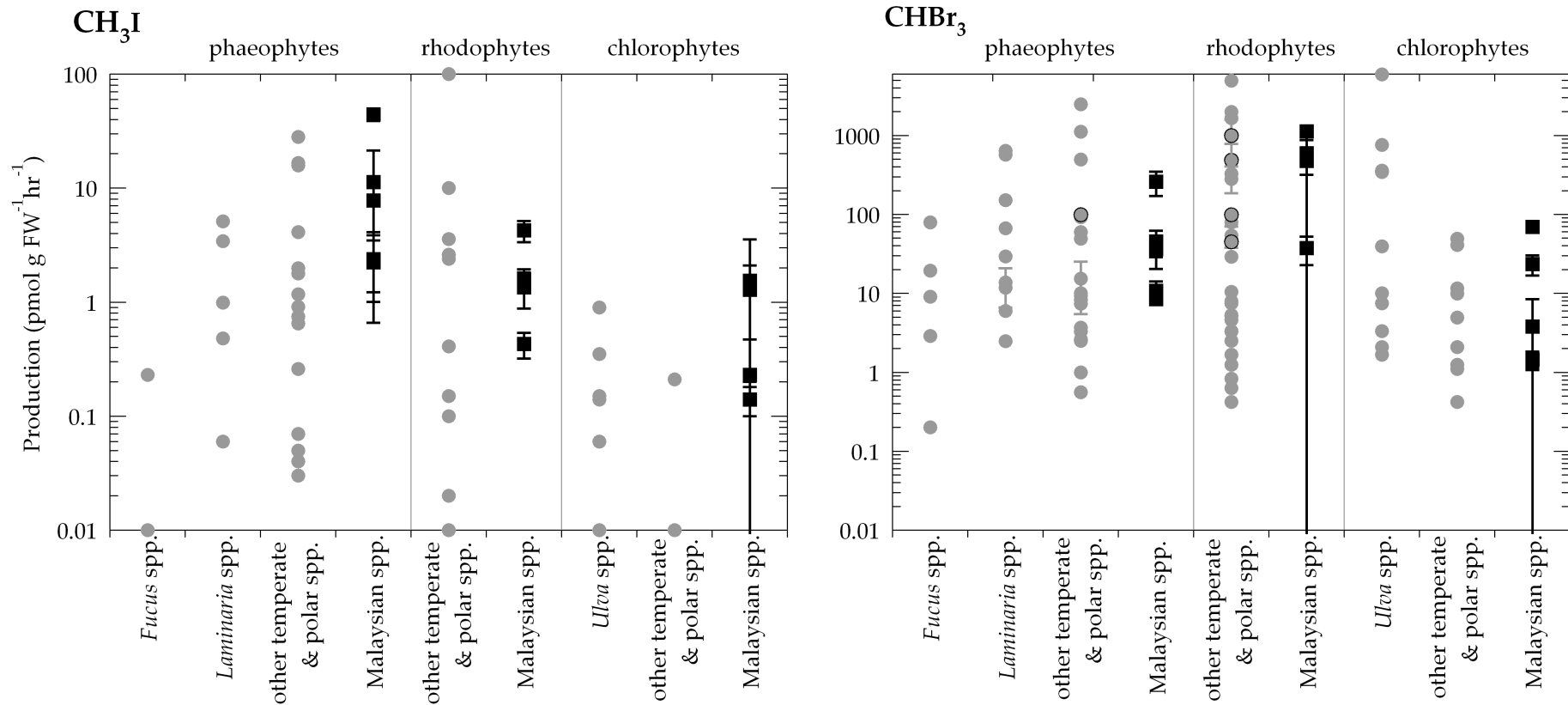


Figure 10. Halocarbon production reported in this and previous studies for CH₃I and CHBr₃. ■ = this study, error bars = 1σ standard deviation. ● = previous studies (black outline = study may include subtropical or tropical strains). Published values were from the following sources: Carpenter et al. (2000); Collen et al. (1994); Ekdahl et al. (1998); Giese et al. (1999); Goodwin et al. (1997a); Itoh and Shinya (1994); Itoh et al. (1997); Klick (1993); Laternus (1996); Laternus et al. (2004); Manley and Dastoor (1987); Manley et al. (1992); Marshall et al. (1999); Pedersen et al. (1996); Schall et al. (1994).

The results of the literature comparison (Fig. 10) show a large range of production values, spanning from negligible or no production to 100 pmol g FW⁻¹ hr⁻¹ for CH₃I and 6000 pmol g FW⁻¹ hr⁻¹ for CHBr₃. Phaeophytes displayed the highest mean production rates for CH₃I, followed by rhodophytes. The chlorophytes showed a considerably lower mean rate; 0.3 pmol g FW⁻¹ hr⁻¹ compared to around 10 and 4 pmol g FW⁻¹ hr⁻¹ for phaeophytes and rhodophytes respectively. Conversely, chlorophytes were, on average, the strongest CHBr₃ producers, with a production range of 0-6000 pmol g FW⁻¹ hr⁻¹ (mean 307) compared to 0-3000 (mean 160) pmol g FW⁻¹ hr⁻¹ for phaeophytes and 0-5000 (mean 288) pmol g FW⁻¹ hr⁻¹ for rhodophytes. These differences between classes may provide assistance in creating emissions budgets if the distribution of chlorophytes, phaeophytes and rhodophytes in an area is known (see Chapter 6 Section 6.2). Species that were recorded as producing no CH₃I or CHBr₃ are not displayed in Fig. 10, but the percentage of species that did not produce CH₃I was higher than for CHBr₃ at ~26% compared to ~10%. The percentage standard deviation across the whole CH₃I and CHBr₃ datasets was similar for both halocarbons at 328 for CHBr₃.

Sequential measurements from the same incubation flask in this study have highlighted the effect incubation time may have on calculated production. The incubation times used by the studies included in Fig. 10 ranged from 30 minutes to 48 hours, so the incubation time could explain some of the variability between studies investigating the same or similar species. Marshall et al. (1999) and Itoh et al. (1997) observed decreases in halocarbon concentrations between 3-48 hours in incubations conducted both in light and dark conditions, both papers proposed biological loss processes. Marshall et al. (1999) conducted further experiments and attributed losses to microbial breakdown whilst Itoh et al. (1997) suggested re-adsorption of the halocarbons onto the algal surface followed by degradation. Our results, which show higher mean production at t4 compared to t24 support these previous findings. The higher values at t4 may also be attributed to incubation preparation, a 'burst' of halocarbon emissions upon immersion into the incubation flask due to stress/exposure when the samples are weighed and checked may be unavoidable. Manley and Dastoor (1987) suggested that iodine limitation in the incubation seawater could account for decreases in CH₃I production as incubations progress. However, as macroalgae can accumulate iodine to far greater concentrations than seawater, up to 30,000 times greater for some *Laminaria* sp., (Küpper et al., 1998 and references herein) this seems unlikely in our 24 hour incubations. Results from several other studies report the opposite effect, with increasing production seen in longer incubations (e.g. Bravo-Linares et al., 2010). It is possible that longer incubation times in enclosed systems may subject the algae to physiological stresses, such as nutrient depletion, build up of exudates or pH shifts, which may cause increases in halocarbon emissions (Mtolera et al., 1996). These varying results suggest that incubation effects may be species or incubation set up specific.

Our production rates for CH₃I and CHBr₃ were within the range of values quoted in the existing literature. For CH₃I and CHBr₃ all but one to two species (*Papenfusiella kuromo* (Itoh et al., 1997), *Gracilaria cornea* (Ekdahl et al., 1998), *Bryopsis* sp. and *Caulerpa* sp. (this study)) fell within +/- 1 SD around the mean for each class (red, brown, green). Methodological differences could have affected the emission rates recorded; for example Itoh et al. (1997) cut disks out of some algae samples for use in incubations which may have triggered defensive emissions leading to the high CH₃I production observed.

Three genera which had been intensively studied, *Fucus*, *Laminaria* and *Ulva*, are highlighted in Fig. 10 to show variability within these groups. The spread of results recorded for species from these three genera measured from different locations and under different conditions is considerable. This variability is probably due to two factors. Firstly, differences in measurement techniques, such as incubation times, could impact calculated production, as discussed previously. Secondly, it is possible that species which share evolutionary traits, and so are grouped in the same genus, can demonstrate differences in physiology. Several studies have measured species from the same genus using the same experimental technique and seen differences in CHBr₃ production of up to 10 ppt between species from the same or similar locations (Carpenter et al., 2000; Laturus, 1996). Thereby, it seems possible that similar species from different locations could show differences in production rates beyond that which may be attributable to different experimental protocols.

3.4 Conclusions

1. Incubations of 15 tropical macroalgae species showed variable production rates covering several orders of magnitude. Brominated halocarbons were dominant, and rhodophytes produced the most bromocarbons. Phaeophytes and chlorophytes showed a stronger propensity towards iodocarbon production, although emissions in general were low for the majority of chlorophytes we studied.
2. Our measurements at two time points during a 24 hour incubation demonstrate that incubation time can also have an impact on determined production rates; production rates were higher at t4 compared to t24. For this reason, comparisons between individual studies should be made with caution.
3. Nonetheless, data from previous studies were compared to our tropical data and the range of production values was similar. As the tropical dataset is considerably smaller than that for polar and temperate species only preliminary conclusions may be drawn at this time. However, from our dataset it seems that tropical species are, on average, not individually stronger producers of halocarbons than their temperate and polar counterparts. Differences in spatial distribution may, instead, drive geographical differences in regional coastal halocarbon emissions; for example, a higher propensity toward strong-producing rhodophytes (natural or farmed) in tropical regions.

3.4.1 Further work

Ratios between halocarbons seen in these incubations will be compared to observed atmospheric halocarbon ratios in Chapter 5.

CHBr_3 and CH_2Br_2 production by tropical macroalgae will be used to derive “bottom up” emission estimates from Malaysian and South East Asian coastal environments in Chapter 6. The contribution of current and projected future aquaculture will also be discussed.

CHAPTER 4

Halocarbon production by macroalgae during desiccation

4.1 Introduction

Many seaweed species commonly experience periods of desiccation or drying. These processes could be natural, for example regular exposure and resubmersion of seaweeds in the intertidal zone. They could also be anthropogenically driven, for example prolonged desiccation when farmed seaweed is harvested and left to dry before processing. These two processes are very different, yet both may cause physiological stress to the algae. Tidal variations in exposure are natural but only certain organisms are adapted to the rapid changes in temperature, light levels and salinity that can occur in a tidal region. Organic and inorganic halide compounds, in their role as antioxidants, may be part of this adaptation strategy in macroalgae (Chapter 1 Section 1.3.3). Conversely, prolonged desiccation during an aquaculture harvest may push the seaweed beyond its natural ability to cope with desiccation, and so may result in a different pattern of halocarbon emissions.

4.1.1 Natural tidal desiccation

In the unique environment of the intertidal zone sessile organisms have to be adapted to both submersion and exposure. Whilst exposure is a natural occurrence for intertidal seaweeds it can still place abiotic stress on the algae; this has been demonstrated by studies which show that individuals from the same species grow faster when continually submerged compared to those that are exposed as part of daily tidal cycles (Williams and Dethier, 2005). The length and extent of an individual plant's exposure depends on weather conditions (such as humidity or wind), tidal patterns, and the position of the seaweed on the shore. This last factor is of particular importance, and it is believed that the ability to cope with desiccation is a strong determinant in zonal positioning and extent of an individual species' range within the tidal region (see summary in Lobban et al., 1985).

Exposure periods cause stress to macroalgae in several ways. Light levels will increase with excessive light causing photoinhibition and a reduction in photosynthesis. Briefly, photoinhibition involves damage to the reaction centre of photosystem II (PSII), which can be irreparable if excessive light conditions persist (Adir et al., 2003 and references herein). Increased exposure to UV will also occur, potentially causing permanent damage to pigments and tissues (Lüning, 1990). Rapid temperature changes can also occur when seaweeds are exposed (Lobban et al., 1985). An increase in temperature from solar radiation is common (Burrirt et al., 2002), although in winter decreasing temperatures and freezing conditions may also cause problems (cold stress is not discussed further here). With many of these stresses, it is the combination of several factors that may cause significant damage. For example, a slight increase in temperature may increase the rate of photosynthesis, and therefore confer a benefit on the algae (Lüning, 1990). However, it is likely that this benefit will be offset by other limiting factors, such as inorganic carbon limitation or stress from dehydration and evaporation. As water evaporates from the surface and intracellular spaces of the algae the salinity of these solutions will increase. Osmotic regulation in algae is a complex topic, but as a brief introduction; an increase in salinity during exposure disrupts the turgor pressure of cells as water flows out of the cells down the osmotic potential gradient. As the cell begins to collapse in on itself the plasmalemma (cell membrane) can tear away from the cell wall causing irreparable damage (Kirst, 1989). Loss of water from these membranes can also cause changes in the structure of phospholipid structures. The now 'leaky' membranes are unable to act correctly as selectively permeable barriers, especially during resubmersion (Burrirt et al., 2002).

Nutrient uptake may be reduced during exposure. Of particular importance is the limitation of inorganic carbon that may occur as CO_2 in the atmosphere is less abundant than the bicarbonate carbon source found in seawater (Lobban et al., 1985). A reduction in available carbon reduces available energy, and as energy is needed to regenerate antioxidants and power other stress-reduction mechanisms (Burrirt et al., 2002) over time a seaweed specimen will become less able to cope with exposure. Unlike vascular plants, macroalgae absorb inorganic ions over their entire surface when submerged in seawater (Chapman, 1979) and so limitation of key macronutrients, nitrate (NO_3^-) and phosphate (PO_4^-), may also occur (Davison & Pearson, 1996).

Two key physiological processes, respiration and photosynthesis, generally decrease with exposure. Respiration declined immediately or shortly after emersion for all species studied by Ji and Tanaka (2002), although they found the reduction was less extreme than for photosynthesis. Increasing rates of photosynthesis with exposure have been reported; Dawes et al. (1978) measuring several species from mangroves and salt marshes, saw higher rates of photosynthesis in exposed samples compared to submerged. However, there are many factors during desiccation that can exert a detrimental effect on photosynthetic ability and a decrease in photosynthetic capacity is commonly seen in field and laboratory examples (Pena et al., 1999; Williams & Dethier, 2005). A common response to desiccation related stresses such as light stress and nutrient limitation is an increase in ROS and oxidative stress, which may be linked to increased halocarbon production, as described in the following section (4.1.2).

4.1.2 Halocarbons and desiccation stress

Intertidal macroalgae cannot avoid emersion and the exposure to heat and light that occur with it. Nor can they prevent loss of water via physical processes, as seen in higher plants closing stomata to conserve water (Lüning, 1990). Instead they must provide coping mechanisms to reduce the effects of desiccation. These mechanisms can act to mitigate damage, for example morphological adaptation to reduce water loss in species with small surface-to-volume ratios. Other mechanisms act to limit the damage and stress once it occurs. One strategy to limit damage is the antioxidant response to oxidative stress, an important feature in macroalgae desiccation tolerance. Antioxidants reduce damage by quenching production or reducing the flux of ROS before they can cause irreparable damage to cell constituents (Lesser, 2006). Many previous studies have demonstrated increases in antioxidants or antioxidant regeneration activity, during periods of dehydration. The role of halogens as antioxidants was discussed in Chapter 1 Section 1.3.

Previous interest in halocarbon emissions during tidal desiccation has been linked to the role of biogenic iodine species in the process $IO \rightarrow \text{particles} \rightarrow \text{aerosols} \rightarrow \text{cloud condensation nuclei}$ (CCN) (Chapter 1 Section 1.6.2). Research at Mace Head, Ireland in 1998-1999 as part of the PARFORCE campaign (New Particle Formation and Fate in the Coastal Environment) demonstrated that new particle events, lasting for several hours, coincided with daytime low tides and were strongly linked to IO (O'Dowd et al., 2002a, b). Pulses of bromocarbon emissions have also been linked to tidal cycles (Nightingale et al., 1995) and a full understanding of these processes is important for accurate quantification of coastal emission budgets.

4.1.3 Prolonged desiccation

As the length of emersion increases the effect of the damaging processes described in 4.1.1 may become too great for the antioxidant systems to overcome (Burritt et al., 2002). In their study, Burritt and coworkers saw differences in the ascorbate-glutathione antioxidant response of samples from the same species collected from high and low shore positions once subjected to desiccation for 12 hours or longer. Specimens from higher on the shore seemed better able to cope with the desiccation and displayed a higher rate of antioxidant generation. Little is known about the halocarbon response to prolonged desiccation or how it may vary between species.

Our main interest in prolonged desiccation is due to its links with aquaculture (see also Chapter 1 Section 1.7.3). Many farms still use a simple air-drying process in which the harvested seaweed is laid out in the open, see Fig. 1. Understanding the emissions during commercial drying of seaweeds is potentially important in our understanding of halocarbon budgets from countries where seaweed farming and drying is common such as Malaysia, Indonesia and the Philippines (Neish, 2003).



Figure 1. Seaweed drying at small-scale farm on Pangkor Island, Malaysia (September 2011). Inset shows detail of seaweed in various states of desiccation.

4.1.4 Aims of this work

Aim

To improve our understanding of bromocarbon emissions during seaweed desiccation.

This includes:

i. Differences in emissions between species

A large body of work has been produced debating the link between zonation on the shore and desiccation tolerance. This has been observed for individuals from the same species (Burritt et al., 2002) and between species of the same genus (Collen & Davison, 1999). The degree of tolerance to desiccation between species does correlate with their vertical limit in the intertidal zone (Pena et al., 1999), albeit as part of a complex biological system. Morphological differences can be important, *Porphyra* species are often found high on the shore but desiccate quickly due to their large surface area (Ji & Tanaka, 2002). On the other hand, the filamentous nature of some algae may allow water to be trapped between layers or filaments, reducing the amount of desiccation (Jones & Norton, 1979; Kirst, 1989). This study will mainly concentrate on two morphologically different species, *Fucus vesiculosus* and *Ulva intestinalis* (Fig. 2) collected from the same position on the shore to investigate differences in emissions. In a separate series of experiments, tropical species were investigated using a flux chamber and this data will also be compared to the temperate laboratory studies.

ii. Rewetting

The resubmersion that follows a period of desiccation does not signal the end of potential damage to the algae. Further changes to the structure of the cell membrane as it is rehydrated can increase cell damage, and a flux of ROS is often seen at this point (Collen & Davison, 1999). Terrestrial plants are known to include rehydration recovery processes as part of their arsenal of dehydration coping mechanisms (Oliver et al., 1998) and a previous study on seaweeds demonstrated a burst of halocarbon emissions upon seawater rewetting (Nightingale et al., 1995). Rewetting could also occur with freshwater, for example rainwater. This reduction in salinity could also affect emissions as the osmotic gradient across the cell boundary can be disrupted such that water moves into the cells causing them to burst (Lobban et al., 1985).



Figure 2. *F. vesiculosus* (left) and *U. intestinalis* (right). Images from www.algaebase.org (2012).

iii. Photosynthesis changes and links to halocarbon production

Photosynthesis is critical to both the growth of macroalgae and their ability to respond to stress factors via (energetically) active means. Photosynthesis is therefore inextricably linked to desiccation, and a reduction in photosynthetic capacity may give some indication that stress processes (as described in Section 4.1.1) are inhibiting algal physiology and that the algae is now less equipped to deal with ongoing desiccation stress. Research into photosynthesis has noted a change in the fluorescence quantum yield (F_v/F_m) as an indicator of the state of PSII efficiency under stress (Liu & Pang, 2010). Previous studies, mainly looking at iodine emissions and their role in atmospheric chemistry (Cainey et al., 2007; Kundel et al., 2012), have not considered the physiological state of the algae during emission tests. We conducted desiccation experiments in which we measured F_v/F_m to investigate links between halocarbon emissions and photosynthetic efficiency.



Figure 3. West Runton, Norfolk. All temperate specimens used in desiccation work were collected from the area between the red lines.

4.2 Methodology

To investigate the impact of desiccation on halocarbon emissions a purpose-built desiccation incubation system was built. Temperate seaweeds samples (Section 4.2.1) underwent desiccation within this system (Section 4.2.2) which provided a controlled flow of air over each sample, the outflow of which could be trapped on Markes sorbent tubes (Section 4.2.3). Sorbent tubes were analysed via GCMS (Section 4.2.4).

4.2.1 Collection of seaweed samples

Samples of *F. vesiculosus*, *U. intestinalis* and *Porphyra* sp. were collected from West Runton on the North Norfolk coast. All samples were collected from a similar position in the intertidal zone (Fig. 3) and returned to UEA within two hours. Samples were sorted and gently cleaned to remove sand and epiphytic organisms before being placed in large tanks of artificial seawater made using Seachem Marine Salt™ (Seachem, USA) and distilled water which was aerated using two aquarium pumps connected to airstones. Salinity was checked regularly and maintained at 32-34. Tanks were stored in a constant temperature room held at 13 °C (± 0.5 °C) with a light level of 180 $\mu\text{mol photons m}^{-2} \text{s}^{-1}$ and a 14:10 light:dark cycle. Samples were used within one week of collection.

4.2.2 Incubation flasks and housing

A diagram of the incubation set up can be seen in Fig. 4 and bracketed letters (e.g. (A)) following components in the text refer to this figure. Incubation flasks comprised 1 l wide-necked glass Duran® bottles (Schott, USA) with rubber bungs (Fischer Scientific, UK). Each bung had two holes drilled in the centre and two glass tubes, 1 mm wider than the diameter of the drilled holes, were threaded through the holes to provide inlet and outlet gas lines. The inlet line extended to about 1 cm above the base of the flask whilst the outlet line extended only half way down to ensure the air flow circulated through the entire flask (G + H). The outlet line of each flask was connected to a ¼ inch Ultra-torr (Swagelok, UK) fitting which allowed the sampling tubes to be easily connected and disconnected whilst maintaining a gas-tight fitting (I). Chilled sorbet tubes were connected to this outlet when samples were required. The inlet line provided a flow of compressed air from a commercial cylinder (BOC). This air was first passed through a hydrocarbon trap (A) to remove potential contamination before passing to the first flow control system (C). This loop, comprising two three-way valves and two needle valves (Swagelok, UK) allowed a 'high' (250 ml min⁻¹) for desiccating and a 'low' (70 ml min⁻¹) flow for sampling to be established before the experiment began and then selected via the switch of a valve during the experiment (referred to henceforth as 'desiccating' and 'sampling' flows). Flow then passed to a series of connecting luer taps that allowed flow to each flask to be controlled individually (D). Each flask was connected via Tygon® tubing (Cole-Parmer, UK) (E) and an individual flow control system (F). These individual flow control systems worked in the same way as (C) to allow two pre-determined flows to be delivered to each flask. Safety measures were provided by a pressure relief valve (B) set at 10 psi and a Perspex screen in front of the flasks.

After system assembly all connections were leak checked using a flow of helium and an electronic leak detector (Agilent, UK). Flow through the whole system was also checked for consistency to ensure there were no leaks or blockages. No major modifications were made to the system after set up, but periodic checks that the flow remained constant throughout the system were made, and the liquid leak detector SNOOP® (Swagelok, UK) was also used to check the system was gas tight. During each experiment the outflow from each incubation flask was checked regularly (see Section 4.3.2) with an electronic flow meter (Phenomenex, Korea) to ensure each flask was receiving the correct volume of air. A thermometer attached to the frame provided daily temperature readings, during the ~5 month spread of experiments temperature varied between 19 – 22 °C.

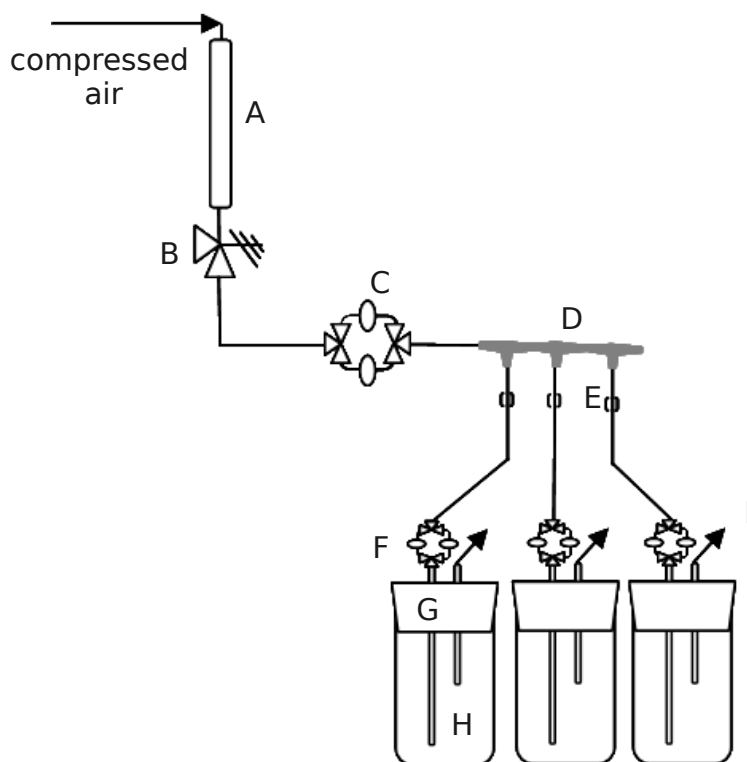


Figure 4. Desiccation chamber diagram, including:

- A** Hydrocarbon trap.
- B** Pressure release valve.
- C** Flow control system 1 (system comprises two three-way valves and two needle valves allowing either a high or low flow to be selected, see main body of text).
- D** Luer taps to turn flow on/off to individual flasks.
- E** Mini hose clamp to control flow through Tygon® tubing.
- F** Flow control system 2 (as C).
- G** Bung through which glass tubes provide air inlet and outlet to (H).
- H** Glass incubation vessel, seaweed sample sits at bottom of vessel.
- I** Outlet flow of air, sorbent tube was connected here during sampling.

4.2.3 Sorbent tube sampling

To measure halocarbon emissions thermal desorption tubes (Markes, UK) containing three sorbents; Tenax TA, Carbograph 1TD and Carboxen 1000 arranged in order of increasing sorbent strength (as listed here), were used. The use of tubes for the analysis of halocarbon samples has been previously validated at UEA (Hughes et al., 2009; 2012). Tubes were selected for these experiments as they have the potential to provide high time resolution data. The minimum time between sample analyses via our P&T GCMS is 30 minutes, including the time needed to trap and preconcentrate the sample. The only limit with sorbent tube sampling is the time needed to trap the sample, in this case 10 minutes. Air samples were passed through the sorbent tubes and halocarbons remain trapped on the sorbents removing them from the bulk air and providing a conveniently sized sample. A flow meter connected to the tube ensured each sample came from a known volume of air. To facilitate efficient trapping tubes were also wrapped in frozen gel packs for the duration of sampling. The temperature within the gel packs was commonly 0-2 °C with a maximum of 5 °C. Post-sampling, tubes were capped with ¼ inch brass caps and PTFE ferrules and stored in a -18 °C freezer until analysis.

To retain all analytes passing through the tube the sample volume must not exceed the breakthrough volume (BV), the volume of gas that can be sampled before analytes elute from the vent end of the sorbent tube (U.S. E.P.A., 1999). Markes guidelines (Markes International, 2012) give greater safe sampling volumes (SSVs, two thirds of the BV) on Tenax TA and Carbograph 1TD than the 700 ml sampling volume used in these experiment. The SSV for CHBr_3 is 100 L and 1.9 l for Tenax TA and Carbograph 1TD respectively. Data for CH_2Br_2 was not available, however, CHBrCl_2 (which has a similar GC elution time) had a SSV of 9 l on Tenax TA. Markes SSV values are determined at 20 °C, far higher than the trapping temperatures used in our experiments.

We also conducted two experiments to determine if high concentrations and high flow rates lead to breakthrough of CHBr_3 from the sorbent tubes. These tests were performed using seawater samples purged using the system described in Chapter 2 Section 2.2 with a sorbent tube, chilled to $1\text{ }^\circ\text{C}$ using a Peltier cooler, in place of the trap (see (Hughes et al., 2009; 2012)). Fig. 5 shows that breakthrough of CHBr_3 was not seen at concentrations up to $\sim 950\text{ pmol l}^{-1}$ (Panel a) or at flow rates up to 150 ml min^{-1} (Panel b). Whilst the sorbent tubes used in desiccation experiments were filled with direct air samples, not gases purged from seawater, the response of the GCMS is still comparable between these tests and the desiccation experiments. A concentration of $\sim 950\text{ pmol l}^{-1}$ corresponds to a peak area response of $\sim 2,500,000$. With the exception of two samples (which fell above but close to this value) all other air samples analysed showed responses less than 2,500,000, the majority falling well below this value. Therefore, it seems unlikely that breakthrough posed a problem in any of the work discussed in this chapter. Fig 4a also demonstrates the linear response of the system to concentrations higher than generally seen in this work. Panel b shows that, at flow rates up to 150 ml min^{-1} , breakthrough was not observed. A flow rate of 70 ml min^{-1} was used during this work, well within this range. Our chosen sampling flow rate of 70 ml min^{-1} was also within the $10\text{-}200\text{ ml min}^{-1}$ range recommended by Markes International (2008).

Previous investigations in our laboratory have shown that sorbent tubes maintain stable concentrations of bromocarbons for up to 16 months when stored at $-18\text{ }^\circ\text{C}$ (Hughes et al., 2009) the majority of samples for this experiment were analysed within 1-7 days of collection, and all were analysed within two weeks. Due to concerns over the stability of trapped halocarbons and the baseline background concentrations of some compounds, only data for CH_2Br_2 and CHBr_3 were quantified during this experiment.

After use, tubes were conditioned in a Markes TC-20TM multi-tube conditioner, which heated the tubes for 20 minutes each at $100\text{ }^\circ\text{C}$, $200\text{ }^\circ\text{C}$, $300\text{ }^\circ\text{C}$ and $320\text{ }^\circ\text{C}$ whilst a flow of clean OFN was passed through them. Once capped, these tubes were stored in the freezer for reuse, thus providing ready-chilled tubes for sampling. With access to over 200 tubes a large number of samples could be taken during individual experiments. 1 in 10 tubes was run as a 'blank' (removed from the freezer and placed directly into the ULTRATM racks) to ensure that tube cleaning and storage were effective at providing low background halocarbon levels on sample tubes. 'Background' halocarbon concentrations observed in the blank tubes acted as a detection limit, tubes with halocarbon concentrations below that which was seen in the blank tubes were treated as zero. The quantity of bromocarbon in the blank tubes was tracked over time to monitor changes, no problems with contamination in blank tubes was observed during this set of experiments.

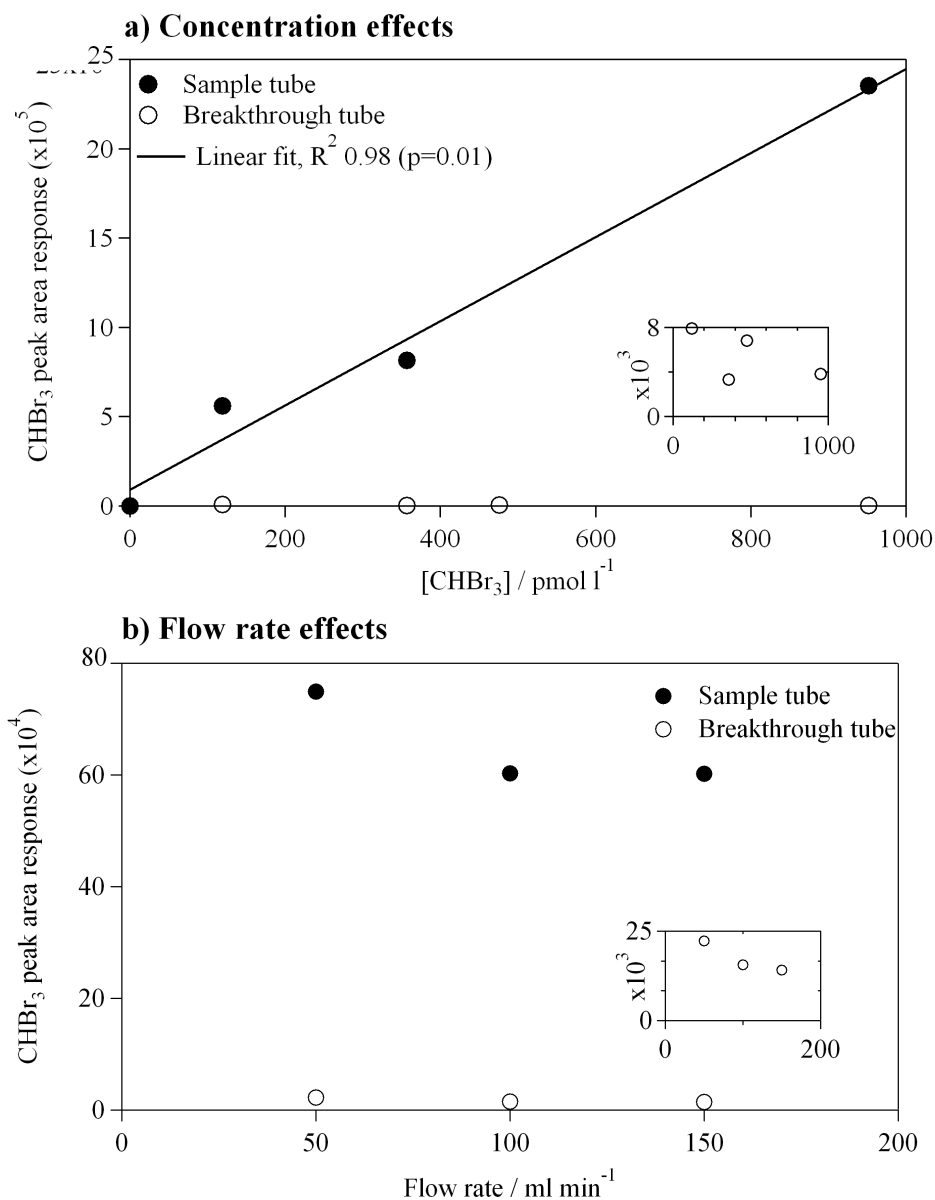


Figure 5. Testing Markes sorbent tubes for CHBr₃ breakthrough at (a) high concentrations and (b) high flow rates. Two tubes were connected in series: one to collect the sample and a second tube to monitor for breakthrough (see main body of text). Samples were pre-purged seawater samples spiked with a known concentration of CHBr₃. In (a) increasing concentrations of CHBr₃ were purged at a constant 70 ml min^{-1} flow rate. In (b) ~ 476 pmol l^{-1} of CHBr₃ was purged at varying flow rates. Inset graphs in both panels show the second, 'breakthrough', tube in more detail.

4.2.4 Analysis of sorbent tubes

Samples were analysed using a Markes ULTRA™ and UNITY™. The ULTRA™ system provided automated analysis of up to 100 tubes arranged in racks of 10 tubes. Prior to analysis a tube was moved into the 'active position' where it was sealed into the path of the helium carrier gas and a leak test was performed. Tubes that passed the leak test were purged at ambient temperature to remove residual air, a necessary step to prevent oxidation during the heating process which could interfere with analysis or reduce sorbent lifetime. The tube was then heated to 300 °C for 5 minutes, allowing the trapped analytes to be desorbed into a flow of helium and transferred along a short, insulated line to the UNITY™ cold trap held at -10 °C. Commercially packed cold traps (Markes, UK) containing glass wool, Tenax TA, Carbograph 1TD and Carboxen 1000 were used. Post-desorption the tube was returned to its position in the ULTRA™ racks and the next tube was selected. Whilst the ULTRA™ can hold up to 100 tubes, to minimise losses or migration of halocarbons within the tubes as they sat at ambient temperature a maximum of 10 tubes were loaded at any one time. Each batch of 10 tubes included; one blank, 2-3 standards and 6-7 samples. The use of Markes DiffLok™ caps reduced diffusion into and out of the tubes whilst they sat in the ULTRA™ racks. After trapping of the sample on the UNITY™ cold trap the trap was heated to 300 °C for 15 minutes to desorb the analytes into a flow of helium and along a 200 °C heated transfer line to the GC column. An Agilent GCMS, as described in Chapter 3 Section 3.2.5, was used for analysis. Sample concentrations were calculated relative to an air standard (SX074) calibrated to the NOAA scale (Chapter 5 Section 5.2.5). The standard was trapped onto chilled sorbent tubes in the same manner as sample collection to provide a calibration of the entire analytical system. Tubes filled with labelled surrogate analytes; deuterated methyl iodide (CD₃I) and ¹³C-labelled dibromoethane (¹³C₂H₄Br₂) (see Chapter 3 Section 3.2.6) were also used. During each day sample and blank tubes were interspersed with these two types of standard to provide a measure of system sensitivity drift throughout the day. Fig. 5 demonstrates that the system provides a linear response to increasing concentration up to and beyond that seen in sampling.

4.2.5 Experimental protocols

For each experiment the following protocol was followed:

- Seaweed samples (1-2) were removed alongside seawater from the storage tank and kept, submerged, in individual flasks. *F. vesiculosus* samples comprised whole, individual plants and *U. intestinalis* samples comprised groups of *U. intestinalis* fronds. The use of whole plantlets was discussed in Chapter 3 Section 3.2.1. There was an increase in temperature of 5-7 °C between storage and desiccation so samples were left submerged for approximately 1 hour in the laboratory to acclimatise to experimental light and temperature conditions. Similar changes in temperature were also recorded in other studies, for example Kumar et al. (2011).
- Gas supply to the incubation flasks was established to flush existing air from the system. Flow rate and leak checks were carried out.
- Samples were gently blotted dry to remove excess water and weighed. Samples were immediately placed in individual incubation chambers and the first sample was taken.
- The flow of OFN to each incubation flask was maintained for the duration of the experiment, alternating between high flow for periods of desiccation and lower flow for sampling. One of two sampling patterns was usually followed; either 10 minutes sampling, 10 minutes desiccation (repeated) or 10 minutes sampling, 20 minutes desiccation (repeated).
- For each experiment one flask was used as a control. Tube sorption efficiency may be affected by air moisture levels (Markes International, 2012) For this reason a small spray, ~10 ml, of seawater taken from the seaweed storage tank was added to the control flask at the start of each experiment to ensure blank samples contained some degree of moisture. Control flasks were observed to still contain signs of moisture at the end of each experiment.
- At the end of each experiment samples were removed and reweighed. Dry weight was also calculated (see Chapter 3 Section 3.2.3). Incubation flasks were washed and left to air dry between experiments.

If an experiment involved rewetting the specimen then a pipette was used to delivery ~50 ml of water through the outlet glass tube of the flask. The flask was gently swirled to ensure the seaweed was covered and then sampling continued. This volume was enough to ensure the entire specimen was just covered, without creating too large a volume of water that could physically alter the halocarbon flux. A detailed list of individual experiments and their conditions can be seen in Table 1.

Table 1. Summary of desiccation experiments. Experimental codes are abbreviations of descriptions given in column 2.

Code	Description	Date of experiments	# replicates	# control samples	Description
Halocarbon production					
FS1	<i>F. vesiculosus</i> short desiccation	31.01.12	1	1	Samples taken every 10 minutes for 2 hours.
FS2		03.02.12	1	1	Samples taken every 10 minutes for 3 hours.
FS3		14.02.12	1	1	As FS2
FL1	<i>F. vesiculosus</i> long desiccation	12.03.12	2	1	Samples taken every 20 minutes for 8 hours.
FL2		20.03.12	2	1	Samples taken every 20 minutes for 5 hours.
US1	<i>U. intestinalis</i> short desiccation	23.02.12	1	1	Samples taken every 10 minutes for 2 hours.
US2		02.03.12	1	1	Samples taken every 10 minutes for 3 hours.
UL	<i>U. intestinalis</i> long desiccation	14.03.12	2	1	Samples taken every 20 minutes for 8 hours.
P1	<i>Porphyra</i> sp. desiccation	13.06.12	2	1	Samples taken every 10 minutes for 2 hours then every 20 minutes for 5 hours (total desiccation = 7 hours).
URFW1	<i>U. intestinalis</i> desiccation followed by rewetting in freshwater	12.04.12	2	1	Dried for 5 hours. Samples taken every 10 minutes for 1 hour then specimens rewetted with distilled water followed by sampling every 10 minutes for 2 hours (total desiccation = 6 hours followed by 2 hours rewetted).
URFW2		26.04.12	2	1	Samples taken hourly for 3.5 hours. Specimens then rewetted with distilled water followed by samples taken every 10 minutes for 2.5 hours.
URFW3		01.05.12	2	1	Samples taken every 20 minutes for 8 hours followed by rewetting with distilled water. Samples then taken every 10 minutes for 2 hours.

Table 1 cont.

Code	Description	Date of experiments	# replicates	# control samples	Description
Mass loss experiments					
FM1	<i>F. vesiculosus</i> mass	21.03.12	3	x	Specimens dried as per halocarbon production experiments but removed from desiccation chambers and weighed 3 times an hour.
FM2	loss during desiccation	23.03.12	2	x	
UM	<i>U. intestinalis</i> mass	22.03.12	3	x	
	loss during desiccation				
F_v/F_m experiments					
FP	<i>F. vesiculosus</i> photosynthetic performance during desiccation	19.06.12	3	x	Specimens dried on laboratory bench in petri dishes. F _v /F _m samples taken twice an hour.
UP1	<i>U. intestinalis</i> photosynthetic performance during desiccation	19.06.12	3	x	
UP2	<i>U. intestinalis</i> photosynthetic performance during desiccation	21.06.12	3	x	

4.2.6 Water loss and photosynthesis changes

To complement the halocarbon emission incubations measurements were also conducted to determine the effect of desiccation on both water loss and photosynthesis (also in Table 1).

i. Mass (water) loss experiments

To determine the rate at which water was lost from *F. vesiculosus* and *U. intestinalis* as they dried, and how this may correlate with halocarbon emissions or vary between species, mass loss experiments were conducted. Samples were dried in the incubation system and removed to be weighed at regular intervals. Unfortunately, due to the need to remove the samples before weighing them, halocarbon emissions could not be measured concurrently, but all system parameters remained consistent between mass loss and halocarbon experiments. The mass loss experiment was conducted twice on *F. vesiculosus* (FM1 and FM2) and once on *U. intestinalis* (UM1).

ii. Photosynthetic capacity during desiccation

To measure the effect of desiccation on photosynthetic capacity a Walz 'Pulse-Amplitude-Modulation' (PAM) fluorometer (Heinz Walz GmbH, Germany) was used. The PAM fluorometer tests how stress has affected PSII by comparing the dark-adapted fluorescence state, with a saturated state (achieved by the application of a saturated light pulse to the dark-adapted sample so that its reaction centres close). The resulting value, the maximum potential quantum efficiency (F_v/F_m), is lower in stressed samples where more reaction centres are shut and so there is less difference between the two states.

Due to the need to dark adapt samples before fluorescence measurements can be taken it was not practical to desiccate samples within the incubation chambers. Instead, samples were dried under the same light and temperature conditions but in shallow glass petri dishes which were coated in black tape to block light from the sides and underneath and placed on a lab bench. A household fan was used to provide movement of air to aid desiccation. Cooling of air by the fan was within the range of laboratory temperatures observed during the experimental period (Section 4.2.2). Two Walz PAM systems were used, a DIVING-PAM and a PHYTO-PAM with EDF attachment, but they both provide a photosynthesis reading in the same way. Specimens were collected and stored in the same manner as previous experiments. The first F_v/F_m measurement of each sample was made when the specimen was submerged in a small volume of water from the seaweed storage tank. This water was then removed and the alga weighed. Periods of desiccation were interspersed with periods of 15 minute dark adaptation followed immediately by F_v/F_m measurements. Dark adaptation was provided by covering the petri dish with waterproof thick cardboard. During UP2 light and temperature fluctuations in the lab were recorded; light levels varied between 78 and 110 $\mu\text{mol photons m}^{-2} \text{s}^{-1}$ and the temperature fluctuated between 22.5 and 23.5 °C (light levels were measured using a Biospherical Instruments Inc. light meter model QSL-2102).

4.2.7 Flux chamber experiments

During fieldwork in Malaysia (2010) three tropical macrophytes; *Sargassum baccularia*, *Padina australis* and *Caulerpa* sp. were removed from a submerged position in the intertidal region and placed on dry sand under a flux chamber, as described in Chapter 2 Section 2.3. Air samples from the flux chamber were collected into canisters and returned to UEA for analysis via NCI-GCMS (Chapter 5 Section 5.2.4).

4.3 Results

Details of individual experiments and the abbreviation that represents them in the following text can be found in Table 1.

Note – displaying desiccation results relative to flow not time

As described in Section 4.2.2 flow rates were altered between periods of sampling and desiccation to create balance between the flows needed to dry seaweed and those which fall within recommended values for sorbent tube sampling. Short (2-3 hour) and long (up to 8 hour) incubations followed slightly different protocols in terms of the length of time samples were under desiccating flow rates (see Table 1). To account for this, all halocarbon production experiments (Figs. 10-14) are expressed in terms of total flow passing through the flask, not incubation time. It is hoped this aids comparison between individual experiments.

4.3.1 Replicate variability and the use of standardised concentration values

Within halocarbon desiccation experiments (Figs. 8-14 and 17-18) individual replicates showed the same pattern of halocarbon production but the magnitude of emission varied considerably. For example, in FL2 the maximum concentration seen in replicate a is about four times higher than that seen in replicate b (~100 ppt compared to ~25 ppt). This is not unexpected, in Chapter 3 Section 3.3.4 the variation between specimens in incubation studies was discussed. Variations in halocarbon production due to differences in age, environmental history or natural biological variation were not uncommon in our incubation studies, or the existing literature. Ball et al. (2010) saw up to a factor of 10 difference in I₂ emissions from drying seaweeds, which they attributed to using samples in different stages of decay. Selecting only healthy looking specimens in this study probably allows better comparisons between results of individual specimens, and also reduces the range of variability between replicates. As the replicate variability exists in total measured concentration, not pattern of emissions, concentrations have been standardised by assigning the initial concentration as 1 and converting subsequent values accordingly. This should allow clearer comparisons between experiments. Figures containing standardised halocarbon emission data (Figs. 10-14, 17-18) contain the original concentration range to the right of each plot for reference.

4.3.2 Treatment of potential sources of errors

Calibration of the tube samples used 2-3 tubes filled with a gas standard for every 3-6 sample tubes (Section 4.2.4). The error bars in all figures represent the error associated with this calibration method and the variation in chromatographic peak area associated with these standards. Other potential sources of error are listed below, alongside methods to constraint them:

1. **Variations in flow rate during the experiment.** The incubation flasks were housed in a set up that allowed two flows to be obtained via switching of several valves (Section 4.2.2). This meant that desiccating and sampling flows could be accurately set prior to each experiment and selected via a switch of a valve, negating the need to constantly alter flows with needle valves or other restrictors during the experiment. Flow to each flask could also be controlled individually and was checked for each flask every 10 minutes during the first hour and then at least every 30 minutes to 1 hour thereafter. These methods ensured consistent, accurate flows throughout each experiment.
2. **Biological variability.** As each point on Figures 8-14 and 17-18 represents one biological replicate the variation between samples has been considered in the overall differences in concentration through the entire set of experiments (e.g. Section 4.3.6).
3. **Errors in the known concentration of the standard.** This remained constant throughout the experiment, at 6.1% for CH_2Br_2 and 4% CHBr_3 .

4.3.3 Mass loss experiments

Results of the mass loss experiments can be seen in Table 2. Two mass loss experiments (FM1 and FM2) were performed on *F. vesiculosus*, the results of which were similar and so have been averaged in further analyses. Total percentage water content results were similar to Bravo-Linares et al. (2010) who reported 77% for *F. vesiculosus* and 79% for *U. intestinalis*. However, rates of water loss differed; Bravo-Linares et al. (2010) reported a faster rate of water loss for *F. vesiculosus* (7.4 % h⁻¹ compared to 4 % hr⁻¹ for *U. intestinalis*). As shown in Table 2, both the total percentage water loss and the percentage loss rate per hour were greater for *U. intestinalis*. Previous studies (e.g. Davison & Pearson, 1996) have suggested that overlapping algal fronds support water conservation and reduce water loss. In this experiment a mass of *U. intestinalis* fronds were spread out to form a mat, perhaps this reduced the protective ability of overlapping fronds and increased the rate of water loss. What we can see from these experiments is that *U. intestinalis* has a higher water content and, in our desiccation set up, dries more rapidly. These factors will be considered when comparing the differences between halocarbon emission rates of different species.

In following sections concentrations measured at each time point are converted to production (pmol g FW⁻¹ hr⁻¹). To calculate the mass of a sample at each time point during the halocarbon desiccation experiments (all FS, FL, US and UL coded experiments) percentage mass loss rates from these mass loss experiments (FM and UM) were applied to starting masses from FS, FL, US and UL. Differences in rate of water loss during FM and UM were observed depending on whether samples were taken several times an hour (an analogue for FS1-3 and US1-2) or hourly (an analogue for FL1-2 and UL). This is due to different exposures to 'desiccating' and 'sampling' flow rates (see Section 4.2.2). To account for this, mass loss rates for these two scenarios are also shown in Table 2, and the two rates were applied to starting masses as appropriate.

Table 2. Mass (water) loss rates during desiccation.

	<i>F. vesiculosus</i>	<i>U. intestinalis</i>
Percentage water content	75	88
Total percentage water loss (7 hours of desiccation)	77	85
Mean Rate of water loss (% hr ⁻¹)	7	12
% loss rate if 3 samples per hour	4.4	6.7
	1σ = 1.2	1σ = 1.6
% loss rate if 1 sample per hour	11.0	16.5
	1σ = 4.1	1σ = 4.0

4.3.4 F_v/F_m experiments

Measurements of changes in photosynthetic capacity during desiccation for both *F. vesiculosus* and *U. intestinalis* can be seen in Fig. 6. Care must be taken when comparing F_v/F_m results between studies as environmental factors can play a role in determining F_v/F_m . A higher F_v/F_m for one sample does not mean it has a higher photosynthetic capacity than another as variations in light and temperature can play a role in determining F_v/F_m (Walz, 1998). For this reason optimal or maximum F_v/F_m values for a 'healthy' sample are more a matter of relative measurements in an individual experiment than a hard-and-fast rule. For plants, F_v/F_m values of 0.8 to 0.835 in true dark-adapted samples have been observed (Walz, 1998), and previous studies on algae have reported F_v/F_m values in healthy *F. vesiculosus* and *U. intestinalis* samples of ~0.7-0.8 (Lewis et al., 2001; Magnusson, 1997; Pearson et al., 2000). Initial measurements of all replicates were made when the specimens were submerged in a small volume of seawater, and were around 0.7. Whilst some differences are observed between replicates in Fig. 6, the overall pattern was one of decline, with a quicker overall decline in F_v/F_m for UP1 compared to UP2. In FP a similar pattern was seen as in UP1, despite these experiments occurring on different days, with a period of stable F_v/F_m measurements followed by significant decreases occurring in hours 3 and 4.

Several of the replicates showed increases in the final F_v/F_m measurement. As we could find no previous records of this in the literature we attribute it to a sampling artefact. For comparable measurements a constant difference between the PAM and the sample must be maintained. As the algae dried considerably it could have shrunk away from the PAM attachment therefore altering readings.

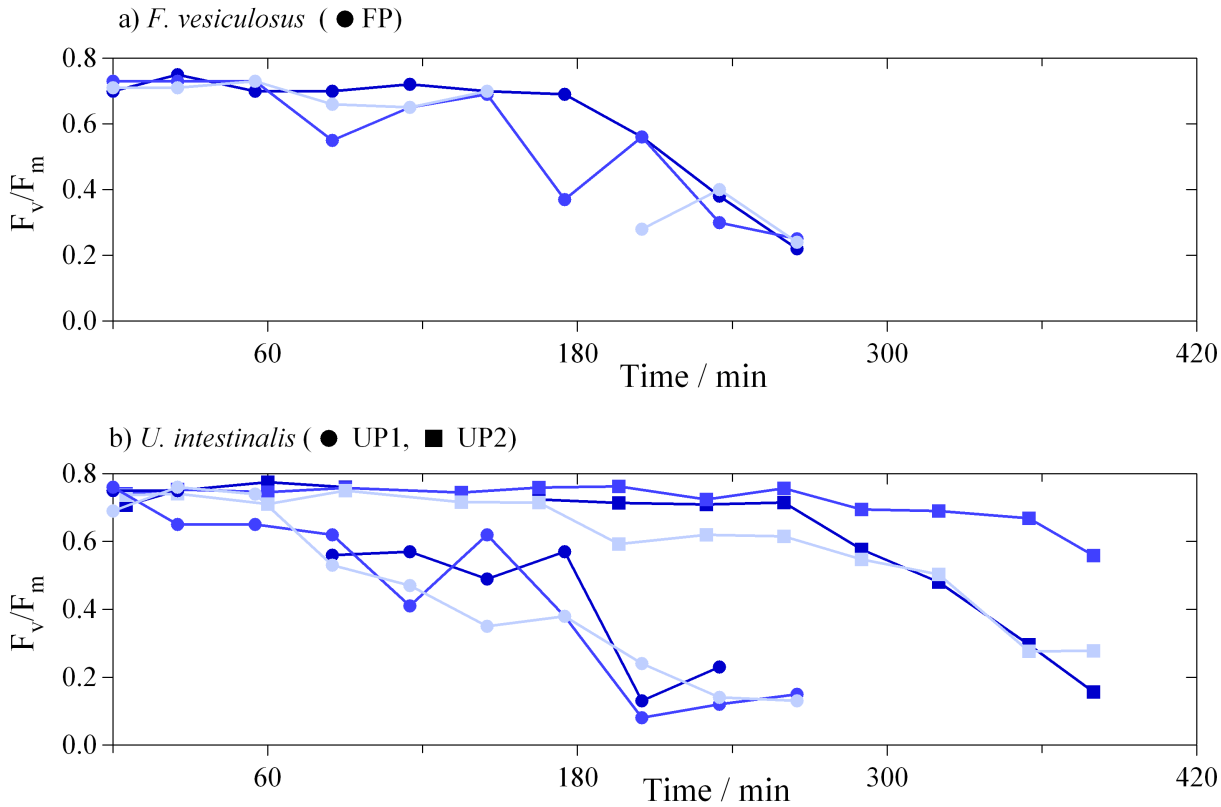


Figure 6. Changes in photosynthetic capacity (F_v/F_m) over time during desiccation of (a) *F. vesiculosus* (FP) and (b) *U. intestinalis* (UP1 and UP2). Blue lines/markers represent individual replicates in each experiment. Original in colour.

As described in Section 4.2.6, the F_v/F_m experiments (FP, UP1-2) were conducted on a bench in open petri dishes due to the need to dark adapt the samples before each measurement. Desiccation was faster in the F_v/F_m experiments compared to the halocarbon experiments (FS, FL, US and UL) and mass loss experiments (FM and UM), possibly as the samples were more exposed in open petri dishes compared to enclosed flasks. For example, the *F. vesiculosus* percentage mass loss after 3 hours was ~30% in FM experiments but 54% in FP. Fig. 7 shows the same F_v/F_m values as Fig. 6 plotted against percentage water loss (which was measured at several intervals during the F_v/F_m experiments). This allows a measure of comparison between the halocarbon (FS, FL, US, UL) and mass loss (FM and UM) experiments and these F_v/F_m experiments. For *F. vesiculosus* it appears that significant decreases in F_v/F_m do not begin to occur until about 50-60% of water is lost. For *U. intestinalis* the photosynthetic response varied, with some replicates showing a decline in F_v/F_m at water loss levels between 30 and 40% whilst other replicates did not show significant declines in photosynthetic capacity until up to 60% of water had been lost from the algal specimen.

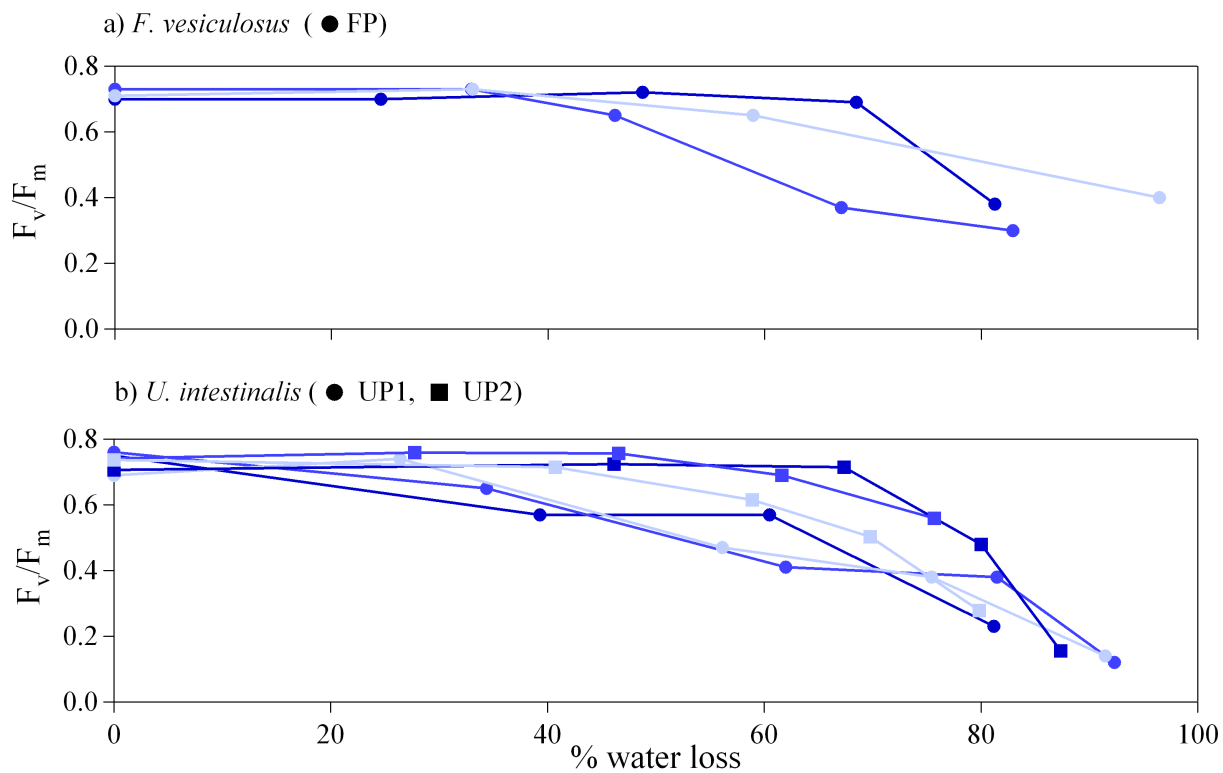


Figure 7. Changes in photosynthetic capacity (F_v/F_m) during desiccation of (a) *F. vesiculosus* (FP) and (b) *U. intestinalis* (UP1 and UP2) where state of desiccation is demonstrated by percentage water loss. Blue lines/markers represent individual replicates in each experiment. Original in colour.

4.3.5 Halocarbons emission patterns: submerged vs. exposed macroalgae

Five experiments (FS1-3 and US1-2) started with the algal specimen in the incubation flask whilst still submerged in 100 ml seawater (taken from the macroalgae storage tank). These experiments are shown in Fig. 8 (*F. vesiculosus* FS1-3) and Fig. 9 (*U. intestinalis* US1-2). Low headspace concentrations are observed when samples were submerged, followed by a rapid increase in both bromocarbons when the sample was exposed. A previous study by Ashu-Ayem et al. (2012) investigating I₂ emissions in a chamber saw similar effects; low emissions when the sample was submerged followed by a strong rapid-onset pulse upon full exposure which lasts 15-20 minutes before emissions began to slow or stopped.

To examine the partitioning between the water and headspace during the submerged portion of FS1-3 and US1-2 the dimensionless Henry's Law constant (k_H^{cc}), defined as the ratio of the aqueous phase concentration (c_a) over the gas phase concentration (c_g) was used. This constant is defined in Equation 1, alongside its relationship to the Henry's Law coefficient with respect to solubility (k_H), where R is the Ideal Gas Constant and T is temperature (in K).

$$k_H^{cc} = \frac{c_a}{c_g} = k_H \cdot RT \quad (1)$$

Equation 1 was used to calculate aqueous phase bromocarbon concentration in pmol L⁻¹ which could then be converted to production rates in pmol g FW⁻¹ hr⁻¹. Production rate ranges submerged samples in FS1-3 and US1-2 are show in Table 3 alongside production rates from exposed samples (FS, FL, US and UL experiments) and submerged samples from incubation experiments (details in Chapter 3). Samples used for seawater incubations were collected from the same site as desiccation samples and GCMS conditions post-sample injection were identical. Two of the seawater incubations were also conducted within a similar time period as the desiccation experiments. The bulk of halocarbon desiccation experiments were conducted between 31st January and 14th March 2012 and the seawater incubations of *U. intestinalis* and *Porphyra* sp. were conducted on the 24st January and 16th February 2012 respectively (Table 1). However, the incubation of *F. vesiculosus* was on 30th July 2012. Previous studies have demonstrated seasonal differences in internal halide and halocarbon concentrations (Itoh & Shinya, 1994), however we assume no significant differences in this study. No mass loss experiments were conducted on *Porphyra* sp. so this could not be compared quantitatively with its respective seawater incubation.

Patterns remained the same between both desiccation and submerged incubation experiments; production by *U. intestinalis* was greater than *F. vesiculosus* and CHBr_3 production was greater than CH_2Br_2 . These results show that at least some of the pulse in halocarbon emissions upon seaweed exposure is linked to emissions being directly to the atmosphere as opposed to into seawater followed by sea-air flux. This is shown by comparable production rates in seawater incubation experiments and from inferred seawater concentrations (using Henry's Law constants) during desiccation experiments (both highlighted in darker blue, Table 3) but lower production rates from the headspace of submerged samples (highlighted in light blue, Table 3). As seawater is removed, emissions are into a smaller volume of seawater leading to a larger bromocarbon concentration and therefore a greater flux (McFiggans et al., 2004). Emissions may also directly flux to the atmosphere upon exposure.

However, mean production rates for exposed *F. vesiculosus* and *U. intestinalis* were two to three orders of magnitude lower than production during seawater incubations for both CH_2Br_2 and CHBr_3 . The reduced production rates observed from exposed samples could be due to several factors. Firstly, a film of water covering the samples may be trapping some emissions in the aqueous phase, as discussed above. However, as samples were blotted dry to remove excess water before desiccating, this seems unlikely. Secondly, differences could be due to the use of two analytical techniques. A comparison between these two experiments (desiccation and seawater incubation) involves a comparison between two analytical techniques:

1. The purging, trapping and direct analysis of halocarbons in seawater (Chapter 3).
2. Trapping of halocarbons on sorbent tubes for subsequent desorption and analysis via a commercial Markes system (this chapter).

To further investigate, Table 3 also includes a comparison between seawater and atmospheric measurements using a different air sampling technique. Tropical species; *S. baccularia*, *Caulerpa* sp. and *P. australis*, were incubated in seawater (Chapter 3) and also placed in flux chambers (see Section 4.2.7). Again, these results show higher production from seawater incubations compared to exposed samples. Finally, it seems unlikely that losses of halocarbons during trapping onto the Markes tubes or subsequent storage of the tubes are wholly responsible for differences between desiccation experiments and seawater incubations for three reasons:

- Section 4.2.3 (and Fig. 5) demonstrated minimal analyte breakthrough.
- Tube storage without significant losses for up to 16 months demonstrated by Hughes et al. (2009).
- Table 3 also demonstrates lower atmospheric measurements for whole air samples.

Previous studies have demonstrated high levels of bromocarbons during low tide when in situ measurements have been made in a coastal environment (e.g. Carpenter et al., 1999) and, as discussed in the introductory section of this chapter as well as Chapter 1 Sections 1.3.3 and 1.6.2, the production of halocarbons in response to exposure and oxidative stress is well documented. It seems likely that some of the disparity between calculated production from seawater and atmospheric samples is, at least in part, linked to differences in measurement techniques, this will be discussed further in Section 4.4.3. The need to further our collective understanding of the roles different experimental and analytical techniques play in results observed in different studies is discussed further in Chapter 6 Section 6.4.1.

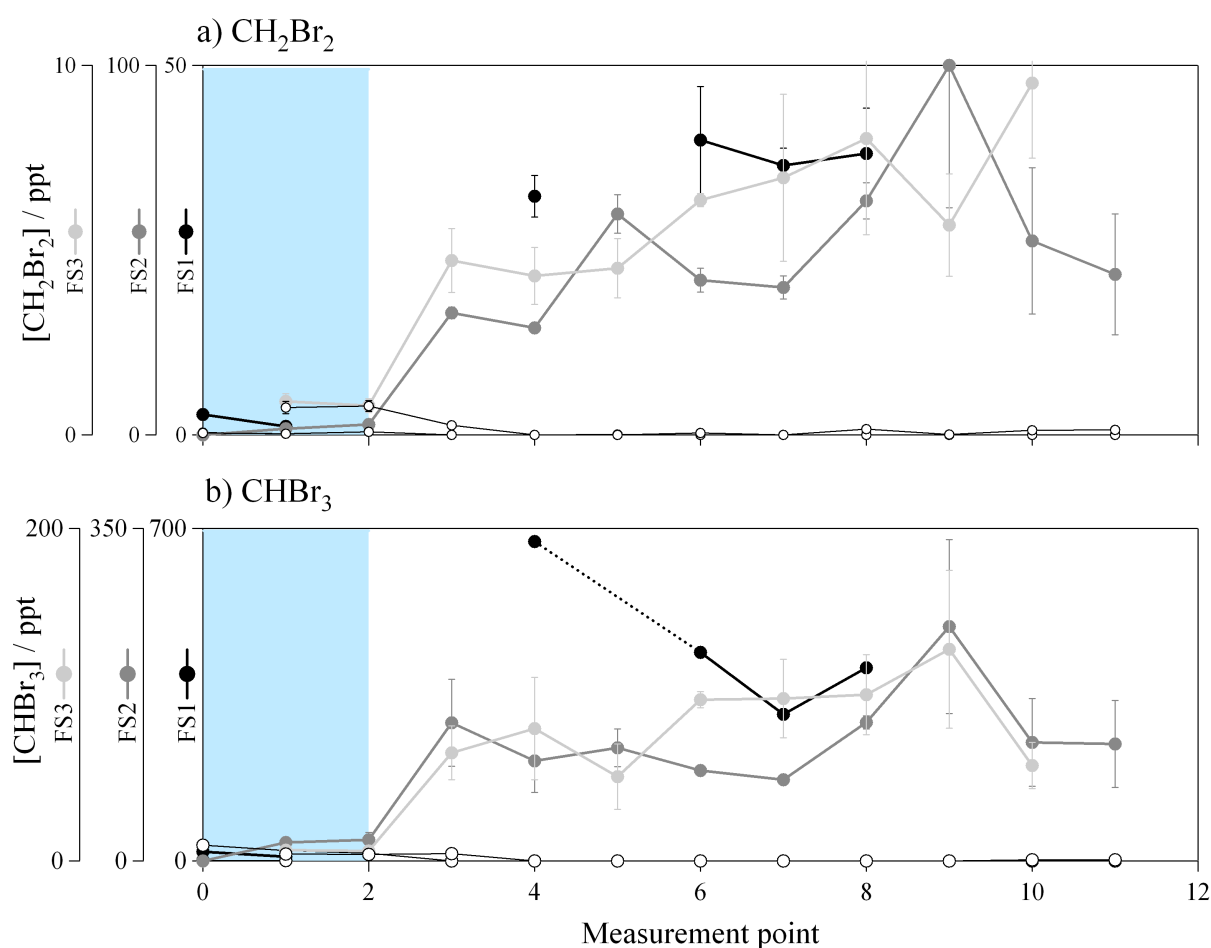


Figure 8. Concentration of (a) CH_2Br_2 and (b) CHBr_3 observed in flasks when *F. vesiculosus* specimens are submerged (blue background) and exposed (white background). These are experiments FS1-3. Closed circles are algal replicates, open are controls. Error bars are described in Section 4.3.2. Original in colour.

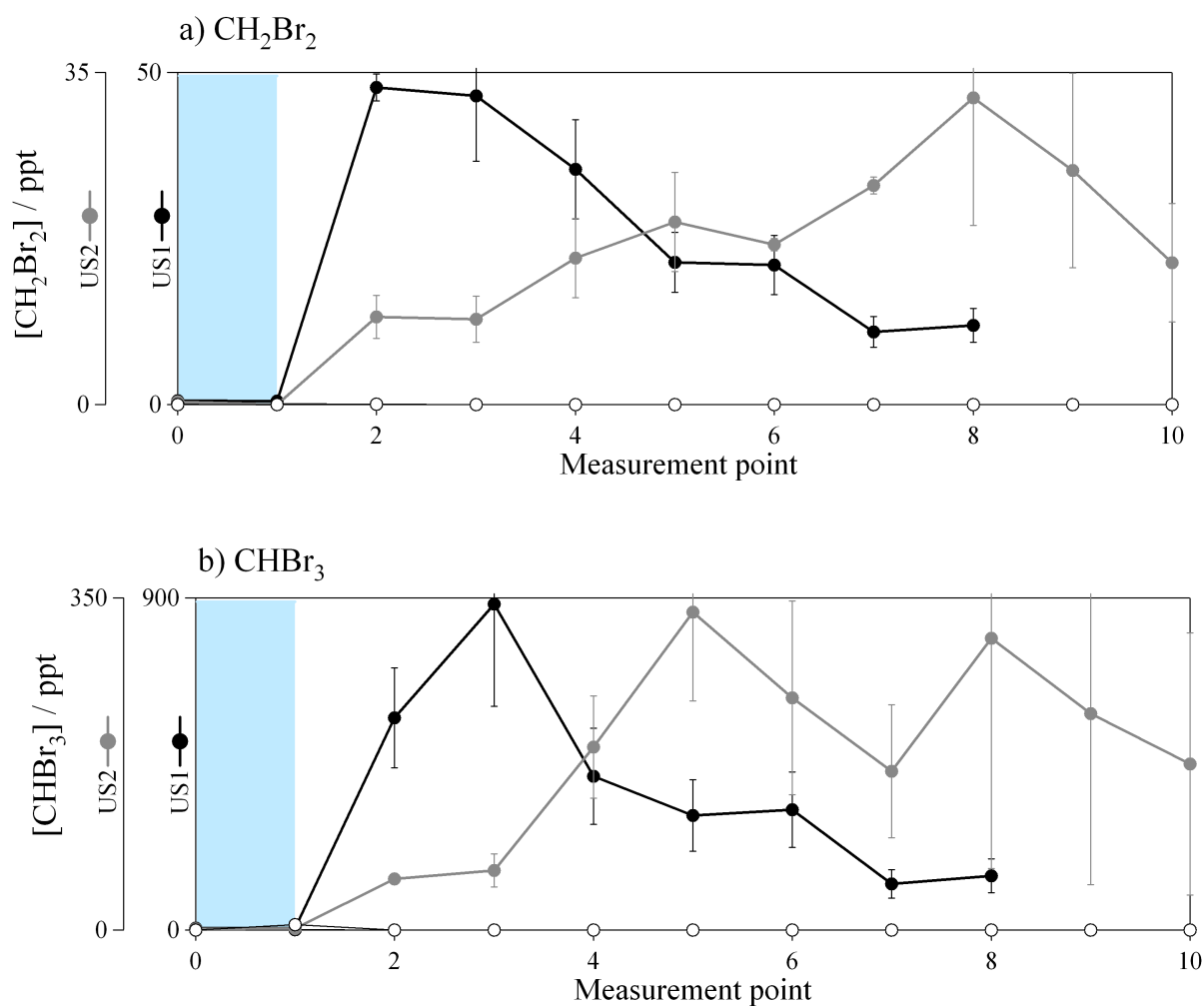


Figure 9. Concentration of (a) CH₂Br₂ and (b) CHBr₃ observed in flasks when *U. intestinalis* specimens are submerged (blue background) and exposed (white background). These are experiments US1-2. Closed circles are algal replicates, open are controls. Error bars are described in Section 4.3.2. Original in colour.

Table 3. Production (pmol g FW⁻¹ hr⁻¹) during desiccation/exposure experiments and seawater incubations.

Experiment n= individual data points included in range	Production / pmol g FW ⁻¹ hr ⁻¹	
	CH ₂ Br ₂	CHBr ₃
<i>F. vesiculosus</i>		
Desiccation experiments, submerged samples – production calculated from inferred seawater concentrations (FS1-3, n=6)	69 - 200	615 - 1140
Desiccation experiments, submerged samples – production calculated from headspace concentrations (FS1-3, n=6)	0.02 - 0.06	0.2-0.4
Desiccation experiments, exposed samples (FS1-3 & FL1-2, n=43)	0 - 4	0 - 19
Incubation experiments, submerged samples (t24, n=2)	21 - 122	217 - 954
<i>U. intestinalis</i>		
Desiccation experiments, submerged samples – production calculated from inferred seawater concentrations (US1-2, n=4)	30 - 43	183 - 626
Desiccation experiments, submerged samples – production calculated from headspace concentrations (US1-2, n=4)	0.01 - 0.02	0.1 - 0.2
Desiccation experiments – exposed (US1-2 & UL1, n=28)	0.4 - 2	1 - 27
Incubation experiments (t24, n=3)	524 - 907	1994 - 2648
Tropical incubations		
<i>S. baccularia</i>		
Seawater incubation (t24, n=2)	6 - 11	8-13
Desiccation (n=2)*	0.3	0.6
<i>Caulerpa sp.</i>		
Seawater incubation (t24, n=3)	1-12	0.4-9
Desiccation (n=1*)	0.02	0.07
<i>P. australis</i>		
Seawater incubation (t24, n=2)	6-8	8-9
Desiccation (n=1*)	0.02	0.08

All desiccation flux chamber experiments were comprised of 1 (or 2 in the case of *S. baccularia*) flux chambers under which a seaweed sample was placed for 30 minutes of exposure. One air sample was collected and analysed at least twice, the average of these analyses are provided here.

4.3.6 Halocarbons emission patterns during desiccation of macroalgae

i. F. vesiculosus

The first set of experiments studied the bromocarbon production of *F. vesiculosus* over a short desiccation period of 2-3 hours (FS1, FS2 and FS3). Each of these experiments comprised one flask containing a seaweed sample and one control flask. Desiccation over a longer period of up to 8 hours was investigated in FL1 and FL2, each of which used two samples and one control (full details in Table 1). Results for CH_2Br_2 and CHBr_3 can be seen in Figs. 10 and 11 respectively. *F. vesiculosus* samples showed emission of bromocarbons in all experiments. The concentrations in the sample flasks were significantly higher than in the control at the start of the experiment and control flasks maintained low concentrations, 0-2 ppt for CH_2Br_2 and 0-3.7 ppt for CHBr_3 , for the duration of the incubations. No consistent increases or decreases with time were seen in any of the control flasks despite the fact control flasks had been wetted with a small amount of seawater likely to contain halocarbons. Halocarbon concentrations seen in sample flasks are therefore likely to be due to production by the seaweed or release from the surface of the algae, not evaporation of seawater. Regular blank tubes (at least 1 in 10) were run through the analytical system and these also failed to show any patterns in background bromocarbon levels. Any changes in sample flask concentrations are therefore attributable to the algal samples.

In FS1 CH_2Br_2 concentrations remained steady for the 2 hour duration of the experiment. In FS2 and FS3 concentrations rose or remained steady until around 2 hours when they began to increase. Concentration in the sample flask was greater than in the control at the end of all three experiments.

In the 'FL' labelled experiments, which exposed the seaweeds to desiccating conditions for longer time periods, the responses of individual specimens can be broadly divided into two groups. In FL1 CH_2Br_2 concentrations were highest at the start of the experiment, with a general decrease from this point onwards. In FL2 decreases in concentration at the start of the experiment were followed by later peaks, up to 4 hours into desiccation. As only one sample an hour was taken during FL2 the peak is only visible in one sample, returning to previous levels by the 5th hour. However, peaks of carbon tetrachloride (CCl_4), a compound which is not biogenically produced, remained the same as previous samples during this peak in CH_2Br_2 and CHBr_3 (data not shown). This supports a biological source for this peak and not analytical error. Concentrations remained similar to that at the start for several hours before decreasing. In the majority of longer desiccation samples concentrations had reached, or were close to, control levels within 5 hours of exposure.

Short (FS and US) and long (FL and UL) desiccation experiments, varied slightly in their protocol, the FL and UL experiments exposed the seaweeds to higher flow rates for a longer period of time (see Table 1). This could help explain some of the difference between replicates, for example the period in which emissions increases or remained stable is longer in FS1-3 than in FL1-2 (Fig. 10). No differences in the range of concentrations were observed between the FS and FL experiments. For example, the range of CH_2Br_2 concentrations was 6-167 ppt in FS1-3 and 0-163 ppt in FL1-2. CHBr_3 concentrations were also similar between FS and FL experiments (Fig. 11), as were the range of both CH_2Br_2 and CHBr_3 concentrations in US1-2 and UL1 (Figs. 12 and 13).

The CHBr_3 emission patterns (Fig. 11) were similar to that of CH_2Br_2 for all experiments except FS3, in which CHBr_3 showed a slightly prolonged period of increase compared to CH_2Br_2 . This is not unexpected given that incubation experiments in Chapter 3 showed a correlation between CH_2Br_2 and CHBr_3 . A discussion of the relationship between these halocarbons can be found in Chapter 3, Section 3.3.3.

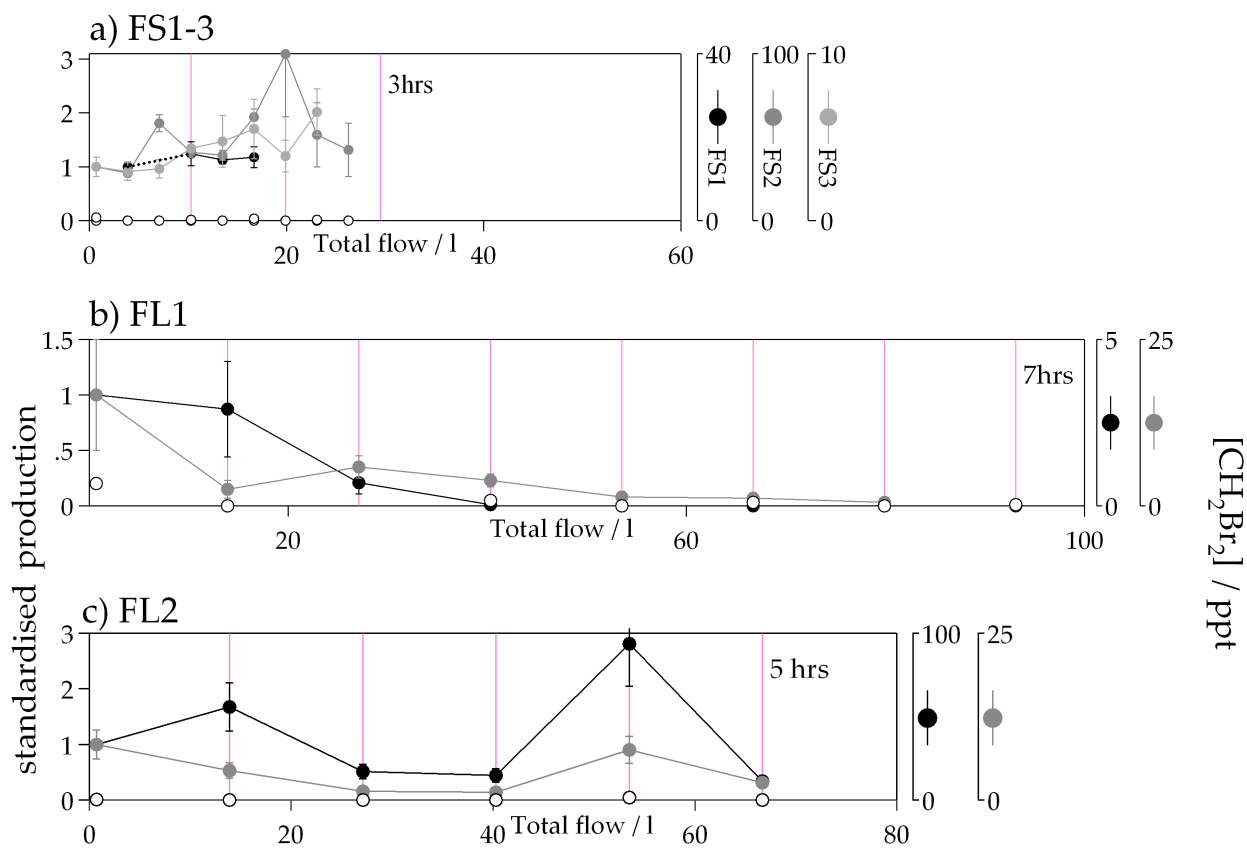


Figure 10. Changes in CH₂Br₂ concentration during desiccation of *F. vesiculosus*. Left axis shows standardised production, floating right axis shows concentration (ppt). Changes are expressed against total flow (l) through the incubation system. Closed circles are algal replicates, open are controls. Time (hours) shown by vertical pink bars. Error bars are described in Section 4.3.2. Original in colour.

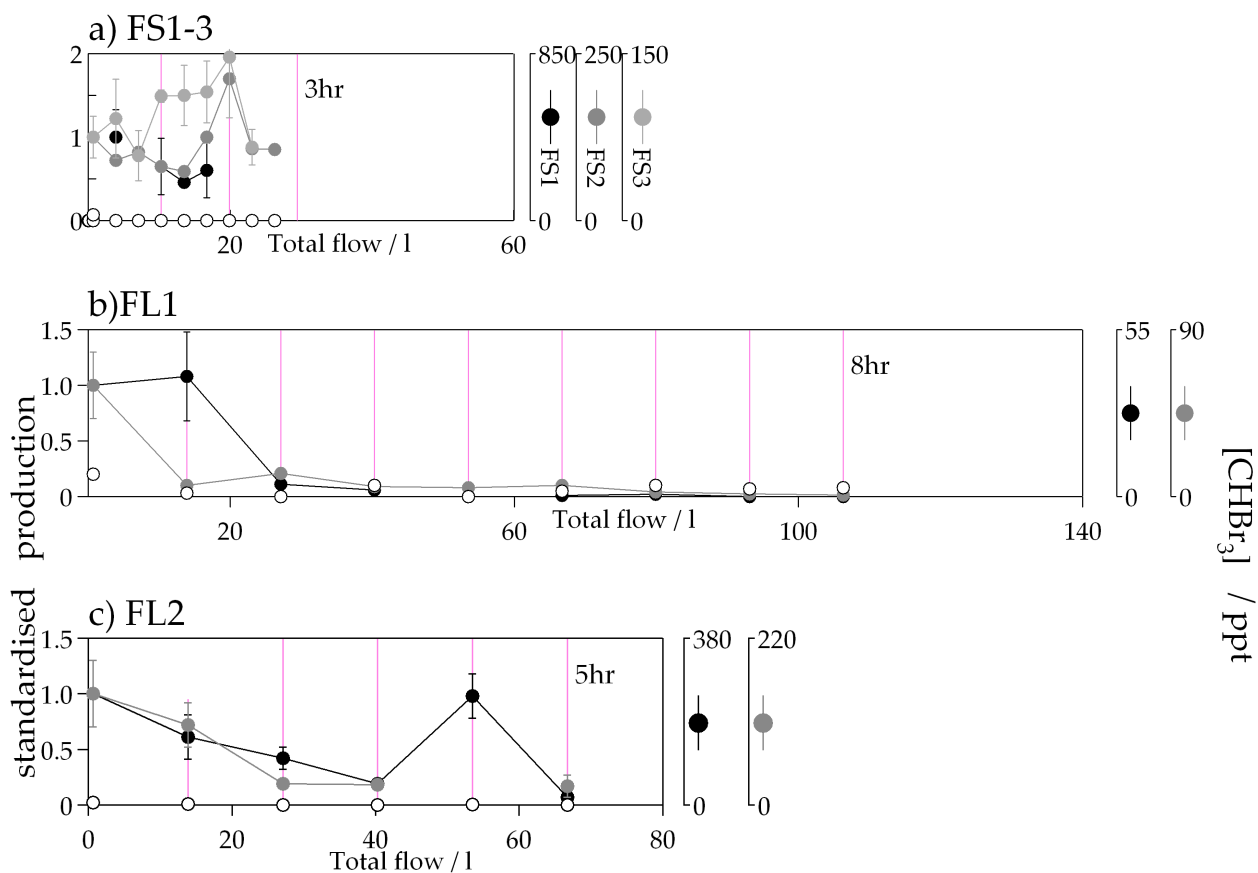


Figure 11. Changes in CHBr₃ concentration during desiccation of *E. vesiculosus*. Left axis shows standardised production, floating right axis shows concentration (ppt). Changes are expressed against total flow (l) through the incubation system. Closed circles are algal replicates, open are controls. Time (hours) shown by vertical pink bars. Error bars are described in Section 4.3.2. Original in colour.

ii. *U. intestinalis*

CH_2Br_2 and CHBr_3 emission by *U. intestinalis* during desiccation can be seen in Figs. 12 and 13 respectively. The first short *U. intestinalis* incubation (US1) showed similar results to many of the *F. vesiculosus* desiccation incubations in that concentrations of CH_2Br_2 and CHBr_3 peaked at or near the start of the experiment and then decreased steadily. Unfortunately, analytical problems occurred and the US1 hour 3 samples were lost. CHBr_3 concentrations in US2 (Fig. 13) show an interesting 'saw-tooth' double peak within a short period of time, although much of this may be within the error range. It could be that other experiments, where measurements were obtained less frequently, miss some of these features. The longer *U. intestinalis* incubation, UL, showed sustained halocarbon concentrations that were not seen in many of the FL experiments. Concentrations of both CH_2Br_2 and CHBr_3 remained similar to starting concentrations up to 5-7 hours after the experiment began.

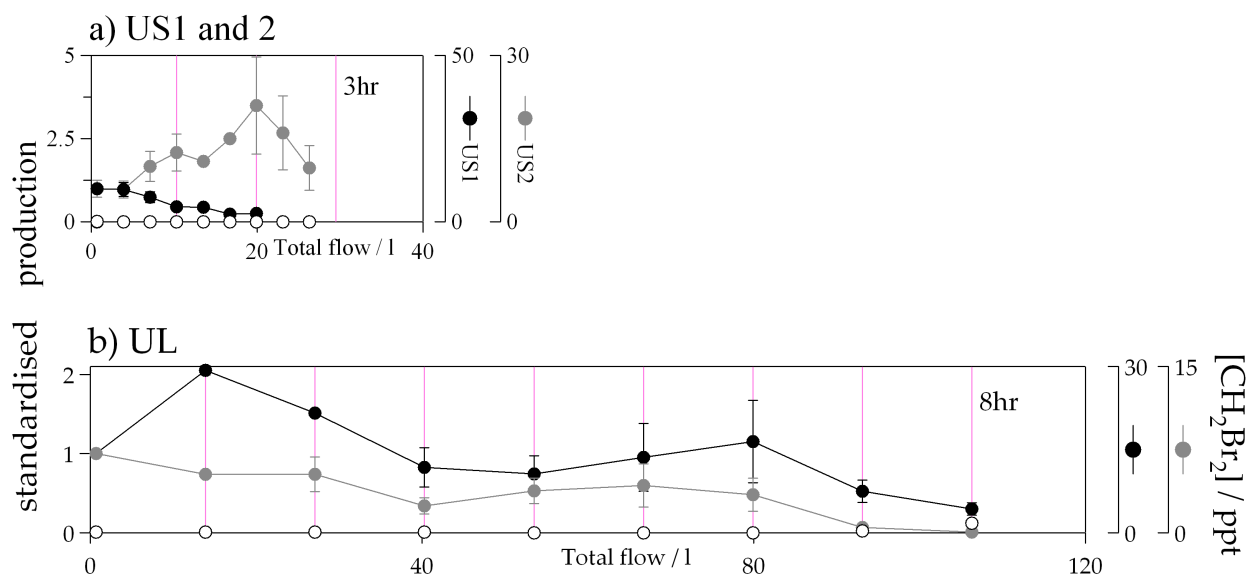


Figure 12. Changes in CH_2Br_2 concentration during desiccation of *U. intestinalis*. Left axis shows standardised production, floating right axis shows concentration (ppt). Changes are expressed against total flow (l) through the incubation system. Closed circles are algal replicates, open are controls. Time (hours) shown by vertical pink bars. Error bars are described in Section 4.3.2. Original in colour.

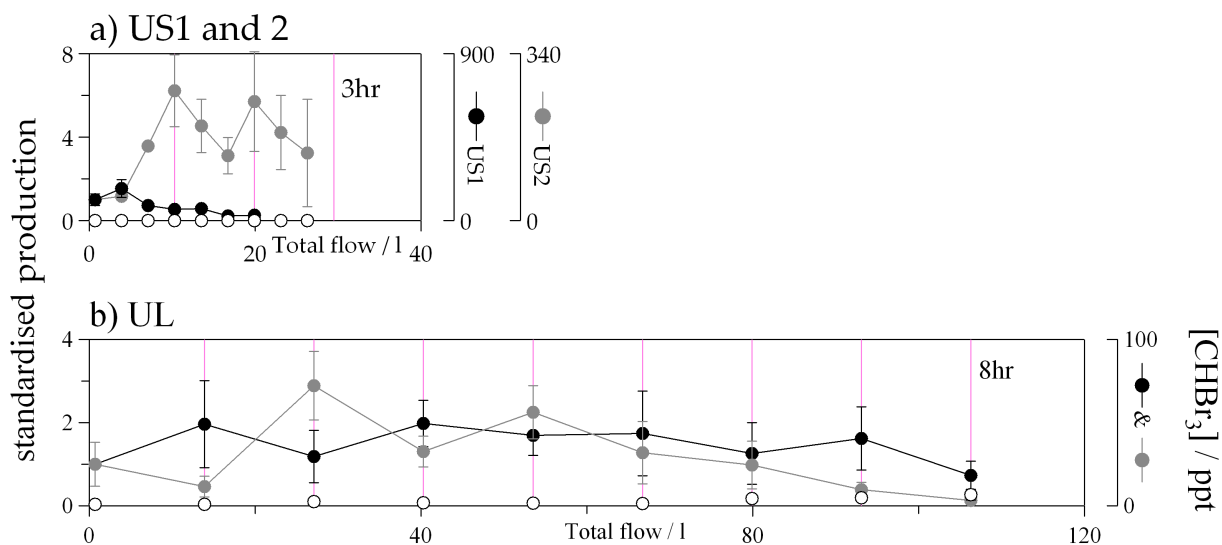


Figure 13. Changes in CHBr₃ concentration of during desiccation of *U. intestinalis*. Left axis shows standardised production, floating right axis shows concentration (ppt). Changes are expressed against total flow (l) through the incubation system. Closed circles are algal replicates, open are controls. Time (hours) shown by vertical pink bars. Error bars are described in Section 4.3.2. Original in colour.

iii. *Porphyra sp.*

Only one experiment was conducted on *Porphyra sp.* in which the two replicates were incubated for nearly 8 hours, emissions of both CH_2Br_2 and CHBr_3 can be seen in Fig. 14. CH_2Br_2 emissions peak at the start of the experiment and decrease steadily until they reach control levels between 2-3 hours into the experiment. CHBr_3 concentrations in the control were higher than all other *F. vesiculosus* and *U. intestinalis* experiments; the mean control value was ~11 ppt (with a range of 0-31 ppt) compared to mean control values of between 0.3-5 ppt for the other experiments. As the CHBr_3 concentrations in the *Porphyra* incubations were low, with a mean value of 5.7 ppt and only one value falling above 20 ppt, little can be said about significant patterns of CHBr_3 emission from *Porphyra* in this incubation due the higher concentrations in the control.

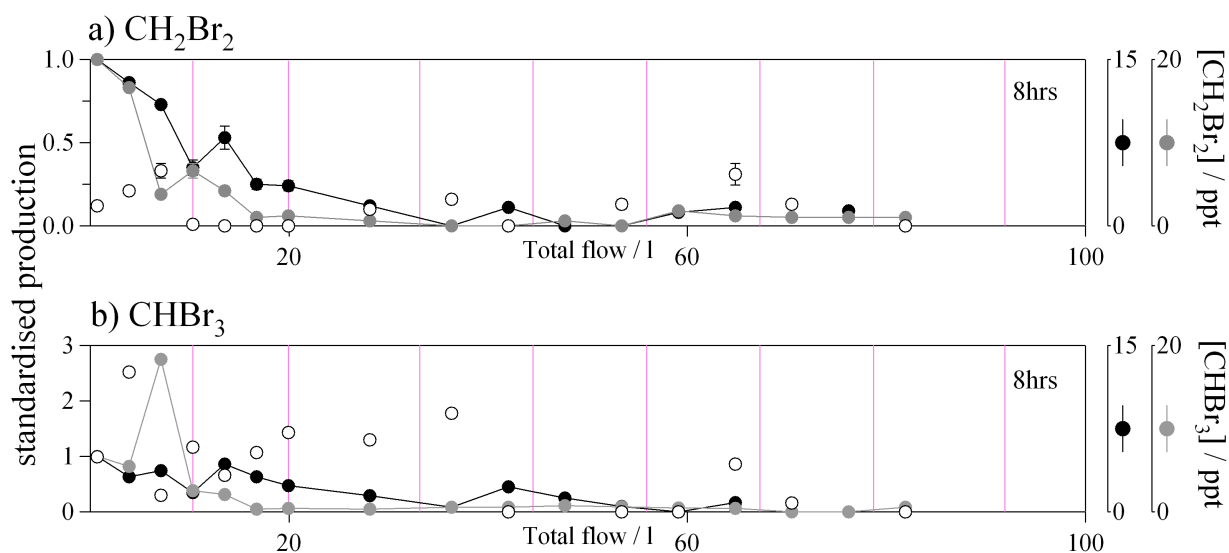


Figure 14. Changes in concentration of (a) CH_2Br_2 and (b) CHBr_3 during desiccation of *Porphyra sp.* Left axis shows standardised production, floating right axis shows concentration (ppt). Closed circles are algal replicates, open are controls. Changes are expressed against total flow (l) through the incubation system. Time (hours) shown by vertical pink bars. Error bars are described in Section 4.3.2. Original in colour.

4.3.7 Halocarbon production/emission rates

To compare with other studies; both previous desiccation studies and also seawater incubations (Section 4.3.5) a production rate is needed. To calculate production per gram of fresh weight we used the mass loss experiments FM1 and FM2 (total $n=5$) and UM ($n=3$). Mass loss rates described in Section 4.3.3 were applied to the known starting mass for FS1-3 and FL1-2 to provide an estimated mass to correspond with every halocarbon measurement. As air was constantly flowing through each flask, and as the total flow through the flask between samples (2.5-5 l) was at least double that of the flask volume (1 l) we assume that any bromocarbons measured during sampling were released from the seaweed during the 10 minute sampling period. This information can then be used to calculate a production rate in $\text{pmol g FW}^{-1} \text{ min}^{-1}$. This process was then repeated for *U. intestinalis*.

In terms of patterns during the individual desiccation experiments (Figs. 10-13) the patterns of emission peaks and declines remain the same whether bromocarbon production rates or concentrations are used. The benefit of calculated production values lies in the ability to make comparisons between species, and also between this and other studies.

Firstly, to compare production between species histogram distributions of production values for both *F. vesiculosus* and *U. intestinalis* can be seen in Figs. 15 and 16 respectively. These histograms include production data from FS1-3 and FL1-2 (51 values in total) for *F. vesiculosus* and US1-2 and UL (34 values) for *U. intestinalis*. For *F. vesiculosus* about 60% of the CH_2Br_2 values and 50% of the CHBr_3 values are in the lowest bin. The values that fall within this bin have been binned again, and this histogram is superimposed in black. The main difference between the *F. vesiculosus* (Fig. 15) and *U. intestinalis* (Fig. 16) histograms is that the spread of values is far more even for *U. intestinalis* than for *F. vesiculosus*. The maximum CH_2Br_2 production rate was from a *F. vesiculosus* experiment, at $\sim 4 \text{ pmol g FW}^{-1} \text{ h}^{-1}$. However, more production rates over $1 \text{ pmol g FW}^{-1} \text{ h}^{-1}$ were recorded for *U. intestinalis*, and *U. intestinalis* also demonstrated the highest CHBr_3 production rate at $27 \text{ pmol g FW}^{-1} \text{ h}^{-1}$ compared to $16 \text{ pmol g FW}^{-1} \text{ h}^{-1}$ for *F. vesiculosus*. A statistical comparison was conducted on the complete *F. vesiculosus* and *U. intestinalis* datasets (using data from individual experiments: FS1-3, FL1-2, US1-2 and UL). As the data failed normality tests ($p < 0.001$) a non-parametric Mann-Whitney Rank Sums Test was used. The results showed a statistically significant difference between *F. vesiculosus* and *U. intestinalis* production rates of both CH_2Br_2 and CHBr_3 (both $p < 0.001$). Possible reasons for these differences will be discussed in further detail in Section 4.4.1.

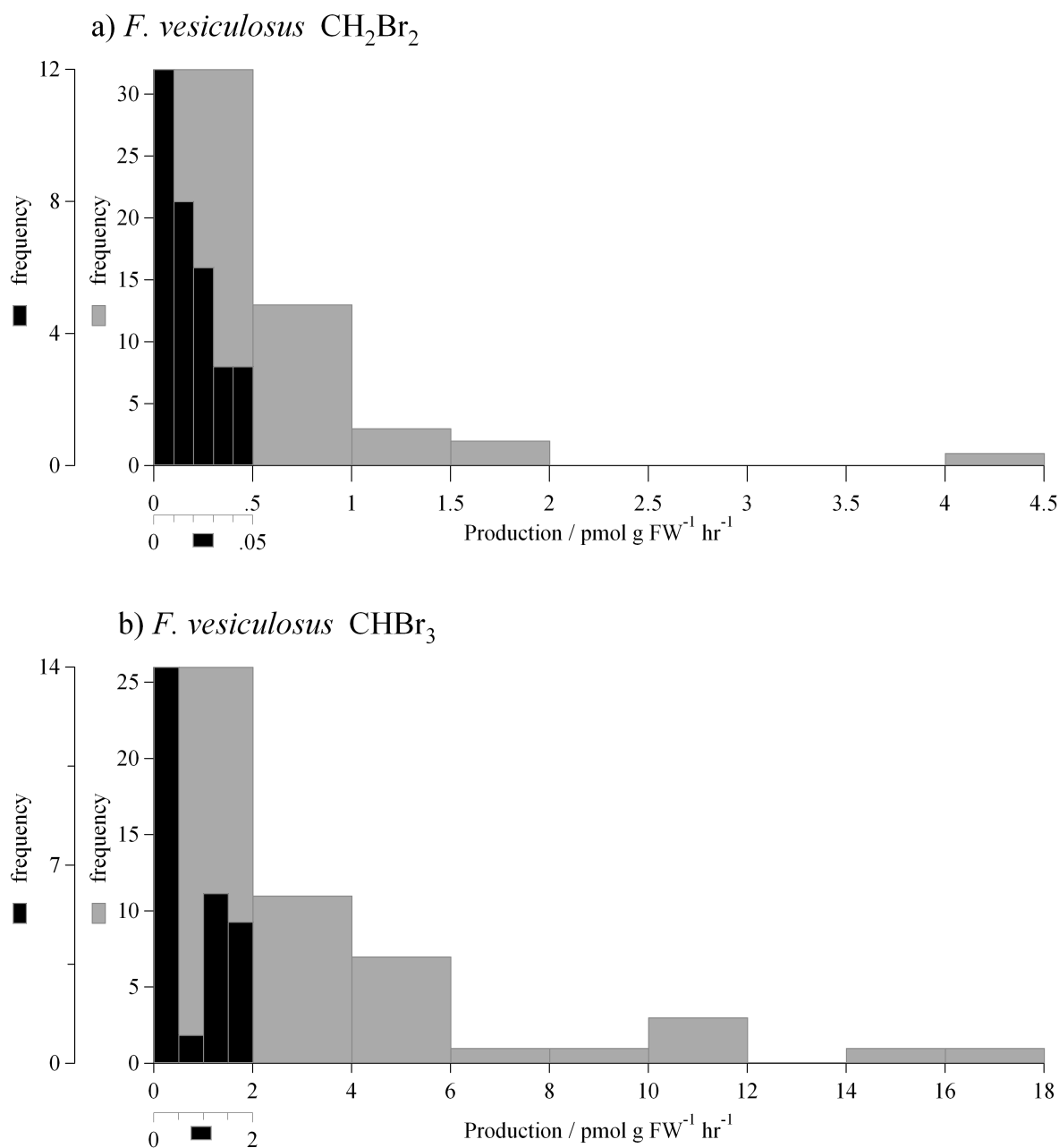


Figure 15. Distribution of (a) CH₂Br₂ and (b) CHBr₃ production rates (n=51) during desiccation of *F. vesiculosus*. Black overlaid histogram represents the distribution of values within the first grey bin.

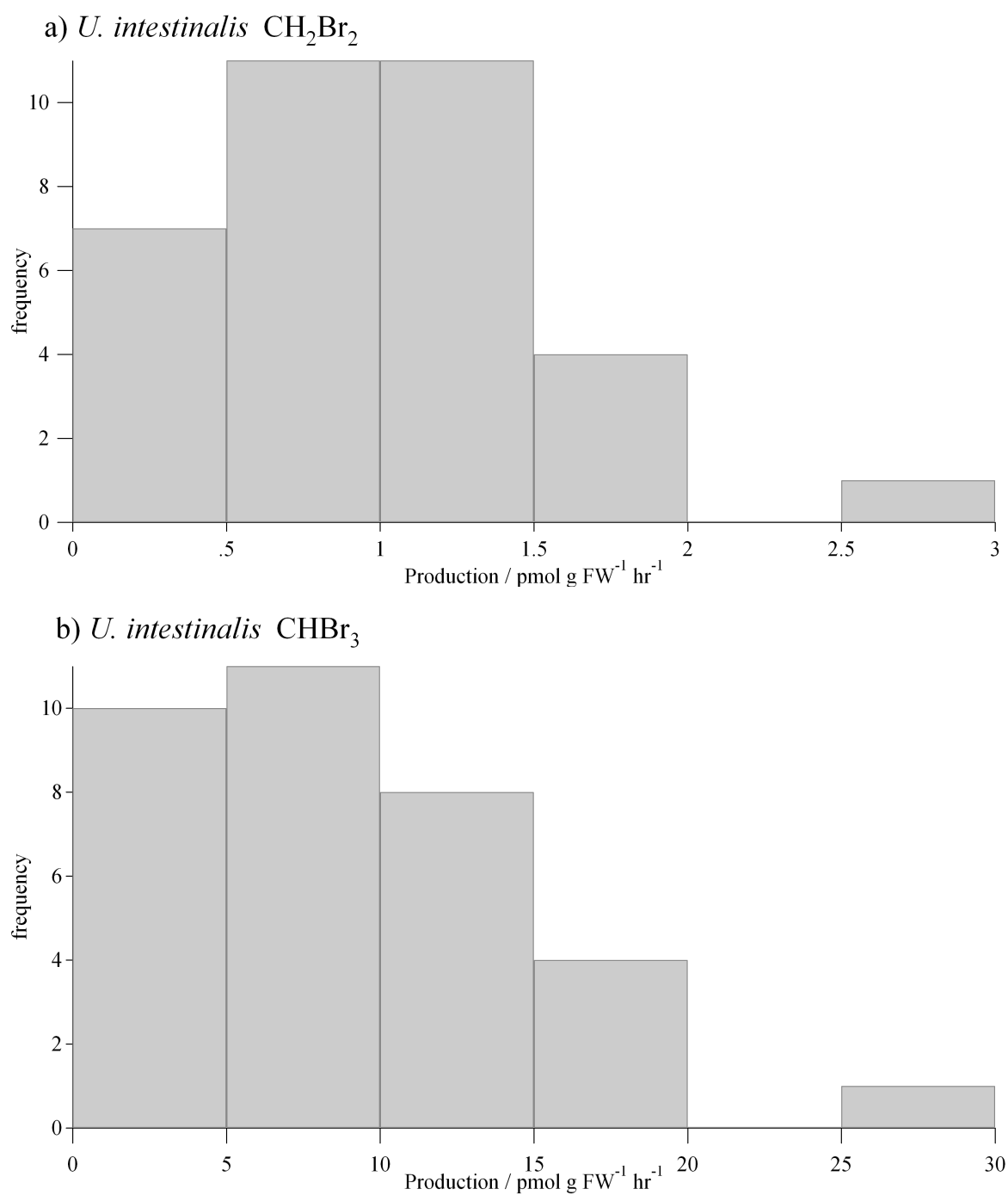


Figure 16 Distribution of (a) CH₂Br₂ and (b) CHBr₃ production rates (n=34) during desiccation of *U. intestinalis*.

4.3.8 Rewetting experiments

As described in Section 4.1.2, physiological damage may also be caused by freshwater rewetting of the alga during desiccation. To investigate this, a series of experiments (URFW1-3) were conducted, rewetting *U. intestinalis* with freshwater after a period of desiccation were conducted. It was hoped this may replicate the effect of rewetting with rainwater. Desiccation using the incubation set up followed the same principle as for previous experiments (e.g. US1-2 and UL), then after a period of desiccation varying from ~3-8 hours (see Table 1) samples were rewetted as described in Section 4.2.6. The results can be seen in Fig. 17 (CH_2Br_2) and Fig. 18 (CHBr_3). URFW1 and URFW3 (panels a and c in both diagrams) rewetted the seaweed after a long period of desiccation, ~6 and 8 hours respectively. During URFW1 halocarbon samples were not taken for the first 5 hours as the experimental aim was to concentrate on the rewetting process. However, measuring halocarbon emissions for only 1 hour before rewetting makes it difficult to determine changes in emission patterns upon rewetting and for subsequent experiments (URFW2-3) halocarbon measurements were taken frequently throughout the entire experiment.

In URFW3 little change is observed after rewetting, potentially a slight increase in both CH_2Br_2 and CHBr_3 can be observed. However, this is of no greater magnitude than other fluctuations during the desiccation process, for example URFW3 replicate 'a' between 5-7 hours. URFW2, however, showed an increase in both CH_2Br_2 and CHBr_3 emissions after freshwater rewetting. The increase in emissions is considerable, rising to over half the maximum emission near the start of the experiment. At the time sampling finished for URFW2 the concentration of CH_2Br_2 and CHBr_3 in the flasks appeared to still be increasing.

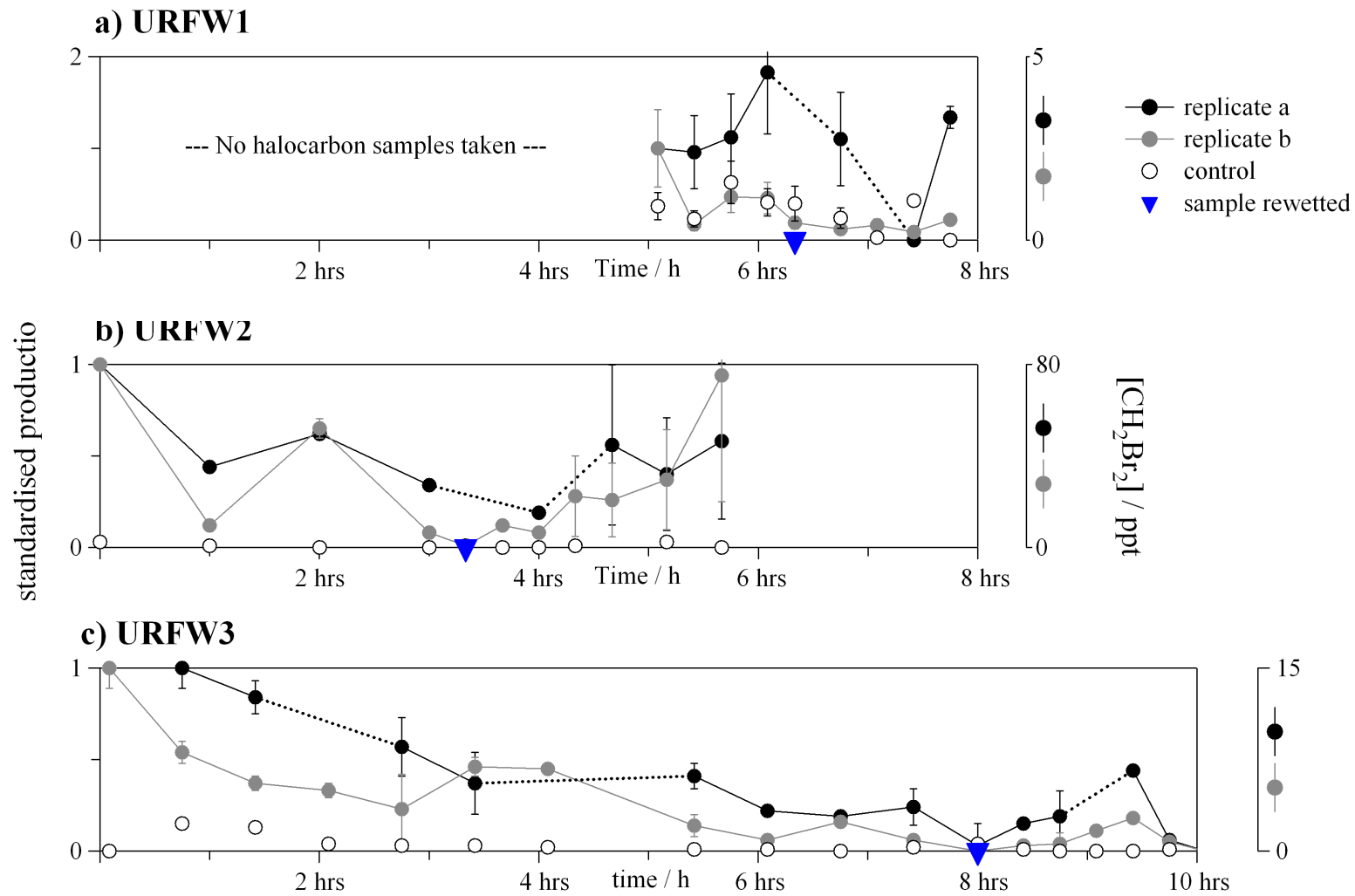


Figure 17. Changes in CH_2Br_2 concentration during desiccation and freshwater rewetting of *U. intestinalis*. Left axis shows standardised production, floating right axis shows concentration (ppt). Closed circles are replicates, open are control. Error bars are described in Section 4.3.2. Original in colour.

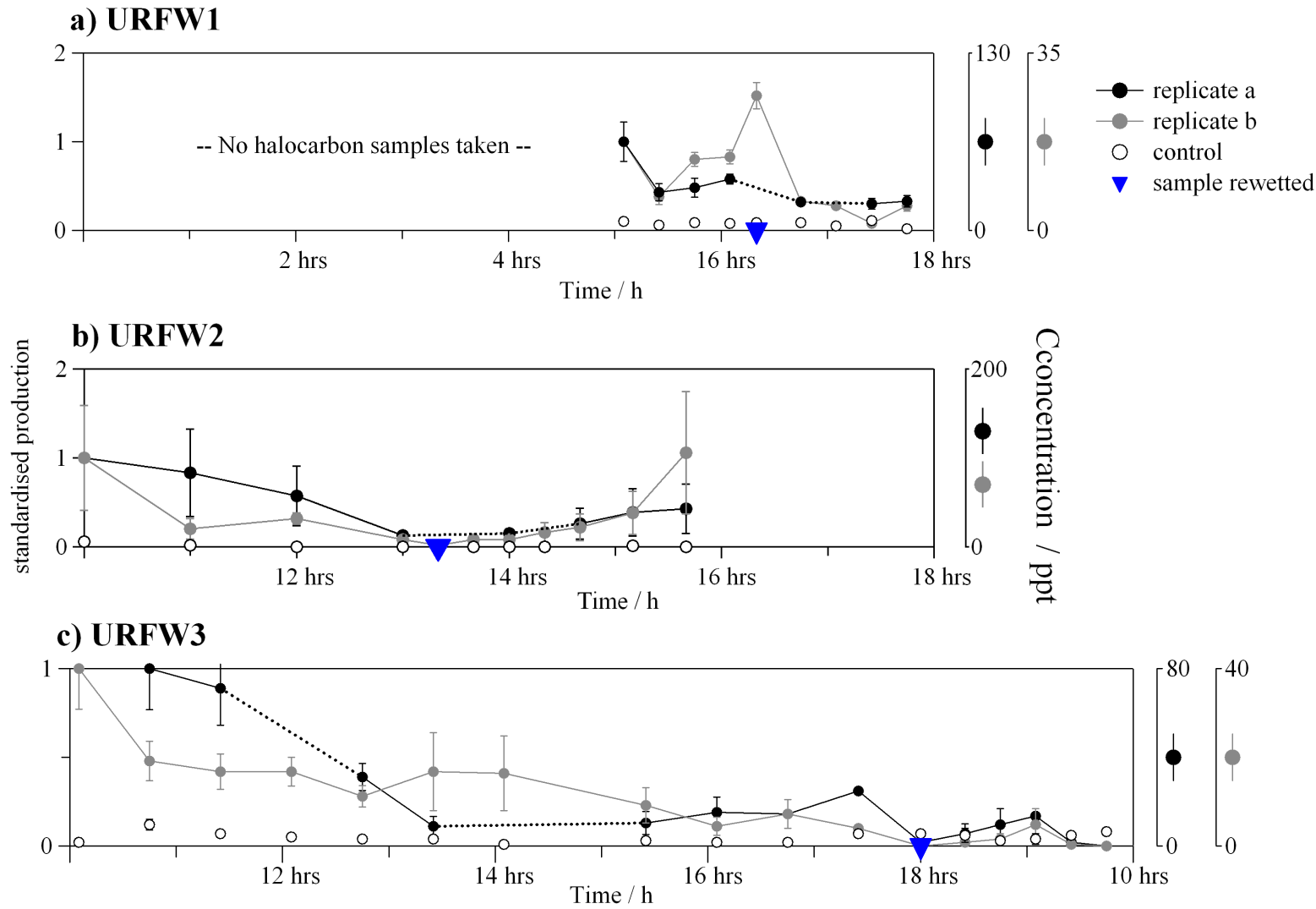


Figure 18. Changes in CHBr_3 concentration during desiccation and freshwater rewetting of *U. intestinalis*. Left axis shows standardised production, floating right axis shows concentration (ppt). Closed circles are replicates, open are control. Error bars are described in Section 4.3.2. Original in colour.

4.4 Discussion - the halocarbon response to desiccation

Much of the early work on halocarbon emissions during desiccation was driven by the interest in iodine and its role in particulate formation. Early studies identified tidal cycles in measurements of polyhalomethanes (including CHBr_3) over seaweed beds, alongside bursts of iodine-containing particles at low tide (Carpenter et al., 1999; Mäkelä et al., 2002). To investigate this further chamber studies were used, commonly using the phaeophyte *L. digitata* (Caine et al., 2007; McFiggans et al., 2004; Palmer et al., 2005). Bursts of particulate production linked to emission of molecular I_2 were reported, but these studies did not include details of the duration of these bursts. Often the chamber experiments altered environmental conditions during the duration of desiccation, for example switching ozone or light on and off, making it hard to judge the magnitude of these emissions under natural desiccation conditions. Less work has been done on bromocarbon production during desiccation. The studies that are available focused on natural halocarbon production in coastal waters and so also did not concentrate on the timescale of emissions. Nightingale et al. (1995) desiccated algae for several hours to mimic a tidal cycle but measurements were made to simulate the resubmergence of seaweeds after exposure, not during exposure itself. A pulse of halocarbon emissions was reported upon reimmersion, but, as described in Section 4.1.4 damage can be caused by both exposure and reimmersion, and so the magnitude of this peak cannot be attributed to either. Another study which desiccated and then measured halocarbon production upon reimmersion saw a general decrease in brominated compounds after desiccation but a general increase in iodinated compounds (Bravo-Linares et al., 2010). Again, this response could be linked to reimmersion stress as well as desiccation itself. Two recent studies have looked at the time profiles of emissions during desiccation. Ball et al. (2010) measured time profiles of molecular iodine, I_2 , in a set of 10 incubations of 7 temperate phaeophytes. Their results showed that, in some incubations, short bursts of I_2 did occur near the start of the experiment and in others that there was a gentle rise up to higher concentrations of I_2 . All experiments in the Ball et al. study lasted less than one hour and increases, peaks and decreases were seen within this time. Another study, by Kundel et al. (2012), also conducted I_2 time series for several species. Again, they saw an I_2 response that was either rapid pulses with durational maxima of 20-30 minutes or gradually increasing emissions. Emissions of various iodocarbons were also measured, although time series were not reported.

Our results build on previous I_2 experiments by showing that bromocarbon emissions may also display rapid peaks early on in the desiccation process before emissions fall to zero within a few hours. Several replicates in our study showed quickly evolving peaks (e.g. FL2a, US2) which were seen previously (e.g. Kundel et al., 2012). The high sampling frequency of our experiments allowed the observation of these bursts which has seldom been possible in previous desiccation studies.

Similarities between the two species included an initial halocarbon burst followed by decreasing emissions over time. The main difference between the two species, despite collecting both species from the same site and position on the shore, is a prolonged emission from *U. intestinalis* (UL1, Figs. 12 and 13) compared to *F. vesiculosus* (FL1-2, Figs. 10 and 11). Emission patterns pre-rewetting in URFW2 and URFW3 (Figs. 17 and 18) act as replicates for UL as they were conducted in the same way. They also show emissions taking longer to decrease than seen in the *F. vesiculosus* experiments. Sharper peaks in emissions were noted during *F. vesiculosus* experiments compared to *U. intestinalis*. These differences will be discussed in more detail in subsequent sections.

4.4.1 Variation in desiccation rate between species

Both *F. vesiculosus* and *U. intestinalis* demonstrated a relatively linear pattern of water loss, as seen in previous studies (Bravo-Linares et al., 2010, Ji & Tanaka, 2002). Rates of water loss, however, differed between the two species (Table 2). After four hours of desiccation *F. vesiculosus* samples had lost ~35% of their mass, similar to Lüning (1990) who reported water loss of 20-30% in fucoid species after 4 hours. The loss rate was higher for *U. intestinalis* at ~50% after 4 hours. Morphological differences may explain differences in water loss. *F. vesiculosus*, a phaeophyte, is a perennial species with a differentiated form comprising air bladders and tough hold fasts, stipes and blades. *U. intestinalis*, a chlorophyte, is an annual and has a simple form comprised of blades or tubes one or two cells thick. It generally forms dense clumps or mats on the shore. In contrast to our results, Bravo-Linares et al. (2010) found that *U. intestinalis* was better than *F. vesiculosus* at retaining water due to its structure, trapping water between its fronds to prevent it drying out. In our study, *U. intestinalis* was spread out to form a thin mat, potentially negating the benefits conveyed by the multiple fronds trapping water. This could increase the surface area of the alga exposed to desiccation, making the *U. intestinalis* more like flatter *Ulva* species, such as *U. lactuca* and *U. pertusa*, which had higher rates of water loss in previous studies due to their larger surface area (Bravo-Linares et al., 2010; Ji and Tanaka, 2002). This result demonstrates that differences between in situ and laboratory conditions may affect experimental outcomes. It also provides a potentially interesting example of how artificial desiccation, for example during drying of harvested algae to create a market product, may vary from natural tidal desiccation. During commercial drying processes the algae is spread into thin mats to increase the speed of drying and ensure drying occurs before rotting (Fig. 1), increasing the rate at which the algal biomass dries and potentially increasing the rate of exposure to stress.

4.4.2 Variation in F_v/F_m between species

To further investigate differences between species, F_v/F_m was recorded as a measure of photosynthetic health for *F. vesiculosus* and *U. intestinalis*. Other studies have recorded decreases in photosynthesis with desiccation (Pena et al., 1999; Williams & Dethier, 2005), our study supports these findings (Figs. 6 and 7). When combined, the experiments in this chapter show an overall pattern; halocarbon emissions may peak at first emersion but then decrease as water is lost and F_v/F_m decreases. However, a closer inspection reveals little connection between F_v/F_m and halocarbon emissions. During the first hour the F_v/F_m values for all *F. vesiculosus* (FP) replicates and the majority of *U. intestinalis* replicates (UP1-2) remained relatively constant or even increased slightly. This has been reported by other studies (Ji & Tanaka, 2002; Kumar et al., 2011; Pena et al., 1999), and has been attributed to a greater demand for energy for desiccation tolerance mechanisms or an increased availability of CO₂ as diffusion into the cell is enhanced. Decreases in F_v/F_m began after an hour for some replicates (e.g. in UP1). In other replicates large decreases were not noted until 2-3 hours into the experiment. A decrease in F_v/F_m occurs as inorganic carbon becomes limited, oxidative damage affects the photosynthetic apparatus and electron flows between PSI and PSII are interrupted (Kumar et al., 2011; Sampath-Wiley et al., 2008).

Differences in F_v/F_m may also help explain differences between the two species. *U. intestinalis* dried quicker than *F. vesiculosus* but its F_v/F_m did not necessarily decrease quicker (it decreased faster in UP1 but not UP2). Also, halocarbon production decreased more slowly for *U. intestinalis* (UL and URFW2-3) than for *F. vesiculosus* (FL1-2). **A potential link between these factors is that as *U. intestinalis* has a faster rate of water loss during desiccation it is subjected to a higher level of oxidative stress and therefore produces more halocarbons for a longer period of time.** The difference in the rate of F_v/F_m decline between UP1 and UP2 could be indicative of previous in situ environmental histories affecting laboratory results. Previous studies investigating oxidative bursts show the initial burst to be the largest (Küpper et al., 2001), therefore samples with different stress histories may respond differently to laboratory stresses.

4.4.3 Reasons for decreasing bromocarbon emissions over time

An initial peak in bromocarbon production, as demonstrated in many of our experiments, is likely caused by two factors. Firstly, direct flux of bromocarbons into the atmosphere/flask headspace as opposed to into seawater and then a reduced water-air flux (Section 4.3.5) and, secondly, as a response to the stress the algae is subjected to upon emersion, including increasing light levels and temperature (Section 4.1.1). However, this increase in emissions, which in the majority of experiments occurred at the start of exposure, was short lived, particularly during *F. vesiculosus* experiments. As halocarbon emissions are described as an oxidative stress response, and are therefore expected to increase with increasing desiccation/exposure, it may seem counter-intuitive that our results show *F. vesiculosus* emissions decreasing quickly, in some instances within an hour. It is unlikely that halide limitation drives this decrease in emissions as seaweeds concentrate halides from seawater (Saenko et al., 1978, Chapter 1 Section 1.3.1), therefore other causes must be proposed. Previous studies (e.g. Burritt et al., 2002) have seen effects, such as a decreasing ability to regenerate antioxidants (their study centred on the ascorbate-glutathione antioxidant response), when desiccation persists for 12 hours or more. It seems unlikely that the factors they link to decreasing antioxidant capabilities, such as nutrient limitation, are factors in decreasing halocarbon emissions within 1-2 hours. It also seems unlikely that carbon/energy limitation drives our observed decrease in halocarbon emissions, as F_v/F_m values remained stable or even increased slightly within the first 1-2 hours of desiccation (Section 4.3.4) and uptake of inorganic carbon may increase in the early stages of desiccation (Section 4.1.4). It also seems unlikely that the majority of oxidative damage occurs within the first hour or so, especially as our results show that F_v/F_m values begin decreasing later than this. Therefore, it seems likely that this apparent initial flux is largely due to an increased flux as bromocarbons volatilise from the algal surface once the majority of seawater is removed and a remaining seawater layer begins to evaporate. This is supported by Table 4 which shows lower production rates for exposed algae compared to those submerged (although this comparison includes three analytical techniques, see Section 4.3.5). Although the rate of evaporation may be similar for both species, *U. intestinalis* is a stronger bromocarbon producer in seawater (Section 4.3.7 and Table 4) and so is likely to have more bromocarbons at or near its surface. This may lead to the larger fluxes compared to *F. vesiculosus*, even if evaporation was an important driver of bromocarbon concentrations observed in the flasks. However, as other studies working on *Laminaria* (Küpper et al., 2008; Palmer et al., 2005) have reported halocarbons as a response to oxidative stresses (such as the addition of oligogulonates which elicits an oxidative burst) it seems likely that active production/emission of halocarbons to cope with desiccation does occur. In particular, this is supported by the *U. intestinalis* experiments where emissions remain above the level for the control for several hours.

Reasons for the rapid decrease in bromocarbon emissions in *F. vesiculosus* could be linked to the 'desensitisation' effect discussed by Küpper et al. (2001) who saw a strong oxidative burst after the first treatment with oligoguluronates (which mimic oxidative stress) but no subsequent response for up to three hours after the initial response.

4.4.4 The effects of rewetting with freshwater after a period of desiccation

In URFW2 and URFW3 freshwater rewetting was linked to an increase in bromocarbon emissions (Figs. 17 and 18). However, the magnitude of this increase was dependent on the length of time the specimen had been exposed for. In URFW2 the algae were exposed for ~3.5 hours before they were rewetted and concentrations of CH₂Br₂ and CHBr₃ returned to levels similar to the start of the experiment. In contrast, algal samples in URFW3 were desiccated for 8 hours and increases in emissions were less than half the magnitude of the original peak. Rewetting in freshwater causes an extra osmotic stress to the cells, the larger increase in halocarbon emissions in samples rewetted earlier may represent the fact that the algae still had the physiological capability (substantial F_v/F_m decreased were observed between 3-6 hours) and/or internal halide, nutrient and energy stores to produce a halocarbon response to the stress of freshwater osmotic shock. It should be noted that *U. intestinalis* is a salinity-tolerant species found in a wide range of salinities in the natural environment (Edwards et al., 1988). Therefore the response of *U. intestinalis* to freshwater rewetting may not represent that of all species.

4.5 Conclusions

This study has enhanced our knowledge of bromocarbon release during desiccation of temperate macroalgae in the following ways:

1. A burst of bromocarbons was observed upon exposure during desiccation experiments FS1-3 and US1-2, linked to both oxidative stress and a direct bromocarbon flux into the headspace. However care must be taken when comparing production rates of exposed and submerged samples where different measurement techniques (i.e. seawater vs. air samples) are used. Future comparisons should use the same measurement platform for both determining both submerged and exposed emissions; taking care to account for the partitioning of bromocarbons into the headspace of incubation vessels (see Chapter 3 Section 3.2.3).

2. *U. intestinalis* dried faster and lost a larger percentage of its water content than *F. vesiculosus* under the conditions of our study.

3. Production during exposure was higher for *U. intestinalis* compared to *F. vesiculosus*, as seen for seawater incubations in Chapter 3. Patterns of emissions also differed during longer desiccation experiments (FL1, FL2 and UL1); *U. intestinalis* tended to show prolonged emissions whilst *F. vesiculosus* showed a peak followed by a rapid decrease in emissions. As *U. intestinalis* is a stronger bromocarbon producer perhaps it has larger bromocarbon stores available to supply prolonged emission. However, as the halide/halocarbon response of *U. intestinalis* to oxidative stress is less well known when compared to phaeophytes (e.g. *Laminaria*, see Section 4.4) further work is needed to determine differences in emissions between *F. vesiculosus* and *U. intestinalis*.

4. Decreases in F_v/F_m were variable between replicates experiments of the same species (UP1 and UP2) and so conclusive differences between changes in F_v/F_m between *F. vesiculosus* and *U. intestinalis* could not be made. Changes in F_v/F_m did not match changes in halocarbon emissions. From these results it seems likely that a halocarbon pulse upon exposure may be a response to short-term stress, such as O₃ exposure (Ashu-Ayem et al., 2012) but not the effects of prolonged desiccation such as carbon and nutrient limitation or disruption of photosynthesis.

A desensitisation effect may also play a role.

4.5.1 Further work

Chapter 6 Section 6.2 emission estimates include a discussion of the changing flux of halocarbons to the atmosphere during daily tidal exposure of tropical macroalgae.

CHAPTER 5

Atmospheric distribution of halocarbons around Malaysia

5.1 Introduction

Alongside the incubation of tropical macroalgae discussed in Chapter 3 a variety of other in situ measurements were also made to further our understanding of tropical halocarbon production in the coastal zone. These measurements were made in 2010 and 2011 during two field campaigns, the details of which are discussed in Section 5.2. Results and discussions (Section 5.3 and 5.4) focus on mapping the distribution of halocarbon concentrations in Malaysia, linking this data to macroalgae incubations and previous ambient measurements.

Data used in this chapter were collected during two campaigns covering both peninsular and eastern Malaysia (Borneo) from a variety of measurement platforms: ground-based sampling, small boat near-shore transects, a larger research vessel (R/V Sonne) and a research aircraft (Falcon). The SHIVA, 'Stratospheric Ozone: Halogens in a Varying Atmosphere', campaign (SHIVA11) was part of an EU funded project (ref: 226224-FP7-ENV-2008-1) studying the oceanic emission strength, atmospheric transport, chemical transformation and contribution to stratospheric inorganic bromine of a suite of halogenated VSLS, with a particular focus on the tropical South East Asian region. The project involved measurement and modelling studies to improve our understanding of these processes in terms of both current conditions and potential future changes to the climate system. For more information see <http://shiva.iup.uni-heidelberg.de/>.

5.2 Methodology

Table 1 provides a summary of campaigns, measurements taken, and acronyms that will be used herein. The location column is expanded in Fig. 1, a map of sampling sites. The two campaigns involved a variety of techniques to collect, store and analyse samples for the determination of halocarbon concentrations in both air and seawater samples. Table 1 also highlights the techniques used and refers to the relevant methodology sections that describe sample analysis techniques in further detail. Data collected by other research groups during the SHIVA campaign will be compared to our dataset and, where possible, used to extend our range of halocarbon measurements. Refer to citations in Table 1 for methodologies corresponding to these datasets.

Table 1. Measurement platforms, techniques and analytical methods used to map the distribution of halocarbons in Malaysia.

Campaign code	Dates	Location	Platform	Sample medium	Sample collection	Sample analysis and responsible scientist/institutions¹
JAM10	July – Aug 2010	Peninsular Malaysia: Langkawi & Port Dickson	Ground	Air	Canisters (ambient & flux chamber)	GC-NCIMS in Sept-Oct 2010, Section 5.2.4.
SHIVA11	Nov 2011	Borneo	Ground	Air	Canisters	GC-NCIMS in Jan-Mar 2012, Section 5.2.4.
			Small boats	Air	Canisters	GC-NCIMS in Jan-Mar 2012, Section 5.2.4.
			Falcon	Air	Canisters	Mills & Oram (UEA) ³ , GC-NCIMS during campaign Technique as used for ground/small boat samples but separate GCMS instrument used.
			R/V Sonne	Air	Canisters	Atlas (RSMAS) ² .
				Air	In situ samples	Robinson (U. Cambridge), μ Dirac, see Gostlow et al. (2010).

¹ when data has been obtained from other sources, ² a description of shipboard air measurements can be found in Tegtmeier et al. (2012), air samples were collected between 15.11.11 to 29.11.11 from a pole reaching 4 m out from the port side of the boat 15 m above the sea surface. ³ Samples collected into Pyrex flasks and analysed in a manner similar to that described in Section 5.2.3.



Figure 1a. ● Ground measurements or launch points for small boat transects, including:

La: Langkawi

PD: Port Dickson, including Cape Rachado, Pantai Dickson and Pantai Purnama

Ku: Kuching

KK: Kota Kinabalu

sem: Semporna region

Figure 1b. SHIVA11 campaign activities including R/V Sonne ship track, Falcon aircraft base at Miri and aircraft range (see inset legend). Map b taken from <http://shiva.iup.uni-heidelberg.de/>.

5.2.1 Sampling sites - SHIVA11

This chapter will mainly focus on the results from the SHIVA11 campaign. From Kuching on the 19th November 2011 and from Kota Kinabalu (KK) on the 23rd November 2011 a small boat conducted a transect out to meet the R/V Sonne at ~20 km from the shore. Flask samples were filled from the bow of the boat at Kuching and from port side stern at KK. Air samples were taken directly at the edge of the boat, about 1-2 m above the sea surface. Fig. 2 illustrates the vessels used in (a) Kuching and (b) KK. A small boat was also used as part of a three day measurement campaign in Semporna:

- Bohey Dulang (BD) - 25.11.11 – hourly samples taken between 09:00 and 16:00 (local time) on a small island.
- Small boat cruise (hereafter abbreviated to “semcruise”) - 26.10.11 – around islands, mangroves and seaweed colonised areas was conducted between 06:47-13:22 (local time).

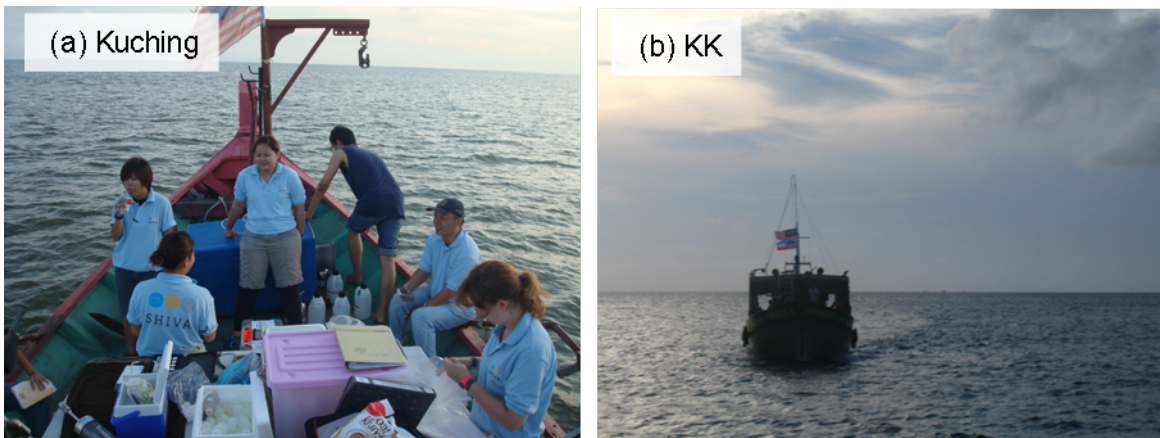


Figure 2. Boats used for transects at (a) Kuching and (b) KK during SHIVA11. Full details given in Table 1.

5.2.2 Sampling sites – JAM10

Whilst the majority of this chapter focuses on SHIVA11, comparisons will also be made with the JAM10 ('July and August Malaysia') campaign. This was a small campaign, mainly in conjunction with the University of Malaya. During JAM10 samples were taken at a variety of sites (Fig. 3), including mangrove stands (e.g. Pantai Dickson), sandy beaches with heavily macroalgae-colonised intertidal reefs (e.g. Cape Rachado) and areas without macroalgae (e.g. Langkawi).

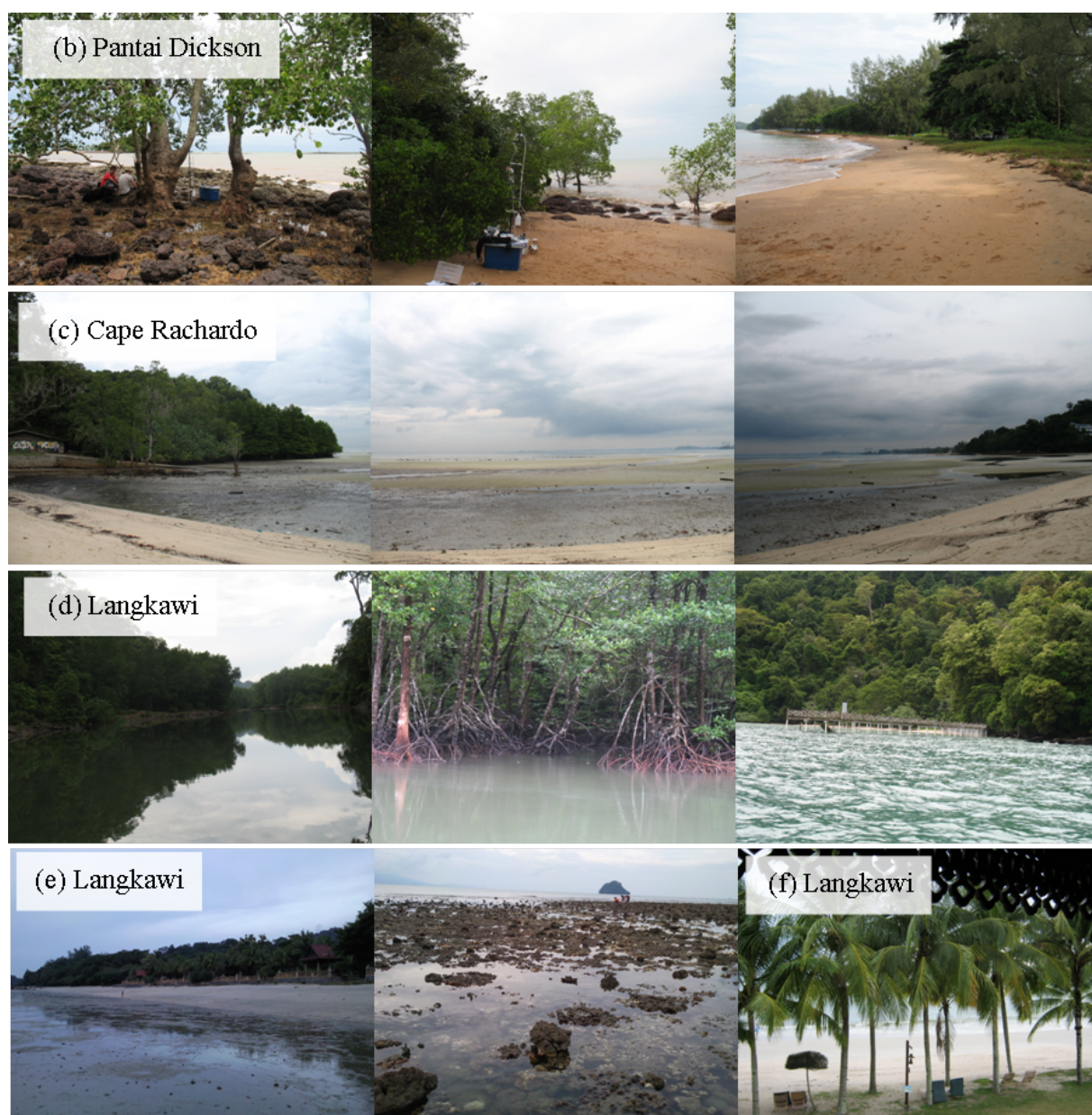


Figure 3. Sampling locations visited during JAM10. For further details see Table 1.

5.2.3 Sample collection

Restek SilcoCan® air monitoring canisters were used to collect whole air samples in the field. Samples were collected into pre-evacuated canisters via a line of PFA tubing (¼ inch diameter) connected to the diaphragm valve on the top of the canister. A small pump (Air Dimensions, Inc., USA) connected to a rechargeable 12 V battery allowed filling of the flasks to 40 psi. Before sampling the tubing was flushed for several minutes. The canister was then connected, filled to ~30 psi and vented twice to flush the flask. A third fill to 40 psi provided the sample. Samples were returned to UEA for analysis within 4 months. A study by Brinckmann et al. (2012) demonstrated good stability of samples in moist (typical tropospheric H₂O mixing levels) air for up to five months; including CHBr₃ which is less stable in dry air samples. Water vapour in humid samples adsorbs onto the inner wall of the canister, preventing some of the analytes from doing so and therefore increasing stability (Dewulf & van Langenhove, 1997).

5.2.4 Sample analysis

A Markes Air Server™ allowed the connection of up to 6 canister samples to a Markes UNITY™ thermal desorption system (Worton et al., 2008). Automated sets including blanks, calibrant gas samples and air samples could be established and controlled via the UNITY™ software. After a 3 minute pre-purge (25 ml min⁻¹) of the sample line a 500 ml sample was collected over 20 minutes at 25 ml min⁻¹. Samples were trapped on a cold trap packed in-house with Carboxen 1003 (used for its hydrophilic properties) and held at -30 °C by the use of a Peltier cooling system. The trap was then quickly heated to 300 °C and held at this temperature for 15 minutes to desorb the analytes and send them along a 120 °C heated transfer line to the GC column.

An Agilent 6890 GC with a 105 m (nominal length), 0.32 mm internal diameter, 1µm film Rtx 502.2 capillary column (Restek) was used for analyte separation. The oven temperature programme was set at 35 °C for 8 minutes followed by a temperature ramp at 10 °C min⁻¹ to 150 °C where the temperature was held for 10 minutes before a second ramp at 15 °C min⁻¹ to 260 °C where the oven was held for 15 minutes.

An Agilent 5973 quadrupole MS operating in negative ion chemical ionisation (NCI) mode was used for analysis of canister samples. Chemical ionisation uses a reagent gas, in this instance high purity methane, to ionise the sample, resulting in a soft ionisation that generates less fragmentation (Kellner et al., 2004). The use of this system for high sensitivity analysis of halogenated compounds has been reported by Worton et al. (2008) and the analysis of samples in this work follows their protocols. The system is run in SIM (see Chapter 3 Section 2), monitoring m/z 35 for chlorinated compounds, 79 and 81 for brominated compounds and 127 for iodinated compounds throughout the chromatographic run. Peaks are identified via two methods; retention time relative to known standards and the use of EI mode to match full mass spectra with known standards and spectral libraries (Worton et al., 2008). Each flask was analysed at least twice. Point calibration was conducted using a gas standard, which is discussed further in Section 5.3.5, introduced to the system in the same way as flask samples via the UNITY™ system. A working standard was sampled at regular intervals during daily sample analyses to help correct for daily sensitivity drift.

After use, flasks were connected to a rig, evacuated to $\sim 8 \times 10^{-2}$ mb and baked (whilst under vacuum) at 130 °C for at least 12 hours. 10% of flasks are then filled with clean nitrogen and analysed as a quality control mechanism to ensure minimal contamination levels have been obtained.

5.2.5 Air standard concentrations, calibrations and intercalibrations

Absolute mixing ratios in the working standard were derived via an ongoing calibration system which involves the intercomparison of standards both at UEA and between UEA and other organisations. Determining the magnitude of drift in a standard over time is complex; different standards may drift at different rates relative to each other and so even multiple intercomparisons may not be able to accurately track changes over time. Intercalibrations also provide some measure of drift in standards. Two standards were used during the work described in this chapter.

i. UEA 'Jana' standard

This was used to calibrate JAM10 analyses. The standard comprises an aluminium tank filled to a high-pressure with non-dried ambient air from Mainz, Germany in April 2004. Mixing ratios for this standard were obtained via comparison with NOAA standards during several intercomparisons since 2004. The latest intercalibrations were with the University of York in 2010 and the University of Cambridge in 2012. The concentration values used for this work were obtained from a 2010 intercomparison. Our data suggest that there is no significant drift in the Jana standard between May 2010 and October 2011 (a period covering the data in this chapter) for the mixed bromochloro compounds (CHBr_2Cl , CHBrCl_2 and CHBr_2Cl) as well as CH_2Br_2 . CHBr_3 does show significant drift in the Jana standard (36% between 2008 and 2012), this is corrected for via regular comparisons with other NOAA standards. For the purpose of this work an intercomparison done in 2010 is timely and is likely to minimise the effects of drift on our results.

ii. UEA SX074 standard

2011 analyses were run relative to the UEA 'SX074' standard and concentration values are on a NOAA scale derived from intercomparisons with standards owned by the University of Cambridge as well as other UEA standards. Samples were analysed in January 2012 and intercomparisons to determine concentration values were conducted in March and September 2012. Based on these intercomparisons we assume negligible drift in the standard between the start of analyses in January 2012 and the first intercomparison in March 2012.

5.2.6 A comparison of system precision and detection limits

Table 2 contains information on the following parameters, given for each campaign discussed in this chapter.

- Precision of the system was determined by the variability on replicate analyses of the standard and is given as percentage standard deviation (1σ) for each compound.
- The given error on the standard concentration taken from the original NOAA scale numbers and intercalibrations, (Section 5.2.5)
- The detection limit (in ppt) of the system during each campaign. Five calibrated blank runs were used to determine the standard deviation (σ) on the blank mean (\bar{x}) using Eq. 1 (Kaiser, 1970).

$$\text{Detection limit} = \bar{x} + 3\sigma \quad (1)$$

During JAM10 the variability for CH_3I and CHBr_3 in particular was higher on the first four samples analysed on the first day, from this point onwards the frequency of calibration analyses was increased to reduce variation due to drift, removing this error would reduce overall 1σ to 8.84% for CH_3I and 15.0% for CHBr_3 .

Table 2. Precision ($\%1\sigma$), given error on standard concentrations (1σ) and detection limits (ppt) for two Malaysian campaigns; JAM10 and SHIVA11. n = number of standard pairs used to determine precision.

	CH₃I			CHBrCl₂			CH₂Br₂			CHBr₂Cl			CHBr₃		
	Precision	Error on standard	Detection limit	Precision	Error on standard	Detection limit	Precision	Error on standard	Detection limit	Precision	Error on standard	Detection limit	Precision	Error on standard	Detection limit
JAM10	9.88 (n=40)	0.08	0.76	3.90 (n=44)	x	0.05	7.75 (n=43)	0.09	0.15	6.75 (n=44)	0.03	0.09	16.9 (n=43)	0.36	0.92
SHIVA11	8.50 (n=47)	0.76	0.30	3.64 (n=48)	0.004	<0.01	3.39 (n=48)	0.01	0.00	4.01 (n=48)	0.01	<0.01	2.93 (n=48)	0.05	0.06

5.3 Results and discussion

5.3.1 Data overview

An overview of halocarbon concentrations observed during SHIVA11 is shown in Table 3. This table includes data collected from ground stations, small boats, the Falcon and the R/V Sonne. Air samples collected aboard the Falcon were taken at altitudes ranging from 39 to ~10900 m. Fig. 4a shows the vertical profile of concentrations observed from Falcon samples for four compounds (CH_2Br_2 , CHBrCl_2 , CHBr_2Cl and CHBr_3). A decrease in concentration with altitude is observed, as also reported by Blake et al. (1997, 1999) and Park et al. (2010) for biogenically produced halocarbons with short atmospheric lifetimes. For the purpose of comparison with ground samples we have selected only those samples believed to be taken within the boundary layer, which has been approximated at 760 m based on Robinson et al. (2012). Boundary layer samples can be seen in Fig. 4b and it is this subsection of measurements referred to in Table 3 and subsequent analyses throughout this chapter.

Table 3. A summary of halocarbon concentrations observed during SHIVA11. All values in ppt. nr = not recorded. Values in each grid box show:

mean / ppt
(range)
percentage standard deviation

Site (n = sample no.)	CH ₃ I	CHBrCl ₂	CHBr ₂ Cl	CH ₂ Br ₂	CHBr ₃
UEA Ground/small boat measurements (SHIVA11)					
Kuching (7)	1.30 (0.94-1.95) 29.2	0.30 (0.26-0.37) 13.8	0.22 (0.2-0.26) 10	1.03 (0.85-1.42) 17.5	1.46 (1.27-1.64) 8.6
KK (5)	2.38 (1.36-3.54) 41.9	1.0 (0.47-1.67) 52.2	0.61 (0.33-0.94) 42.7	1.20 (1.13-1.25) 4.6	2.73 (1.99-3.61) 22.1
BD (8)	1.16 (0.86-1.42) 15.1	0.39 (0.20-0.47) 21.7	0.42 (0.23-0.50) 20.2	1.25 (1.15-1.38) 6.8	2.65 (2.12-3.24) 15.4
semcruise (14)	2.11 (1.2-3.05) 27.7	0.51 (0.41-0.63) 14.2	0.50 (0.35-0.66) 17.7	1.35 (1.18-1.64) 11.3	2.83 (1.5-4.27) 30.2
All ground/small boat data	1.70 (0.71-3.45) 45.3	0.54 (0.2-1.67) 54.3	0.47 (.2-.94) 37	1.28 (0.85-1.76) 14.7	2.59 (1.27-4.82) 34.8
Other SHIVA11 measurements - aircraft and shipboard measurements					
Falcon aircraft canisters <760 m altitude (116) (UEA)	nr	0.33 (0.22-0.67) 21.2	0.30 (0.17-0.63) 30	1.04 (0.8-1.5) 13.5	1.68 (0.82-3.67) 29.3
R/V Sonne canisters (195) (RSMAS)	0.39 (0.19-0.78) 23.1	nr	0.28 (0.11-5.87) 146.4	1.17 (0.71-1.98) 16.1	2.08 (0.79-18.42) 65.4
R/V Sonne μ Dirac (227) (UCAM)	0.32 (0.05-3.39) 112.5	nr	nr	0.74 (0.37-1.48) 23	2.82 (1.32-6.81) 30.1

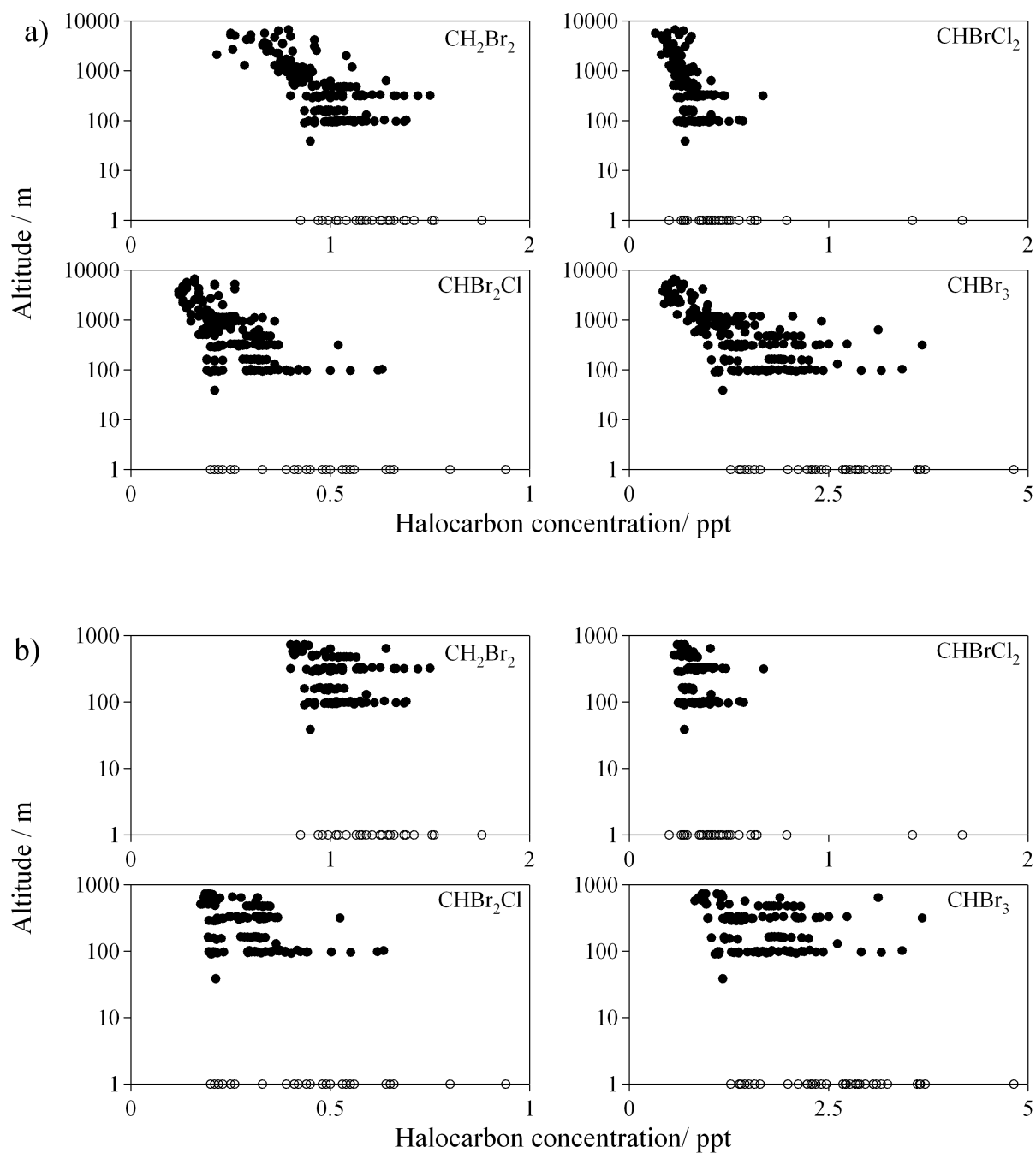


Figure 4. Vertical distributions of halocarbons sampled at (a) all altitudes and (b) < 760 m only. Data represent UEA canister samples taken aboard the Falcon aircraft (●) or from ground/local boat stations (○).

5.3.2 Differences between SHIVA11 sites

Relatively similar concentration ranges are seen at all ground-based and small boat sites visited during SHIVA11 with a CHBr_3 concentration range, for example, of 1.5-2.8 ppt (a comparison with other studies will be made in Section 5.3.3). Comparisons between sites can be made using statistical tests. A non-parametric ranked ANOVA test was conducted as not all datasets passed normality and/or equal variance tests, and some of the sites had a small sample size. The ranked ANOVA test was performed on the ground/small boat sites (Kuching, KK, BD and semcruise). Ranked ANOVA tests were performed both on differences between individual halocarbons at each site and also on a combined dataset of all halocarbons at each site. Significant differences ($p < 0.05$) were observed for both sets of tests. Dunn's post-hoc test (Dunn's test was selected as groups did not contain the same amount of data) showed that a large proportion of this significant difference could be attributed to differences between Kuching and other sites, in particular KK and semcruise. This is likely due to the lower concentrations observed at Kuching, which will be discussed in further detail in Section 5.3.5.

5.3.3 Extending range of halocarbon measurements with other datasets

Data from the Falcon and R/V Sonne, which extend the geographical range of measurements, does not greatly increase the range of halocarbon concentrations measured at ground/small boat stations during SHIVA11. One difference of note was a substantially lower mean CH_2I concentration measured in canister samples taken aboard the R/V Sonne when compared to ground/small boat samples. Previous studies have shown a decreasing gradient in atmospheric concentration of CH_2I away from the coast (Grose et al., 2007 and review by Saiz-Lopez et al., 2012). Commonly, but not exclusively (see Chapter 1, Section 1.7), these high coastal concentrations tend to be recorded in areas of macroalgae colonisation. No macroalgae were observed from the launch sites at Kuching or KK, but floating seaweed debris was observed during the local boat transects which could indicate that it is found in, or relatively near, the coastal regions we sampled.

CHBr_2Cl and CHBr_3 measured in canisters from the R/V Sonne (RSMAS) were lower than all ground/small boat sites apart from Kuching. Again, highly productive coastal regions tend to show higher concentrations of bromocarbons (Quack & Wallace, 2003; Yokouchi et al., 2005). One R/V Sonne canister CHBr_3 measurement of 18.4 ppt is much higher than all other CHBr_3 measurements made aboard the vessel which fell below ~ 5 ppt. If this sample is removed from the dataset the CHBr_3 mean value measured in canisters aboard the R/V Sonne decreases to 2.0 ppt (range 0.8-7 ppt) whilst little difference is observed in the mean and range of the other halocarbons listed in Table 3. Aboard the R/V Sonne another measurement technique, the μDirac , was also used to measure halocarbon concentrations. CHBr_3 concentrations measured with the μDirac were slightly higher than those measured using the RSMAS canister samples. Canister samples (analysed by UEA) and μDirac CHBr_3 measurements have agreed well in past campaigns (Gostlow et al., 2010) and time series of canister and μDirac samples taken aboard the R/V Sonne generally correlated well (B. Quack pers. comm. 2012, data not shown).

Falcon measurements were generally lower concentrations than those seen for all other platforms, apart from the local boat samples taken at Kuching. As a decreasing halocarbon concentration with increasing altitude is observed (Fig. 4) this is likely due to deriving mean concentrations from a range of altitudes. However, regional patterns (e.g. areas of high and low concentrations) observed by the Falcon match those from other measurement platforms, this will be discussed in the following section.

CH_2Br_2 concentrations cover a smaller range and have lower standard deviations in all the datasets. As the longest lived VSLs discussed in this chapter, with a lifetime of 120 days compared to 7-78 days for the other halocarbons (Montzka et al., 2010) it is likely to exhibit less spatial and temporal variation in concentration than some of the shorter-lived species such as CHBr_3 .

Measurements were also made at several locations in Peninsular Malaysia during JAM10. Between 2-4 flasks were filled at each site. Table 4 provides information on these results. Concentrations of CHBr_3 and CH_2Br_2 reached higher values than measured in Borneo during SHIVA11; CHBr_3 ranged from 0.25-14.09 ppt and CH_2Br_2 0.52-2.28 ppt. However, at some sites (e.g. Langkawi S1) the percentage standard deviation was high, suggesting that high CHBr_3 concentrations were 'events' rather than a background state. For example, at Langkawi S1, over 48 hours, CHBr_3 concentrations varied from 0.3-14 ppt. The CH_3I range was closer to that from SHIVA11, ranging from 0.43 to 2.24 ppt. These measurements were made within regions of potentially strong halocarbon emissions, for example near macroalgae beds at Cape Rachado, and therefore higher concentrations may be expected. Laboratory incubations of species found at these sites (see Chapter 3) demonstrated high levels of halocarbon production from many species. These measurements indicate localised emission 'hot spots' which are related to coastal biology.

Table 4. A summary of halocarbon concentrations observed during JAM11. All values in ppt. nr = not recorded. Values in each grid box show:

Site* (n = sample no.)	mean / ppt				
	(range)				
	percentage standard deviation				
	CH_3I	CHBrCl_2	CHBr_2Cl	CH_2Br_2	CHBr_3
Langkawi S1 (4) [§]	3.41 (2.73-5.69) 49.6	0.78 (0.33-1.62) 59.2	0.39 (0.22-0.60) 40.4	1.20 (0.65-2.28) 47.5	3.91 (0.25-14.09) 124.74
Langkawi S2 (2) [¶]	1.39 (0.82-1.97) 50.0	0.21 (0.17-0.25) 14.4	0.23 (0.20-0.25) 10.4	1.00 (0.86-1.15) 11.9	1.88 (0.94-2.80) 40.3
Cape Rachado (4)	0.86 (0.43-1.35) 36.4	0.87 (0.29-2.45) 87.4	0.33 (0.16-0.58) 36.8	1.12 (0.92-1.37) 12.82	2.34 (0.76-3.8) 51.8
Pantai Dickson (2)	1.27 (0.84-1.81) 34.7	0.79 (0.49-1.14) 43.1	0.66 (0.41-0.92) 32.2	1.58 (1.21-1.89) 18.5	6.58 (3.11-12.32) 61.9

* See Figs. 1-3). [§] A beach site, Fig 3f. [¶]Boats in mangrove/coast area Fig. 3d

5.3.4 A comparison with previous studies

The range of concentrations shown in Table 3 are consistent with previous measurements of halocarbons in the MBL. Table 5 presents a range of observations from other published studies. Our mean CHBr_3 concentrations ranged from 1.68 to 2.83 ppt, slightly higher than the mean values reported for other tropical research cruises of ~ 1 ppt (Butler et al., 2007; Carpenter et al., 2009). Cruise measurements tend to focus on open ocean or continental shelf samples and our higher measurements are consistent with stronger production and emissions from coastal waters (see summary in Quack & Wallace, 2003). As many research cruise vessels cannot come close to shore, small boat transects, such as the ones conducted during SHIVA11, form an important, and potentially under-utilised, source of information on marine halocarbon emissions. CHBr_3 concentrations were lower than the mean value of 7.9 ppt (range 2-27) reported by O'Brien et al. (2009) for measurements made at Cape Verde and Yokouchi et al. (2005) who measured up to a mean of 31 ppt near tropical islands in various locations. The fact that coastal concentrations higher than those from the open ocean have been identified in regions that do not have high levels of seaweed colonisation (Ku and KK from this study and Cape Verde) suggest other sources may also play an important role in elevated coastal halocarbon concentrations. Chapter 1 Section 1.3 provided information on other potential marine halocarbon sources.

Table 5. CHBr₃, CH₂Br₂ and CH₃I atmospheric mixing ratios (ppt) from a range of previous studies. Where available both the mean value and the range (in brackets) are shown. For several studies only the range is given. * = 90% range given.

Location	CHBr ₃ / ppt	CH ₂ Br ₂ / ppt	CH ₃ I / ppt	Reference
“Tropics” (average from several cruises)	1 (0.4-2.1)*	0.9 (0.6-1.3)*	0.6 (0.2-11)*	Butler et al. (2007)
Open ocean data				
Tropical and subtropical N. Atlantic	1.7 (0.5-9.9)	1.3 (0.9-1.6)	0.9 (0.6-1.3)	Fuhlbrügge et al. (2012)
Equatorial Pacific	1.9 (0.8-3.5)	1.3 (0.5-2)	nr	Yokouchi et al. (2005)
Equatorial Pacific 17 °N – 14 °S	3.1 (0.5-6.7)	1.7 (1.2-2.2)	1.1 (0.7-1.8)	Atlas et al. (1993)
W. Pacific	1.1 (<0.1-2.5)	1 (0.5-1.5)	nr	Yokouchi et al. (2005)
W. Pacific	1.2 (0.4-10.7)	nr	nr	Quack and Suess (1999)
Tropical Atlantic upwelling	1.1 (0.5-2)*	0.4 (0.2-0.4)*	nr	Carpenter et al. (2003)
Coastal data				
Coastal waters (average from several cruises)	0.8 (0.2-1.99)*	1 (0.6-1.9)*	0.8 (0.4-1.6)*	Butler et al. (2007)
Tropical and subtropical N. Atlantic	4.2 – 6.58	1.96 – 3.14	max 3.3	Fuhlbrügge et al. (2012)
Java Island	0.9 (0.4-1.6)	0.9 (0.6-1.5)	nr	Yokouchi et al. (2005)
Tropical islands (San Cristobal and Christmas Island)	13.8 (1.4-43.6)	2.6 (1.4-7.6)	nr	Yokouchi et al. (2005)
Cape Verde	7.9 (2-27.2)	1.97 (0.8-1.8)	nr	O'Brien et al. (2009)
Mace Head, Ireland	6.8 (1-22.7)	1.3 (0.3-3.4)	3.8 (1.3-12)	Carpenter et al. (2003)

5.3.5 Mapping emissions

Figs. 5-9 display the atmospheric distribution of (in order) CH_3I , CH_2Br_2 , CHBr_3 , CHBrCl_2 and CHBr_2Cl around Borneo, determined from measurements made during the SHIVA11 campaign. Data is taken from UEA local boat/ground station canisters, UEA Falcon canisters, R/V Sonne canisters (RSMAS) and μDirac measurements (UCAM).

A few important points to help interpretation of Figs 5-9:

- All values are in ppt.
- The large map panel (at the top of each page) shows all the available data from all measurement platforms on the same colour scale. This map is designed to allow for an overall comparison of regional differences in halocarbon concentrations.
- Smaller map panels (a-d) show data collected from an individual measurement technique. For example UEA local boat data is shown in map panel a in each figure. Each smaller map has its own colour scale. This prevents high measurements on one scale obscuring patterns that may otherwise be observed from other measurement platforms.

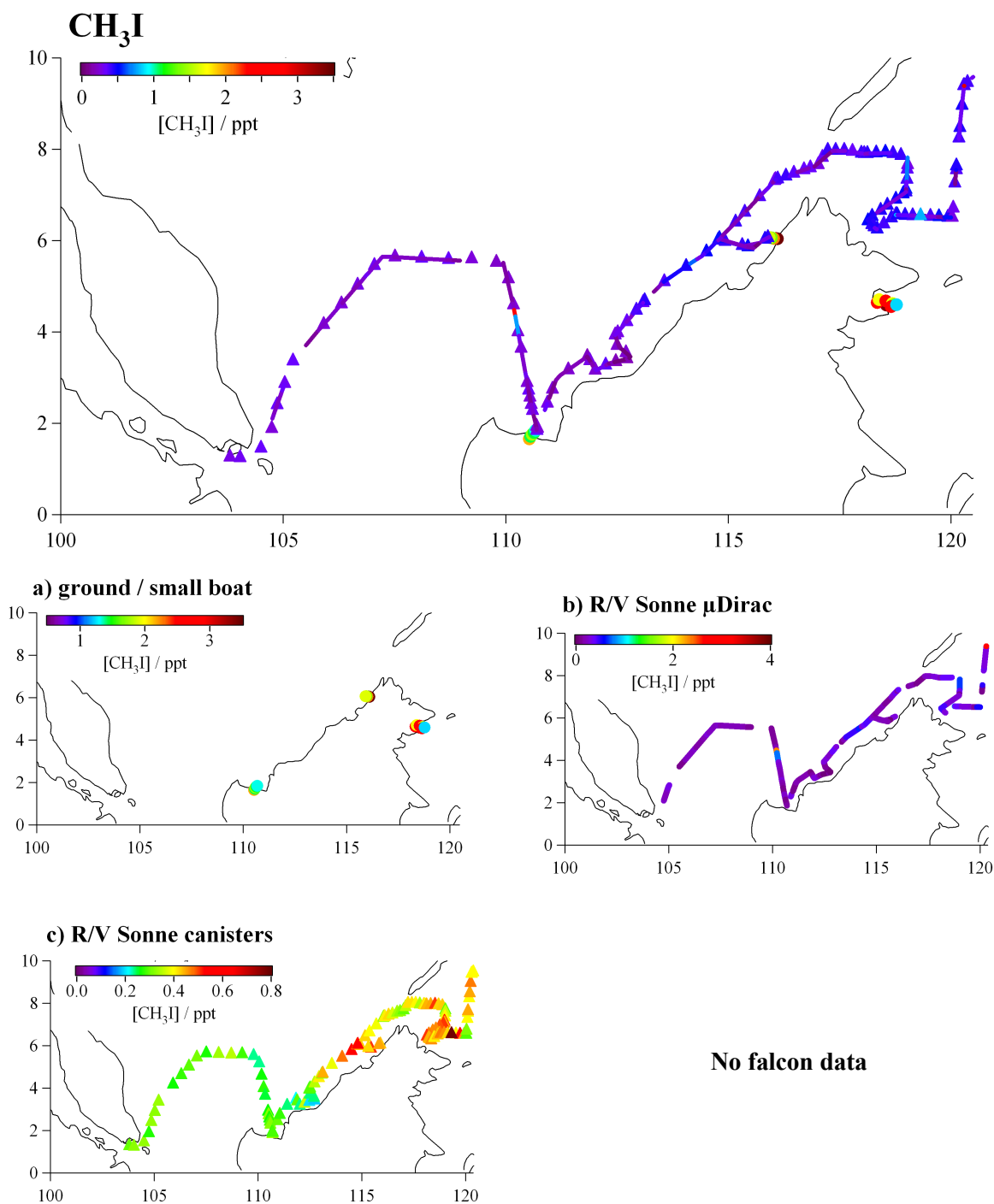


Figure 5. Atmospheric distribution (ppt) of CH₃I around Malaysia determined from measurements made during SHIVA11:

- = Local boat or ground samples (UEA)
- ▲ ● R/V Sonne canister samples (RSMAS)
- (continuous) = R/V Sonne μ Dirac samples (UCAM)

Original in colour.

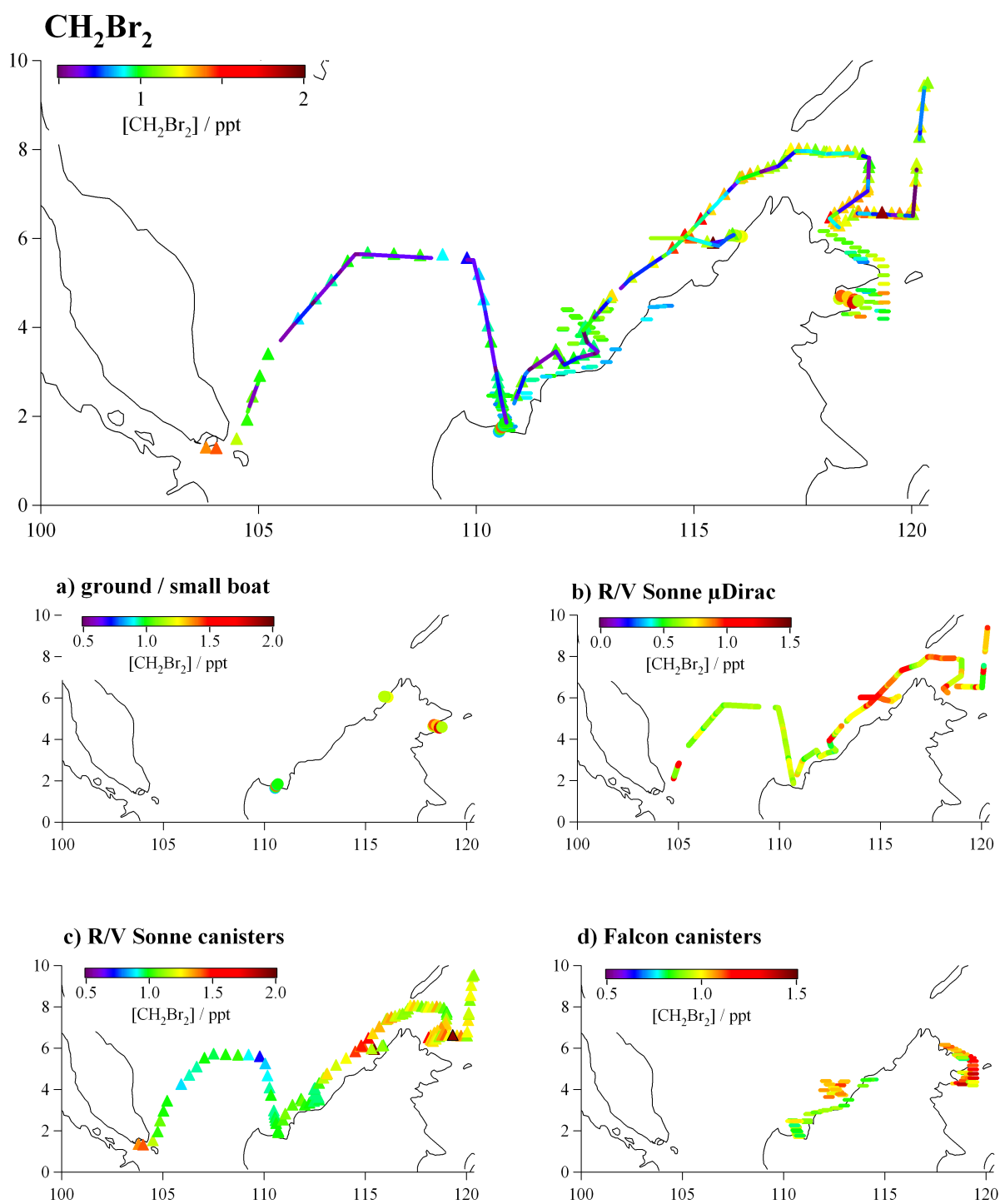


Figure 6. Atmospheric distribution (ppt) of CH₂Br₂ around Malaysia determined from measurements made during SHIVA11:

- = Local boat or ground samples (UEA)
- ▲ = R/V Sonne canister samples (RSMAS)
- (continuous) = R/V Sonne μ Dirac samples (UCAM)
- - = Falcon samples (UEA)

Original in colour.

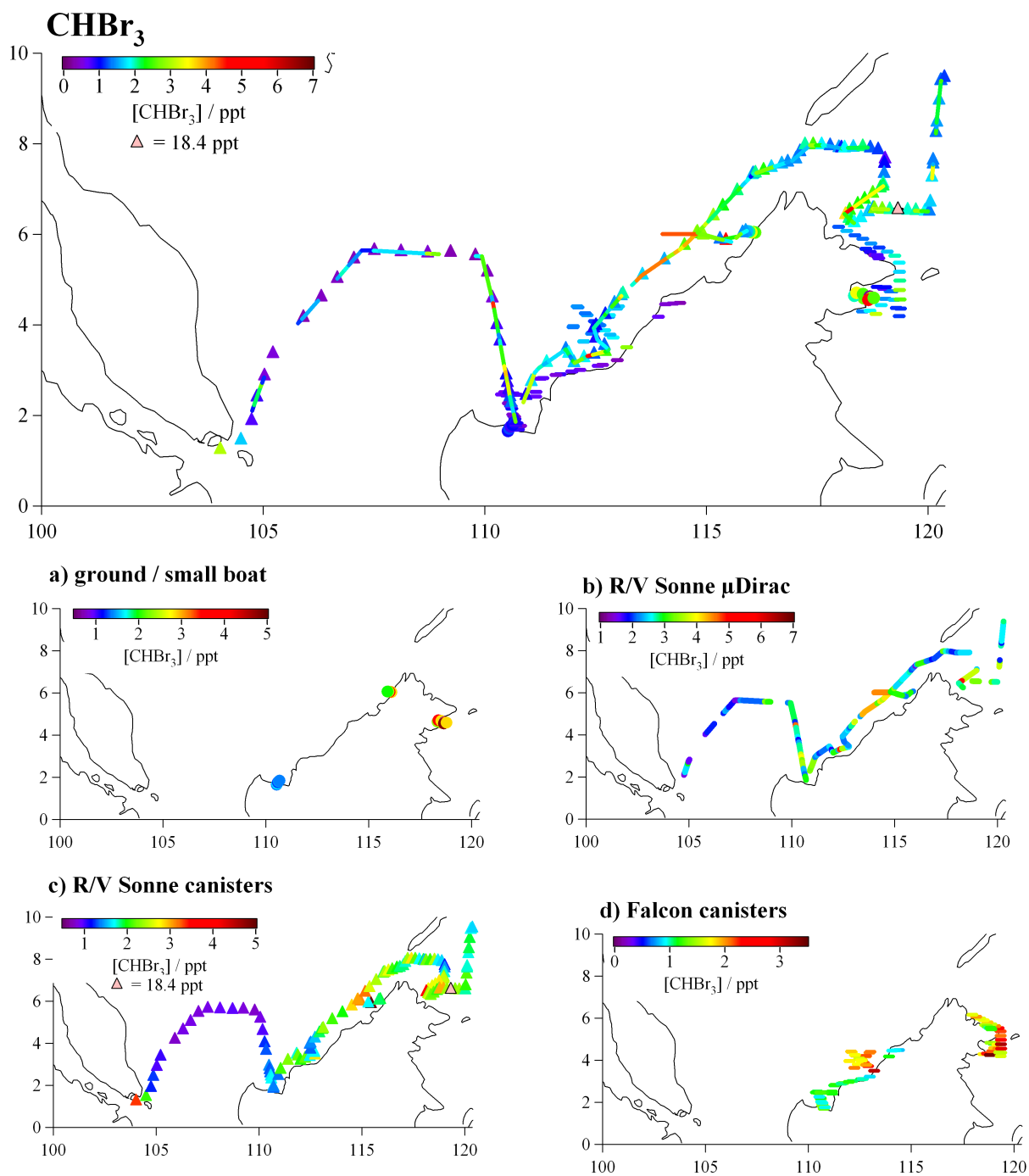


Figure 7. Atmospheric distribution (ppt) of CHBr₃ around Malaysia determined from measurements made during SHIVA11:

- = Local boat or ground samples (UEA)
- ▲ = R/V Sonne canister samples (RSMAS)
- (continuous) = R/V Sonne μDirac samples (UCAM)
- - = Falcon samples (UEA)

Original in colour.

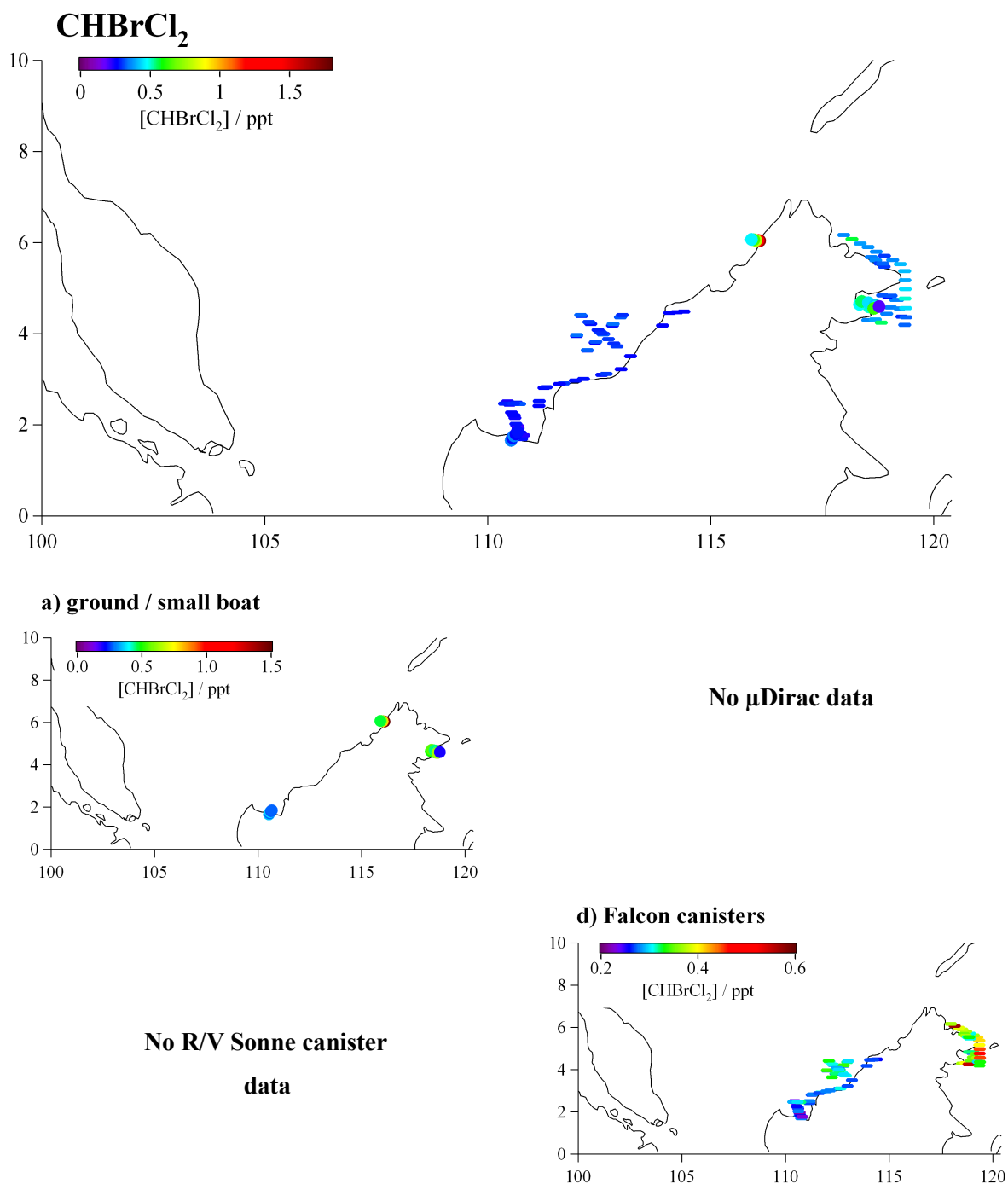


Figure 8. Atmospheric distribution (ppt) of CHBrCl₂ around Malaysia determined from measurements made during SHIVA11:

● = Local boat or ground samples (UEA)

– = Falcon samples (UEA)

Original in colour.

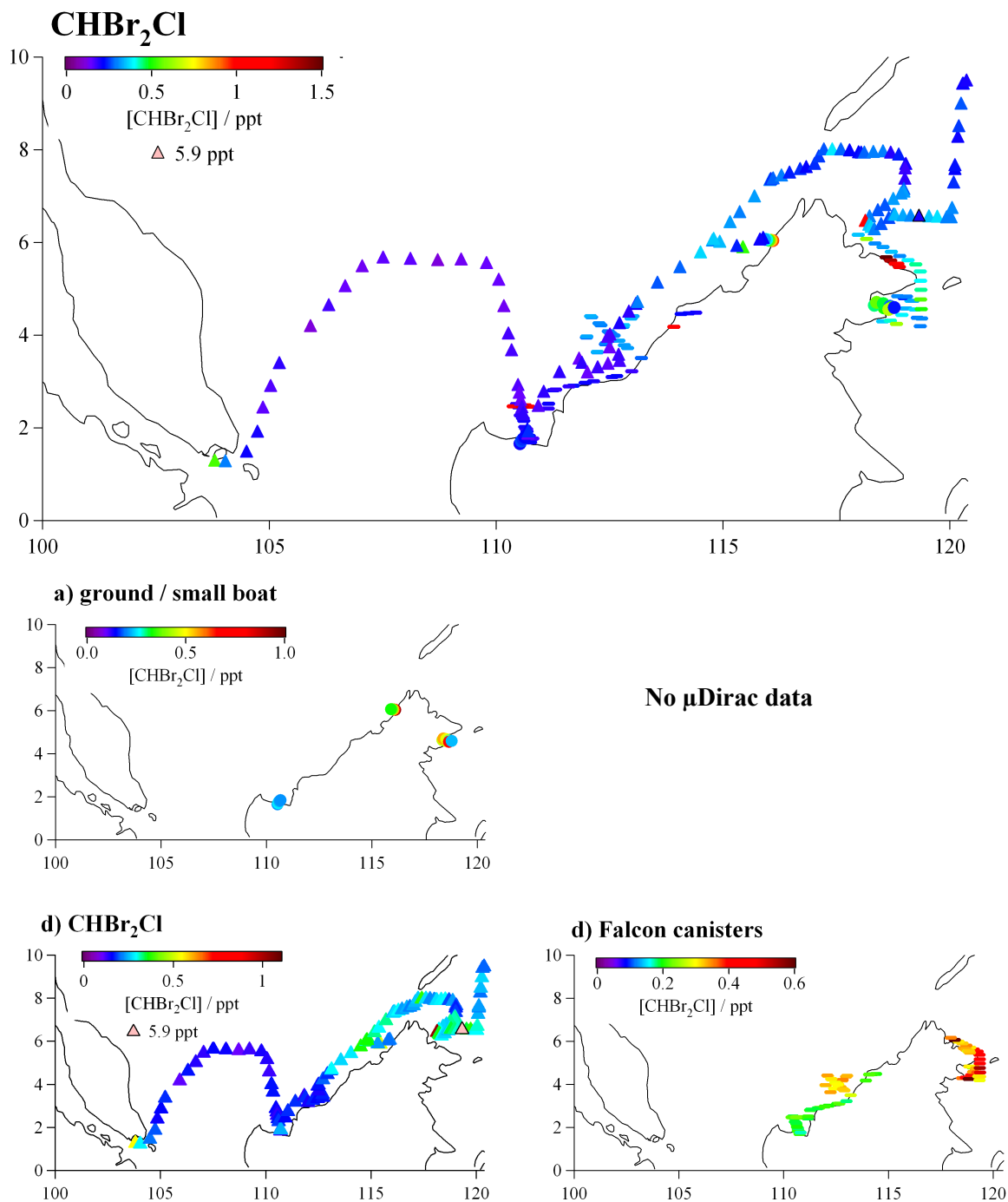


Figure 9. Atmospheric distribution (ppt) of CHBr₂Cl around Malaysia determined from measurements made during SHIVA11:

● = Local boat or ground samples (UEA)

– = Falcon samples (UEA)

Original in colour.

Studying the halocarbon distribution around Borneo we see the following patterns for all halocarbons (Figs. 5-9):

- Low concentrations were observed as the ship passed through the South China Sea (SCS, see Fig. 1 for reference). Open ocean regions are often characterised by lower concentrations, see Chapter 1 Section 1.7.
- These low halocarbon concentrations in the open ocean could be linked to low biological productivity in these regions. Previous studies have found links between chlorophyll-a (as a marker of biological activity) and halocarbon distributions in open ocean regions (Arnold et al., 2010). A satellite map of chlorophyll-a concentrations averaged over the SHIVA11 campaign (Fig. 10) shows lower concentrations in the SCS compared to regions nearer the Borneo coast.
- However, low concentrations were also observed close to the coast in the Kuching area (south west Borneo) by the local boats and the Falcon. The R/V Sonne also measured low concentrations in this region.
- Higher concentrations were observed as the R/V Sonne traveled northward up the Borneo coast and into the Sulu Sea, local boat measurements were also higher at KK compared to at Kuching. This stretch of coastline showed variable production, with some low as well as high concentrations. Variations could be due to changes in biological productivity, meteorology or other factors such as river inputs. This will be discussed in further detail in Section 5.3.5.
- Higher concentrations were also observed from the Falcon and local boat/ground measurements in the Semporna region, an area of extensive macroalgae farms. Again, this is discussed further in Section 5.3.5.

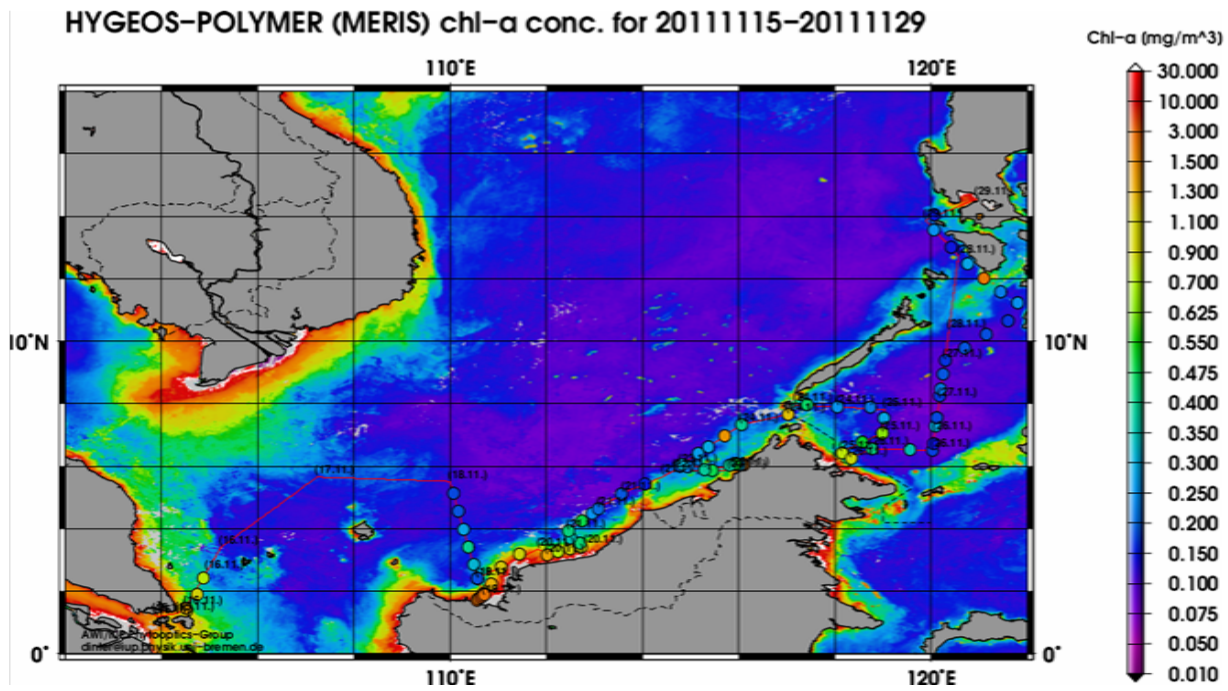


Figure 10. Two week composite map of satellite chlorophyll-a derived from the MERIS sensor and based on HYGEOS-POLYMER algorithm. The red line shows the R/V Sonne cruise track and coloured circles are in-situ chlorophyll-a concentrations measured using high performance liquid chromatography (HPLC). Map courtesy of Wee Cheah and Astrid Bracher (AWI) and François Steinmetz (HYGEOS), February 2013.

5.3.6 Back trajectories and air mass differences between sites

Differences between sites can be investigated further using back trajectories to establish movement of air masses in the hours or days preceding sampling. The Air Resources Laboratory's HYbrid Single-Particle Lagrangian Integrated Trajectory (HYSPLIT) model (Draxler & Rolph, 2013; Rolph, 2013) was used to compute back trajectories using NCEP/NCAR reanalysis data. The data are first generation reanalysis on a $2.5^\circ \times 2.5^\circ$ latitude-longitude grid with a horizontal resolution of ~ 210 km and 28 vertical levels (Kistler et al., 2001). Back trajectories were performed every 6 hours over the 48 hour period preceding 12:00 local time (LT) (04:00 UTC) on the day air samples were taken. A 48 hour time period was chosen as trajectories become increasingly unreliable the further back they are projected and also as VSLs source regions are believed to be relatively local. This procedure was repeated for three vertical levels; 100 m, 500 m and 1000 m. Fig. 11 shows a composite image of HYSPLIT trajectories at three vertical levels for each local boat site to demonstrate that, in general, little difference was seen between levels, a trend observed for almost all the back trajectories calculated during this period. Fig. 12 shows HYSPLIT trajectories for 12:00 LT for each day of the R/V Sonne cruise alongside additional trajectories, where needed, for local boat/ground and Falcon flights.

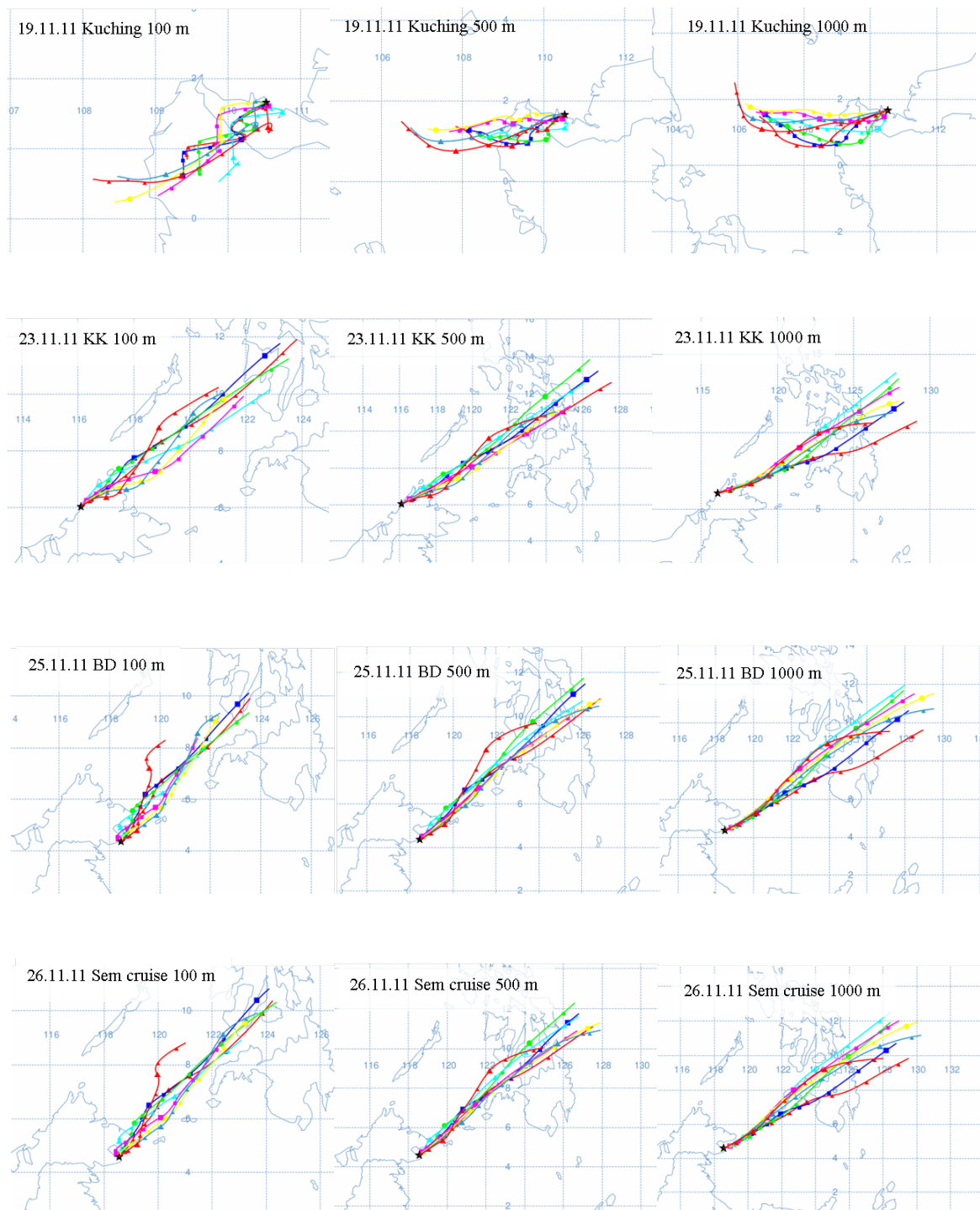


Figure 11. HYSPLIT back trajectories for local boat/ground stations. Trajectories were computed every 6 hours for 48 hours preceding 12:00 LT. Trajectories were calculated at three vertical levels; 100 m, 500 m and 1000 m. Colour represents starting time of back trajectory (oldest to youngest): red, dark blue, green, turquoise, purple, yellow, blue and red again. Original in colour.

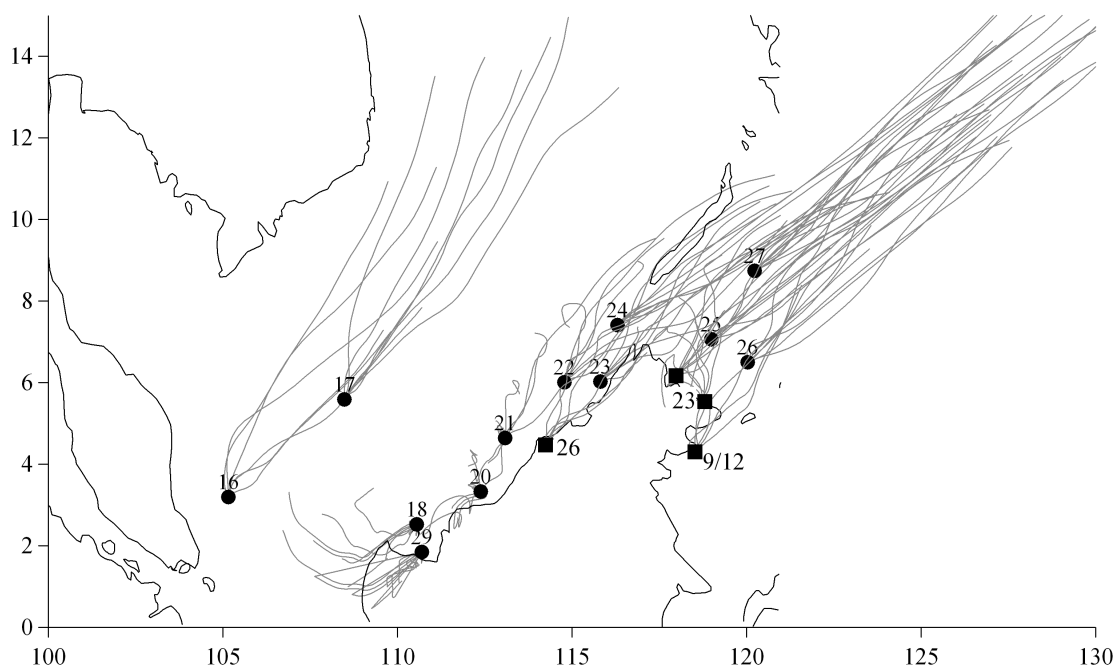


Figure 12. HYSPLIT back trajectories for R/V Sonne cruise and Falcon flights. ● = Starting back trajectory location for 12:00 LT for each day of the R/V Sonne cruise track, number = date (all November 2011) shown. ■ = Starting location for back trajectories for Falcon flights that did not coincide with the R/V Sonne. Again, dates shown next to marker (23 and 26th November, 9th December 2011).

The back trajectories allow us to identify four regions which support the concentration maps shown in Figs. 5-9. A visual summary showing a basic outline of these regions are shown in Fig. 13 and Table 6 provides a summary of measurements taken in each region. The four regions cover:

Region 1 (R1):

Low concentrations and back trajectories crossing the open ocean as the R/V Sonne crosses the SCS.

Region 2 (R2):

Some of the lowest concentrations were observed in this region – refer back to Section 5.3.2 where Kuching data were significantly different to those measured at other local boat/ground stations. Back trajectories typically crossed over land or out over the open ocean, but did not travel along coastal regions.

Region 3 (R3):

This region comprises the western Borneo coast. Back trajectories are predominantly from the Sulu Sea, in a northeasterly direction passing close to the Borneo coast. Some areas of elevated concentrations are observed in this region.

Region 4 (R4):

This region comprises measurements made in the Semporna area, a region known for macroalgae aquaculture (Neish, 2003). Back trajectories come from a similar direction to Region 3.

Observed halocarbon concentrations in these four regions can now be potentially attributed to local sources, air mass history or a combination of factors. To develop this idea the next section will utilise relationships between different halocarbons to further investigate the differences between these regions.

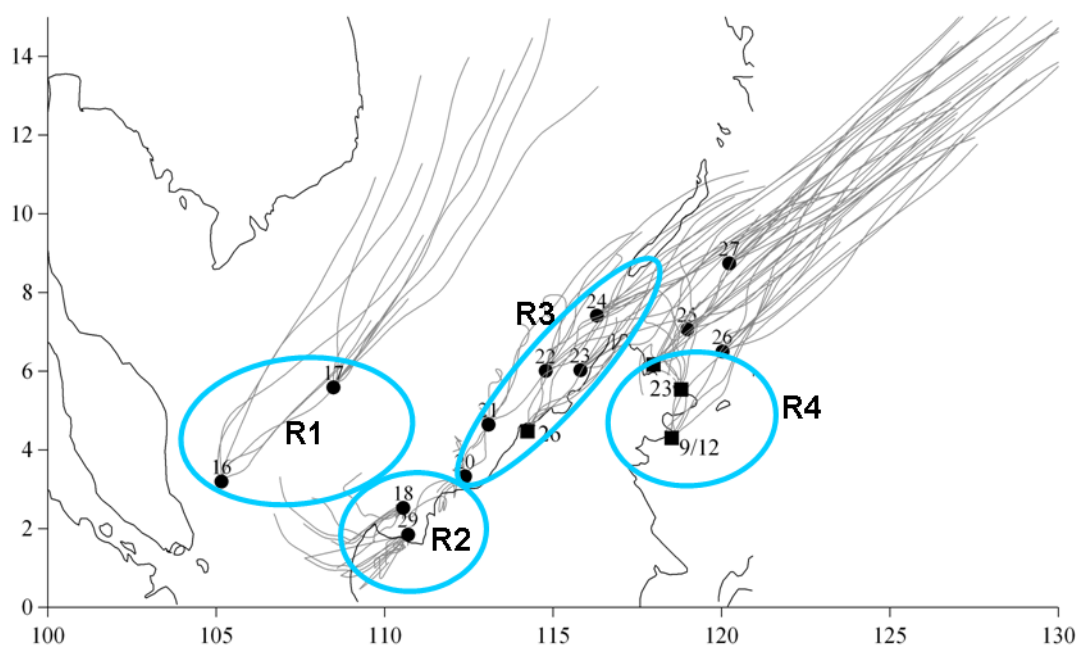


Figure 13. An overview of regions R1=R4 identified using back trajectories, halocarbon concentrations and chl-a concentrations. See text for further details.

Table 6. A summary of measurements taken in each of the four regions (R1-4) characterised by halocarbon concentrations and air mass back trajectories. x = no data available for this region.

	R1	R2	R3	R4
R/V Sonne	Transect across the SCS 15-18/11	18-19/11	Travelling northward parallel to the Borneo coast	x
Falcon	x	16/11 19/11	21/11 26/11	23/11 9/12
Local boat/ ground station	x	Kuching 19/11	KK 23/11	BD 25/11 semcruise 26/11

5.3.7 Halocarbon correlations in different regions of Borneo

In Chapter 3 correlations between halocarbons produced during macroalgae incubations were discussed. Significant correlations ($p < 0.001$) between CHBr_3 , CH_2Br_2 and CHBr_2Cl with R^2 values between 0.79-0.94 suggested a common biological source. Relationships between halocarbons have been exploited to provide information on source regions and the history of sampled air masses (Brinckmann et al., 2012; O'Brien et al., 2009; Yokouchi et al., 2005). Here we use relationships between three halocarbons, CHBr_3 , CHBr_2Cl and CH_2Br_2 , three compounds which have:

- A common, mainly marine biological, source.
- An assumed constant emission ratio in this region.
- Different atmospheric lifetimes ($\text{CHBr}_3 < \text{CHBr}_2\text{Cl} < \text{CH}_2\text{Br}_2$).

Carpenter et al. (2003) defined scenarios which could be identified using relationships between these three halocarbons to determine if they were sampling near or at a distance from the halocarbon source region. A similar technique will be used here, using two relationships to help define air masses sampled in Regions 1 to 4.

1. Correlations

Strong correlations suggest a close proximity to source regions. Fig. 14 and Table 7 show correlation plots and associated information for CHBr_3 vs CH_2Br_2 and CHBr_3 vs CHBr_2Cl . Orthogonal distance regression (ODR) was used to calculate the regression line slopes as this calculation allows for error in both the x and y variables.

Both Pearson Product-Moment Correlation Coefficient and Spearman's Rank Correlation Coefficient can be used as a measure of statistical confidence (p) in these correlations (Table 7). Whilst it is commonly assumed that the Pearson test should be performed on data that pass normality tests and the Spearman test on data that fail this is not the case, for non-ranked data Pearson's is generally the test of choice (see Howell, 2007 for a full description of selecting statistical correlation tests). Both tests can be conducted on non parametric data (and many of the regional halocarbon datasets failed Shapiro-Wilk normality tests at $p=0.05$) and can provide information on the reliability of the correlation, as will be discussed in more detail following Figs. 14 and 15.

2. Two-factor correlations to determine chemical decay

If measurements are taken at some distance from a site and it is assumed that diffusion and transport affect the three halocarbons equally then differences in concentrations are linked to chemical decay. A decay curve plotted on a plot of $\ln([\text{CH}_2\text{Br}_2]/[\text{CHBr}_3])$ vs $\ln([\text{CHBr}_3])$ or $\ln([\text{CHBr}_2\text{Cl}]/[\text{CHBr}_3])$ vs $\ln([\text{CHBr}_3])$ (Fig. 15, Table 8) should demonstrate an increasing ratio of $\ln([\text{CH}_2\text{Br}_2]/[\text{CHBr}_3])$ or $\ln([\text{CHBr}_2\text{Cl}]/[\text{CHBr}_3])$ with decreasing $\ln([\text{CHBr}_3])$ concentrations. This relationship exists as the shorter lifetime of CHBr_3 leads to more pronounced changes in the concentration of CHBr_3 relative to longer lived VSLS (CHBr_2Cl and CH_2Br_2). For example, in older or more diluted air there will be relatively more longer-lived CH_2Br_2 (Yokouchi et al., 2005).

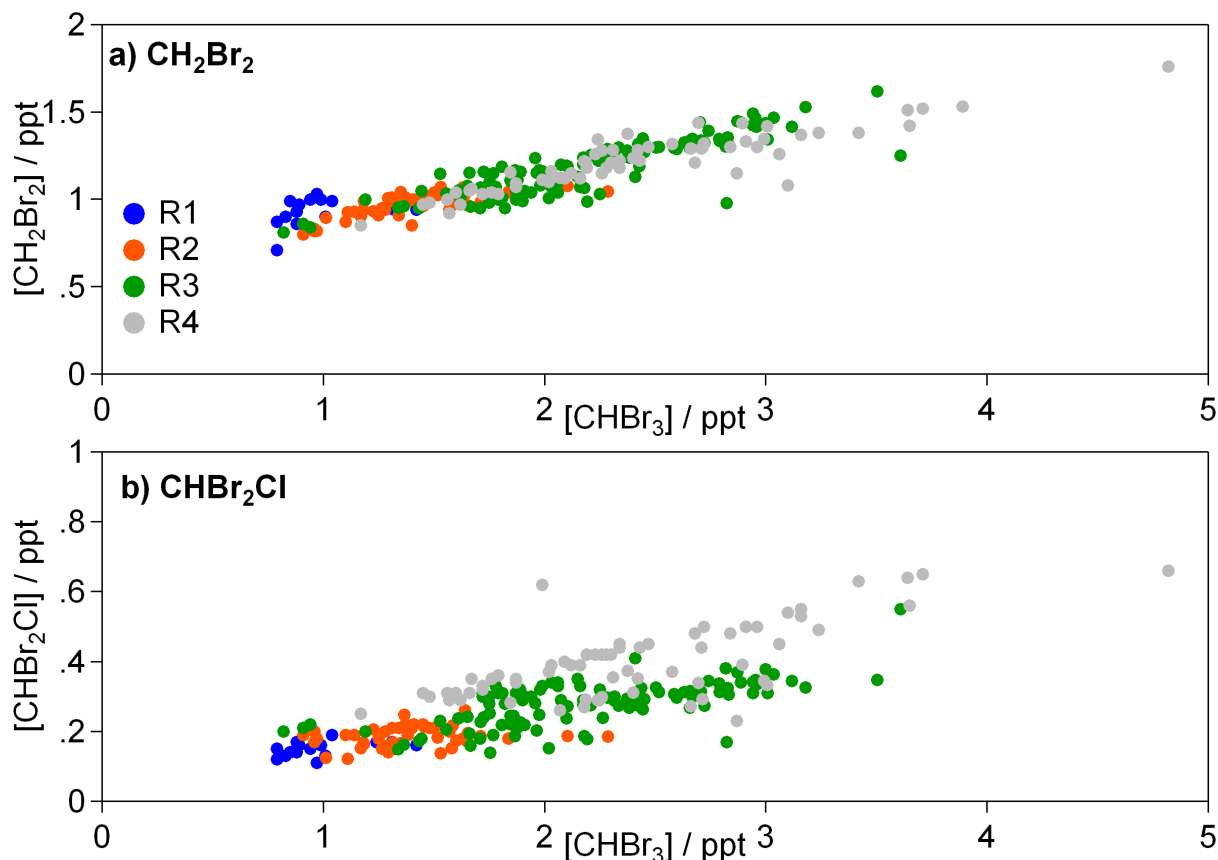


Figure 14. Bromoalkane correlations measured during SHIVA11. Data includes R/V Sonne, Falcon and local boat/ground station measurements. Points are coded according to region (see inset legend). See Table 7 for regression line equations. Original in colour.

Table 7. Descriptive statistics for bromoalkane correlations displayed in Fig. 14. The table includes ODR line equations; standard deviation (σ) on the slope (m); R^2 values; p values for Pearson's (p_r) and Spearman's (p_p) correlation tests.

n	CH ₂ Br ₂ – CHBr ₃					CHBr ₂ Cl – CHBr ₃					
	Equation ($y = mx + c$)	σ m	R^2	p_r	p_p	Equation	σ m	R^2	p_r	p_p	
R1	17	$y = 0.14x + 0.80$	0.09	0.11	0.19	0.07	$y = 0.04x + 0.11$	0.02	0.21	0.07	0.04
R2	49	$y = 0.19x + 0.70$	0.03	0.54	<0.001	<0.001	$y = 0.02x + 0.16$	0.02	0.04	0.16	0.05
R3	111	$Y = 0.27x + 0.58$	0.01	0.80	<0.001	<0.001	$y = 0.08x + 0.11$	0.01	0.50	<0.001	<0.01
R4	65	$Y = 0.22x + 0.67$	0.01	0.82	<0.001	<0.001	$y = 0.14x + 0.07$	0.02	0.51	<0.001	<0.01

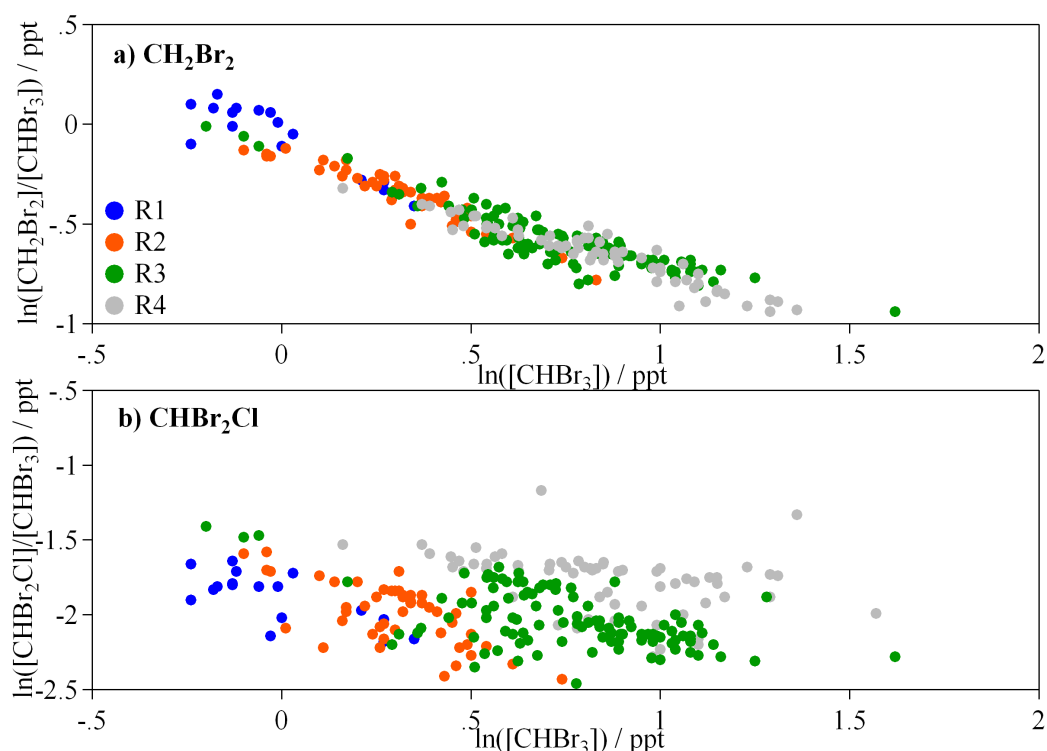


Figure 15. Logarithmic bromoalkane correlations measured during SHIVA11. Data includes R/V Sonne, Falcon and local boat/ground station measurements. Points are coded according to region (see inset legend). See Table 8 for regression line equations. Original in colour.

Table 8. Descriptive statistics for bromoalkane correlations displayed in Fig. 15. The table includes ODR line equations and R^2 values.

	n	CH ₂ Br ₂ / CHBr ₃ v CHBr ₃		CHBr ₂ Cl/ CHBr ₃ v CHBr ₃	
		Equation	R ²	Equation	R ²
R1	17	$y = -0.92x - 0.07$	0.79	$Y = -0.90x - 1.90$	0.52
R2	49	$y = -0.72x - 0.12$	0.89	$y = -1.22x - 1.62$	0.48
R3	111	$y = -0.56x - 0.17$	0.81	$y = -0.66x - 1.56$	0.26
R4	65	$y = -0.56x - 0.18$	0.88	$y = -0.59x - 1.29$	0.14

Regional differences are clearly shown in Figs. 14 and 15. Correlations of both CH₂Br₂ and CHBr₂Cl with CHBr₃ are weakest in regions 1 and 2. Region 1 is an open ocean area where low halocarbon production was observed. Weak correlations are expected, as seen by Yokouchi et al.

Regional differences are clearly shown in Figs. 14 and 15. Correlations of both CH_2Br_2 and CHBr_2Cl with CHBr_3 are weakest in regions 1 and 2. Region 1 is an open ocean area where low halocarbon production was observed. Weak correlations are expected, as seen by Yokouchi et al. (2005) who reported weak or nonexistent correlations at open ocean sites where $\text{CHBr}_3 < 3.5$ ppt. Region 2, however, is coastal and so higher concentrations may be expected here. The observed weak correlations in Region 2 could be linked to back trajectories crossing over the land, bringing diluted air into the sampling region. As will be discussed further during emission budget estimates in Chapter 6 Section 6.2, little data exists on the distribution of macroalgae around the Malaysian coast. We did see macroalgal debris during the Kuching cruise, but low concentrations in this region could be indicative of limited macroalgae colonisation.

Correlations (Fig. 14) were stronger in regions 3 and 4 where air passed along coastlines, sometimes crossing Philippine islands to the north. Air masses sampled in these two regions had potentially spent longer in highly productive regions. The strongest CH_2Br_2 vs CHBr_3 correlation was observed in Semporna (R4), known as an area of macroalgae colonisation (Phang et al., 2010) and also a site of previously high halocarbon measurements (Pyle et al., 2011). Fig 15 supports R4 as a source region; R4 $\ln([\text{CH}_2\text{Br}_2]/[\text{CHBr}_3])$ vs. $\ln([\text{CHBr}_3])$ data is clustered in the lower part of the plot, with relatively higher CHBr_3 concentration suggesting proximity to source.

As discussed earlier in this section, differences between Spearman and Pearson correlation tests can provide further information on the datasets. As Table 7 shows, R3 and R4 showed statistically significant correlations ($p = < 0.01$) for both relationships under both tests, as did the CH_2Br_2 vs. CHBr_3 relationship at R2. Stronger correlation coefficients for Pearson tests compared to Spearman are indicative of strong linear relationships. However, weaker or failed correlations were seen at R1 and R2.

Fisher's z-statistic can be used to determine if statistical significances exist between correlations. Performing Fisher's z statistical test according to Howell (2007) for the Pearson's p_r values displayed in Table 7 we produce a matrix (Table 9) which supports the trends discussed earlier. Regions 1 and 2 and regions 3 and 4 are grouped, with little or no statistical difference between correlations, whilst differences exist between these pairings (R1 and R2 compared to R3 and R4). This is of interest as Zhou et al. (2008) observed differences in both mixing ratios and the slope of linear regressions between sites but no significant differences between the correlations. They attributed this a pervasive influence of marine air throughout their sampling region, which we do not appear to see in our Borneo results.

The relationship between CHBr_2Cl and CHBr_3 both for correlations (Fig. 14) and logarithmic ratios (Fig. 15) is weaker than the one between CH_2Br_2 and CHBr_3 . Carpenter et al. (2003) also saw a weaker relationship for CHBr_2Cl vs. CHBr_3 . They attributed this to changes in relationship (seen by changes in the slope of the regression line) at higher CHBr_3 concentrations. An analysis of the combined dataset from R1-R4 shows no difference between the ODR slope for data containing the lowest and highest 50% of CHBr_3 concentrations (after Carpenter et al., 2003). Brinckmann et al. (2012) noted deviations from the general CHBr_2Cl vs CHBr_3 relationship pattern due to unexpectedly high CHBr_2Cl mixing ratios in coastal regions. They attributed this to independent sources or a higher emissions of this compound in localised regions of the western Pacific. As the results from seaweed incubations (Chapter 3) showed strong correlations between CHBr_2Cl and CHBr_3 the source of these discrepancies must lie in other (non macroalgal) source regions or in other processes that have yet to be fully quantified in tropical regions (e.g. loss or exchange processes in seawater).

Table 9. Fisher's z-statistic test results for Pearson correlation p_r values determined for CH_2Br_2 vs. CHBr_3 and CHBr_2Cl vs. CHBr_3 in regions 1-4. $z > 1.96$ demonstrates a significant difference at $p=0.05$.

CH_2Br_2 vs. CHBr_3				CHBr_2Cl vs. CHBr_3			
	R1	R2	R3	CHBr_2Cl	R1	R2	R3
R1				R1			
R2	1.99			R2	0.89		
R3	3.80	2.68		R3	1.42	3.83	
R4	4.00	2.97	0.67	R4	1.36	3.46	0

5.3.8 Three-factor correlations to determine regional emission ratios

Several studies have used more complex relationship calculations to determine region emissions. A principle outlined by McKeen and Liu (1993) demonstrates that by using three compounds with common sources and constant regional emission rates one can also investigate the effect of chemical decay and dilution on sampled air masses and from this information determine regional emission ratios.

Using the principles of McKeen and Liu (1993) a log-log plot of $\text{CHBr}_3/\text{CH}_2\text{Br}_2$ against $\text{CHBr}_2\text{Cl}/\text{CH}_2\text{Br}_2$ for a regional dataset should be bound in an envelope of two lines representing two scenarios. The first is a 'dilution line' which has a slope of 1 on a log-log plot. This is representative of a situation where all three species are inert and background concentrations of CHBr_3 and CHBr_2Cl are zero. The second is a 'chemical decay line' where decay is governed by pseudo first order chemical reaction, the slope (m) of which is predicted by Eq. 2 where k is the rate constant for each halocarbon, in this case the rate of decay which can be determined from the lifetime (τ) of CHBr_3 , CHBr_2Cl and CH_2Br_2 as shown in Eq. 3. Commonly the chemical decay line slope has been calculated to be 4.89 (e.g. Yokouchi et al., 2005) based on lifetimes of 26, 69 and 120 days for CHBr_3 , CHBr_2Cl and CH_2Br_2 respectively. Recently, Brinckmann et al. (2012) reduced the slope to 2.84 to represent shorter tropical lifetimes of 16, 29 and 52 days based on Hossaini et al. (2010).

$$m = \frac{(k_{\text{CHBr}_3} - k_{\text{CH}_2\text{Br}_2})}{(k_{\text{CHBr}_2\text{Cl}} - k_{\text{CH}_2\text{Br}_2})} \quad (2)$$

$$\tau = \frac{1}{k} \quad (3)$$

Previous studies have used the intercept of these two lines to estimate both regional and global oceanic halocarbon fluxes by scaling the emissions to a co-emitted compound for which an absolute emission rate is believed to be known with the most confidence, in this case CH_2Br_2 due to its longer atmospheric lifetime. Fig. 16a shows the data from SHIVA11 overlaid with emission estimates from three previous studies. Point A refers to Brinckmann et al. (2012) who infer an emission ratio of 0.35, 9 (all ratios given as CHBr_2Cl , CHBr_3) using the updated chemical decay line slope of 2.84 and data from mid latitudes as well as the tropical west Pacific. Point B represents a ratio of 0.46, 9 taken from O'Brien et al. (2009) determined from measurements at Cape Verde. Finally, point C is taken from Yokouchi et al. (2005) and represents their ratio of 0.7, 9 from data collected at a range of sites (including tropical islands and open ocean data). Both the O'Brien and Yokouchi studies use a slope of 4.89. In Fig 16b dilution and chemical decay lines that best fit our data have also been plotted. The CHBr_2Cl , CHBr_3 'apex' of Yokouchi et al. (point C on both Fig 16a and b) fits our data well when combined with the chemical decay line slope derived for tropical sites by Brinckmann et al. (2012).

Across all studies a regional emission ratio of 9 for CHBr_3 (relative to CH_2Br_2) was determined. However, differences arise in the CHBr_2Cl results which range from 0.35 to 0.7 (again relative to CH_2Br_2). Carpenter et al. (2003) reported differences in the CHBr_2Cl vs. CHBr_3 regression slope at higher concentrations (as discussed in Section 5.3.6). Perhaps differences in proximity to emission sources between these studies may account for differences in the relationship between CHBr_2Cl and other bromocarbons.

As it is commonly assumed that macroalgae are an important halocarbon source it is useful to compare this atmospherically-derived ratio (0.7, 9) to that determined from tropical incubations in Chapter 3. Averaging all 15 incubated species the mean incubation ratio is 4 (range 0.2-17) for $\text{CHBr}_3/\text{CH}_2\text{Br}_2$ and 0.3 (range 0.03-1) for $\text{CHBr}_2\text{Cl}/\text{CH}_2\text{Br}_2$. These ratios are not dissimilar to those determined by Carpenter et al. (2000) for a range of temperate species. When macroalgae are fully submerged (as we commonly observed in peninsular Malaysia) then the emissions are first to seawater, and then to the atmosphere, so observed emissions will be modified according to the relative solubility of the gases. Using the Henry's Law coefficients for halocarbons in seawater from Moore et al. (1995) gives relative solubilities for $\text{CHBr}_3/\text{CH}_2\text{Br}_2$ and $\text{CHBr}_2\text{Cl}/\text{CH}_2\text{Br}_2$ of 1.5 and 0.8 respectively. Correcting the above ratios for equilibrium partitioning between water and gas phases results in atmospheric emission ratios of 3 and 0.4 respectively for the same halocarbon pairs averaged across all species incubated. In general, these compare well to the emission ratios derived from atmospheric concentrations, although macroalgae incubations displayed a wide range of ratios highlighting the need for caution when using them to determine 'bottom up' emission estimates of regional emissions (Chapter 6 Section 6.2).

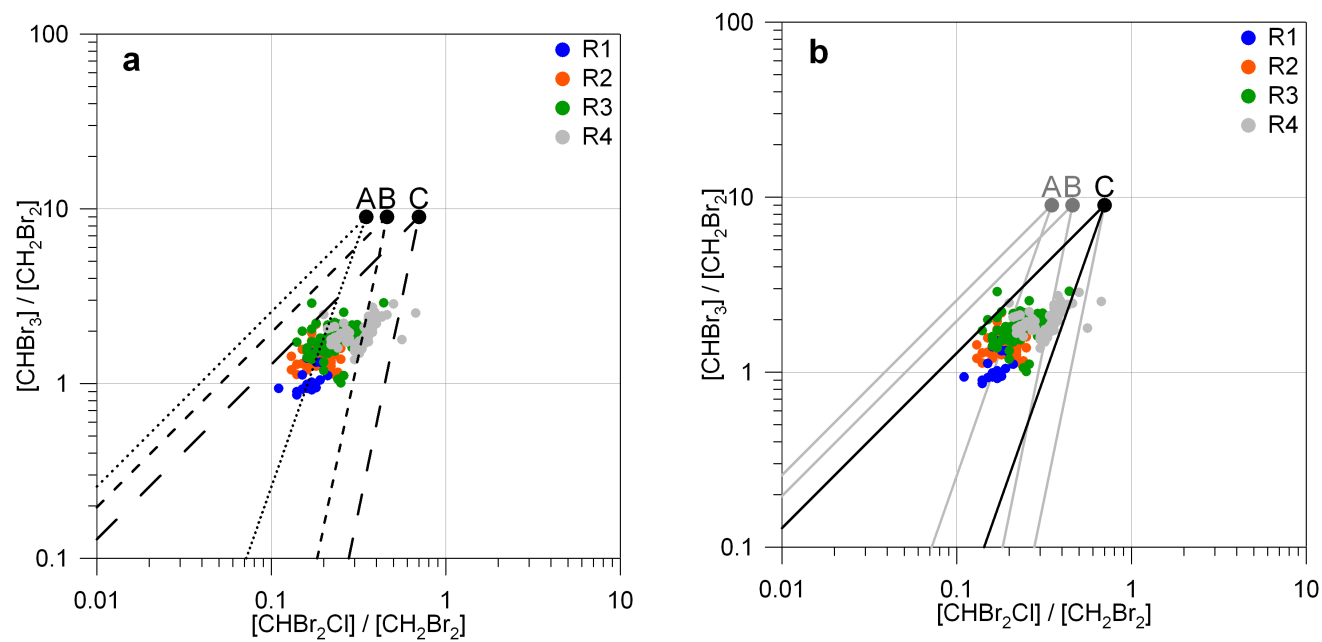


Figure 16. Ratios of $[\text{CHBr}_3]/[\text{CH}_2\text{Br}_2]$ plotted against $[\text{CHBr}_2\text{Cl}]/[\text{CH}_2\text{Br}_2]$ on a log-log scale. Data points are colour-coded with respect to region (see inset legend). Points A, B and C are described in the main body of text. Dilution and chemical decay lines (see main body of text) in panel a are taken from Brinckmann et al. (2012), O'Brien et al. (2009) and Yokouchi et al. (2005). Panel b shows these lines (now in grey) with the addition of dilution and chemical decay lines derived in this study (black). Original in colour.

5.3.9 Contribution of biogenic VSLS to stratospheric bromine

As discussed in Chapter 1 Section 1.7.2, tropical regions are believed to be important with regards to the capacity of tropical deep convection to transport biogenic VSLS from the MBL to the TTL and so act as an important source region for the biogenic VSLS contribution to stratospheric Br_y (Br_y^{VSLS}) (Aschmann et al., 2009). The tropical west Pacific, including the region of interest to SHIVA, is situated within the West Pacific Warm Pool, an area containing some of the warmest waters in the world (Anderson et al., 1996). These warm surface waters provide moist warm air to feed strong convective systems which can transport short lived halocarbons to tropical tropopause layer (see Section 1.7). Fig. 17. shows visible band satellite images from the MTSAT-1R geostationsary satellite for 06:00UTC daily from 19th – 25th November 2011, a period covering many of the SHIVA measurements. Large convective clouds appear as bright white clouds on the visible satellite images, and are clearly visible within the measurement region, supporting the idea that this region can provide convective transport for VSLS to the upper troposphere. As well as physical transport, physical and chemical loss processes will impact the amount of emitted VSLS that reach the upper troposphere, the rest of this section provides preliminary calculations as to the percentage of ground-level emissions transported to higher altitudes.

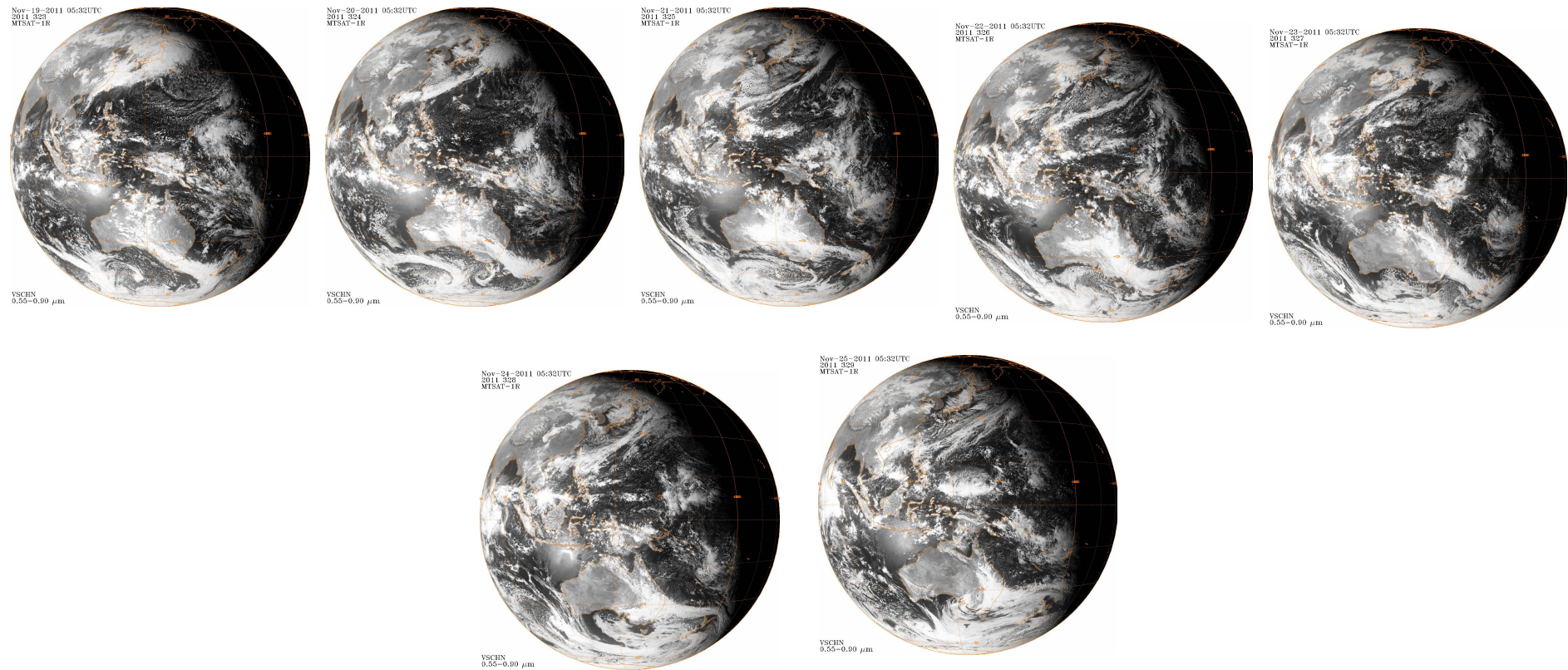


Figure 17. Visible band satellite images from the MTSAT 1R satellite for 06:00 UTC daily from 19^h – 25th November 2011. Images are in chronological order left to right and top to bottom. Images are from the NOAA National Climatic Data Center archives, accessed May 2013 from <http://www.ncdc.noaa.gov/gibbs/year> (NCDC, 2013).

Current estimates place the contribution of biogenic VSLS to stratospheric bromine at 6 (1-8) ppt (Montzka et al., 2010; see also Chapter 1 Section 1.6.4). As a key aim of the SHIVA project was to contribute to reducing the uncertainty in this figure, it seemed pertinent to consider how the atmospheric concentrations discussed in this chapter may contribute to stratospheric $\text{Br}_y^{\text{VSLS}}$. The mean boundary layer mixing ratios for five brominated VSLS calculated from SHIVA11 are shown in Table 10. Referring to modelling work by Hossaini et al. (2012b) we see that approximately 77% of bromine from VSLS produced in the tropical boundary layer may form stratospheric $\text{Br}_y^{\text{VSLS}}$. Hossaini et al. (2012b) used five VSLS we measured in Borneo (CH_2Br_2 , CHBr_3 , CH_2BrCl , CHBrCl_2 , CHBr_2Cl), as well as bromoethane ($\text{C}_2\text{H}_5\text{Br}$) which we did not measure. Our calculations, based only on the mean concentrations observed during SHIVA11 (see Table 3), suggest a preliminarily calculated contribution to stratospheric $\text{Br}_y^{\text{VSLS}}$ from measurements made around Borneo of ~ 7 ppt. Model results from Hossaini et al (2012b) calculate a tropical contribution of 4.9-5.2 ppt. A lower contribution was estimated by Tegtmeier et al. (2012) with an average contribution of 0.4 pptv Br and a maximum of 2.3 pptv Br, based on measurements made in the west Pacific. Their results are based only on CH_2Br_2 and CHBr_3 , and the reader's attention should be drawn to the online reviewer comments for this article, which make a comprehensive discussion regarding these low figures and the possibility that they are unusually low due to their basis on measurements made during one campaign where Tegtmeier and coworkers observed low to moderate oceanic bromocarbon emissions). Comparing our value (which includes a significant number of coastal observations) to the previous studies, a preliminary conclusion would be that coastal regions potentially contribute significantly to stratospheric bromine loading in the tropical zone. Our measurements are higher than Hossaini et al. (2012b), who use more spatially averaged halocarbon concentrations. They are also higher than open ocean measurements made by Tegtmeier et al. (2012), although a better comparison may be to compare the contribution from our oceanic region (R1) at 5 ppt Br, with our stronger coastal source regions (R3 and R4) at 9 and 10 ppt Br respectively. Further calculations to constrain the strength of these emissions are beyond the scope of this chapter.

5.4 Conclusions – regional halocarbon distributions around Malaysia

Previous studies have commonly used emission estimates derived from the log-log plots discussed in Section 5.3.7 to determine global halocarbon emissions, scaling the ratio of CHBr_2Cl and CHBr_3 to global CH_2Br_2 emission estimates from Montzka et al. (2010). As we derived the same or similar ratio as many previous studies this task has not been repeated here. However, this dataset still provides useful information regarding regional atmospheric distributions of halocarbons around Borneo, which will be summarised below. The following chapter (6) will bring together results from this study, alongside the incubation work in Chapter 3, to look at regional halocarbon emission estimates in more detail.

Tropical coastal atmospheric halocarbon measurements made in Malaysia fell within the range of previous studies (Table 5). Halocarbon concentrations were higher than tropical open ocean data supporting a coastal halocarbon source in these regions (Section 5.3.3). However, observations made during SHIVA11 were lower than some other coastal studies (e.g. Yokouchi et al., 2005). Due to the short lived nature of these halocarbons, distribution is patchy (Section 5.3.4). High concentrations were observed in areas of heavy macroalgae colonisation in peninsular Malaysia (e.g. Port Dickson) but the impact of coastal halocarbon distributions appeared to be spatially limited. Prevailing wind conditions appear to also play a potential role in halocarbon distributions; air coming from productive coastlines or islands in the northeast are linked to regions of higher halocarbon concentrations. However, reliable predictions of regional halocarbon distributions cannot be made without first gaining better information on the distribution of macroalgae beds around the Malaysian coastline.

Previous modelling studies (Pyle et al., 2011; Warwick et al., 2006) have often assumed strong emission sources around entire stretches of tropical coastline. Strong production during laboratory incubations of tropical macroalgae (Chapter 3) support this theory, in situ atmospheric measurements do not. Semporna, a region of large aquaculture sites where rhodophytes (which laboratory studies have determined to be prolific halocarbon producers) are cultivated, did not show significantly higher concentrations of halocarbons than other regions in this, or previous studies. Yokouchi et al. (2005), when plotting data from a wide range of coastal and open ocean sources on a log-log plot similar to Fig. 16, saw coastal measurements falling on or close to the dilution line, an indicator that these are source regions as the ratios had not been affected by chemical decay. Our data from Semporna (which forms part of R4 in Fig. 16) does not follow this pattern, suggesting influences of dilute, background air even in regions of potentially strong halocarbon sources.

For logistical reasons it was not possible to make measurements of halocarbon concentrations in the seawater around Semporna. Further work should focus on obtaining both atmospheric and seawater samples to provide measurements of in situ halocarbon fluxes. Our data suggests that care should be taken when extrapolating 'bottom up' macroalgae production to produce regional emission estimates as additional in situ processes may occur. For example, halocarbon breakdown processes (e.g. bacterial breakdown (Goodwin et al., 1997b)) may have a greater effect in the tropics (see Chapter 1 Section 1.4, 1.7 and 1.8). The need for further measurements of both seawater and atmospheric halocarbon measurements are supported by a weaker relationship between CHBr_2Cl and CHBr_3 compared to CH_2Br_2 in coastal regions seen in this study and others, which has not fully been explained (Brinckmann et al., 2012; Carpenter et al., 2003). Little discussion has also been given to the CH_3I or the relationship between iodocarbons and inorganic iodine species (such as IO) in this region. Measurements of this type were made during SHIVA11, see Chapter 6 Section 6.4.

Overall, it seems that 'hot spots' of halocarbon production exist around the Malaysian coastline, potentially associated with productive coastal regions such as macroalgae beds. However, data from such regions should not be extrapolated to determine emissions for entire coastal regions. Further information on halocarbon sources, sinks and transport in this region are needed to provide a full picture of regional halocarbon emission budgets.

CHAPTER 6

Regional estimates of annual bromocarbon emissions and concluding remarks

6.1 Introduction

The aim of this chapter is to bring together knowledge gained in the previous research-focused chapters. It contains three sections:

Section 6.2 calculates annual bromocarbon emission estimates from Malaysia and south east Asia. In this section production rates from tropical macroalgae calculated in Chapter 3 are used to derive a bottom up estimate of emission budgets. Section 6.2 also considers the impacts of tropical macroalgae aquaculture, at both current and predicted future levels, on regional halocarbon emissions estimates. This section of work can also be found in Leedham et al. (2013).

Section 6.3 brings together the outputs from Chapters 3-5 to provide an overview of this thesis. Overarching themes and outcomes are discussed.

Section 6.4 builds on the previous two sections and identifies ideas for further development of this research field.

6.2 A semiquantitative analysis of the halocarbon flux from macroalgae

The tropical region, especially the Pacific, has often been considered an important source region with regards to the global halocarbon budget, as described in Chapter 1 Section 1.7. Tropical fluxes have been proposed as globally important on the basis of observed high atmospheric mixing ratios and surface seawater concentrations, a proposed strong macroalgal source and strong deep convective systems (Butler et al., 2007; Montzka et al., 2010; Pyle et al., 2011; Yokouchi et al., 2005). As Chapter 3 provided the first direct measurements of tropical macroalgal halocarbon production it is worthwhile to use the incubation-derived halocarbon production values to estimate regional fluxes of CHBr_3 and compare these values to existing estimates. Papers referred to multiple times are abbreviated after first use for brevity. At the end of Section 6.2. all data used in these estimates, alongside any assumptions or calculations made, are summarised in Table 1 and a comparison with other studies is made in Table 2.

6.2.1 Determining macroalgal biomass

To estimate macroalgal biomass along the Malaysian coastline, biomass transects conducted by the University of Malaya (UM) at Port Dickson (Chapter 3, Fig. 1) were used (Keng et al., 2013) [Keng13]. Biomass evaluations were made several times over an 18 month period between March 2010 and June 2011. These biomass surveys are entirely the work of UM, but are used in the further evaluation presented here. During each visit triplicate 100-130 m long transects each comprising 10 to 13 quadrats were conducted. All seaweed in each 0.09 m² quadrat was collected and returned to the laboratory to determine total fresh (FW) and dry (DW) biomass as well as species abundance. Average biomass values during this 18 month period were 7.0, 5.2 and 0.1 kg FW m⁻² for phaeophytes, chlorophytes and rhodophytes respectively.

No other published biomass data for the tropics was available for comparison, however Hameed and Ahmed (1999) [HA99] measured localised biomass on the Pakistan coast and provide mean annual biomass values of 13.6, 11.0 and 4.1 kg FW m² for phaeophytes, chlorophytes and rhodophytes. Both studies show the same distribution of biomass: phaeophyte > chlorophyte > rhodophyte. However, total biomass per square kilometre from HA99 is roughly double that of Keng13. Previous studies estimating the contribution made by macroalgae to the global halocarbon flux (Gschwend et al., 1985; Nightingale et al., 1995) used biomass values determined from a 1975 FAO report (Michanek, 1975 - out of print, summary in Naylor, 1976) [Mich75] which estimated a global standing stock of phaeophyte and rhodophyte biomass of 1.5×10^{10} and 2.7×10^9 kg FW respectively. There are no data for chlorophytes in the Mich75 dataset, and it is biased to species that are harvested or farmed for commercial purposes. A comprehensive discussion of the Mich75 estimation and the errors attached to it, with regard to temperate coastlines, can be found in Carpenter and Liss (2000) [CL2000] who conclude that it is an underestimation. Charpy-Roubaud and Sournia (1990) defined a potential global coastal area inhabited by macroalgae of 6.8×10^{12} m². Attempts to distribute the global standing stock given by Mich75 over this area results in biomass estimates of $\sim 2.2 \times 10^{-3}$ kg FW m² for phaeophytes and 3.9×10^{-4} kg FW m² for rhodophytes. These are much lower than both the Keng13 and HA99 estimates. This is not unexpected as seaweed distribution is variable and errors would arise from scaling in either direction. On one hand, individual biomass studies are likely conducted in areas of high macroalgal biomass and therefore enhanced research potential. On the other, global standing stock estimates are difficult to reduce to regional biomass estimates, especially in the tropics given that much of the current data is based on temperate and/or economic species. An example of a potential source of error when estimating halocarbon emissions can be seen in the significantly lower proportion of rhodophytes in the Keng13 database compared with both HA99 and Mitch75. We have shown tropical rhodophytes to be prolific producers of halocarbons and an overestimation of rhodophyte biomass could therefore lead to an overestimation in emission budgets. For these reasons, our ability to use regional biomass data, albeit from one site, will hopefully benefit the following Malaysian emission estimates, and, assuming similar species are found throughout south east Asia, (Phang et al., 2008), to a wider regional emission estimate as well.

6.2.2 Determining regional fluxes and annual emissions

To calculate the potential CHBr_3 flux from tropical macroalgae we assume that the coastal area covered by macroalgae extends 200 m from the shore with a constant gradient to a water depth of 6 m (Fig. 1). Whilst the Keng13 biomass study extended to a maximum of 130 m, for safety reasons, visual inspection confirmed that seaweed extended out beyond this depth. We then defined three potential coastal scenarios. Within each scenario the following assumptions remained constant:

Assumption 1 (A1): We assume that seaweeds are distributed evenly along the base of the coastal wedge defined in Fig. 1 in the same amount per square metre as recorded in the Port Dickson transects. Tidal ranges are discussed further in individual scenarios. Errors on biomass studies (Keng13) were included in the error associated with our flux rate, see A2.

Assumption 2 (A2): We averaged production rates for phaeophytes, rhodophytes and chlorophytes from the incubations conducted in Chapter 3 and multiplied this by the Keng13 biomass data to give a production/flux rate of $378 \text{ nmol CHBr}_3 \text{ m}^{-2} \text{ hr}^{-1}$. The main errors associated with this flux rate are from the calculated production rates and the estimations of regional biomass from Keng13. To account for this, the individual standard deviations on species' production rates (Appendix 1) were propagated with the standard deviation error associated with the biomass studies over an 18 month period to give a percentage standard deviation (%SD) error on our production rate of 61% (range $147\text{-}609 \text{ nmol CHBr}_3 \text{ m}^{-2} \text{ hr}^{-1}$). This is similar to the $\sim 70\%$ error on global CHBr_3 annual emission from macroalgae given by Carpenter and Liss (2000). A large proportion of this error is due to intra-species variability observed in the incubation experiments (see Chapter 3 Section 3.3.2) and the patchy distribution of rhodophytes at the Port Dickson sampling site. This error is discussed further in the following sections as this flux rate is used to determine regional emission estimates.

Assumption 3 (A3): Taking into account results from Carpenter et al. (2000) [Car2000] who show average diel production over a 24 hour light:dark cycle to be only 60% of that under constant illumination, we reduce our production values, which were determined under constant light, by the same amount. Light and biogenic halocarbon production was discussed further in Chapter 1 Section 1.3.3. Light levels are also likely to play a role in abiotic halocarbon production (Chapter 1 Section 1.2.2) which is not considered further here (Section 6.4).

Assumption 4 (A4): Where emissions are into seawater we assume instant mixing within this volume of water. We assume that the flux to the atmosphere is the major loss process for CHBr_3 in seawater since it has a long lifetime in seawater relative to all other known loss processes i.e. hydrolysis, biotic and abiotic reductive dehalogenation, halogen substitution and photolysis (Chapter 1 Section 1.4).

Assumption 5 (A5): Flux calculations are made using mean seawater concentrations calculated in each scenario and Eqs. 1 and 2 below; where K_w is the transfer velocity expressed from the liquid phase and ΔC is the concentration difference between the liquid (C_w) and gaseous (C_a) phases. A mean atmospheric concentration of 3.2 ppt was determined from the local boat data collected as part of the SHIVA11 campaign discussed in Chapter 5 (see Section 5.2.1) to represent a mean coastal atmospheric CHBr_3 concentration. The range of CHBr_3 concentrations measured was 0.9-6 ppt. A sensitivity analysis showed that high seawater concentrations (see Scenario 1) dominate the flux and that altering the atmospheric concentration within the range observed during SHIVA has little effect on the calculated flux rate. The dimensionless Henry's Law constant (H) was calculated using a mean 10 °N-10 °S latitudinal water temperature of 27 °C and a mean oceanic surface wind speed of 5.47 m s⁻¹ (Quack & Wallace, 2003) [QW03] and the procedure described in Johnson (2010). Flux rates and the factors affecting them were discussed in more detail in Chapter 1 Section 1.5.

$$\text{Flux} = -K_w \Delta C \quad (1)$$

$$\Delta C = \frac{C_a}{H} - C_w \quad (2)$$

Assumption 6 (A6): To estimate annual emissions from Malaysia and the south east Asian (SEA) region we assume that, as our calculations included both a mean annual seaweed biomass and a correction for reduced halocarbon production during darkness, our fluxes remain constant throughout the year. We use coastal lengths from the World Resources Institute (WRI, 2012) who provide comparable data for all countries discussed in this study. Our definition of SEA includes the coastlines of the following countries: Brunei, Burma, Cambodia, Christmas Island, Indonesia, Malaysia (both peninsular and eastern), the Philippines, Singapore, Thailand, Timor-Leste and Vietnam. No detailed information is available on the percentage of shoreline that supports seaweed in the Malaysian/SEA region. Based on our limited visual experience we guess that just under half the coastline may be populated by seaweeds and assign 40% of the coastline as potential macroalgal source regions (Table 1). We assume that an even distribution of macroalgae exists within this area, in the density reported by Keng13.

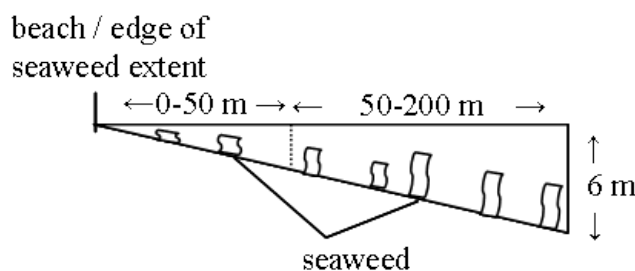


Figure 1. Visual representation of the seawater wedge used with assumptions A1-A6 (see text) to calculate emission scenarios. Technique after Carpenter et al. (2000).

Scenario 1:

Seaweeds are never exposed at low tide and emit constantly into the ‘wedge’ (Fig. 1) of water extending 200 m from the shore to a maximum depth of 6 m, a volume of 6×10^6 l for every metre of coastline. We assume the volume of seawater remains constant but refer to the Car2000 methodology whose calculations suggest that, due to tidal flushing, daily mean CHBr_3 concentration in the seawater wedge is similar to that which would be seen after 6 hours of constant emissions into the seawater. This may be somewhat of an overestimate due to a larger tidal range in Car2000; 3 m at Mace Head compared to 1.7 m at Port Dickson. Under scenario 1 we estimate a mean daily CHBr_3 concentration of 755 pmol l^{-1} . Unfortunately, for logistical reasons seawater measurements have not been made in this region (see also Chapter 5 Section 5.4 and this chapter Section 6.4). However, our value falls within the range of coastal values given by QW03 of 36-2000 pmol l^{-1} and is higher than the 388 pmol l^{-1} mean reported by Car2000 from measurements at Mace Head, Ireland (Table 2). The Car2000 value assumes that a depth of 10 m was reached 200 m from the shore. Increasing our water depth to 10 m would reduce our seawater concentration to 454 pmol l^{-1} , closer to the Car2000 value.

The resulting mean CHBr_3 flux from Malaysian coastal seawater influenced by seaweed beds to the atmosphere is $45 (17-73) \text{ nmol CHBr}_3 \text{ m}^{-2} \text{ hr}^{-1}$. Scaling this up to cover Malaysia and SEA (using A6) gives an annual flux of 1 (0.3-1.4) Mmol Br yr^{-1} for Malaysia and 15 (6-27) Mmol Br yr^{-1} for SEA (Mmol is 1×10^6 moles). These values are collated in Table 2.

Scenario 2:

In this scenario a tidal cycle is applied to the same coastal wedge. Between 0-50 m from the shore macroalgae beds are periodically exposed and submerged during a semi-diurnal tidal cycle. Between 50-200 m the macroalgae remain constantly submerged. The volume of water within the entire 200 m wedge fluctuates with the tidal cycle, with a maximum tidal range of 1.7 m (from Malaysian Admiralty tidal data logs). We assume that, when exposed, the average production rate of 378 nmol CHBr₃ m⁻² hr⁻¹ (A2) is emitted directly to the atmosphere and when submerged a flux rate is calculated using A5. Scaling up this flux rate using A6 gives an annual emission from Malaysia and SEA of 2 and 40 Mmol Br yr⁻¹ respectively.

In this scenario we make no alteration to emissions to account for stress during tidal exposure, as discussed in Chapter 1 Section 1.3.3 and 1.6.2. The impact of desiccation on bromocarbon emissions was investigated in Chapter 4, an increased pulse of emissions was seen, which generally lasted less than an hour. As the range of species studied in Chapter 4 was limited to one chlorophyte (*U. intestinalis*) and one phaeophyte (*F. vesiculosus*), both of which are temperate species, data from those experiments will not be applied here. It is worth noting, however, that emissions during exposure may increase due to exposure-related stress. Further experiments would help better constrain this pulse of emissions upon exposure.

Scenario 3:

In Scenarios 1 and 2 an assumption is made that CHBr₃ flushed from the coastal wedge during the tidal cycle is effectively lost and does not reach the atmosphere. However, as the lifetime of CHBr₃ in seawater is on the order of several years (see Carpenter et al., 2009 [Car09]; Hense & Quack, 2009; and Chapter 1 Section 1.4), CHBr₃ flushed from this coastal wedge may still evade to the atmosphere. With this in mind, Scenario 3 assumes all emissions from seaweed (at a rate of 378 (±61%SD) nmol CHBr₃ m⁻² hr⁻¹ (A2)) enters the atmosphere without an intermediate step via seawater. This represents an upper limit estimation and, when combined with scenarios 1 and 2, provides a flux rate range to compare to other studies. The annual emissions from Scenario 3 for Malaysia and SEA are 7 (3-12) and 140 (53-224) Mmol Br yr⁻¹ respectively (Table 2).

6.2.3 A comparison of estimated fluxes and emissions

The idealised scenarios described above place bounds on the likely coastal emissions from the SEA region and can be compared to previous estimates (Table 2). Comparisons between flux rate estimates should be made with caution as different studies use different flux calculations. Numerous factors can affect calculated fluxes, including approximations of wind speed, Schmidt number and CHBr_3 diffusivity (Chapter 1 Section 1.5). However, if we compare our flux rate range of 17-610 $\text{nmol CHBr}_3 \text{ m}^{-2} \text{ hr}^{-1}$ to the median global coastal flux derived by QW03 of 101 $\text{nmol CHBr}_3 \text{ m}^{-2} \text{ hr}^{-1}$ and their global range of 4-430 $\text{nmol CHBr}_3 \text{ m}^{-2} \text{ hr}^{-1}$, our values are not too dissimilar. Our upper estimate falls above theirs, however, our upper limit is based upon an assumption that all CHBr_3 produced by macroalgae reaches the atmosphere, a likely overestimate due to seawater loss processes (see A5). The QW03 data were heavily biased towards measurements in temperate and polar regions, and many were taken within the Atlantic, so this comparison suggests that tropical coastlines are not outliers in terms of global coastal fluxes. Physical, chemical and biological processes will vary in tropical coastlines compared to their temperate and polar counterparts. A description of potential differences is given in Chapter 1 Section 1.7, one example is increased rates of chemical loss processes due to warmer temperatures. Comparisons can also be made with Car09 who give a temperate (50-60 °N) coastal flux rate of 10 (5-13) $\text{nmol CHBr}_3 \text{ m}^{-2} \text{ hr}^{-1}$ and Butler et al. (2007) [BTL07] who provide an average global coastal flux rate of 9 (<0.1-21) $\text{nmol CHBr}_3 \text{ m}^{-2} \text{ hr}^{-1}$. These flux rates both fall below our Scenario 1 lower estimate, however both datasets are from research ship cruises which are very unlikely to represent waters directly influenced by macroalgae emissions well. The potential importance of macroalgae in determining coastal fluxes can be seen in a comparison with observations from the Cape Verde observatory (16.8 °N, 24.9 °W, tropical Atlantic) where intertidal seaweeds are not abundant. A localised flux rate of 7 $\text{nmol m}^{-2} \text{ hr}^{-1}$, derived by O'Brien et al. (2009) from model studies attempting to replicate local sources of the high atmospheric CHBr_3 concentrations observed at Cape Verde, is also lower than our range. In addition, our flux rates are higher than a range of open ocean CHBr_3 flux rates of 0.1 – 0.5 $\text{nmol CHBr}_3 \text{ m}^{-2} \text{ hr}^{-1}$ (BTL07; QW03; Tegtmeier et al., 2012) (Table 2). Our calculations suggest that in the tropics, as in temperate regions, there is a higher flux rate in a narrow coastal region compared to the open ocean.

Other chapters in this thesis have also considered differences between halocarbon biogeochemistry in different geographical regions. In Chapter 3 Section 3.3.4 halocarbon production by temperate, polar and tropical macroalgae was compared. Little difference was seen between production rates and it was concluded that differences in biomass distribution, for example, may be a more important driver in geographical differences in halocarbon emissions.

A collection of flux rates should be accompanied by estimates of total annual emissions for meaningful comparisons; a high flux in a narrow coastal band may contribute less than a lower open ocean flux covering a large area. Previous work (e.g. Warwick et al., 2006) has estimated that tropical coastlines act as an important global, as well as regional, halocarbon source, so we estimate regional CHBr_3 emissions based on our flux rates to allow comparisons with regional and global emission estimates. No other nation-specific data are available for comparison, but Pyle et al. (2011) [Pyle11] used atmospheric CHBr_3 measurements from inland and coastal sites with back trajectory and chemical transport models to estimate SEA regional emissions. They calculated an annual emission from their SEA region of between 180-350 Mmol Br yr^{-1} (assuming their 'Scenario 5' emissions are distributed evenly between coastal and open ocean regions). These values are lower than original estimates using a similar model with a coarser spatial resolution (Warwick et al., 2006) which predicted $\sim 7050 \text{ Mmol CHBr}_3 \text{ yr}^{-1}$ using similar scenarios). This earlier study suggested that the tropics must be a dominant source of halocarbon emissions in order to account for the observed atmospheric distribution of CHBr_3 . Our SEA annual emission range of 6-224 Mmol Br yr^{-1} , is lower than Pyle11, with our upper limit similar to their lower estimate. However a number of differences between these studies could account for this disparity. Firstly, both studies define SEA differently, the Pyle11 SEA region covers a larger area and includes more coastline, than ours. Secondly, whilst they do not specify the coastal width used in their model it is likely larger than our 200 m strip (scenarios in Warwick et al., 2006, which remain similar in Pyle11, use data from QW03 who quote a coastal area up to 2 km from the shore). It is highly likely that strongly seaweed-influenced fluxes are limited to a coastal zone much narrower than 2 km, and should not be extrapolated to cover such a large coastal region. Elevated concentrations in shelf regions are potentially attributable to other sources. One example, with respect to iodocarbons, is abiotic production requiring DOM (Chapter 1 Section 1.2.2). This process may have a stronger source in coastal and shelf waters where there is a higher DOM concentration. However, abiotic production of bromocarbons in this manner has not been reported. Other coastal sources, such as mangroves and coral reefs (see Chapter 1 Section 1.1 and 1.2) remain to be quantified and may need to be parameterised independently in model scenarios. This result highlights an important point made by Car09; that to compare coastal fluxes and emissions the community needs to create a standardised definition of coastal, shelf and open ocean zones.

If one compares our annual emissions to a wider dataset that provides global coastal annual emission estimates ranging from 1600 (CL2000) to 8100 (BTL07) Mmol Br yr⁻¹ (Table 2) our upper limit (Scenario 3) SEA value provides between 2-9% of total coastal CHBr₃ emissions. Previous studies have estimated the contribution of tropical oceans to the global halocarbon budget at ~75% (Palmer and Reason, 2009 (±46%), Yang et al., 2005). Our lower value suggests other areas, such as the open oceans, may be important in terms of global CHBr₃ emissions. Whilst lower CHBr₃ fluxes are seen in the open ocean its large area suggests it may provide a significant contribution to regional emission budgets. The impact of coastal and open oceans with respect to their contribution to stratospheric bromine in the SEA region was touched upon in Chapter 5 Section 5.3.8, where the importance of coastal regions was highlighted.

Several potential sources of error could affect our calculations which scale up biomass from one site to cover the SEA region. One example is the percentage of total macroalgae biomass comprised of phaeophytes, rhodophytes and chlorophytes. Data from Keng13 suggests rhodophyte biomass is <1% of total seaweed biomass per square metre yet rhodophytes were the dominant halocarbon producers during our incubation studies. For example, increasing rhodophyte biomass to 10% in Scenario 1 leads to a doubling of the scenario 1 mean flux rate from 45 nmol CHBr₃ m⁻² hr⁻¹ to 93 nmol CHBr₃ m⁻² hr⁻¹. This simple test highlights the benefit and need to conduct localised biomass studies alongside halocarbon production measurements. We also recognise, however, that Port Dickson was selected for this study in part because of prominent macroalgae colonisation. Other coastal areas we inspected along the western Malaysian shore were notably devoid of visible seaweed beds. Species selection was representative of common Malaysian species, including dominant genera such as *Sargassum* and *Gracilaria*, but a wide variety of species remain unquantified in terms of halocarbon emissions. For example, only 3 out of the 39 Malaysian *Sargassum* species recorded by Phang et al. (2008) were incubated. It should also be recalled that macroalgae produce CH₂Br₂ and mixed bromochloro- compounds alongside CHBr₃. These gases are also atmospherically important, Hossaini et al. (2012b) suggest they contribute ~1.2 ppt Br_y to the stratosphere, a not-unimportant amount compared to the contribution of ~4.9-5.2 ppt from CH₂Br₂ and CHBr₃ (see also Chapter 5 Section 5.3.8). Repeating the calculations made for CHBr₃ Section 6.2.2 we estimate the annual emission of CH₂Br₂ from SEA to be ~2-136 Mmol Br yr⁻¹ (Tables 1 and 2). This is not inconsiderable when compared to the same value for CHBr₃ (1-140) and when one considers the longer atmospheric lifetime of CH₂Br₂ and, therefore, its potential to dominate over CHBr₃ in terms of the flux of bromine from very short lived gases to the stratosphere.

Upon consideration of all factors, it seems likely that macroalgae may play an important role, regionally and within a narrow coastal band. However, across a larger coastal area emissions from tropical coastal macroalgae cannot account for all of the annual emissions predicted by models.

6.2.4 The impact of tropical aquaculture

Having established estimates for current Malaysian/SEA emissions it is of interest to consider how these are influenced by seaweed mariculture today, and how this may change in the future. Rhodophyte genera such as *Gracilaria*, *Gelidium* and *Kappaphycus*, which were all found to emit large quantities of bromocarbons (Chapter 3, in particular Sections 3.3.2 and Fig. 7) are commonly farmed for food or commercial products in SEA (John et al., 2011; McHugh, 2003).

As the seaweed found at Port Dickson is naturally occurring we assume the parameters used to calculate regional biomass in the flux calculations (Table 1) represent the natural biomass of Malaysia. We also estimate that current farmed seaweed biomass at ~ 6000 t DW yr⁻¹ (Neish, 2009; Phang et al., 2010) is in addition to this. Using these parameters to calculate halocarbon production from natural and farmed biomass we estimate that aquaculture currently makes up 0.7% of total Malaysian biomass but contributes $\sim 2\%$ of Malaysian CHBr₃ macroalgae emissions, due to the fact that farmed seaweeds in this region are all rhodophytes which are strong emitters of bromocarbons. There is a strong interest in increasing the amount of seaweed aquaculture in Malaysia; various studies suggest the potential increase could lead to a 6 to 11-fold increase in the area under cultivation (Goh & Lee, 2010; Neish, 2009; Phang et al., 2010). These predictions are based upon recent increases in production as well as projections of total cultivatable area. Increases of this magnitude could occur within the next decade, based on recent increases in growth. If we assume naturally produced halocarbon emissions remain constant this increase could lead to a corresponding increase in the relative contribution of CHBr₃ emissions from aquaculture, making it responsible for 12-20% of total annual CHBr₃ emissions from Malaysian macroalgae.

Clearly caveats must be applied to these calculations. Variations in production rate both within and between species (see Chapter 3) may affect our estimated macroalgae emissions. The percentage change estimates for the effects of aquaculture only consider production from macroalgae and not other potential coastal sources such as benthic microalgae, phytoplankton or mangroves. It is assumed that air-sea gas exchange processes are equal for natural and farmed algae and that the rate of these processes will not change in the future. Many factors, some unique to the coastal region, mean determining coastal flux rates are difficult. These processes include wave damping, drag (in shallower waters the ocean floor will exert a greater effect), higher wind speeds, thermal stratification (increased warming by light on shallower waters), changes in salinity due to precipitation and increased surfactants (Upstill-Goddard, 2006 and references herein). Accurate emission budgets would also need to include emissions that may occur during harvesting and post-harvest processing. We assume halocarbon production from natural and farmed algae is the same, despite the fact that artificial aquaculture environment places increased physiological stress on the algae due to increased prevalence of pests, disease and/or herbivores; increased light stress and potential nutrient limitation (Ask & Azanza, 2002).

It is also important to consider aquaculture on a global scale. Around 94% of seaweed production within the SEA region occurs in Indonesia and the Philippines (Phang et al., 2010) and market analyses suggest production in all of SEA is likely to increase (Neish, 2009), with consequent increases in regional halocarbon emissions. There are also other important non-tropical producers. China is the world leader, harvesting 1.2 million tonnes (DW) of seaweed in 2007, over five times the amount produced in the entire SEA region (Tang et al., 2011). These potentially larger emissions are, however, at a distance from the region of tropical deep convective systems. The range of cultivated species also differs, with China producing mainly *Laminaria* and *Porphyra* (Tang et al., 2011). *Laminaria* sp. in particular, are strong producers of iodinated species. This was introduced in Chapter 1 (e.g. Section 1.6.2) and Chapter 3 (Section 3.3.2) also demonstrated the propensity of phaeophytes to produce more iodocarbons relative to rhodophytes and chlorophytes. A larger percentage of phaeophyte biomass in Chinese aquaculture may mean the impact on local atmospheric chemistry may vary between the two regions.

Table 1. A summary of data sources, assumptions and calculations used to determine emission estimates in Section 6.2. Bracketed letters in the text, e.g. (a), refer to the first reference column. This table is a summary only, more detailed definitions of the processes used in these sections are given in the main body of the text.

Ref	Step	Data source, assumptions, modifications and notes	Value
Section 6.2.1 Determining macroalgal biomass			
a	Malaysian & south east Asian (SEA) seaweed biomass distribution	Keng et al. (2013) mean biomass from an annual study at one site in peninsular Malaysia (Port Dickson, see Chapter 3, Fig. 1).	Phaeophytes: 7.0 kg FW m ⁻² Chlorophytes: 5.2 kg FW m ⁻² Rhodophytes: 0.1 kg FW m ⁻²
Section 6.2.2 Determining regional fluxes and annual emissions			
b	Volume of water impacted by seaweed emissions	A wedge of water (see Fig. 1) extending out to 200 m and to a depth of 6 m (supported by Port Dickson biomass surveys) containing 6 x10 ⁵ l of seawater for every metre of coastline. Seaweed density along the base of this wedge is taken from (a).	See Fig. 1
c	Area of Malaysian and SEA coastline where seaweed is found	Total coastal length from (WRI, 2012). Based on very limited visual experience we estimate just under half (~40%) of Malaysian coastline may contain seaweed and assume this % extends to the whole SEA region. Flux rates covers area out to 200 m as in (b).	Malaysia: 7.5 x10 ⁸ m ² SEA: 1.4 x10 ¹⁰ m ²
d	CHBr ₃ emissions	Average rhodophyte, phaeophyte & chlorophyte production rates from our study (pmol g FW ⁻¹ hr ⁻¹) reduced by 60% to account for diel light cycles (Carpenter et al., 2000). Production multiplied by biomass (a).	378 (61%SD) nmol CHBr ₃ m ⁻² hr ⁻¹

Table 1 cont.

Ref	Step	Data source, assumptions, modifications and notes	Value
e	Scenario 1: CHBr ₃ concentration in coastal seawater	Macroalgae remain constantly submerged and volume of water remains constant (b). Emissions instantly mixed within seawater wedge (b). A loss for tidal flushing assumed from Carpenter et al. (2000) is applied.	755 pmol l ⁻¹
f	Scenario 1: CHBr ₃ flux	Flux calculated using mean seawater [CHBr ₃] from (e), mean atmospheric [CHBr ₃] of 3.2 ppt from measurements during the SHIVA campaign (Chapter 5), mean 10 °N-10 °S latitudinal water temperature of 27 °C and a mean oceanic surface wind speed of 5.47 m s ⁻¹ (Quack & Wallace, 2003) and the procedure described in Johnson (2010). A lower limit estimate.	45 (17-73) nmol CHBr ₃ m ⁻² hr ⁻¹
g	Scenario 1: Annual emission	Flux rate (from f) scaled to annual emission and applied to Malaysian and SEA coastal area where seaweed is found (c).	Malaysia: 1 (0.3-1.4) Mmol Br yr ⁻¹ SEA: 15 (6-27) Mmol Br yr ⁻¹
h	Scenario 2: Annual emission	Flux calculations as for Scenario 1 (d-f) but a tidal range of 1.7 m is applied to alter volume of coastal wedge. Seaweeds between 0-50 m from the shore are periodically exposed, increasing flux to atmosphere during this time. Hourly emissions using this varying flux rates are used to calculate a daily and then annual emission for the same area (c) as Scenario 1.	Malaysia: 2 Mmol Br yr ⁻¹ SEA: 40 Mmol Br yr ⁻¹
i	Scenario 3: Annual emission	All mean CHBr ₃ emissions per square metre reaches the atmosphere with no intermediary step via seawater. Emissions cover same area (c) as Scenarios 1 and 2. An upper limit estimate.	Malaysia: 7 (3-12) Mmol Br yr ⁻¹ SEA: 140 (53-244) Mmol Br yr ⁻¹
Section 6.2.4 Impact of tropical aquaculture			
j	Emissions from Malaysian aquaculture	Current Malaysian farmed biomass and future increases based on: Goh and Lee (2010), Neish (2009) and Phang et al. (2010). Assumes natural emissions are the same as in Section 6.2.2 and these remain constant in the future.	Current: ~6000 t Potential future: 6 to 11-fold increases

Table 2. A comparison of seawater concentrations, flux rates and annual emission estimates calculated in this study (Section 6.2) and the existing literature.

Study	Geographical region	Oceanic zone	Information source	CHBr ₃
Seawater concentrations				Seawater concentration / pmol⁻¹
This study	Tropical: Port Dickson, Malaysia	Coastal waters to 200 m, macroalgae area	Based on Malaysian macroalgae incubations and biomass studies (Scenario 1).	755
	Tropical: Port Dickson, Malaysia	Coastal waters	Samples taken over areas containing macroalgae and areas without.	up to ~410
Quack and Wallace (2003)	10-40 °N	Coastal <2 km from coast ("shore")	Review of oceanic and atmospheric measurements, various sources.	36-2000
Carpenter et al. (2000)	Temperate: Mace Head, Ireland	Coastal waters to 200 m, 5-15 m deep, macroalgal area	Site-specific seawater measurements.	388 (1σ=166)
		Shelf waters 2-10 km, 20-45 m deep ("offshore")		104 (1σ=12)
Flux rates				Flux to atmosphere / nmol CHBr₃ m⁻² hr⁻¹
This study	Tropical	As previous	As previous (Scenario 1 – Scenario 2).	17-610
Tegtmeier et al. (2012)	Extratropical and tropical western Pacific	Cruise track (mainly open ocean)	Seawater & atmospheric cruise data.	0.5
		Case study "hot spot"		3-5
Quack and Wallace (2003)	Globally averaged	Coastal <2 km from coast ("shore")	As previous.	101 (4-430)
		Shelf waters		4.4 (1-40)
	Atlantic	Open ocean		0.4
Butler et al. (2007) ^a	Tropical	Open ocean	Seawater & atmospheric data from seven cruises.	0.4
	Global	All		9 (<0.1-21)
Carpenter et al. (2009) ^a	temperate: Atlantic 50-60 °N	Coastal	Seawater & atmospheric data from two cruises.	10 (5-13)

Table 2 cont.

Study	Geographical region	Oceanic zone	Information source	CHBr ₃
Annual emissions				Mmol Br yr⁻¹
This study	Tropical	Malaysia	Bottom-up incubations of macroalgae combined with site-specific biomass study. Scenario 2 with Scenario 1 (min) and 3 (max) in brackets.	2 (0.3-12)
		SEA		40 (6-244)
Warwick et al. (2006)	Tropical, global	All	Model estimates attempting to reproduce observed atmospheric CHBr ₃ distributions. Their Scenario 5 places emission in tropical oceans.	7050
Pyle et al. (2011)	Tropical: south east Asia	Coastal	A refinement of Warwick et al. (2006) scenarios updated using regional atmospheric measurements from Borneo.	180
		All		350
Carpenter et al. (2009)	Global	Waters to depth of 180 m	Extrapolation of cruise/site specific measurements.	2500
Butler et al. (2007)	Global	All	As previous.	10000
		Open ocean		1900
		Coastal		8100
Palmer and Reason (2009)	Tropical	All	Flux value (above) scaled to estimated area of tropical oceans. Assumes no strong, coastal macroalgae source.	4350
Quack and Wallace (2003)	Global	Coastal ("shore")	As previous.	2300
Carpenter and Liss (2000)	Global	Coastal	Temperate measurements in macroalgal-rich areas scaled up using estimates of coastal length, fluxes and macroalgae biomass.	1600

^a Original value quoted as nmol CHBr₃ m⁻² d⁻¹, assumption that daily rate constant over 24 hours and converted as such.

6.3 A discursive summary of work covered in Chapters 3-5

In this section results from Chapters 3, 4 and 5 will be brought together to provide an overview of the research conducted and how it builds on previous data.

6.3.1 Regional halocarbon distributions around Malaysia

In Chapter 5 halocarbon measurements were made from a research ship, a research aircraft, small boats and from ground sites. Data were combined to create maps of regional emissions around Malaysia. Combining this data with chlorophyll-a satellite data and HYSPLIT back trajectories allowed us to outline four regions (Chapter 5 Section 5.3.5). Statistically significant differences in halocarbon concentrations and ratios in these regions were attributed to differences in source strength and meteorology. For example, region 2 (R2) was a region of low concentrations, potentially due to an input of air from over the land. Region 4 (R4) was a region of higher concentrations, potentially due to strong halocarbon sources in this area (Semporna) which is known for its macroalgal aquaculture (Phang et al., 2010). This links well with incubation studies conducted in Chapter 3, the results of which showed strong halocarbon production by a commonly farmed rhodophyte, *Kappaphycus alvarezii*. Halocarbon ratios were used to explore these regions, further, as described in Section 6.3.4.

6.3.2 Tropical macroalgae – incubations and emission estimates

In Chapter 3 halocarbon production rates for 15 tropical macroalgae species were investigated using laboratory incubations of macroalgae. Production of all 9 halocarbons (CH_3I , CH_2I_2 , CH_2Br_2 , CHBr_3 , CH_2BrCl , CHBrCl_2 , CHBr_2Cl , CH_2ClI and CH_2BrI) was observed. CH_2BrCl was produced in the smallest quantities, and production was not observed for some species. Apart from production of CH_3I from *Ulva reticulata*, all other halocarbons were produced from all other species.

Variation within replicates of the same species was sometimes considerable. An extreme example being variation between three individual plantlets of *Gracilaria changii* collected from the same site and incubated at the same time gave production rates ranging from 82 – 875 pmol g FW⁻¹ hr⁻¹. Despite this inherent variability, differences between species and class were still seen. In general, the rhodophytes were the strongest bromocarbon producers. Rhodophytes, for example *K. alvarezii*, are commonly farmed in Malaysia and south east Asia. This information was used in Chapter 6 Section 6.2 to discuss potential impacts of current and predicted future aquaculture on regional halocarbon emissions in south east Asia. Annual emission budget estimates were calculated based on biomass data from one site of peninsular Malaysia and so were made with many caveats. However, using these preliminary calculations, we estimated that due to the predominance of red algae in aquaculture, aquaculture currently contributes ~2% of Malaysian CHBr₃ emissions despite accounting for only 0.7% of Malaysian macroalgal biomass. Our projections of future aquaculture emissions based on potential aquaculture expansion data suggests that aquaculture could be responsible for up ~12-20% of total macroalgal emissions if all the predicted cultivatable area in Malaysia was to be realised.

Strong bromocarbon producers during incubation studies were often strong producers of other halocarbons too. This was investigated during the ranking exercise conducted in Chapter 3 Section 3.3.2. However, many species showed a spread of rank values and differences were seen between difference classes. For example, phaeophytes were strong iodocarbon producers, as seen for temperate species (Carpenter & Liss, 2000; Küpper et al., 2008). Chlorophytes were generally the weakest producers, with the exception of *Bryopsis* sp.. As *Bryopsis* is a fast-growing and opportunistic algae questions may be raised about whether halocarbon production assists in rapid colonisation of an area, perhaps by suppressing grazing or epiphytes in a similar way to how halogenated secondary metabolites may act (e.g. Paul & Pohnert, 2010). Future research ideas are discussed in Section 6.4.

The variation in halocarbon production rates from a range of species collected from a small range of sites demonstrates that species-specific halocarbon production measurements should be made, and combined with biomass data, to best determine halocarbon emission budgets from coastal macroalgae. A preliminary experiment combining incubation and biomass data is discussed in Section 6.2, using data from one site in Peninsular Malaysia. Differences were observed between biomass data from several different studies (Section 6.2.1), highlighting the need for a better understanding of regional biomass distributions to improve regional halocarbon emission estimates.

6.3.3 Macroalgae incubations – comparisons between different studies and methodologies

Measurements were made at two time points during the tropical species incubations which allowed us to investigate how incubation time may affect results. We found that calculated production rates did vary between measurements made after 4 (t4) and 24 (t24) hours. Over half of the measurements made at t4 were significantly higher than corresponding measurements made at t24. This could be linked to a variety of factors which were discussed in detail in Chapter 3 Section 3.3.4 and include re-adsorption of halocarbons onto the algal surface, microbial losses, abiotic losses (e.g. nucleophilic substitution) and stress processes during the incubations. However, patterns remained the same between t4 and t24: the relative amounts of halocarbons produced by each algae and the fact that some algae were strong producers and others weak remained the same at t4 and t24.

Our results suggest that care should be taken when comparing production rates between studies, in particular with regards to quantitative results. Despite this caveat, we conducted literature comparisons between our tropical production rates, temperate production rates calculated via the same system, and existing temperate and polar data (Chapter 3 Section 3.3.4). A large range of production values were reported in the literature, for example CHBr_3 production ranged from little or no production to $6000 \text{ pmol g FW}^{-1} \text{ hr}^{-1}$. Production rates from this study were within the range of literature values and there was no overall pattern to suggest tropical species were, overall, weaker or stronger halocarbon producers than those from other geographical regions. From our results it seems more likely that the species distribution in an area is an important factor in regional differences in halocarbon budgets, as we saw a large range of production values (little or no to over $1000 \text{ pmol g FW}^{-1} \text{ hr}^{-1}$) from 15 species collected from 4 sites.

6.3.4 Halocarbon ratios

Ratios between halocarbons were discussed in Chapters 3, 4 and 5. In Chapter 3 they were discussed with regards to halocarbon production during incubations. Significant correlations were common for polyhalogenated halocarbons but not the methyl halide CH_3I which only correlated with CH_2ClI and CH_2I_2 . This supports the wealth of literature on halocarbon production mechanisms (Chapter 1 Section 1.3.2) which propose methyl halide production via methyl halide transferase-catalysed methylation of halides and polyhalocarbon production via vanadium-dependent haloperoxidase mediated reactions. Ratios also help investigate the potential for non-biological production or conversion between halocarbons (e.g. Chapter 1 Section 1.4). Previous studies have suggested, amongst other processes, conversion from CHBr_3 to CHBr_2Cl and CH_2I_2 to CH_2ClI (Class & Ballschmiter, 1988; Jones & Carpenter, 2007; Moore & Tokarczyk, 1994). Our t4 and t24 incubation results did not conclusively show these conversion processes, in the case of CHBr_3 to CHBr_2Cl this is likely due to the experimental duration (max 24 hours) being less than the lifetime of CHBr_3 with respect to nucleophilic substitution (5 years at 25 °C, see Chapter 1 Table 3).

The strongest correlations during incubations were observed between CH_2Br_2 , CHBr_3 and CHBr_2Cl . During the desiccation experiments, strong correlations were also observed between CH_2Br_2 and CHBr_3 (Chapter 4 Section 4.3.6). A common biological source for these three halocarbons allowed them to be used to provide information on source regions and air mass history around Borneo in Chapter 5 Section 5.3.6, building on previous studies such as Brinckmann et al. (2012), Carpenter et al. (2003), O'Brien et al. (2009) and Yokouchi et al. (2005). Correlations between atmospheric concentrations of these three halocarbons measured around Borneo and differences in ratios supported the four regions we identified (Chapter 5 Section 5.3.6). For example, stronger correlations and higher halocarbon concentrations were seen in proposed source regions, such as the Semporna region. Three-factor correlations (Chapter 5 Section 5.3.7) provided an emission ratio similar to that from previous studies (Brinckmann et al., 2012; O'Brien et al., 2009; Yokouchi et al., 2005). This result supports previous use of these ratios to derive regional or global halocarbon emission estimates as similar results have now been seen from data collected at several sites, including coastal areas with and without (e.g. Cape Verde) macroalgae and open ocean cruises.

Of interest is the use of an updated chemical decay line to reflect different atmospheric lifetimes in the tropics. Many processes; biological emissions, the air-sea flux and seawater and atmospheric loss processes, differ between temperate and tropical regions. Some of these factors (e.g. biological loss processes in seawater) remain unconstrained and many may change with a changing climate (Chapter 1 Section 1.8). Opportunities for future research will be discussed further in Section 6.4.

6.3.5 Desiccation of macroalgae

Due to proposed links between halocarbons and oxidative stress (Chapter 1 Section 1.3.3 and Chapter 4 Section 4.1.2) the effect of desiccation on halocarbon production was discussed in Chapter 4. The main focus of this chapter was the effect of desiccation on halocarbon emissions from two common temperate species; *Fucus vesiculosus* and *Ulva intestinalis*. A measure of changing photosynthetic capacity during desiccation was made using F_v/F_m measurements (Section 4.2.6). This study is the first time an attempt has been made to describe some measure of photosynthetic stress alongside organohalogen emissions.

When air samples were measured from a flask containing submerged algae that was then exposed emissions were seen to increase (Chapter 4 Section 4.3.5). Calculations using Henry' Law constants suggests this is, at least partly, due to bromocarbons remaining in the aqueous phase when seawater was present in the desiccation flasks. Attempts were made to describe this further by comparing with seawater measurements made during incubations (those carried out in Chapter 3 Section 3.2.2). Mean bromocarbon production from both *F. vesiculosus* and *U. intestinalis* were 2 to 3 orders of magnitude greater in seawater than measurements made during the desiccation experiments in Chapter 4. This comparison included two measurement techniques, seawater samples and air samples trapped on sorbent tubes. Despite attempts to understand potential differences between these techniques, for example investigating sorbent trapping efficiency (Chapter 4 Section 4.2.3) and seawater measurements with whole air canister samples (Chapter 4 Section 4.3.5), we cannot exclude the fact that differences could be due to the use of two different sampling techniques. We conclude that, for successful comparisons between halocarbon production rates of submerged and exposed algae, the same measurement technique should be used, ensuring that partitioning between the seawater and headspace is accounted for when the algae is submerged.

Our desiccation experiments provided information on halocarbon emission patterns immediately following exposure. Halocarbon emissions tended to quickly increase, peak and then decrease again. The overall pattern was that, following exposure, water loss began in a linear manner whilst halocarbon emissions increased and F_v/F_m remained stable or increased slightly. Differences were seen between species; halocarbon production was higher for *U. intestinalis* compared to *F. vesiculosus*, and a prolonged period of emissions was observed in a couple of the *U. intestinalis* experiments. Decreases in F_v/F_m (representing photosynthetic stress and a decrease in photosynthetic capacity) did not correlate with a peak in halocarbon emissions. From these results it seemed likely that a halocarbon pulse upon immediate exposure may be linked to short-term stress, such as ozone exposure, but not long term desiccation stresses such as nutrient limitation.

Freshwater rewetting of *U. intestinalis* led to an increase in bromocarbon emissions. However this increase was dependent on the length of the preceding exposure period. Freshwater rewetting would potentially add an extra osmotic stress during desiccation, and could increase the flux of halocarbons from exposed algae. However, this study was conducted on one species of algae, in particular one that is somewhat euryhaline (Edwards et al., 1988) and so further studies in this area are advised.

6.4 Future work ideas

This section includes ideas for further research that have either been raised during data interpretation and discussion in previous chapters, or have come to light during my research over the past three years.

6.4.1 Halocarbon measurement techniques

i. Incubation protocols and temporal variability in halocarbon emissions

Our observed differences between halocarbon production rates measured at t4 compared to t24 suggest that incubation time may be important in calculated production rates. Other analytical aspects that may differ between studies have not been considered here, and should form a component of future work that aims to compare halocarbon production between different species, regions or methodological techniques. For example, McFiggans et al. (2004) noted that increasing age led to increasing variability in emissions. Most incubation studies are short-term and we do not fully understand how age or temporal variability affects halocarbon emissions. Internal iodine concentrations were shown to vary seasonably in temperate macroalgae by Mairh et al. (1989). In tropical regions seasonal differences may be linked to the changing monsoons affecting seawater temperatures which may, in turn, impact upon macroalgal growth, abundance and halocarbon emissions.

ii. Intercalibrations

Whilst extensive efforts have been made in recent years to conduct inter-laboratory intercalibrations of standards for atmospheric halocarbon measurements (Jones et al., 2011), it is also important to intercalibrate standards for seawater analyses (Butler et al., 2010). Seawater standards are made more frequently than air standards (see Chapter 3 Section 3.2.6 for a description of calibration techniques at UEA), and often need to be kept cool or frozen, making intercomparisons potentially more difficult than those involving compressed air canisters (Chapter 5 Section 5.2.5). However, as previous research have demonstrated the potential importance of sampling-induced artefacts when using liquid DMS samples (Hill & Dacey, 2001) these intercalibrations should not be ignored if comparisons are to be made between different studies.

6.4.2 Halocarbons and their ecosystem role

Chapter 1 Section 1.3.5 introduced the potential role of halocarbons as a chemical defence compound and this area has several strands that could form potentially interesting future studies. If bacteria use CH_2Br_2 as an energy source, as suggested by Goodwin et al. (1997b), then they are likely to also utilise other halocarbons as well. The role that bacterial breakdown may play has not been fully quantified and could form part of a study that helps bridge together Chapters 3 and 5 of this thesis. Whilst these two chapters form useful studies in their own right, the link between laboratory production of halocarbons by seaweed (Chapter 3) and atmospheric halocarbon concentrations (Chapter 5) would benefit from in situ seawater measurements. As mentioned previously, seawater measurements in coastal regions (such as Semporna, where higher atmospheric concentrations were observed) could not be made. Measurements at aquaculture sites would also be highly beneficial. Seawater measurements could also include seawater incubations to determine the impact of processes, such as abiotic production (Chapter 1 Section 1.2.2) and bacterial production, or loss on the tropical coastal halocarbon flux.

The role of many other tropical ecosystems such as benthic muds and corals have yet to be studied with respect to their impact on halocarbon budgets. Mangrove stands form an important part of tropical coastal ecosystems and there is some evidence that they may contribute significantly to global CH_3I budgets (Manley et al., 2007). More could also be done to determine the role halocarbons may play as an epiphyte or grazing deterrent, as discussed in Chapter 3 Section 3.3.2.

6.4.3 Halocarbon emissions in a changing climate

Firstly, there is the impact that climate change may have on seaweed biodiversity; distribution and other ecosystem processes, which is currently poorly understood (Harley et al., 2012). These changes may impact halocarbon source strengths, as might changes to aquaculture (Section 6.2) which may increase the seaweed biomass significantly in certain areas. Work in this thesis has highlighted several potential research areas with respect to aquaculture and halocarbon emissions, including; the impact of aquaculture stresses (e.g. disease, nutrient limitation and light stress) , the impact of post-harvest processing (e.g. desiccation, Chapter 4) and the production rates of species commonly used in aquaculture.

Source strength is not likely to be the only factor in the halocarbon biogeochemical system affected by climate change. As described in Chapter 1 Section 1.8, model studies also suggest that physical changes to deep convection and OH chemistry may have an impact on the contribution of biogenic VSLS to stratospheric bromine. In particular, Hossaini et al. (2012a) predict an increase in SG injection from biogenic VSLS on 0.3-1 ppt, depending on the warming scenario used.

Climate change aside, other anthropogenic factors may impact emissions in the coastal environment in general. For example, megacities are predicted to be important drivers of change in the coastal zone. Pollution may impact marine and coastal ecosystems, urban heat islands may affect atmospheric transport of trace gases and excess nutrients may increase the occurrence of algal blooms (von Glasow et al., 2013). All of these processes may affect VSLS biogeochemical cycles and have yet to be investigated.

This page intentionally blank.

Appendix 1 – Production of halocarbons by tropical macroalgae at two time points in a 24 hour incubation, 4 hours and 24 hours.

All values in pmol g FW⁻¹ hr⁻¹.

Species	PRODUCTION at t4 (pmol/g FW/hr)								
	CH ₃ I	CH ₂ BrCl	CH ₂ Br ₂	CHBrCl ₂	CH ₂ ClI	CHBr ₂ Cl	CH ₂ BrI	CHBr ₃	CH ₂ I ₂
<i>Gelidium elegans</i>	3.12	2.18	57.42	7.16	2.13	18.11	8.29	294.84	25.14
<i>Kappaphycus alvarezii</i>	nm	0.14	121.81	1.98	0.27	65.48	119.07	1731.45	47.73
<i>Gracilaria changii</i> 1	11.60	1.67	1014.39	10.83	1.57	326.47	710.72	4461.73	333.31
<i>Gracilaria changii</i> 2	9.36	0.73	875.48	8.47	1.05	171.99	620.30	4264.50	412.91
<i>Gracilaria salicornia</i> 1	1.40	0.44	263.21	2.77	1.04	65.32	365.96	1572.33	393.56
<i>Gracilaria salicornia</i> 2	3.72	6.14	382.40	14.19	3.98	114.28	50.83	3205.25	74.27
<i>Padina australis</i>	not measured at t4								
<i>Turbinaria conoides</i>	30.24	0.93	553.71	8.91	nd	22.40	561.78	554.17	501.66
<i>Sargassum baccularia</i>	not measured at t4								
<i>Sargassum binderi</i>	3.24	0.29	140.91	2.30	0.19	9.52	35.89	118.16	18.12
<i>Sargassum siliquosum</i>	not measured at t4								
<i>Bryopsis</i> sp.	not measured at t4								
<i>Caulerpa racemosa</i>	1.14	nd	2.55	nd	0.04	0.21	1.66	3.00	2.33
<i>Caulerpa</i> sp.	1.43	nd	0.36	nd	0.02	0.06	0.46	0.67	0.39
<i>Cladophora</i> sp.	0.08	0.02	13.65	0.07	0.01	0.60	0.41	3.08	0.46
<i>Ulva reticulata</i>	0.82	nd	30.45	0.43	0.07	9.36	4.15	157.09	2.30

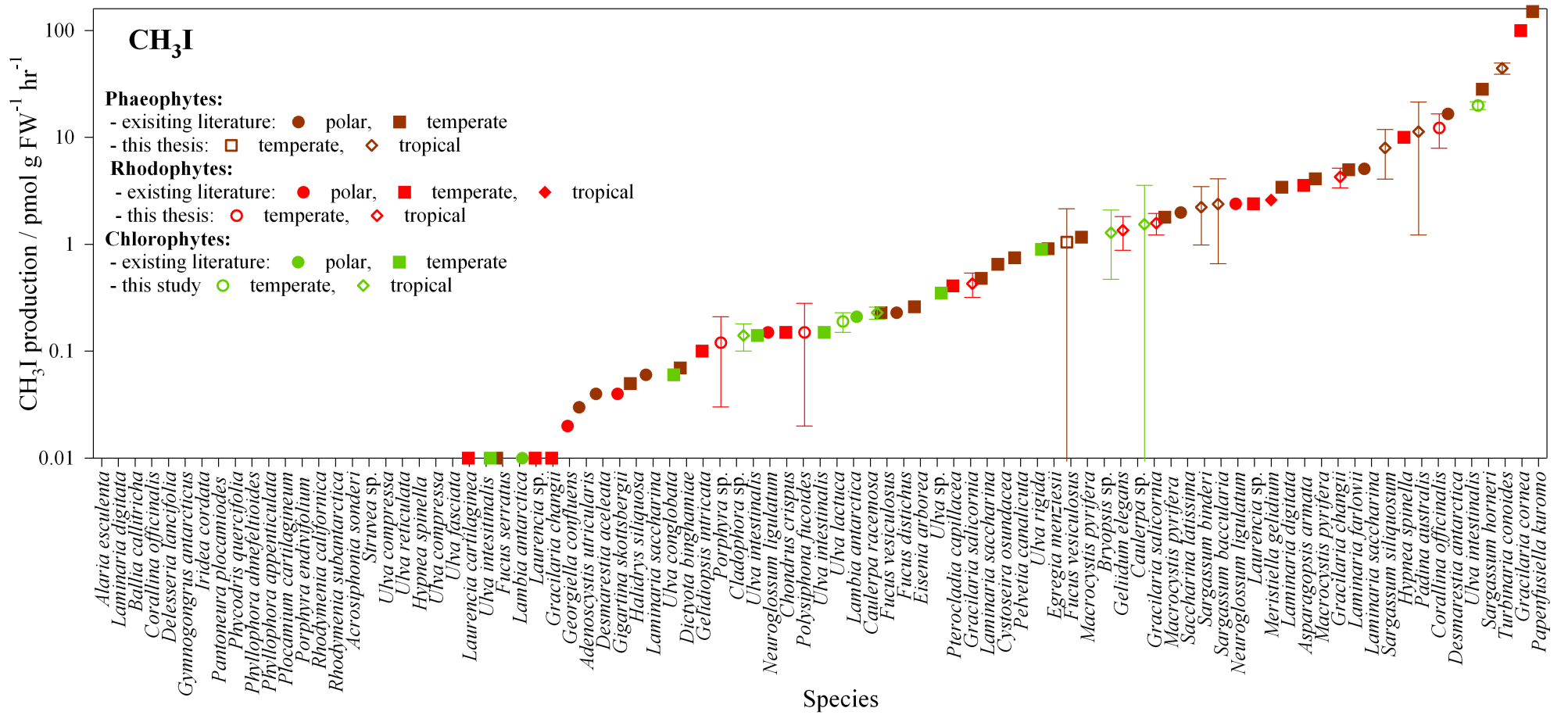
Species	STANDARD DEVIATION (n=2-3) on PRODUCTION VALUES (above)								
	CH ₃ I	CH ₂ BrCl	CH ₂ Br ₂	CHBrCl ₂	CH ₂ ClI	CHBr ₂ Cl	CH ₂ BrI	CHBr ₃	CH ₂ I ₂
<i>Gelidium elegans</i>	0.31	0.49	20.34	1.28	0.22	7.04	2.62	165.87	4.81
<i>Kappaphycus alvarezii</i>	nm	0.05	57.91	0.89	0.31	30.33	57.71	335.91	29.82
<i>Gracilaria changii</i> 1	2.71	0.41	93.25	2.15	0.16	69.13	143.64	189.30	232.54
<i>Gracilaria changii</i> 2	3.66	0.52	256.29	1.38	0.30	16.72	370.90	477.54	291.94
<i>Gracilaria salicornia</i> 1	0.62	0.41	164.91	0.19	0.73	13.62	130.65	209.83	130.64
<i>Gracilaria salicornia</i> 2	0.38	0.64	36.29	1.62	1.29	12.46	15.11	577.43	33.77
<i>Padina australis</i>	not measured at t4								
<i>Turbinaria conoides</i>	6.60	0.28	130.05	0.84	nd	3.88	161.75	105.08	184.48
<i>Sargassum baccularia</i>	not measured at t4								
<i>Sargassum binderi</i>	0.76	0.16	71.06	2.25	0.07	5.05	16.58	53.46	5.56
<i>Sargassum siliquosum</i>	not measured at t4								
<i>Bryopsis</i> sp.	not measured at t4								
<i>Caulerpa racemosa</i>	0.04	0.02	4.16	1.27	0.00	0.05	0.00	0.00	0.00
<i>Caulerpa</i> sp.	0.03	nd	2.72	nd	0.03	0.16	0.24	1.54	0.39
<i>Cladophora</i> sp.	1.07	nd	0.51	nd	0.01	0.00	0.11	0.30	0.26
<i>Ulva reticulata</i>	0.13	0.02	11.38	0.07	0.00	0.48	0.21	2.11	0.45

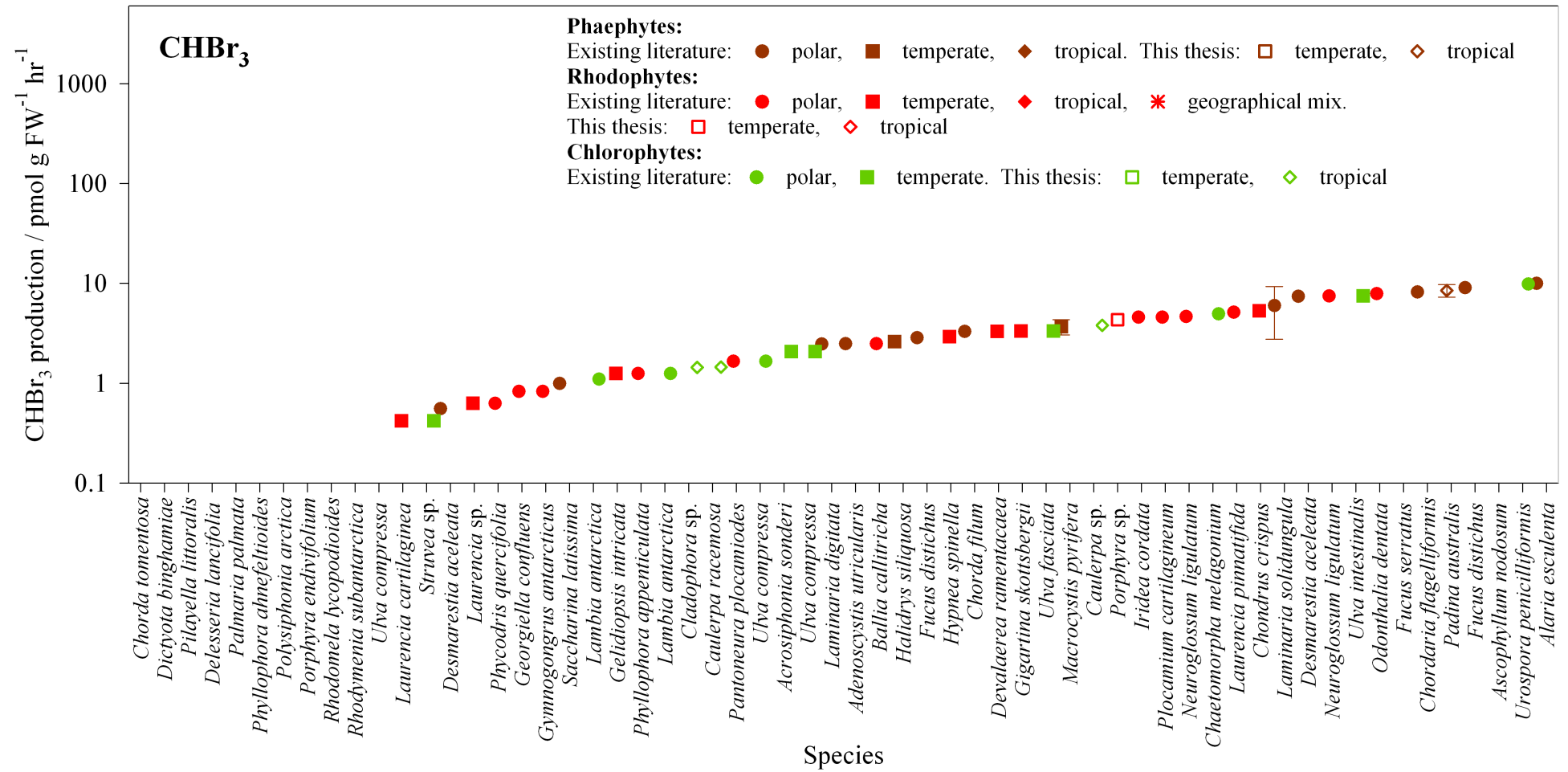
Species	PRODUCTION at t24 (pmol/g FW/hr)								
	CH ₃ I	CH ² BrCl	CH ₂ Br ₂	CHBrCl ₂	CH ₂ ClI	CHBr ₂ Cl	CH ₂ BrI	CHBr ₃	CH ₂ I ₂
<i>Gelidium elegans</i>	1.35	0.71	28.65	1.26	0.58	6.11	1.23	37.63	3.20
<i>Kappaphycus alvarezii</i>	nm	0.28	226.93	2.07	0.47	76.71	78.39	512.03	11.44
<i>Gracilaria changii</i> 1	4.27	0.10	86.00	3.04	0.22	100.32	53.59	1129.07	105.55
<i>Gracilaria changii</i> 2	not measured at t24								
<i>Gracilaria salicornia</i> 1	0.43	0.08	78.86	1.57	0.12	52.01	53.48	478.44	57.47
<i>Gracilaria salicornia</i> 2	1.58	0.49	35.17	3.26	0.30	30.76	1.93	595.04	5.05
<i>Padina australis</i>	11.31	nd	6.57	0.68	0.20	1.33	0.98	8.45	16.06
<i>Turbinaria conoides</i>	44.31	1.02	251.06	2.93	5.74	12.39	490.46	259.91	485.21
<i>Sargassum baccularia</i>	2.38	nd	8.60	0.72	0.15	1.49	1.52	10.82	1.79
<i>Sargassum binderi</i>	2.23	0.09	45.44	3.15	0.06	6.79	4.56	45.26	1.68
<i>Sargassum siliquosum</i>	8.00	nd	18.55	1.27	0.21	3.47	6.67	36.14	6.96
<i>Bryopsis</i> sp.	1.28	nd	29.40	0.01	0.50	2.17	21.51	69.15	9.18
<i>Caulerpa racemosa</i>	0.23	0.01	4.35	nd	0.03	0.15	1.10	1.45	1.22
<i>Caulerpa</i> sp.	1.54	0.01	4.77	0.08	0.01	0.41	0.57	3.78	0.36
<i>Cladophora</i> sp.	0.14	0.02	3.77	0.10	0.03	0.29	0.18	1.44	1.27
<i>Ulva reticulata</i>	nd	nd	12.72	0.09	0.01	1.52	0.95	23.51	0.34

Species	STANDARD DEVIATION (n=2-3) on PRODUCTION VALUES (above)								
	CH ₃ I	CH ² BrCl	CH ₂ Br ₂	CHBrCl ₂	CH ₂ ClI	CHBr ₂ Cl	CH ₂ BrI	CHBr ₃	CH ₂ I ₂
<i>Gelidium elegans</i>	0.47	0.12	6.78	0.52	0.03	2.37	0.38	14.80	1.35
<i>Kappaphycus alvarezii</i>	nm	0.12	103.06	1.03	0.26	34.12	47.30	40.77	6.01
<i>Gracilaria changii</i> 1	0.90	0.06	34.89	0.64	0.10	20.55	24.32	125.83	27.65
<i>Gracilaria changii</i> 2	not measured at t24								
<i>Gracilaria salicornia</i> 1	0.11	0.05	32.48	0.28	0.05	13.18	27.84	560.91	6.51
<i>Gracilaria salicornia</i> 2	0.36	0.13	11.89	0.24	0.14	1.99	1.07	277.90	1.69
<i>Padina australis</i>	10.09	nd	1.52	0.53	0.01	0.77	0.19	1.22	10.79
<i>Turbinaria conoides</i>	5.43	0.15	172.81	0.71	1.16	3.16	184.14	87.73	65.58
<i>Sargassum baccularia</i>	1.72	nd	3.22	0.54	0.09	0.71	0.51	3.45	0.49
<i>Sargassum binderi</i>	1.24	0.00	5.64	0.87	0.02	0.67	2.33	16.45	1.19
<i>Sargassum siliquosum</i>	3.92	nd	2.60	1.29	0.01	1.10	1.06	15.75	3.58
<i>Bryopsis</i> sp.	0.81	nd	5.64	0.01	0.19	0.11	10.57	9.27	1.48
<i>Caulerpa racemosa</i>	0.03	0.00	1.85	nd	0.01	0.04	0.13	0.38	0.28
<i>Caulerpa</i> sp.	2.02	0.01	5.96	0.08	0.00	0.55	0.18	4.68	0.09
<i>Cladophora</i> sp.	0.04	0.00	1.07	0.01	0.00	0.15	0.09	0.30	0.22
<i>Ulva reticulata</i>	nd	nd	3.99	0.03	0.00	0.40	0.23	6.64	0.05

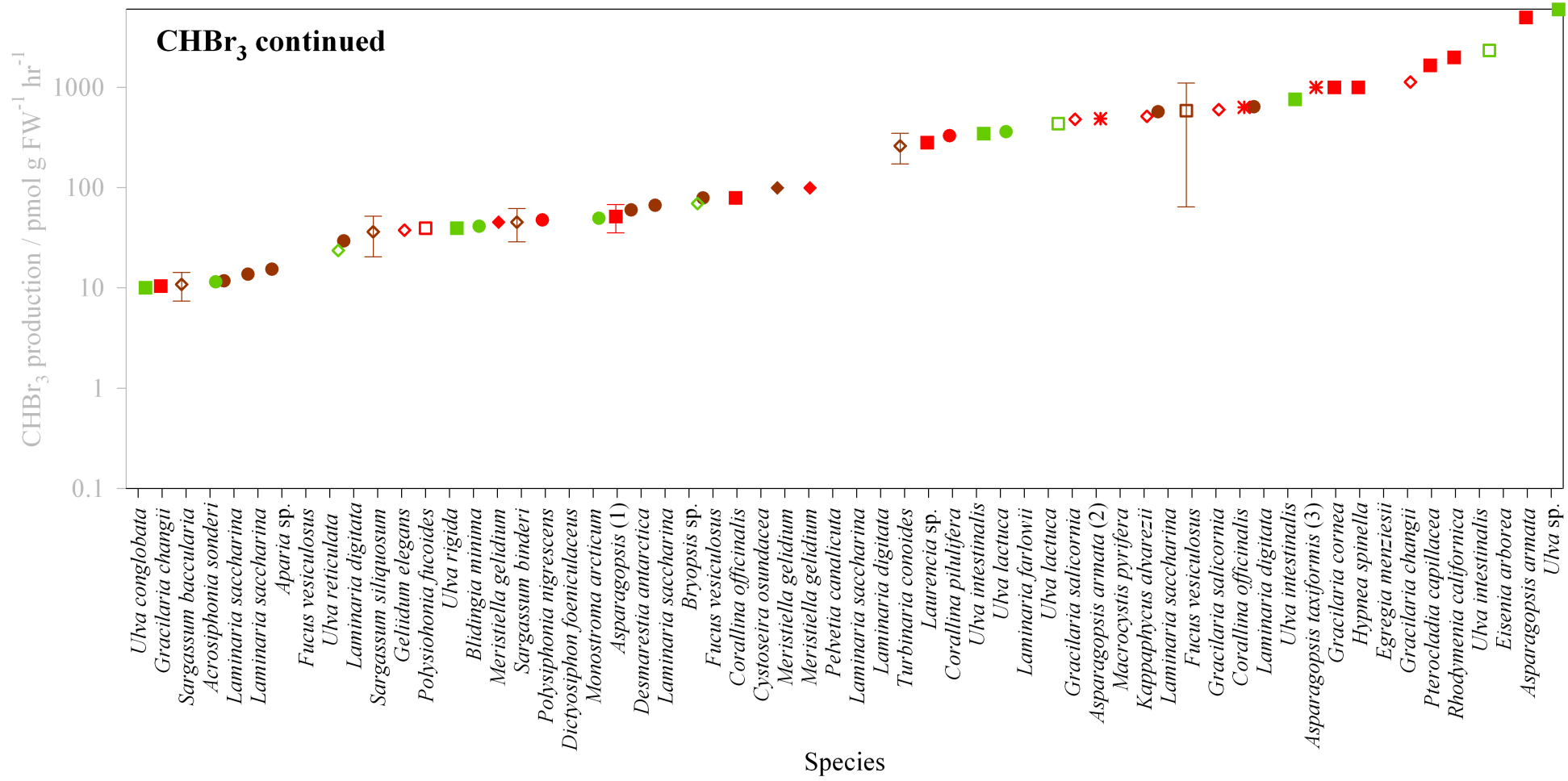
Appendix 2 – A comparison of halocarbon production by macroalgae from this study and the existing literature

These two figures are an extension of Chapter 3 Figure 10 (page 161). A full description of this comparison can be found in Chapter 3 Section 3.3.4. Briefly, these two figures show CH_3I (Fig. 1) and CHBr_3 (Fig. 2) production in $\text{pmol g FW}^{-1} \text{ hr}^{-1}$ for 15 tropical species and 6 temperate species (this thesis). These values have been compared to production rates for temperate and polar species from a range of studies (referenced in Chapter 3 Fig. 10). Each species is listed by name, in order of increasing halocarbon production, with marker colour and shapes defined in the inset figure legends.





Appendix 2, Figure 2 part 1.



Appendix 2, Figure 2 part 2.

References

A

- Adir, N., Zer, H., Shochat, S. and Ohad, I.: Photoinhibition - a historical perspective, *Photosynthesis Research*, 76(1-3), 343-370, doi:10.1023/A:1024969518145, 2003.
- Amachi, S.: Microbial Contribution to Global Iodine Cycling: Volatilization, Accumulation, Reduction, Oxidation, and Sorption of Iodine, *Microbes and Environments*, 23(4), 269-276, doi:10.1264/jsme2.ME08548, 2008.
- Amachi, S., Kamagata, Y., T. K. and Muramatsu, Y.: Bacteria mediate methylation of iodine in marine and terrestrial environments, *Applied and Environmental Microbiology*, 67(6), 2718-2722, doi:10.1128/AEM.67.6.2718, 2001.
- Anderson, S. P., Weller, R. A. and Lukas R. B.: Surface buoyancy forcing and the mixed layer of the Western Pacific Warm Pool: observations and 1D model results, *Journal of Climate*, 9, 3056-3085.
- Aresta, M., Dibenedetto, A. and Barberio, G.: Utilisation of macro-algae for enhanced CO₂ fixation and biofuels production: Development of a computing software for an LCA study, *Fuel Processing Technology*, 86(14-15), 1679-1693, doi:10.1016/j.fuproc.2005.01.016, 2005.
- Arnold, S. R., Spracklen, D. V., Gebhardt, S., Custer, T., Williams, J., Peeken, I. and Alvain, S.: Relationships between atmospheric organic compounds and air-mass exposure to marine biology, *Environmental Chemistry*, 7(3), 232, doi:10.1071/EN09144, 2010.
- Aschmann, J., Sinnhuber, B. M., Atlas, E. L. and Schauffler, S. M.: Modelling the transport of very short-lived substances into the tropical upper troposphere and lower stratosphere, *Atmospheric Chemistry and Physics Discussions*, 9, 18511-18543, 2009.
- Ashu-Ayem, E. R., Nitschke, U., Monahan, C., Chen, J., Darby, S. B., Smith, P. D., O'Dowd, C. D., Stengel, D. B. and Venables, D. S.: Coastal iodine emissions. 1. Release of I₂ by *Laminaria digitata* in chamber experiments., *Environmental Science & Technology*, 46(19), 10413-21, doi:10.1021/es204534v, 2012.
- Ask, E. I. and Azanza, R. V.: Advances in cultivation technology of commercial eucheumatoid species: a review with suggestions for future research, *Aquaculture*, 206(3-4), 257-277, doi:10.1016/S0044-8486(01)00724-4, 2002.
- Atlas, E., Pollock, W., Greenberg, J., Heidt, L. and Thompson, A. M.: Alkyl Nitrates, Nonmethane Hydrocarbons, and Halocarbon Gases Over the Equatorial Pacific Ocean During Saga 3, *Journal of Geophysical Research*, 98(D9), 16933-16947, 1993.

B

- Baker, J. M., Sturges, W. T., Sugier, J., Sunnenberg, G., Lovett, A. A., Reeves, C. E., Nightingale, P. D. and Penkett, S. A.: Emissions of CH₃Br, organochlorines, and organoiodines from temperate macroalgae, *Chemosphere*, 3, 93-106, 2001.
- Ball, S. M., Hollingsworth, A. M., Humbles, J., Leblanc, C., Potin, P. and McFiggans, G.: Spectroscopic studies of molecular iodine emitted into the gas phase by seaweed, *Atmospheric Chemistry and Physics*, 10(13), 6237-6254, doi:10.5194/acp-10-6237-2010, 2010.
- Beerling, D., Gardiner, G., Leggett, G., McLeod, A and Quik, P.: Missing methane emissions from leaves of terrestrial plants, *Global Change Biology*, 14(8), 1821-1826, 2008
- Beissner, R. S., Guilford, W. J., Coates, R. M. and Hager, L. P.: Synthesis of brominated heptanones and bromoform by a bromoperoxidase of marine origin, *Biochemistry*, 20(13), 3724-3731, 1981.

- de Benoist, B., Andersson, M., Egli, I., Takkouche, B. and Allen, H.: Iodine status worldwide, Geneva., 2004.
- Blake, N., Blake, D., Chen, T.-Y., Collins Jr., J. E., Sachse, G. W., Anderson, B. E. and Rowland, S.: Distribution and seasonality of selected hydrocarbons and halocarbons over the western Pacific basin during PEM-West A and PEM-West B, *Journal of Geophysical Research*, 102(D23), 28315-28331, 1997.
- Blake, N., Blake, D., Wingenter, O., Sive, B., Kang, C. H., Thornton, D., Bandy, A., Atlas, E., Flocke, F., Harris, J. and Rowland, F. S.: Aircraft measurements of the latitudinal, vertical, and seasonal variations of NMHCs, methyl nitrate, methyl halides, and DMS during the First Aerosol Characterization Experiment (ACE 1), *Journal of Geophysical Research*, 104(D17), 21803-21817, 1999.
- Bloom, A., Lee-Taylor, S., Madronich, S., Messenger, D. J., Palmer, P. I., Reay, D. S. and McLeod, A.: Global methane emission estimates from ultra violet irradiation of terrestrial plants foliage, *The New Phytologist*, 187(2), 417-425, 2010
- Bloss, W. J., Nikolaisen, S. L., Salawitch, R. J., Friedl, R. R. and Sander, S. P.: Kinetics of the ClO Self-Reaction and 210 nm Absorption Cross Section of the ClO Dimer, *The Journal of Physical Chemistry A*, 105(50), 11226-11239, doi:10.1021/jp012429y, 2001.
- Bondu, S., Cockquempot, B., Deslandes, E. and Morin, P.: Effects of salt and light stress on the release of volatile organic compounds by *Solieria chordalis*: a laboratory incubation study, *Botanica Marina*, 51(6), 485-492, 2008
- Bouwer, E. J. and McCarty, P. L.: Transformations of 1- and 2-Carbon Halogenated Aliphatic Organic Compounds Under Methanogenic Conditions, *Applied and Environmental Microbiology*, 45(4), 1286-1294, 1983.
- Bouwer, E. J., Rittman, B. E. and L, M. P.: Anaerobic degradation of halogenated 1- and 2-carbon organic compounds, *Environmental Science & Technology*, 15(5), 596-599, 1981.
- Bouwman, A. F., Pawłowski, M., Liu, C., Beusen, A. H. W., Shumway, S. E., Glibert, P. M. and Overbeek, C. C.: Global Hindcasts and Future Projections of Coastal Nitrogen and Phosphorus Loads Due to Shellfish and Seaweed Aquaculture, *Reviews in Fisheries Science*, 19(4), 331-357, doi:10.1080/10641262.2011.603849, 2011.
- Bravo-Linares, C. M. and Mudge, S. M.: Temporal trends and identification of the sources of volatile organic compounds in coastal seawater., *Journal of Environmental Monitoring*, 11(3), 628-641, doi:10.1039/b814260m, 2009.
- Bravo-Linares, C. M., Mudge, S. M. and Loyola-Sepulveda, R. H.: Production of Volatile Organic Compounds (VOCs) By Temperate Macroalgae: the Use of Solid Phase Microextraction (SPME) Coupled To GC-MS As Method of Analysis, *Journal of the Chilean Chemical Society*, 55(2), 227-232, doi:10.4067/S0717-97072010000200018, 2010.
- Brinckmann, S., Engel, A., Bönisch, H., Quack, B. and Atlas, E.: Short-lived brominated hydrocarbons – observations in the source regions and the tropical tropopause layer, *Atmospheric Chemistry and Physics*, 12(3), 1213-1228, doi:10.5194/acp-12-1213-2012, 2012.
- Brooks, S. B., Saiz-Lopez, A., Skov, H., Lindberg, S. E., Plane, J. M. C. and Goodsite, M. E.: The mass balance of mercury in the springtime arctic environment, *Geophysical Research Letters*, 33(13), L13812, doi:10.1029/2005GL025525, 2006.
- Brussaard, C. P. D., Wilhelm, S. W., Thingstad, F., Weinbauer, M. G., Bratbak, G., Hekdal, M., Kimmance, S. A., Middelboe, M., Nagasake, K., Paul, J. H., Scheoder, D. C., Suttle, C. A., Vaqué, D. and Wommack, K. E.: Global-scale processes with a nanoscale drive: the role of marine viruses, *The ISME Journal*, 2(6), 575-578, 2008
- Buck, B. H. and Buchholz, C. M.: The offshore-ring: A new system design for the open ocean aquaculture of macroalgae, *Journal of Applied Phycology*, 16(5), 355-368, doi:10.1023/B:JAPH.0000047947.96231.ea, 2004.

References

- Burreson, B. J., Moore, R. E. and Roller, P. P.: Volatile Halogen Compounds in the Alga *Asparagopsis taxiformis* (Rhodophyta), *Journal of Agricultural and Food Chemistry*, 24(4), 856-861, 1976.
- Burritt, D. J., Larkindale, J. and Hurd, C. L.: Antioxidant metabolism in the intertidal red seaweed *Stictosiphonia arbuscula* following desiccation, *Planta*, 215(5), 829-38, doi:10.1007/s00425-002-0805-6, 2002.
- Butler, J., Bell, T. G., Hall, B. D., Quack, B., Carpenter, L. J. and Williams, J.: Technical Note: Ensuring consistent, global measurements of very short-lived halocarbon gases in the ocean and atmosphere, *Atmospheric Chemistry and Physics*, 10(2), 327-330, doi:10.5194/acp-10-327-2010, 2010.
- Butler, J., King, D. B., Lobert, J. M., Montzka, S. A., Yvon-Lewis, S. A., Hall, B. D., Warwick, N. J., Mondeel, D. J., Aydin, M. and Elkins, J. W.: Oceanic distributions and emissions of short-lived halocarbons, *Global Biogeochemical Cycles*, 21(GB1023), doi:10.1029/2006GB002732, 2007.
- C**
- Caine, J. M., Keywood, M., Bigg, E. K., Grose, M. R., Gillett, R. W. and Meyer, M.: Flux chamber study of particle formation from *Durvillaea potatorum*, *Environmental Chemistry*, 4(3), 151-154, doi:10.1071/EN07006, 2007.
- Carlisle, R.: *Scientific American. Inventions and Discoveries*, John Wiley & Sons, Inc., Hoboken, NJ., 2004.
- Carpenter, L. J., Jones, C., Dunk, R., Hornsby, K. and Woeltjen, J.: Air-sea fluxes of biogenic bromine from the tropical and North Atlantic Ocean, *Atmospheric Chemistry and Physics*, 9, 1805-1816, 2009.
- Carpenter, L. J. and Liss, P.: On temperate sources of bromoform and other reactive organic bromine gases, *Journal of Geophysical Research*, 105(D16), 20539-20547, doi:10.1029/2000JD900242, 2000.
- Carpenter, L. J., Liss, P. S. and Penkett, S. A.: Marine organohalogens in the atmosphere over the Atlantic and Southern Oceans, *Journal of Geophysical Research*, 108(D9), doi:10.1029/2002JD002769, 2003.
- Carpenter, L. J., Malin, G., Liss, P. S. and Küpper, F. C.: Novel biogenic iodine-containing trihalomethanes and other short-lived halocarbons in the coastal East Atlantic, *Global Biogeochemical Cycles*, 14(4), 1191-1204, 2000.
- Carpenter, L. J., Sturges, W. T., Penkett, S. A., Liss, P. S., Alicke, B., Hebestreit, K. and Platt, U.: Short-lived alkyl iodides and bromides at Mace Head, Ireland: Links to biogenic sources and halogen oxide production, *Journal of Geophysical Research*, 104, 1679-1689, 1999.
- Chapman, A. R. O.: *Biology of Seaweeds: Levels of Organisation*, University Park Press, Baltimore., 1979.
- Charpy-Roubaud, C. and Sournia, A.: The comparative estimation of phytoplanktonic, microphytobenthic and macrophytobenthic primary production in the oceans, *Marine Microbial Food Webs*, 4(1), 31-57, 1990.
- Chipperfield, M. P. and Pyle, J. A.: Model sensitivity studies of Arctic ozone depletion, *Journal of Geophysical Research*, 103(D21), 28389-28403, doi:10.1029/98JD01960, 1998.
- Chopin, T., Buschmann, A. H., Halling, C., Troell, M., Kautsky, N., Neori, N., Kraemer, G. P., Zertuche-González, J. A., Yarish, C. and Neefus, C.: Minireview. Integrating seaweeds into marine aquaculture systems: a key toward sustainability, *Journal of Phycology*, 37, 975-986, 2001.
- Chuck, A. L., Turner, S. M. and Liss, P. S.: Oceanic distributions and air-sea fluxes of biogenic halocarbons in the open ocean, *Journal of Geophysical Research*, 110(C10), C10022, doi:10.1029/2004JC002741, 2005.

- Class, T. and Ballschmiter, K.: Chemistry of Organic Traces in Air, *Journal of Atmospheric Chemistry*, 6, 35-46, 1988.
- Collen, J. and Davison, I. R.: Reactive oxygen production and damage in intertidal *Fucus* spp. (Phaeophyceae), *Journal of Phycology*, 35, 54-61, 1999.
- Collen, J., Ekdahl, A., Abrahamsson, K. and Pedersen, M.: The involvement of hydrogen peroxide in the production of volatile halogenated compounds by, *Phytochemistry*, 36(5), 1197-1202, 1994.
- Colomb, A., Yassaa, N., Williams, J., Peeken, I. and Lochte, K.: Screening volatile organic compounds (VOCs) emissions from five marine phytoplankton species by head space gas chromatography/mass spectrometry (HS-GC/MS), *Journal of Environmental Monitoring*, 10(3), 325-30, doi:10.1039/b715312k, 2008.
- Commane, R., Seitz, K., Bale, C. S. E., Bloss, W. J., Buxmann, J., Ingham, T., Platt, U., Pöhler, D. and Heard, D. E.: Iodine monoxide at a clean marine coastal site: observations of high frequency variations and inhomogeneous distributions, *Atmospheric Chemistry and Physics*, 11(13), 6721-6733, doi:10.5194/acp-11-6721-2011, 2011.
- Cronin, G., Paul, V. J., Hay, M. E. and Fenical, W.: Are tropical herbivores more resistant than temperate herbivores to seaweed chemical defenses? Diterpenoid metabolites from *Dictyota acutiloba* as feeding deterrents for tropical versus temperate fishes and urchins, *Journal of Chemical Ecology*, 23(2), 289-302, 1997.
- D**
- Daniel, J. S., Solomon, S., Portmann, R. W. and Garcia, R. R.: Stratospheric ozone destruction: The importance of bromine relative to chlorine, *Journal of Geophysical Research*, 104(D19), 23871-23880, 1999.
- Davison, I. R. and Pearson, G. A.: Stress tolerance in intertidal seaweeds, *Journal of Phycology*, 32, 197-211, 1996.
- Dawes, C. J., Moon, R. E. and Davis, M. A.: The Photosynthetic and Respiratory Rates and Tolerances of Benthic Algae from a Mangrove and Salt Marsh Estuary: A Comparative Study, *Estuarine and Coastal Marine Science*, 6(2), 175-185, doi:10.1016/0302-3524(78)90099-3, 1978.
- Dessens, O., Zeng, G., Warwick, N. and Pyle, J.: Short-lived bromine compounds in the lower stratosphere; impact of climate change on ozone, *Atmospheric Science Letters*, 10, 201-206, doi:10.1002/asl, 2009.
- Dewulf, J and van Langenhove, H.: Analytical techniques for the determination and measurement data of 7 chlorinated C1- and C2- hydrocarbons and 6 monocyclic aromatic hydrocarbons in remote air masses: an overview, *Atmospheric Environment*, 1997, 31(20), 3291-3307, 1997
- Dimmer, C. H., Simmonds, P. G., Nickless, G. and Bassford, M. R.: Biogenic fluxes of halomethanes from Irish peatland ecosystems, *Atmospheric Environment*, 35, 321-330, 2001.
- Donner, L. J., Horowitz, L. W., Fiore, A. M., Seman, C. J., Blake, D. R. and Blake, N. J.: Transport of radon-222 and methyl iodide by deep convection in the GFDL Global Atmospheric Model AM2, *Journal of Geophysical Research*, 112(D17), D17303, doi:10.1029/2006JD007548, 2007.
- Dorf, M., Butler, J. H., Butz, A., Camy-Peyret, C., Chipperfield, M. P., Kritten, L., Montzka, S. A., Simmes, B., Weidner, F. and Pfeilsticker, K.: Long-term observations of stratospheric bromine reveal slow down in growth, *Geophysical Research Letters*, 33, L24803, doi:10.1029/2006GL027714, 2006.
- Dorf, M., Butz, A., Camy-Peyret, C., Chipperfield, M. P., Kritten, L. and Pfeilsticker, K.: Bromine in the tropical troposphere and stratosphere as derived from balloon-borne BrO observations, *Atmospheric Chemistry and Physics*, 8, 7265-7271, doi:10.5194/acpd-8-12999-2008, 2008.

References

Draxler, R. R. and Rolph, G. D.: HYSPLIT (HYbrid Single-Particle Lagrangian Integrated Trajectory) Model, access via NOAA ARL READY Website. NOAA AIR Resources Laboratory, Silver Spring, MD [online] Available from: <http://ready.arl.noaa.gov/HYSPLIT.php> (Accessed 4 January 2013), 2013.

E

Edwards, D. M., Reed, R. H. and Stewart, W. D. P.: Osmoacclimation in *Enteromorpha intestinalis*: long-term effects of osmotic stress on organic solute accumulation, *Marine Biology*, 476, 467-476, 1988.

Ekdahl, A., Pedersen, M. and Abrahamsson, K.: A study of the diurnal variation of biogenic volatile halocarbons, *Marine Chemistry*, 63(1), 1-8, 1998.

F

Food and Agriculture Organisation (FAO): The state of world fisheries and aquaculture, edited by I. Nomua, FAO Fisheries and Aquaculture Department, Rome., 2008.

Fahey, D. W. and Hegglin, M. I.: Twenty Questions and Answers about the Ozone Layer: 2010 update, WMO; Geneva., 2010.

Farman, J. C., Gardiner, B. G. and Shanklin, J. D.: Large losses of total ozone in Antarctica reveal seasonal ClO_x/NO_x interaction, *Nature*, 315, 207-210, 1985.

Frische, M., Garofalo, K., Hansteen, T. H., Borchers, R. and Harnisch, J.: The origin of stable halogenated compounds in volcanic gases, *Environmental Science and Pollution Research*, 13(6), 406-413, 2006.

Fuge, R. and Johnson, C. C.: The geochemistry of iodine - a review, *Environmental Geochemistry and Health*, 8(2), 31-54, 1986.

Fuhlbrügge, S., Krüger, K., Quack, B., Atlas, E., Hepach, H. and Ziska, F.: Impact of the marine atmospheric boundary layer on VSLs abundances in the eastern tropical and subtropical North Atlantic Ocean, *Atmospheric Chemistry and Physics Discussions*, 12(12), 31205-31245, doi:10.5194/acpd-12-31205-2012, 2012.

G

Gettelman, A., Lauritzen, P. H., Park, M. and Kay, J. E.: Processes regulating short-lived species in the tropical tropopause layer, *Journal of Geophysical Research*, 114(D13), D13303, doi:10.1029/2009JD011785, 2009.

Giese, B., Latusus, F., Adams, F. C. and Wiencke, C.: Release of Volatile Iodinated C1 - C4 Hydrocarbons by Marine Macroalgae from Various Climate Zones, *Environmental Science and Technology*, 33(14), 2432-2439, 1999.

von Glasow, R. and Crutzen, P. J.: Model study of multiphase DMS oxidation with a focus on halogens, *Atmospheric Chemistry and Physics*, 4(3), 589-608, doi:10.5194/acp-4-589-2004, 2004.

von Glasow, R., Jickells, T. D., Baklanov, A., Carmichael, G. R., Church, T. M., Gallardo, L., Hughes, C., Kanakidou, M., Liss, P. S., Mee, L., Raine, R., et al.: Megacities and large urban agglomerations in the coastal zone: interactions between atmosphere, land, and marine ecosystems., *Ambio*, 42(1), 13-28, doi:10.1007/s13280-012-0343-9, 2013.

von Glasow, R., von Kuhlmann, R., Lawrence, M. G., Platt, U. and Crutzen, P. J.: Impact of reactive bromine chemistry in the troposphere, *Atmospheric Chemistry and Physics*, 4, 2481-2497, doi:10.5194/acpd-4-4877-2004, 2004.

Goh, C. S. and Lee, K. T.: A visionary and conceptual macroalgae-based third-generation bioethanol (TGB) biorefinery in Sabah, Malaysia as an underlay for renewable and sustainable development, *Renewable and Sustainable Energy Reviews*, 14(2), 842-848, doi:10.1016/j.rser.2009.10.001, 2010.

- Goodsite, M. E., Plane, J. M. C. and Skov, H.: A theoretical study of the oxidation of Hg^0 to HgBr_2 in the troposphere., *Environmental Science & Technology*, 38(6), 1772-1776, 2004.
- Goodwin, K. D., North, W. J. and Lidstrom, M. E.: Production of bromoform and dibromomethane by Giant Kelp: Factors affecting release and comparison to anthropogenic bromine sources., *Limnology and Oceanography*, 42(8), 1725-1734, doi:10.4319/lo.1997.42.8.1725, 1997a.
- Goodwin, K. D., Lidstrom, M. E. and Gremland, R. S.: Marine Bacterial Degradation of Brominated Methanes, *Environmental Science & Technology*, 31(11), 3188-3192, 1997b.
- Goodwin, K. D., Schaefer, J. K. and Oremland, R. S.: Bacterial Oxidation of Dibromomethane and Methyl Bromide in Natural Waters and Enrichment Cultures, *Applied and Environmental Microbiology*, 64, 4629-4636, 1998.
- Gostlow, B., Robinson, A. D., Harris, N. R. P., O'Brien, L. M., Oram, D. E., Mills, G. P., Newton, H. M., Yong, S. E. and A Pyle, J.: μDirac : an autonomous instrument for halocarbon measurements, *Atmospheric Measurement Techniques*, 3(2), 507-521, doi:10.5194/amt-3-507-2010, 2010.
- Greenberg, J. P., Guenther, A. B. and Turnipseed, A.: Marine Organic Halide and Isoprene Emissions Near Mace Head, Ireland, *Environmental Chemistry*, 2(4), 291-294, doi:10.1071/EN05072, 2005.
- Gribble, G. W.: The Diversity of Naturally Produced Organohalogens, in *The Handbook of Environmental Chemistry vol. 3 Part P*, vol. 3, pp. 1-15, Springer-Verlag, Berlin Heidelberg., 2003.
- Grose, M. R., Cainey, J. M., McMinn, A. and Gibson, J. A. E.: Coastal marine methyl iodide source and links to new particle formation at Cape Grim during February 2006, *Environmental Chemistry*, 4(3), 172, doi:10.1071/EN07008, 2007.
- Gschwend, P. M., MacFarlane, J. K. and Newman, K. A.: Volatile halogenated organic compounds released to seawater from temperate marine macroalgae, *Science*, 227, 1033-1035, 1985.
- ## H
- Hameed, S. and Ahmed, M.: Seasonal variation in seaweed biomass from the rocky shore of Pacha, near Karachi, Pakistan (Arabian Sea), *Pakistan Journal of Biological Sciences*, 2(3), 1044-1052, 1999.
- Happell, J. D. and Wallace, D. W. R.: Methyl iodide in the Greenland/Norwegian Seas and the tropical Atlantic Ocean: Evidence for photochemical production, *Geophysical Research Letters*, 23(16), 2105, doi:10.1029/96GL01764, 1996.
- Harley, C. D. G., Anderson, K. M., Demes, K. W., Jorve, J. P., Kordas, R. L., Coyle, T. A. and Graham, M. H.: Effects of climate change on global seaweed communities, *Journal of Phycology*, 48, 1064-1078, doi:10.1111/j.1529-8817.2012.01224.x, 2012.
- Helz, G. R. and Hsu, R. Y.: Volatile chloro- and bromocarbons in coastal waters, *Limnology and Oceanography*, 23(5), 858-869, 1978.
- Hense, I. and Quack, B.: Modelling the vertical distribution of bromoform in the upper water column of the tropical Atlantic Ocean, *Biogeosciences*, 6(4), 535-544, doi:10.5194/bg-6-535-2009, 2009.
- Hetzel, B. S. and Mano, M. T.: A review of experimental studies of iodine deficiency during fetal development, *The Journal of Nutrition*, 119(2), 145-151, 1989.
- Hill, R. W. and Dacey, J. W. H.: Sampling-induced artifacts in incubation experiments on biological processing of dimethylsulfide and similarly soluble gases, *Aquatic Microbial Ecology*, 24, 143-151, doi:10.3354/ame024143, 2001.
- Hopkins, F. E.: Ocean acidification and marine biogenic trace gas production, PhD thesis; University of East Anglia., 2010.

References

- Hossaini, R., Chipperfield, M. P., Dhomse, S., Ordóñez, C., Abraham, N. L., Archibald, A., Braesicke, P., Telford, P., Warwick, N., Yang, X. and Pyle, J.: Modelling future changes to the stratospheric source gas injection of biogenic bromocarbons, *Geophysical Research Letters*, 39, L20813, doi:10.1029/2012GL053401, 2012a.
- Hossaini, R., Chipperfield, M. P., Feng, W., Breider, T. J., Atlas, E., Montzka, S. A., Miller, B. R., Moore, F. and Elkins, J.: The contribution of natural and anthropogenic very short-lived species to stratospheric bromine, *Atmospheric Chemistry and Physics*, 12(1), 371-380, doi:10.5194/acp-12-371-2012, 2012b.
- Hossaini, R., Chipperfield, M. P., Monge-Sanz, B. M., Richards, N. A. D., Atlas, E. and Blake, D.: Bromoform and dibromomethane in the tropics: a 3-D model study of chemistry and transport, *Atmospheric Chemistry and Physics*, 10(2), 719-735, doi:10.5194/acp-10-719-2010, 2010.
- Howell, D. C.: *Statistical Methods for Psychology*, 6th ed., Thomson Higher Education, CA, USA., 2007.
- Hughes, C., Franklin, D. J. and Malin, G.: Iodomethane production by two important marine cyanobacteria: *Prochlorococcus marinus* (CCMP 2389) and *Synechococcus* sp. (CCMP 2370), *Marine Chemistry*, 125(1-4), 19-25, doi:10.1016/j.marchem.2011.01.007, 2011.
- Hughes, C., Johnson, M., von Glasow, R., Chance, R., Atkinson, H., Souster, T., Lee, G. A., Clarke, A., Meredith, M., Venables, H. J., Turner, S. M., et al.: Climate-induced change in biogenic bromine emissions from the Antarctic marine biosphere, *Global Biogeochemical Cycles*, 26(GB3019), doi:10.1029/2012GB004295, 2012.
- Hughes, C., Malin, G., Nightingale, P. D. and Liss, P. S.: The effect of light stress on the release of volatile iodocarbons by three species of marine microalgae, *Limnology and Oceanography*, 51(6), 2849-2854, 2006.
- Hughes, C., Malin, G., Turley, C., M., Keeley, B. J. and Nightingale, P.: The production of volatile iodocarbons by biogenic marine aggregates, *Limnology and Oceanography*, 53(2), 867-872, 2008
- I**
- Itoh, N. and Shinya, M.: Seasonal evolution of bromomethanes from coralline algae (Corallinaceae) and its effect on atmospheric ozone, *Marine Chemistry*, 45(1-2), 95-103, doi:10.1016/0304-4203(94)90094-9, 1994.
- Itoh, N., Tsujita, M., Ando, T., Hisatomi, G. and Higashi, T.: Formation and emission of monohalomethanes from marine algae, *Phytochemistry*, 45(1), 67-73, 1997.
- J**
- Ji, Y. and Tanaka, J.: Effect of desiccation on the photosynthesis of seaweeds from the intertidal zone in Honshu, Japan, *Phycological Research*, 50, 145-153, 2002.
- John, R. P., Anisha, G. S., Nampoothiri, K. M. and Pandey, A.: Micro and macroalgal biomass: a renewable source for bioethanol, *Bioresource Technology*, 102(1), 186-93, doi:10.1016/j.biortech.2010.06.139, 2011.
- Johnson, M. T.: A numerical scheme to calculate temperature and salinity dependent air-water transfer velocities for any gas, *Ocean Science*, 6(4), 913-932, doi:10.5194/os-6-913-2010, 2010.
- Jones, C. E., Andrews, S. J., Carpenter, L. J., Hogan, C., Hopkins, F. E., Laube, J. C., Robinson, A. D., Spain, T. G., Archer, S. D., Harris, N. R. P., Nightingale, P. D., et al.: Results from the first national UK inter-laboratory calibration for very short-lived halocarbons, *Atmospheric Measurement Techniques*, 4(5), 865-874, doi:10.5194/amt-4-865-2011, 2011.
- Jones, C. E. and Carpenter, L. J.: Solar photolysis of CH₂I₂, CH₂ICl, and CH₂IBr in water, saltwater, and seawater, *Environmental Science & Technology*, 39(16), 6130-6137, 2005.
- Jones, C. E. and Carpenter, L. J.: Chemical destruction of CH₃I, C₂H₅I, 1-C₃H₇I and 2-C₃H₇I in saltwater, *Geophysical Research Letters*, 34(13), L13804, doi:10.1029/2007GL029775, 2007.

- Jones, C. E., Hornsby, K. E., Sommariva, R., Dunk, R. M., von Glasow, R., McFiggans, G. and Carpenter, L. J.: Quantifying the contribution of marine organic gases to atmospheric iodine, *Geophysical Research Letters*, 37(L18804), doi:10.1029/2010GL043990, 2010.
- Jones, H. G. and Norton, T. A.: Internal factors controlling the rate of evaporation from fronds of some intertidal algae, *New Phytologist*, 83, 771-781, 1979.
- K**
- Kaiser, H.: Part II Quantitation in Elemental Analysis, *Analytical Chemistry*, 42(4), 26A-59A, 1970.
- Kellner, R., Mermet, J.-M., Otto, M., Valcarcel, M. and Widmer, H. M. (eds.): *Analytical Chemistry: A modern approach to analytical science*, 2nd edition, Wiley-VCH, Weinheim, p737-874, 2004
- Keng, F. S.-L., Phang, S.-M., Rahman, N. A., Leedham, E. C., Hughes, C., Robinson, A. D., Harris, N. R. P., Pyle, J. A. and Sturges, W. T.: Volatile halocarbon emissions by three tropical brown seaweeds under different irradiances, *Journal of Applied Phycology*, pre-print, doi:10.1007/s10811-013-9990-x, 2013.
- Kheshgi, H. S., Prince, R. C. and Marland, G.: The potential of biomass fuels in the context of global climate change: focus on transportation fuels, *Annual Review of Energy and the Environment*, 25, 199-244, 2000.
- Kirst, G. O.: Salinity tolerance of eukaryotic marine algae, *Annual Review of Plant Physiology and Molecular Biology*, 40, 21-53, 1989.
- Kistler, R., Kalnay, E., Collins, W., Saha, S., White, G., Woollen, J., Chelliah, M., Ebisuzaki, W., Kanamitsu, M., Kousky, V., Dool, H. V. D., et al.: The NCEP – NCAR 50-Year Reanalysis: Monthly Means CD-ROM and Documentation, *Bulletin of the American Meteorological Society*, 82(2), 247-267, 2001.
- Klick, S.: The release of volatile halocarbons to seawater by untreated and heavy metal exposed samples of the brown seaweed *Fucus Vesiculosus*, *Marine Chemistry*, 42(3-4), 211-221, doi:10.1016/0304-4203(93)90013-E, 1993.
- Krysztofiak, G., Catoire, V., Poulet, G., Marécal, V., Pirre, M., Louis, F., Canneaux, S. and Josse, B.: Detailed modeling of the atmospheric degradation mechanism of very-short lived brominated species, *Atmospheric Environment*, 59, 514-532, doi:10.1016/j.atmosenv.2012.05.026, 2012.
- Kumar, M., Gupta, V., Trivedi, N., Kumari, P., Bijo, A. J., Reddy, C. R. K. and Jha, B.: Desiccation induced oxidative stress and its biochemical responses in intertidal red alga *Gracilaria corticata* (Gracilariales, Rhodophyta), *Environmental and Experimental Botany*, 72(2), 194-201, doi:10.1016/j.envexpbot.2011.03.007, 2011.
- Kundel, M., Thorenz, U. R., Petersen, J. H., Huang, R.-J., Bings, N. H. and Hoffmann, T.: Application of mass spectrometric techniques for the trace analysis of short-lived iodine-containing volatiles emitted by seaweed, *Analytical and Bioanalytical Chemistry*, 402(10), 3345-3357, doi:10.1007/s00216-011-5658-z, 2012.
- Küpper, F. C., Carpenter, L. J., McFiggans, G. B., Palmer, C. J., Waite, T. J., Boneberg, E.-M., Woitsch, S., Weiller, M., Abela, R., Grolimund, D., Potin, P., et al.: Iodide accumulation provides kelp with an inorganic antioxidant impacting atmospheric chemistry, *Proceedings of the National Academy of Sciences of the United States of America*, 105(19), 6954-8, doi:10.1073/pnas.0709959105, 2008.
- Küpper, F. C., Kloareg, B., Guern, J. and Potin, P.: Oligoguluronates elicit an oxidative burst in the brown algal kelp *Laminaria digitata*, *Plant Physiology*, 125(1), 278-291, 2001.
- Küpper, F. C., Schweigert, N., Ar Gall, E., Legendre, J.-M., Vilter, H. and Kloareg, B.: Iodine uptake in Laminariales involves extracellular, haloperoxidase-mediated oxidation of iodide, *Planta*, 207(2), 163-171, doi:10.1007/s004250050469, 1998.

References

L

La Barre, S., Potin, C., Leblanc, C. and Delage, L.: The halogenated metabolism of brown algae (Phaeophyta), its biological importance and environmental significance, *Marine Drugs*, 8(4), 988-1010, 2010

Laternus, F.: Release of volatile halogenated organic compounds by unialgal cultures of polar macroalgae, *Chemosphere*, 31(6), 3387-3395, 1995.

Laternus, F.: Volatile halocarbons released from Arctic macroalgae, *Marine Chemistry*, 55(3-4), 359-366, doi:10.1016/S0304-4203(97)89401-7, 1996.

Laternus, F., Svensson, T., Wiencke, C. and Oberg, G.: Ultraviolet radiation affects emission of ozone-depleting substances by marine macroalgae: results from a laboratory incubation study, *Environmental Science & Technology*, 38(24), 6605-6609, 2004.

Law, K. S. and Sturges, W. T.: Chapter 2. Halogenated Very Short-Lived Substances, in *Scientific Assessment of Ozone Depletion: 2006.*, 2007.

Leedham, E. C., Hughes, C., Keng, F. S. L., Phang, S.-M., Malin, G. and Sturges, W. T.: Emission of atmospherically significant halocarbons by naturally occurring and farmed tropical macroalgae, *Biogeosciences Discussions*, 10(1), 483-528, 2013

Lesser, M. P.: Oxidative stress in marine environments: biochemistry and physiological ecology, *Annual Review of Physiology*, 68(3), 253-278, doi:10.1146/annurev.physiol.68.040104.110001, 2006.

Lewis, S., Donkin, M. E. and Depledge, M. H.: Hsp70 expression in *Enteromorpha intestinalis* (Chlorophyta) exposed to environmental stressors., *Aquatic Toxicology*, 51(3), 277-91, 2001.

Liss, P. S. and Merlivat, L.: Air-sea gas exchange rates: Introduction and synthesis, in *The role of air-sea exchange in geochemical cycling*, edited by P. Buat-Menard, pp. 112-139, D, Reidel, Hingham, MA., 1986.

Liss, P. S. and Slater, P. G.: Flux of gases across the air-sea interface, *Nature*, 247, 181-, 1974.

Liu, F. and Pang, S. J.: Stress tolerance and antioxidant enzymatic activities in the metabolisms of the reactive oxygen species in two intertidal red algae *Grateloupia turuturu* and *Palmaria palmata*, *Journal of Experimental Marine Biology and Ecology*, 382(2), 82-87, doi:10.1016/j.jembe.2009.11.005, 2010.

Lobban, C. S., Harrison, P. J. and Duncan, M. J.: Seashore Communities, in *The Physiological Ecology of Seaweed*, pp. 154-188, Cambridge University Press, New York., 1985.

Lovelock: Natural halocarbons in the air and in the sea, *Nature*, 256, 193-194, 1975.

Lovelock, J. E.: Atmospheric fluorine compounds as indicators of air movements, *Nature*, 397, 1971.

Lovelock, J. E., Maggs, R. J. and Wade, R. J.: Halogenated hydrocarbons in and over the Atlantic, *Nature*, 241, 194-196, 1973.

Lüning, K.: *Seaweeds. Their environment, biogeography and ecophysiology*, John Wiley & Sons, Inc., New York, 1990

M

Magnusson, G.: Diurnal measurements of F_v/F_m used to improve productivity estimates in macroalgae, *Marine Biology*, 130(2), 203-208, doi:10.1007/s002270050239, 1997.

Mahajan, A. S., Plane, J. M. C., Oetjen, H., Mendes, L., Saunders, R. W., Saiz-Lopez, A., Jones, C. E., Carpenter, L. J. and McFiggans, G. B.: Measurement and modelling of tropospheric reactive halogen species over the tropical Atlantic Ocean, *Atmospheric Chemistry and Physics*, 10, 4611-4624, doi:10.5194/acp-10-4611-2010, 2010.

- Mäkelä, J. M., Hoffman, T., Holzke, C., Väkevä, M., Suni, T., Mattila, T., Aalto, P. P., Tapper, U., Kauppinen, E. I. and O'Dowd, C. D.: Biogenic iodine emissions and identification of end-products in coastal ultrafine particles during nucleation bursts, *Journal of Geophysical Research*, 107(D19), doi:10.1029/2001JD000580, 2002.
- Mairh, O. P., Ramavat, B. K., Tewari, A., Oza, R. M. and Joshi, H. V.: Seasonal variation, bioaccumulation and prevention of loss of iodine in seaweeds, *Phytochemistry*, 28(12), 3307-3310, 1989.
- Manley, S.: Phytogenesis of halomethanes: A product of selection or a metabolic accident?, *Biogeochemistry*, 60, 163-180, 2002.
- Manley, S. L. and Barbero, P. E.: Physiological constraints on bromoform (CHBr_3) production by *Ulva lactuca* (Chlorophyta), *Limnology and Oceanography*, 46(6), 1392-1399, 2001.
- Manley, S. L. and Dastoor, M. N.: Methyl halide (CH_3X) production from the giant kelp, *Macrocystis*, and estimates of global CH_3X production by kelp, *Limnology and Oceanography*, 32(3), 709-715, 1987.
- Manley, S. L. and Dastoor, M. N.: Methyl iodide (CH_3I) production by kelp and associated microbes, *Marine Biology*, 98, 477-482, 1988.
- Manley, S. L., Goodwin, K. and North, W. J.: Laboratory production of bromoform, methylene bromide and methyl iodide by macroalgae and distribution in nearshore southern California waters, *Limnology and Oceanography*, 37(8), 1652-1659, 1992.
- Manley, S. L., Wang, N.-Y., Walser, M. L. and Cicerone, R. J.: Methyl halide emissions from greenhouse-grown mangroves, *Geophysical Research Letters*, 34(1), L01806, doi:10.1029/2006GL027777, 2007.
- Markes International: Thermal Desorption Technical Support Note 5: Advice on sorbent selection, tube conditioning, tube storage and air sampling, , 44(0), 2008.
- Markes International: TDTS20: Confirming sorbent tube retention volumes and checking for analyte breakthrough., 2012.
- Marshall, R., Harper, D., McRoberts, W. and Dring, M. T.: Volatile bromocarbons produced by *Falkenbergia* stages of *Asparagopsis* spp. (Rhodophyta), *Limnology and Oceanography*, 44(5), 1348-1352, 1999.
- Martino, M., Liss, P. S. and Plane, J. M. C.: The photolysis of dihalomethanes in surface seawater, *Environmental Science & Technology*, 39(18), 7097-101, 2005.
- Martino, M., Mills, G. P., Woeltjen, J. and Liss, P. S.: A new source of volatile organoiodine compounds in surface seawater, *Geophysical Research Letters*, 36(1), doi:10.1029/2008GL036334, 2009.
- Mata, L., Gaspar, H. and Santos, R.: Carbon/Nutrient Balance in Relation To Biomass Production and Halogenated Compound Content in the Red Alga *Asparagopsis Taxiformis* (Bonnemaisoniaceae), *Journal of Phycology*, 47, 248-253, doi:10.1111/j.1529-8817.2011.01083.x, 2011.
- McFiggans, G., Coe, H., Burgess, R., Allan, J., Cubison, M., Alfarra, M. R., Saunders, R., Saiz-Lopez, A., Plane, J. M. C., Wevill, D., Carpenter, L. J., et al.: Direct evidence for coastal iodine particles from *Laminaria* macroalgae – linkage to emissions of molecular iodine, *Atmospheric Chemistry and Physics*, 4, 701-713, doi:10.5194/acpd-4-939-2004, 2004.
- McHugh, D. K.: FAO Fisheries and Technical Paper No.411 A guide to the seaweed industry, Rome., 2003.
- McKeen, S. A. and Liu, S. C.: Hydrocarbon ratios and photochemical history of air masses, *Geophysical Research Letters*, 20(21), 2363-2366, 1993.
- Michanek, G.: Seaweed resources of the ocean. FAO Fish.Tech.Pap., (138)., 1975.

References

- Molina, M. J. and Rowland, F. S.: Stratospheric sink for chlorofluoromethanes: chlorine atom-catalysed destruction of ozone, *Nature*, 249, 810-812, 1974.
- Monks, P. S.: Gas-phase radical chemistry in the troposphere, *Chemical Society Reviews*, 34(5), 376-395, doi:10.1039/b307982c, 2005.
- Montzka, S. A., Reimann, S., Engel, A., Kruger, K., O'Doherty, S., Sturges, W. T., Blake, D., Dorf, M., Fraser, P., Friodevaux, L., Jucks, K., et al.: Chapter 1. Ozone-Depleting Substances (ODSs) and Related Chemicals, in *WMO Scientific Assessment of Ozone Depletion: 2010*, edited by WMO., 2010.
- Moore, R. M.: A photochemical source of methyl chloride in saline waters., *Environmental Science & Technology*, 42(6), 1933-1937, 2008.
- Moore, R. M., Geen, C. E. and Tait, V. K.: Determination of Henry's Law constants for a suite of naturally occurring halogenated methanes in seawater, *Chemosphere*, 30(6), 1183-1191, 1995.
- Moore, R. M. and Groszko, W.: Methyl iodide distribution in the ocean and fluxes to the atmosphere, *Journal of Geophysical Research*, 104(C5), 11163-11171, doi:DOI: 10.1029/1998JC900073, 1999.
- Moore, R. M. and Tokarczyk, R.: Volatile biogenic halocarbons in the northwest Atlantic, *Global Biogeochemical Cycles*, 7(1), 195-210, 1993.
- Moore, R. M. and Zafiriou, O. C.: Photochemical production of methyl iodide in seawater, *Journal of Geophysical Research*, 99(D8), 16415-16420, doi:10.1029/94JD00786, 1994.
- Mtolera, M. S. P., Collén, J., Pedersén, M., Ekdahl, A., Abrahamsson, K. and Semesi, A. K.: Stress-induced production of volatile halogenated organic compounds in *Eucheuma denticulatum* (Rhodophyta) caused by elevated pH and high light intensities, *European Journal of Phycology*, 31(1), 89-95, doi:10.1080/09670269600651241, 1996.
- N**
- National Climatic Data Center (NCDC): Daily Satellite Images, GIBBS: Global ISCCP B1 Browse System, accessed [20.05.2013] from <http://www.ncdc.noaa.gov/gibbs/year>.
- Naylor, J.: Production, trade and utilisation of seaweeds and seaweed products. *FAO Fish. Tech. Pap.*, (159)., 1976.
- Neish, I. C.: Monograph #1-0703. The ABC of *Eucheuma* Seaplant Production., 2003.
- Neish, I. C.: Tropical red seaweeds as a foundation for integrated multi-trophic aquaculture (IMTA). *SeaPlant Monograph no.HB2E 209 V3.*, 2009.
- Neori, A.: Essential role of seaweed cultivation in integrated multi-trophic aquaculture farms for global expansion of mariculture: an analysis, *Journal of Applied Phycology*, 20(5), 567-570, doi:10.1007/s10811-007-9206-3, 2007.
- Newman, P. A. and Pyle, J. A.: Chapter 3. Polar Stratospheric Ozone: Past and Future, in *Scientific Assessment of Ozone Depletion: 2002*, World Meteorological Society, Geneva., 2002.
- Ni, X. and Hager, L. P.: Expression of *Batis maritima* methyl chloride transferase in *Escherichia coli*, *Proceedings of the National Academy of Sciences of the United States of America*, 96(7), 3611-3615, 1999.
- Nightingale, P. D., G, M., Law, C. S., Watson, A. J., Liss, P. S., Liddicoat, M. L., Boutin, J. and Upstill-Goddard, R. C.: In situ evaluation of air-sea gas exchange parameterisations using novel conservative and volatile tracers, *Global Biogeochemical Cycles*, 14(1), 373-387, 2000.
- Nightingale, P. D., Malin, G. and Liss, P. S.: Production of chloroform and other low molecular-weight halocarbons by some species of macroalgae, *Limnology and Oceanography*, 40(4), 680-689, doi:10.4319/lo.1995.40.4.0680, 1995.

Nylund, G. M., Cervin, G., Persson, F., Hermansson, M., Steinberg, P. D. and Pavia, H.: Seaweed defence against bacteria: a poly-brominated 2-heptanone from the red alga *Bonnemaisonia hamifera* inhibits bacterial colonisation, *Marine Ecology Progress Series*, 369, 39-50, doi:10.3354/meps07577, 2008.

O

Oliver, M. J., Wood, A. J. and Mahony, P. O.: "To dryness and beyond" – preparation for the dried state and rehydration in vegetative desiccation-tolerant plants, *Plant Growth Regulation*, 24, 193-201, 1998.

O'Brien, L. M., Harris, N. R. P., Robinson, a. D., Gostlow, B., Warwick, N., Yang, X. and Pyle, J. a.: Bromocarbons in the tropical marine boundary layer at the Cape Verde Observatory – measurements and modelling, *Atmospheric Chemistry and Physics*, 9, 4335-4379, doi:10.5194/acpd-9-4335-2009, 2009.

O'Dowd, C. D., Hämeri, K., Mäkelä, J. M., Pirjola, L., Kulmala, M., Jennings, S. G., Berresheim, H., Hansson, H.-C., de Leeuw, G., Kunz, G. J., Allen, A. G., et al.: A dedicated study of New Particle Formation and Fate in the Coastal Environment (PARFORCE): Overview of objectives and achievements, *Journal of Geophysical Research*, 107(D19), doi:10.1029/2001JD000555, 2002a.

O'Dowd, C., Jimenez, J. L., Bahreini, R., Flagan, R. C., Seinfeld, J. H., Hämeri, K., Pirjola, L., Kulmala, M., Jennings, S. G. and Hoffmann, T.: Marine aerosol formation from biogenic iodine emissions, *Nature*, 417, 632-636, doi:10.1038/nature00773.1.2.3.4.5.6.7.8.9.10., 2002b.

P

Palmer, C. J., Anders, T. L., Carpenter, L. J., Küpper, F. C. and McFiggans, G. B.: Iodine and Halocarbon Response of *Laminaria digitata* to Oxidative Stress and Links to Atmospheric New Particle Production, *Environmental Chemistry*, 2(4), 282, doi:10.1071/EN05078, 2005.

Palmer, C. J. and Reason, C. J.: Relationships of surface bromoform concentrations with mixed layer depth and salinity in the tropical oceans, *Global Biogeochemical Cycles*, 23(2), 1-10, doi:10.1029/2008GB003338, 2009.

Park, S., Atlas, E. L., Jiménez, R., Daube, B. C., Gottlieb, E. W., Nan, J., Jones, D. B. A., Pfister, L., Conway, T. J., Bui, T. P., Gao, R.-S., et al.: Vertical transport rates and concentrations of OH and Cl radicals in the Tropical Tropopause Layer from observations of CO₂ and halocarbons: implications for distributions of long- and short-lived chemical species, *Atmospheric Chemistry and Physics*, 10(14), 6669-6684, doi:10.5194/acp-10-6669-2010, 2010.

Paul, C. and Pohnert, G.: Production and role of volatile halogenated compounds from marine algae, *Natural Product Reports*, 28(2), 186-195, doi:10.1039/c0np00043d, 2010.

Paul, V. J., Littler, M. M., Littler, D. S. and Fenical, W.: Evidence for chemical defense in tropical green alga *Caulerpa ashmeadii* (Caulerpaceae: Chlorophyta): Isolation of new bioactive sesquiterpenoids, *Journal of Chemical Ecology*, 13(5), 1171-1185, 1987.

Pearson, G., Kautsky, L. and Serrão, E.: Recent evolution in Baltic *Fucus vesiculosus*: reduced tolerance to emersion stresses compared to intertidal (North Sea) populations, *Marine Ecology Progress Series*, 202, 67-79, doi:10.3354/meps202067, 2000.

Pedersen, M., Collen, J., Abrahamsson, K. and Ekdahl, A.: Production of halocarbons from seaweeds: an oxidative stress reaction, *Scientia Marina*, 60(Suppl. 1), 257-263, 1996.

Pena, E. J., Zingmark, R. and Nietch, C.: Comparative photosynthesis of two species of intertidal epiphytic macroalgae on mangrove roots during submersion and emersion, *Journal of Phycology*, 35, 1206-1214, 1999.

Phang, S.-M., Critchley, A. T. and Ang Jr., P. O. (eds.): *Advances in seaweed cultivation in Asia*, University of Malaya Maritime Research Centre; Kuala Lumpur, 2006

References

Phang, S.-M., Wong, C. L. and Sim, M. C.: Checklist of Malaysian Sargassum species, in Taxonomy of Southeast Asian Seaweeds. University of Malaya Monograph Series 2, edited by S.-M. Phang, K. Lewmanomont, and P.-E. Lim, pp. 83-103, Institute of Ocean and Earth Sciences (IOES), University of Malaya, Kuala Lumpur., 2008.

Phang, S.-M., Yeong, H.-Y., Lim, P.-E., Nor, A. R. and Gan, K. T.: Commercial varieties of *Kappaphycus* and *Euचेuma* in Malaysia, *Malaysian Journal of Science*, 29(3), 214-224, 2010.

Platt, U. and Hönniger, G.: The role of halogen species in the troposphere., *Chemosphere*, 52(2), 325-338, doi:10.1016/S0045-6535(03)00216-9, 2003.

Pyle, J. A., Ashfold, M. J., Harris, N. R. P., Robinson, A. D., Warwick, N. J., Carver, G. D., Gostlow, B., O'Brien, L. M., Manning, A. J., Phang, S. M., Yong, S. E., et al.: Bromoform in the tropical boundary layer of the Maritime Continent during OP3, *Atmospheric Chemistry and Physics*, 11(2), 529-542, doi:10.5194/acp-11-529-2011, 2011.

Q

Quack, B., Atlas, E., Petrick, G., Stroud, G., Schauffler, S. and Wallace, D. W. R.: Oceanic bromoform sources for the tropical atmosphere, *Geophysical Research Letters*, 31(L23S05), 2004

Quack, B., Peeken, I., Petrick, G. and Nachtigall, K.: Oceanic distribution and sources of bromoform and dibromomethane in the Mauritanian upwelling, *Journal of Geophysical Research*, 112(C10006), doi:10.1029/2006JC003803, 2007.

Quack, B. and Suess, E. Volatile halogenated hydrocarbons over the western Pacific 43 °N and 4 °N, *Journal of Geophysical Research*, 104(D1), 1663-1678, 1999

Quack, B. and Wallace, D. W. R.: Air-sea flux of bromoform: Controls, rates, and implications, *Global Biogeochemical Cycles*, 17(1), doi:10.1029/2002GB001890, 2003.

R

Read, K. A., Mahajan, A. S., Carpenter, L. J., Evans, M. J., Faria, B. V. E., Heard, D. E., Hopkins, J. R., Lee, J. D., Moller, S. J., Lewis, A. C., Mendes, L., et al.: Extensive halogen-mediated ozone destruction over the tropical Atlantic Ocean., *Nature*, 453(7199), 1232-1235, doi:10.1038/nature07035, 2008.

Reeves, C. E., Penkett, S. A., Bauguitte, S., Law, K. S., Evans, M. J., Bandy, B. J., Monks, P. S., Edwards, G. D., Philips, G., Barjat, H., Kent, J., et al.: Potential for photochemical ozone formation in the troposphere over the North Atlantic as derived from aircraft observations during ACSOE, *Journal of Geophysical Research*, 107(D23), doi:10.1029/2002JD002415, 2002.

Richardson, S. D., DeMarini, D. M., Kogevinas, M., Fernandez, P., Marco, E., Lourencetti, C., Ballesté, C., Heederik, D., Meliefste, K., McKague, A. B., Marcos, R., et al.: What's in the pool? A comprehensive identification of disinfection by-products and assessment of mutagenicity of chlorinated and brominated swimming pool water, *Environmental Health perspectives*, 118(11), 1523-1530, doi:10.1289/ehp.1001965, 2010.

Richter, U. and Wallace, D. W. R.: Production of methyl iodide in the tropical Atlantic Ocean, *Geophysical Research Letters*, 31(23), L23S03, doi:10.1029/2004GL020779, 2004.

Robinson, N. H., Allan, J. D., Trembath, J. A., Rosenberg, P. D., Allen, G. and Coe, H.: The lofting of Western Pacific regional aerosol by island thermodynamics as observed around Borneo, *Atmospheric Chemistry and Physics*, 12, 5963-5983, doi:10.5194/acp-12-5963-2012, 2012.

Rodríguez-Castañeda, A. P., Sánchez-Rodríguez, I., Shumilin, E. N. and Sapozhnikov, D.: Elemental concentrations in some species of seaweeds from La Paz Bay and La Paz Lagoon, south-western Baja California, Mexico, *Journal of Applied Phycology*, 18(3-5), 399-408, doi:10.1007/s10811-006-9040-z, 2006.

Rolph, G. D.: Real-time Environmental Applications and Display sYstem (READY) Website, NOAA Air Resources Laboratory, Silver Spring, MD [online] Available from: <http://ready.arl.noaa.gov> (Accessed 4 January 2013), 2013.

S

- Saenko, G. N., Kravtsova, Y. Y., Ivanenko, V. V. and Sheludko, S. I.: Concentration of Iodine and Bromine by Plants in the Seas of Japan and Okhotsk, *Marine Biology*, 47, 243-250, 1978.
- Saiz-Lopez, A., Plane, J. M. C., Baker, A. R., Carpenter, L. J., von Glasow, R., Martín, J. C. G., McFiggans, G. and Saunders, R. W.: Atmospheric chemistry of iodine., *Chemical Reviews*, 112(3), 1773-1804, doi:10.1021/cr200029u, 2012.
- Saiz-Lopez, A. and Plane, J. M. C.: Novel iodine chemistry in the marine boundary layer, *Geophysical Research Letters*, 31(L04112), doi:10.1029/2003GL019215, 2004.
- Salawitch, R. J.: Biogenic bromine, *Nature*, 439, 275-277, doi:10.1029/2005JD006244, 2006.
- Salawitch, R. J., Weisenstein, D. K., Kovalenko, L. J., Sioris, C. E., Wennberg, P. O., Chance, K., Ko, M. K. W. and McLinden, C. A.: Sensitivity of ozone to bromine in the lower stratosphere, *Geophysical Research Letters*, 32(5), L05811, doi:10.1029/2004GL021504, 2005.
- Sampath-Wiley, P., Neefus, C. D. and Jahnke, L. S.: Seasonal effects of sun exposure and emersion on intertidal seaweed physiology: Fluctuations in antioxidant contents, photosynthetic pigments and photosynthetic efficiency in the red alga *Porphyra umbilicalis* Kützting (Rhodophyta, Bangiales), *Journal of Experimental Marine Biology and Ecology*, 361(2), 83-91, doi:10.1016/j.jembe.2008.05.001, 2008.
- Sander, R.: *Compilation of Henry's Law Constants for Inorganic and Organic Species of Potential Importance in Environmental Chemistry*, Mainz., 1999.
- Sander, R., Rudich, Y., von Glasow, R. and Crutzen, P. J.: The role of BrNO₃ in marine tropospheric chemistry: A model study, *Geophysical Research Letters*, 26(18), 2857-2860, 1999.
- Santelices, B., Bolton, J. and Meneses, I.: Marine Algal Communities, in *Marine Macroecology*, edited by J. D. Witman and K. Roy, pp. 153-194, The University of Chicago Press, Chicago., 2009.
- Sartin, J. H., Halsall, C. J., Hayward, S. and Hewitt, C. N.: Emission rates of C₈-C₁₅ VOCs from seaweed and sand in the inter-tidal zone at Mace Head, Ireland, *Atmospheric Chemistry*, 36, 5311-5321, 2002.
- Sartin, J., Halsall, C., Davison, B. and Owen, S.: Determination of biogenic volatile organic compounds (C₈-C₁₆) in the coastal atmosphere at Mace Head, Ireland, *Analytica Chimica Acta*, 428, 61-72, 2001.
- Saunders, R. W. and Plane, J. M. C.: Formation Pathways and Composition of Iodine Oxide Ultra-Fine Particles, *Environmental Chemistry*, 2(4), 299-303, doi:10.1071/EN05079, 2005.
- Scarratt, M. G. and Moore, R. M.: Production of methyl bromide and methyl chloride in laboratory cultures of marine phytoplankton II, *Marine chemistry*, 59, 311-320, 1998.
- Scarratt, M. G. and Moore, R. M.: Production of Chlorinated Hydrocarbons and Methyl Iodide by the Red Microalga *Porphyridium purpureum*, *Limnology and Oceanography*, 44(3), 703-707, 1999.
- Schall, C., Laturus, F. and Heumann, K. G.: Biogenic volatile organoiodide and organobromine compounds released from polar macroalgae, *Chemosphere*, 28(7), 1315-1324, 1994.
- Seinfeld, J. H. and Pandis, S. N.: *Atmospheric Chemistry and Physics: From air pollution to climate change*, Wiley Blackwell., 1997.
- Seitz, K., Buxmann, J., Pohler, D., Sommer, T., Tschritter, J., Neary, T., O'Dowd, C. and Platt, U.: The spatial distribution of the reactive iodine species IO from simultaneous active and passive DOAS observations, *Atmospheric Chemistry and Physics*, 10, 2117-2128, 2010.
- Singh, A., Nigam, P. S. and Murphy, J. D.: Renewable fuels from algae: an answer to debatable land based fuels, *Bioresource Technology*, 102(1), 10-16, doi:10.1016/j.biortech.2010.06.032, 2011.

References

Smyth, P. P. A., Burns, R., Huang, R. J., Hoffman, T., Mullan, K., Graham, U., Seitz, K., Platt, U. and O'Dowd, C.: Does iodine gas released from seaweed contribute to dietary iodine intake?, *Environmental geochemistry and health*, 33(4), 389-397, doi:10.1007/s10653-011-9384-4, 2011.

Spoerner, M., Wichard, T., Bachhuber, T., Stratmann, J. and Oertel, W.: Growth and thallus morphogenesis of *Ulva mutabilis* (chlorophyta) depends on a combination of two bacterial species excreting regulatory factors, *Journal of Phycology*, 48, 1433-1447, doi:10.1111/j.1529-8817.2012.01231.x, 2012.

Sturges, W. T., Cota, G. F. and T, B. P.: Bromoform emission from Arctic ice algae, *Nature*, 358, 660-662, 1992.

Swain, P. A.: Bernard Courtois (1777-1838), famed for discovering iodine (1811), and his life in Paris from 1789, *Bulletin for the History of Chemistry*, 30(2), 103-111, 2005.

T

Tang, Q., Zhang, J. and Fang, J.: Shellfish and seaweed mariculture increase atmospheric CO₂ absorption by coastal ecosystems, *Marine Ecology Progress Series*, 424, 97-104, doi:10.3354/meps08979, 2011.

Tang, X., Madronich, S., Wallington, T. and Calamari, D.: Changes in tropospheric composition and air quality, *Journal of Photochemistry and Photobiology. B, Biology*, 46(1-3), 83-95, 1998.

Tegtmeier, S., Krüger, K., Quack, B., Atlas, E. L., Pisso, I., Stohl, A. and Yang, X.: Emission and transport of bromocarbons: from the West Pacific ocean into the stratosphere, *Atmospheric Chemistry and Physics*, 12(22), 10633-10648, doi:10.5194/acp-12-10633-2012, 2012.

Theiler, R., Cook, J. C. and Hager, L. P.: Halohydrocarbon synthesis by bromoperoxidase, *Science*, 202, 1094-1096, 1978.

Tokarczyk, R. and Moore, R. M.: Production of volatile organohalogenes by phytoplankton cultures, *Geophysical Research Letters*, 21(4), 285-288, 1994.

Tuckermann, M., Ackermann, R., Golz, C., Lorenzen-Schimdt, H., Senne, T., Stutz, J., Trost, B., Unold, W. and Platt, T.: DOAS-observation of halogen radical-catalysed arctic boundary layer ozone destruction during the ARCTOC-campaigns, 1995 and 1996 in Ny-Alesund, Spitsbergen, *Tellus*, 49B, 533-555, 1997.

U

U.S. Environmental Protection Agency (EPA): Compendium of Methods for the Determination of Toxic Organic Compounds in Ambient Air. Compendium Method TO-17: Determination of Volatile Organic Compounds in Ambient Air Using Active Sampling Onto Sorbent Tubes, Cincinnati, OH., 1999.

U.S. Environmental Protection Agency (EPA): Human health benefits of stratospheric ozone, Washington, DC., 2006.

Upstill-Goddard, R. C.: Air-sea gas exchange in the coastal zone, *Estuarine, Coastal and Shelf Science*, 70(3), 388-404, doi:10.1016/j.ecss.2006.05.043, 2006.

V

de Vooy, C. G. N.: Primary Productivity in Aquatic Environments, in *The Global Carbon Cycle (SCOPE 13)*, edited by B. Bolin, E. T. Degens, S. Kempe, and O. Ketner., 1979.

W

Walz GmbH: UNDERWATER FLUOROMETER DIVING-PAM Submersible Photosynthesis Yield Analyzer Handbook of Operation, , (July), 1998.

Wanninkhof, R.: Relationship between wind speed and gas exchange over the ocean, *Journal of Geophysical Research*, 97, 7373-7382, 1992.

- Warwick, N. J., Pyle, J. A., Carver, G. D., Yang, X., Savage, N. H., O'Connor, F. M. and Cox, R. A.: Global modeling of biogenic bromocarbons, *Journal of Geophysical Research*, 111(D24), 1-12, doi:10.1029/2006JD007264, 2006.
- Watling, R. and Harper, D. B.: Chloromethane production by wood-rotting fungi and an estimate of the global flux to the atmosphere, *Mycological Research*, 102(7), 769-787, 1998.
- Weinberger, F., Coquempot, B., Forner, S., Morin, P., Kloareg, B. and Potin, P.: Different regulation of haloperoxidation during agar oligosaccharide-activated defence mechanisms in two related red algae, *Gracilaria* sp. and *Gracilaria chilensis*, *Journal of Experimental Biology*, 58(15-16), 4365-4372, 2007
- Wever, R., Tromp, M. G. M., Krenn, B. E., Marjani, A. and Van Tol, M.: Brominating Activity of the Seaweed *Ascophyllum nodosum*: Impact on the biosphere, *Environmental Science and Technology*, 25(3), 446-449, 1991.
- Whitehead, D. C.: The distribution and transformations of iodine in the environment, *Environment International*, 10, 321-339, 1984.
- Williams, J., Gros, V., Atlas, E., Maciejczyk, K., Batsaikhan, A., Schöler, H. F., Forster, C., Quack, B., Yassaa, N., Sander, R. and Van Dingenen, R.: Possible evidence for a connection between methyl iodide emissions and Saharan dust, *Journal of Geophysical Research*, 112(D7), 1-11, doi:10.1029/2005JD006702, 2007.
- Williams, S. L. and Dethier, M. N.: High and dry: variation in net photosynthesis of the intertidal seaweed *Fucus gardneri*, *Ecology*, 86(9), 2373-2379, 2005.
- Winter, J. M. and Moore, B. S.: Exploring the chemistry and biology of vanadium-dependent haloperoxidases, *The Journal of Biological Chemistry*, 284(28), 18577-18581, doi:10.1074/jbc.R109.001602, 2009.
- World Resources Institute: Coastal and Marine Ecosystems - Marine Jurisdictions: Coastline length, , check back [online] Available from: <http://www.wri.org/project/earthtrends/text/coastal-marine/variable-61.html>, 2012.
- Worton, D. R., Mills, G. P., Oram, D. E. and Sturges, W. T.: Gas chromatography negative ion chemical ionisation mass spectrometry: application to the detection of alkyl nitrates and halocarbons in the atmosphere, *Journal of Chromatography A*, 1201(1), 112-119, 2008
- Wuosmaa, A. M. and Hager, L. P.: Methyl chloride transferase: a carbocation route for biosynthesis of halometabolites, *Science*, 249, 160-162, 1990.
- Wurl, O., Ed.: *Practical guidelines for the analysis of seawater*, CRC Press, Boca Raton., 2009.
- X**
- Y**
- Yang, X., Cox, R., Warwick, N. J., Pyle, J., Carver, G. D., O'Connor, F. M. and Savage, N. H.: Tropospheric bromine chemistry and its impacts on ozone: A model study, *Journal of Geophysical Research*, 110(D23), 1-18, doi:10.1029/2005JD006244, 2005.
- Yokouchi, Y., Hasebe, F., Fujiwara, M., Takashima, H., Shiotani, M., Nishi, N., Kanaya, Y., Hashimoto, S., Fraser, P., Toom-Saunty, D., Mukai, H., et al.: Correlations and emission ratios among bromoform, dibromochloromethane, and dibromomethane in the atmosphere, *Journal of Geophysical Research*, 110(D23309), doi:10.1029/2005JD006303, 2005.

References

Z

Zemke-White, W. and Ohno, M.: World seaweed utilisation: An end-of-century review, *Journal of Applied Phycology*, 11, 369-376, 1999

Zhou, Y., Mao, H., Russo, R. S., Blake, D. R., Wingenter, O. W., Haase, K. B., Ambrose, J., Varner, R. K., Talbot, R. and Sive, B. C.: Bromoform and dibromomethane measurements in the seacoast region of New Hampshire, 2002–2004, *Journal of Geophysical Research*, 113(D8), D08305, doi:10.1029/2007JD009103, 2008.